

**VISIBLE LIGHT PHOTOREDOX CATALYSIS IN  
sp<sup>3</sup> C-H ACTIVATION OF *t*-AMINES FOR C-C  
BOND FORMATION REACTION**

**THESIS SUBMITTED TO THE**

**UNIVERSITY OF PUNE**

**FOR THE DEGREE OF  
DOCTOR OF PHILOSOPHY**

**(IN CHEMISTRY)**

**BY**

**DEEPAK JADHAV**

**RESEARCH SUPERVISOR**

**Dr. GANESH PANDEY**

**ORGANIC CHEMISTRY DIVISION  
NATIONAL CHEMICAL LABORATORY  
PUNE 411 008**

**APRIL 2014**

*Dedicated to...*

**“My Aai and Baba”**

## CERTIFICATE

This is to certify that the work incorporated in the thesis entitled “**Visible light photoredox catalysis in  $sp^3$  C-H activation of *t*-amines for C-C bond formation reaction**” which is being submitted to the **University of Pune** for the award of **Doctor of Philosophy in Chemistry** by **Mr. Deepak Jadhav** was carried out by him under my supervision at the **National Chemical Laboratory, Pune**. A material that has been obtained from other sources has been duly acknowledged in the thesis.

Date:

**Dr. Ganesh Pandey**  
**(Research Guide)**

## DECLARATION

I hereby declare that the work presented in the thesis entitled “**Visible light photoredox catalysis in  $sp^3$  C-H activation of *t*-amines for C-C bond formation reaction**” submitted for Ph. D. Degree to the **University of Pune**, has been carried out by me at the **National Chemical Laboratory, Pune**, under the supervision of **Dr. Ganesh Pandey**. The work is original and has not been submitted in part or full by me for any degree or diploma to this or any other University /Institute.

Date:

**Deepak Jadhav**

## **Acknowledgement**

It would not have been possible to write this thesis without the generous help and constant encouragement of kind people around me. I would like to extend my appreciation especially, to the following for the support they have rendered for the accomplishment of the work presented in this dissertation.

First and foremost, I would like to express my sincere gratitude to my supervisor Dr. Ganesh Pandey for his invaluable guidance, endless patience, outstanding motivation, amazing enthusiasm, immense knowledge and for the continuous support throughout my Ph.D study and research. I could not have imagined having a better advisor and mentor for my Ph.D study. Indeed, it will be impossible for me to describe in words his contribution in my life.

I am thankful to Dr. (Mrs.) Gadre for her moral support and motivation. I take this opportunity to offer my sincere appreciation to Dr. P. K. Triphati, Dr. S. P. Chavan, Dr. R. A. Joshi and Dr. (Mrs.) R. R. Joshi for their help, valuable suggestions and advice.

I thank my present lab colleagues Rajesh, Binoy, Animesh, Durga, Shiva, Jankiram, Jagadish, Pradeep, Ramkrishna, Akash, Sandip, Rushil, Divya, Pushpendra, Sahani, Pulak, Prachi, Dr. Navnath, Dr. Bhawna, Dr. Atish, Dr. Mantu, Dr. Deepak S. and previous lab members Dr. Sanjay, Dr. Srinivas, Dr. Kishor, Dr. Balakrishna, Dr. Keshrinath, Late Srikant, Dr. Nishant, Dr. Ravindra, Dr. Asha, Dr. Prasanna, Dr. Amrut, Dr. Swaroop, Dr. Rajender , Dr. Debashis Grahacharya, Dr. Dharmendra, Dr. Priyanka, Dr. Sujit, Debasis Dey, Tukaram, Nitesh, Dr. Gumaste, Pawar kaka for making GP Lab, the most desirable place to work.

I am deeply grateful to Prof. Oliver Reiser, University of Regensburg, Germany, for offering an exchange student position and providing me research facilities in his group, through INDIGO Programme. I extend my sincere thanks to all his group members, especially to my colleague Paul Kohls, during my stay there. I would also like to thank BASF SE, Ludwigshafen, Germany for offering me internship opportunity, through INDIGO programme.

Help from Dr. P. R. Rajmohanam, Amol Kotmale, Srikant Kunjir for NMR analyses, (Mrs.) Shantakumari for mass analyses and Dr. Rahul Banerjee, Pradip Pachfule for X-ray analyses is greatly acknowledged. Special thanks to Pradip and Amol for their immense help out.

It is difficult for me to acknowledge a long friend list of mine, but I should not forget to mention name of Dr. Ankur Pandey, Dr. Ankush Biradar, Dr. Kishan H., Dr. Sudhir B., Dr. Atul Prashar, Dr. Pandurang C., Dr. Abasaheb, Dr. Manmath, Dr. Bharat, Dr. Prasad W., Dr. Devendra B., Dr. Abhijit P., Dr. Ganesh K., Dr. Prakash S., Dr. Digambar S., Dr. Dhanraj S., Pradip Pachfule, Ankush Bhise, Pankaj Daramwar, Kiran Patil, Majid, Chinmoy, Shekhar, Nagesh, Mangesh Mahajan, Atul, Bhausahab, Milind, Dnyaneshwar, Govind, Achintya, Prasenjit, all friends from GJ hostel and NCL who helped me directly and indirectly. I would like to specially thank Kiran Patil and Majid for their constant help and brotherhood support. Further, I could not have even imagined, beginning my research career without support and motivation of my M. Sc. friends Dr. Avinash Puyad, Shyam Patil and Dayanand Jadhav.

I thank CSIR New Delhi, for the award of Research Fellowship and Director, CSIR-NCL, for the infrastructure and facilities.

Last but not least I would like to thank my parents, my sisters and my entire family for giving unconditional love, constant support and encouragement without which I never would have been able to achieve my goals. Lastly, I would like to express my heartfelt gratitude to Shona, who is god's greatest gift in my life, was there cheering me up and stood by me through the good and bad times.

Deepak Jadhav

| <b>Contents</b>  |  |              |
|------------------|--|--------------|
| Abbreviations    |  | i            |
| General Remarks  |  | ii           |
| Thesis Abstract  |  | iii-viii     |
| <b>Chapter 1</b> | <b><math>sp^3</math> C-H Activation of <i>t</i>-Amines</b>   | <b>1-30</b>  |
| 1.1              | Introduction   | 2            |
| 1.2              | $\alpha$ $sp^3$ C-H activation of <i>t</i> -amines   | 8            |
| 1.3              | $\alpha$ $sp^3$ C-H activation of <i>t</i> -amines: Non-photochemical approaches                                   | 9            |
| 1.3.1            | $\alpha$ C-H functionalization of <i>t</i> -amines by $\alpha$ -lithiation reaction with alkyllithium/diamine      | 9            |
| 1.3.2            | Transition metal-catalyzed $\alpha$ C-H activation of <i>t</i> -amines   | 9            |
| 1.3.3            | $\alpha$ -aminoalkyl radical based C-H functionalization of <i>t</i> -amines                                       | 11           |
| 1.3.4            | Iminium ion based $\alpha$ C-H functionalization of <i>t</i> -amines   | 13           |
| 1.3.4.I          | Electrochemical oxidation  | 13           |
| 1.3.4.II         | Transition metal catalyzed oxidation   | 14           |
| 1.4              | $\alpha$ $sp^3$ C-H activation of <i>t</i> -amines: Photochemical approaches                                       | 17           |
| 1.4.1            | Background   | 17           |
| 1.4.2            | UV photochemistry for $\alpha$ $sp^3$ C-H activation of <i>t</i> -amines   | 19           |
| 1.4.3            | Visible light photoredox catalysis for $\alpha$ $sp^3$ C-H activation of <i>t</i> -amines                          | 21           |
| 1.5              | Objective of present dissertation  | 25           |
| 1.6              | References   | 26           |
| <b>Chapter 2</b> | <b>Visible Light Photoredox Catalysis: <math>\alpha</math> <math>sp^3</math> C-H Activation of <i>t</i>-Amines</b> | <b>31-83</b> |
| 2.1              | Introduction   | 32           |
| 2.2              | Background of our concept  | 34           |
| 2.3              | Results and discussion   | 35           |
| 2.3.1            | $\alpha$ $sp^3$ C-H activation reaction of <i>t</i> -amines with electron deficient alkenes                        | 35           |

|       |   |    |
|-------|---|----|
| 2.3.2 | Control experiments                           | 36 |
| 2.3.3 | Experimental set-up                           | 37 |
| 2.3.4 | Proposed reaction mechanism                   | 37 |
| 2.3.5 | Evaluation of the generality of the reactions | 39 |
| 2.3.6 | Intramolecular coupling reaction              | 41 |
| 2.4   | Summary                                       | 43 |
| 2.5   | Experimental section                          | 44 |
| 2.6   | References                                    | 55 |
| 2.7   | Spectra                                       | 57 |
| 2.8   | Single crystal structure analysis             | 80 |

|                  |  |               |
|------------------|--|---------------|
| <b>Chapter 3</b> | <b>Visible Light Photoredox Catalysis: Investigation of Distal <math>sp^3</math> C-H Activation of <i>t</i>-Amines</b> | <b>84-181</b> |
|------------------|--|---------------|

|       |   |     |
|-------|---|-----|
| 3.1   | Introduction / Background of our concept  | 85  |
| 3.2   | Earlier reports   | 86  |
| 3.2.1 | Non-photochemical approaches  | 86  |
| 3.2.2 | Photochemical approaches  | 89  |
| 3.3   | Results and discussion  | 91  |
| 3.3.1 | $\gamma$ $sp^3$ C-H activation reaction of <i>t</i> -amines with electron deficient alkenes | 91  |
| 3.3.2 | Evaluation of the generality of the reaction  | 92  |
| 3.3.3 | Proposed reaction mechanism   | 95  |
| 3.3.4 | Synthesis of acridone   | 95  |
| 3.3.5 | Intramolecular coupling reaction  | 96  |
| 3.4   | Investigation of substrate scope of this reaction for various other <i>t</i> -amines        | 97  |
| 3.4.1 | Initial results   | 97  |
| 3.4.2 | Evaluation of the generality of the reaction  | 98  |
| 3.4.3 | Proposed reaction mechanism   | 100 |
| 3.5   | Proposed rationale for different deprotonation site of <i>t</i> -amines                     | 101 |



|      |                                   |     |
|------|-----------------------------------|-----|
| 3.6  | Summary                           | 103 |
| 3.7  | Experimental section              | 104 |
| 3.8  | References                        | 121 |
| 3.9  | Spectra                           | 124 |
| 3.10 | Single crystal structure analysis | 178 |

**Publications, symposia and awards**

**Erratum**

---

## Abbreviations

|  |   |                |   |
|--|---|----------------|---|
| aq.                                    | Aqueous   | mg             | Milligram                                   |
| AcrH <sub>2</sub>                      | 10-methyl-9,10-dihydroacridine                      | MHz            | Megahertz                                   |
| Cat.                                   | Catalytic/catalyst                                  | min            | Minutes                                     |
| CH <sub>2</sub> Cl <sub>2</sub> or DCM | Dichloromethane                                     | mL             | Millilitre                                  |
| CH <sub>3</sub> CN or MeCN             | Acetonitrile  | mM             | Millimolar                                  |
| COSY                                   | Correlated Spectroscopy                             | mmol           | Millimoles                                  |
| DEPT                                   | Distortionless Enhancement by Polarization Transfer | MVK            | Methyl Vinyl Ketone                         |
| DMF                                    | <i>N,N</i> -dimethylformamide                       | MS             | Mass spectrometry                           |
| DMSO                                   | Dimethylsulfoxide                                   | MW             | Molecular weight                            |
| Et <sub>3</sub> N or TEA               | Triethylamine                                       | nm             | Nanometer                                   |
| EtOAc                                  | Ethyl acetate                                       | NMR            | Nuclear Magnetic Resonance                  |
| EtOH                                   | Ethanol   | NOESY          | Nuclear Overhauser Enhancement Spectroscopy |
| g                                      | Gram  | ORTEP          | Orthogonal Thermal Ellipsoid Plots          |
| h                                      | Hours   | Pet-ether      | Petroleum ether                             |
| Hg                                     | Mercury   | PET            | Photoinduced Electron Transfer              |
| HMBC                                   | Heteronuclear Multiple Bond Correlation             | ppm            | Parts per million                           |
| HRMS                                   | High Resolution Mass Spectrometry                   | Py             | Pyridine                                    |
| HSQC                                   | Heteronuclear Single Quantum Coherence              | R <sub>f</sub> | Retention factor                            |
| Hz                                     | Hertz   | rt             | Room temperature                            |
| IR                                     | Infra red   | THF            | Tetrahydrofuran                             |
| L                                      | Liter   | TLC            | Thin layer chromatography                   |
| LCMS                                   | Liquid Chromatography-Mass Spectrometry             | UV             | Ultraviolet                                 |
| LED                                    | Light Emitting Diode                                | μL             | Microliter                                  |
| M                                      | Molar   | μM             | Micromolar                                  |
| MeOH                                   | Methanol  |                |   |

## General Remarks

- All the solvents were purified according to literature procedure.<sup>1</sup>
- Reactions were carried out in Schlenk flask or round bottom flask under argon atmosphere, either by using HPLC grade or dry solvent.
- The irradiation was performed by using 3 W blue LED (light emitting diodes) (~455 nm) as a light source.
- Reaction progress was monitored by TLC. TLC was performed E-Merck pre-coated 60 F254 plates and the spots were visualized by using either UV light, or Iodine, phosphomolibdic acid, *o*-Anisol, KMnO<sub>4</sub> stains.
- Petroleum ether used in the experiments was of 60–80 °C boiling range.
- Column chromatographic separations were carried out by gradient elution with suitable combination of two solvents and silica gel (60–120 mesh/100–200 mesh/230–400 mesh).
- IR spectra were recorded on FTIR instrument, for solid either as nujol mull, neat in case of liquid compounds or their solution in chloroform.
- NMR spectra were recorded on Bruker AV 200 (200 MHz <sup>1</sup>H NMR and 50 MHz <sup>13</sup>C NMR), Bruker AV 300 (300 MHz <sup>1</sup>H NMR and 75 MHz <sup>13</sup>C NMR), Bruker AV 400 (400 MHz <sup>1</sup>H NMR and 100 MHz <sup>13</sup>C NMR) and Bruker DRX 500 (500 MHz <sup>1</sup>H NMR and 126 MHz <sup>13</sup>C NMR).
- <sup>1</sup>H NMR chemical shifts are reported in ppm. Proton coupling constants (J) are reported as absolute values in Hz and peak splitting as: bs, broadened; s, singlet; d, doublet; t, triplet; dd, doublet of doublet; dt, doublet of triplet; td, triplet of doublet; m, multiplet.
- <sup>13</sup>C NMR chemical shifts are reported in ppm relative to the central line of CDCl<sub>3</sub> (δ 77.0). <sup>13</sup>C peak multiplicity assignments were made based on DEPT data.
- High resolution mass spectra (HRMS) were recorded on Finnigan MRT 95, Thermo scientific Q-exactive model and Agilent Q-TOF 6530 spectrometers.
- Numbering of compounds, schemes, tables, referencing and figures for each chapter as well as abstract are independent.

-----  
1) Perrin, D. D.; Armarego, W. L. F. Purification of Laboratory Chemicals, 4<sup>th</sup> ed. Butterworth Heinemann, 1999.

## Thesis Abstract

The present dissertation is divided into three chapters.

### Chapter 1. $sp^3$ C-H Activation of *t*-Amines

This chapter starts with a brief account on the importance of C-H activation strategy in modern research interest. The C-H activation concept allows the chemists to exploit organic compounds in previously unimaginable ways resulting ultimately a revolution in synthetic methodologies for the synthesis of complex natural products and pharmaceuticals. Functionalized, nitrogen-containing heterocycles constitute a widespread structural motif in biologically active compounds and not surprisingly, efficient methods to synthesize these systems are of great significance.

Intense research activities by several research groups have resulted in the development of many useful protocols for the direct  $\alpha$   $sp^3$  C-H activation of *t*-amines. In this endeavor, initially key examples of metal mediated and metal-catalyzed processes (non-photochemical) have been referred.

Further, photoinduced electron transfer (PET) processes have been utilized to generate potentially reactive intermediates i.e. **3** or **4** (Figure 1) from *t*-amines **1** owing to their low oxidation potential. As a result many useful reactions and fascinating transformations for the direct  $\alpha$   $sp^3$  C-H activation of *t*-amines have been developed. A comprehensive detail of generation and exploitation of iminium ion (**4**) by UV and visible light PET processes and examples of  $\alpha$ -aminoalkyl radical (**3**) chemistry is delineated.

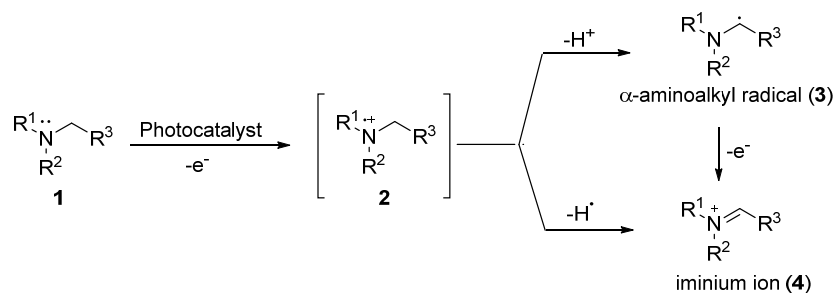
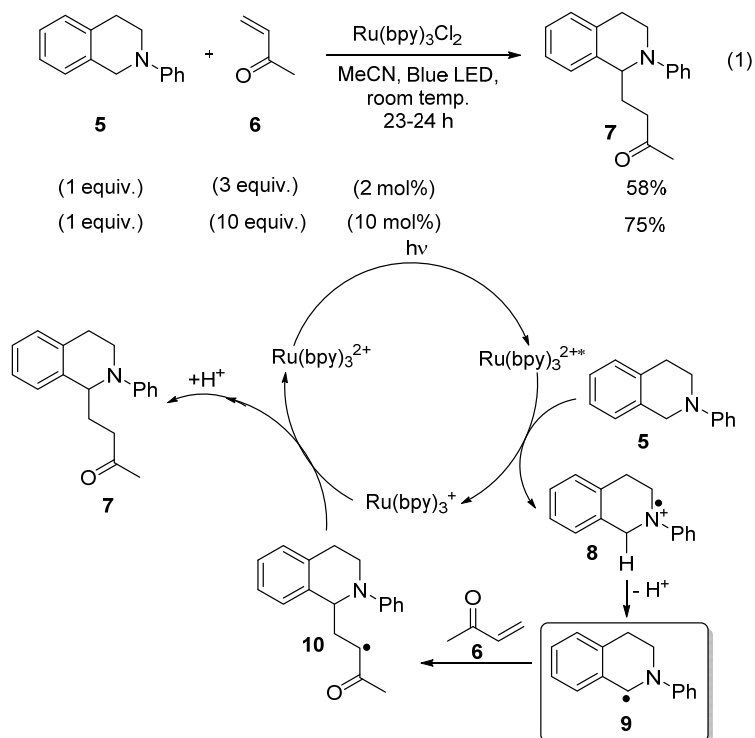


**Figure 1:** Photochemical different modes of reactivity of *t*-amines.

**Chapter 2. Visible Light Photoredox Catalysis:  $\alpha$   $sp^3$  C-H Activation of *t*-Amines**

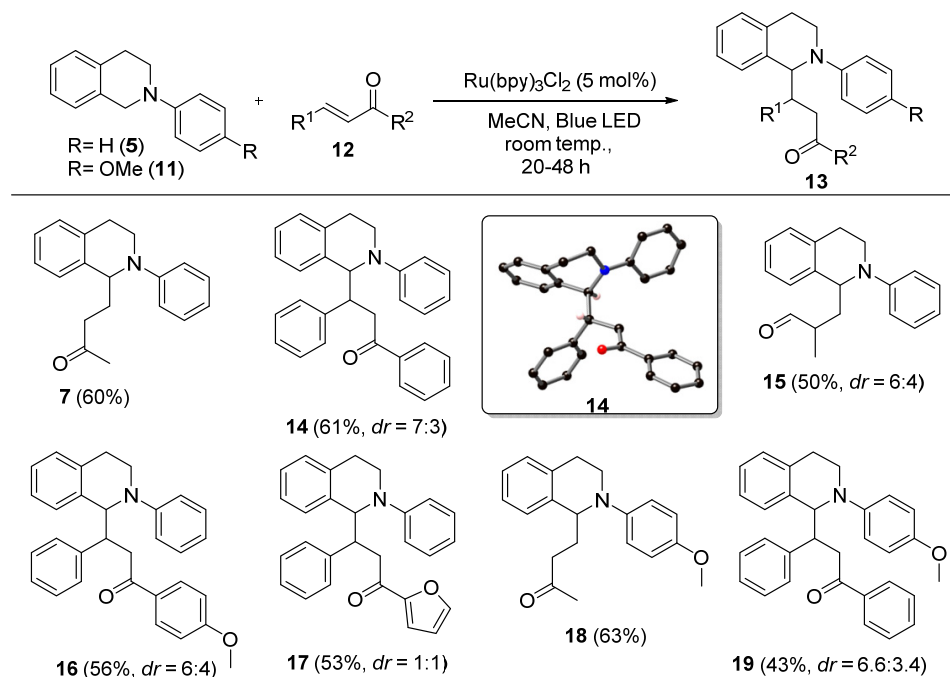
This chapter deals with the synthetic perspectives of  $\alpha$   $sp^3$  C-H activation of *N*-aryltetrahydroisoquinoline using  $Ru(bpy)_3Cl_2$  as photoredox catalyst. The resultant  $\alpha$ -aminoalkyl radical was found to add to various Michael acceptors resulting in novel C-C bond forming reaction.

The plausible reaction mechanism is shown in Scheme 1.



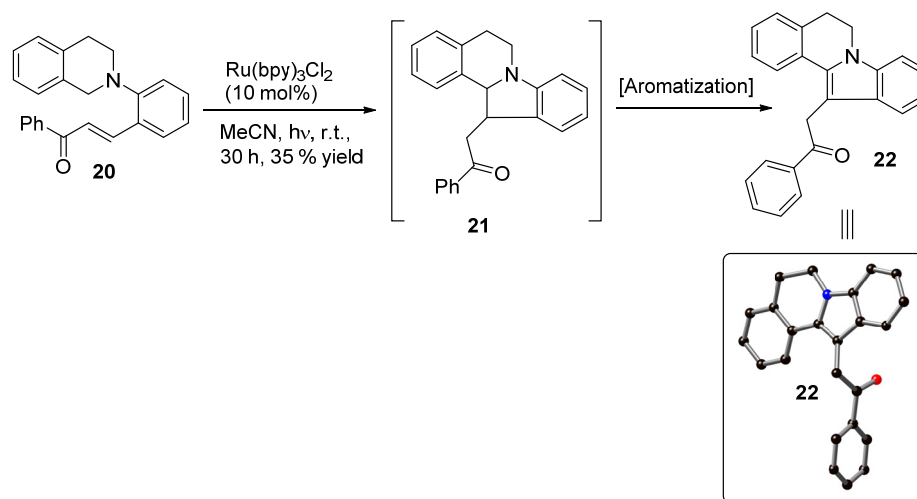
**Scheme 1:** Photoredox  $\alpha$   $sp^3$  C-H functionalization of **5** with **6**.

The generality of this mild and green approach has been evaluated and results are shown in Scheme 2.



**Scheme 2:** Photoredox  $\alpha$   $\text{sp}^3$  C-H functionalization of **5** or **11** with **12**.

Furthermore, the importance of this strategy was demonstrated by carrying out intramolecular cyclization of **20** (Scheme 3) for the synthesis of important heterocyclic scaffold (**22**), a class of framework that have been found to exhibit significant immunosuppressive activity against IL-2, IL-10, and IFN- $\gamma$ .



**Scheme 3:** Synthesis of 5,6-dihydroindolo[2,1-a]-tetrahydroisoquinoline (**22**).

### Chapter 3. Visible Light Photoredox Catalysis: Investigation of Distal $sp^3$ C-H Activation of *t*-Amines

This chapter details the investigations carried out pertaining to distal  $sp^3$  C-H activation of *t*-amines for C-C bond formation reaction, through an unprecedented, mechanistically interesting and synthetically useful one electron oxidative chemistry by visible light (Blue LED) photoredox catalysis.

It was found that, in presence of  $Ru(bpy)_3Cl_2$  catalyst, visible light (Blue LED) mediated activation of 10-methyl-9,10-dihydroacridine (**23**) with electron deficient alkenes leads to  $\gamma$   $sp^3$  C-H alkylation involving  $\gamma$ -amino alkyl radicals as an intermediate. The generality of this reaction was evaluated by studying a number of substrates as shown in Table 1.

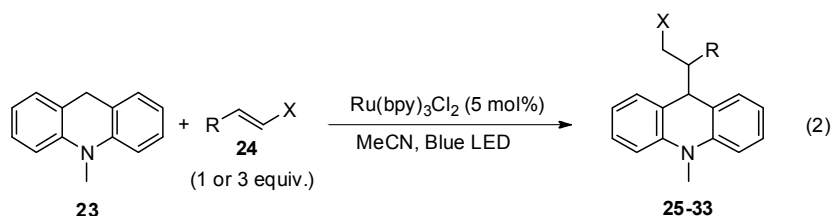


**Table 1.** Photocatalyzed  $\gamma$ - $sp^3$  C-H alkylation of **23** with electron deficient alkenes.

| Entry | Alkene ( <b>24</b> ) |                   | Equiv. | <i>t</i> [h] | Product   | Yield [%] <sup>[a]</sup> |
|-------|----------------------|-------------------|--------|--------------|-----------|--------------------------|
|       | R                    | X                 |        |              |           |                          |
| 1     | H                    | COCH <sub>3</sub> | 3      | 20           | <b>25</b> | 70                       |
| 2     | H                    | CHO               | 3      | 18           | <b>26</b> | 47                       |
| 3     | Ph                   | COCH <sub>3</sub> | 1      | 27           | <b>27</b> | 87                       |
| 4     | Ph                   | CHO               | 3      | 22           | <b>28</b> | 60                       |
| 5     | 2-Furyl              | COCH <sub>3</sub> | 1      | 27           | <b>29</b> | 41                       |
| 6     | Ph                   | COPh              | 1      | 20           | <b>30</b> | 56                       |
| 7     | Ph                   | NO <sub>2</sub>   | 1      | 21           | <b>31</b> | 40                       |
| 8     | Cyclohexenone        |                   | 3      | 21           | <b>32</b> | 58                       |
| 9     | Coumarin             |                   | 1      | 20           | <b>33</b> | 30                       |

<sup>[a]</sup> Yield based on consumption of **23** after column chromatography.

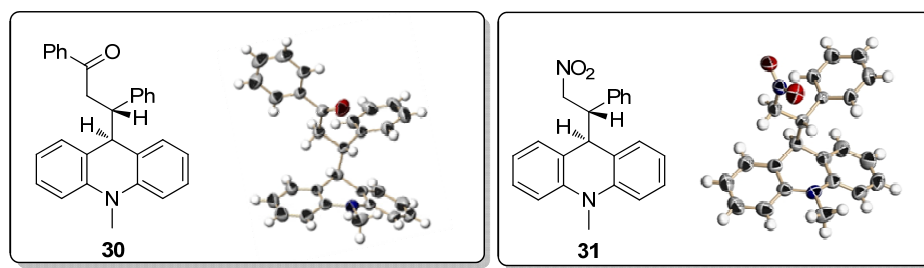


**Figure 3:** X-ray structure of **30** and **31**.

A proposed plausible reaction mechanism of this reaction is shown in Figure 4.

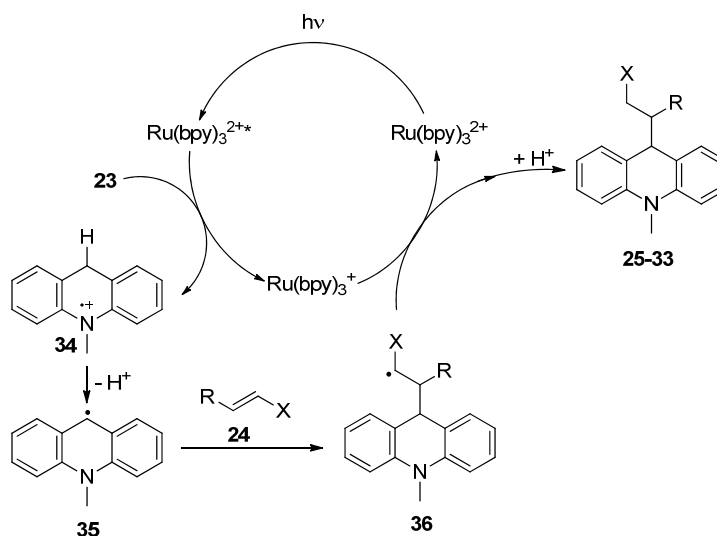
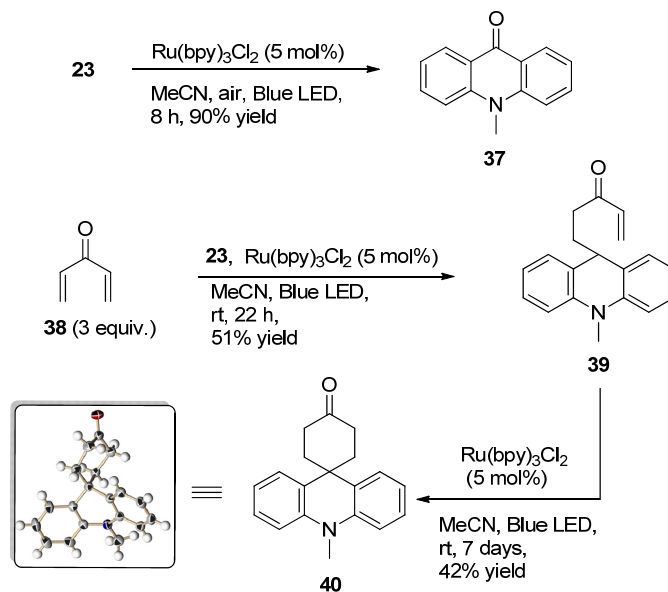


**Figure 4:** Proposed mechanism for photocatalytic  $\gamma$  C-H alkylation of **23**.

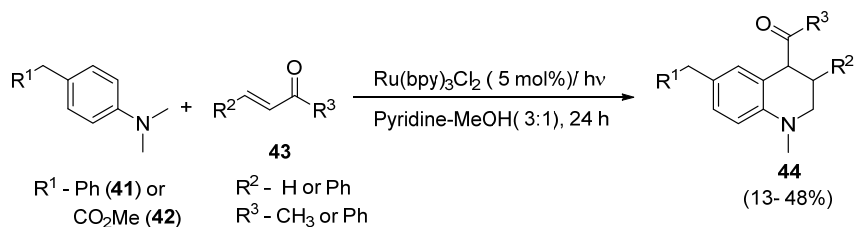
Acridone and their derivatives show a wide range of biological and pharmacological activities including anti-HIV, antiviral etc. Hence, the importance of this strategy was shown by the quantitative conversion of **23** to **37** by PET activation in presence of air without using any consumable agent (Scheme 5). Furthermore, the significance of the methodology was demonstrated by sequential photoredox catalyzed alkylation of **23** with **38** to produce challenging all carbon quaternary spirocyclic product **40** (Scheme 5).



**Scheme 5:** Various photocatalytic reactions of **23**.

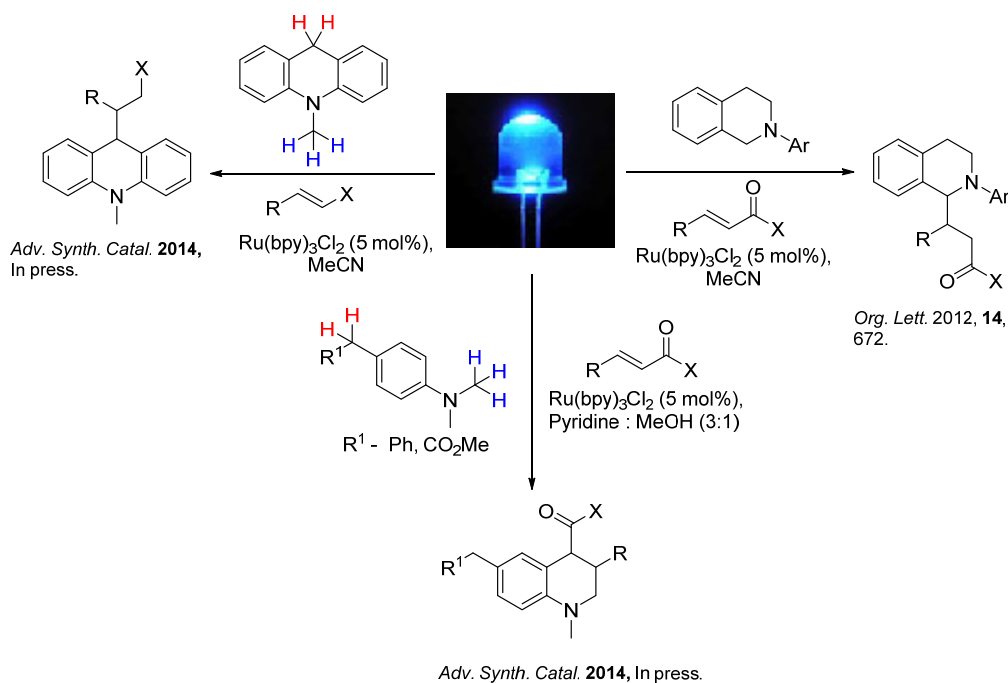


Unexpectedly, identical PET activation of 4-alkyl-*N,N*-dimethylanilines (**41** or **42**) in the presence of enones (**43**) in degassed dry pyridine-MeOH (3:1) using Ru(bpy)<sub>3</sub>Cl<sub>2</sub> (5 mol%) produced tetrahydroisoquinoline frameworks (**44**) in low to moderate yields (13-48%) through  $\alpha$  sp<sup>3</sup> C-H alkylation/ cyclization sequence (Scheme 6).



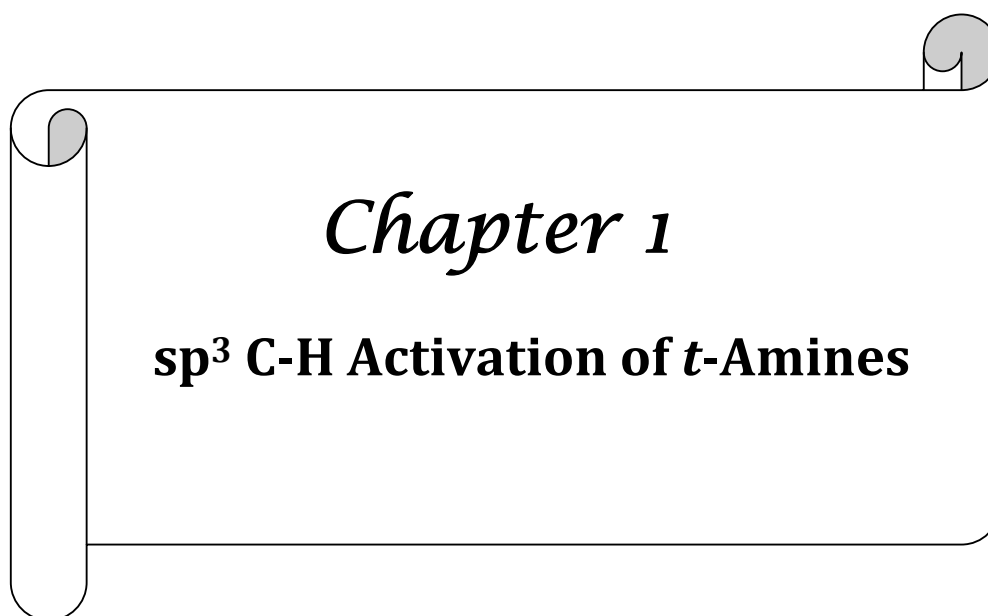
**Scheme 6:** Photocatalytic reaction of *t*-anilines (**41** or **42**) with **43**.

The overall results of this thesis are summarized with the help of Scheme 7.



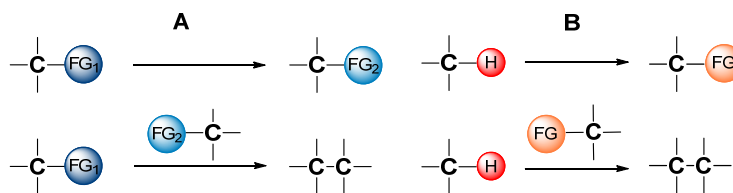
**Scheme 7:** sp<sup>3</sup> C-H functionalization of *t*-amines.

(Note: Compounds numbers in the abstract are different from those in the thesis).

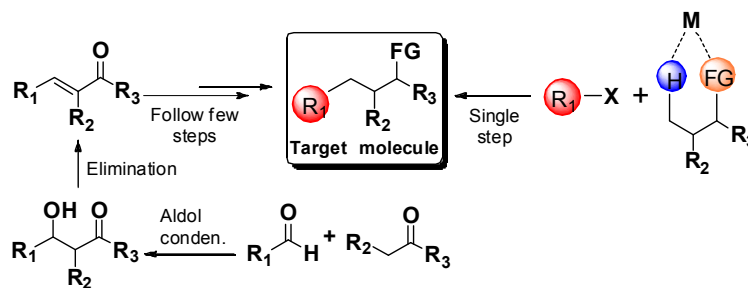


## 1.1 Introduction:

Organic synthesis depends on the functional group transformations or structural features exhibiting relatively high chemical reactivity. In traditional organic synthesis approach, the product formation is typically incorporated by means of pre-functionalized material requiring sequence of steps. However, in modern synthetic organic chemistry, direct transformation of C-H bond into product reduces needless pre-functionalization of starting materials and represents a more atom and step economy strategy (Scheme-1).<sup>1</sup> This straightforward and concise approach of C-H activation rather than sequential traditional approach is further illustrated by the synthesis of the target molecule, in a single step by displacement of the hydrogen atom (Scheme 2).<sup>1</sup>



**Scheme 1:** (A) Organic synthesis by traditional approach (B) Organic synthesis by C-H functionalization.

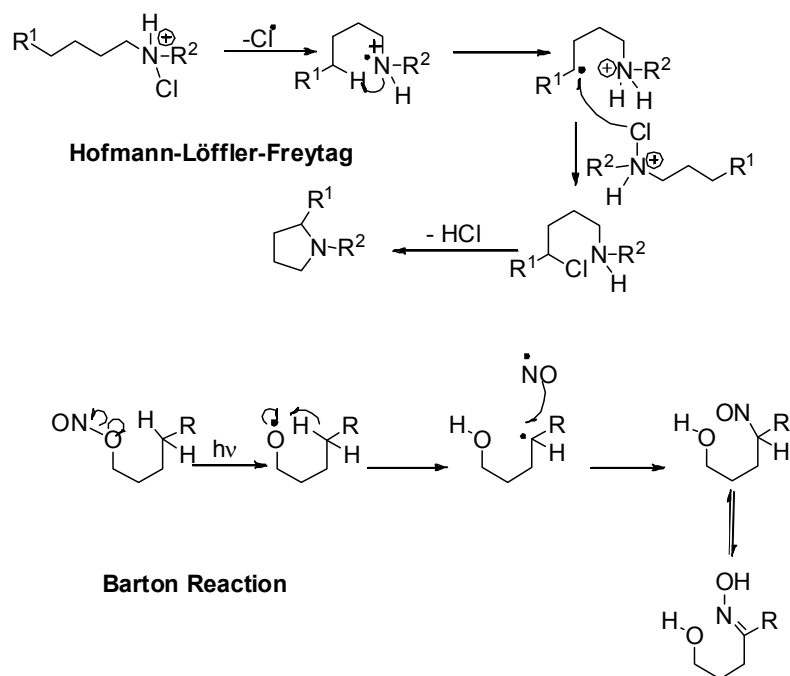


**Scheme 2:** Evolution in organic synthesis.

In general, for the term “C-H activation synonyms include C-H functionalization / C-H transformation”. In a broad sense, the term C-H activation or C-H functionalization can be defined as conversion of carbon-hydrogen bonds into carbon-carbon or carbon-heteroatom bonds. Consequently, this categorization is done on the basis of the net structural change (C-H bond to C-C / C-Y bond) engendered by the given transformation which does not necessarily categorize them on the basis of the mechanism by which they occur.<sup>2</sup>

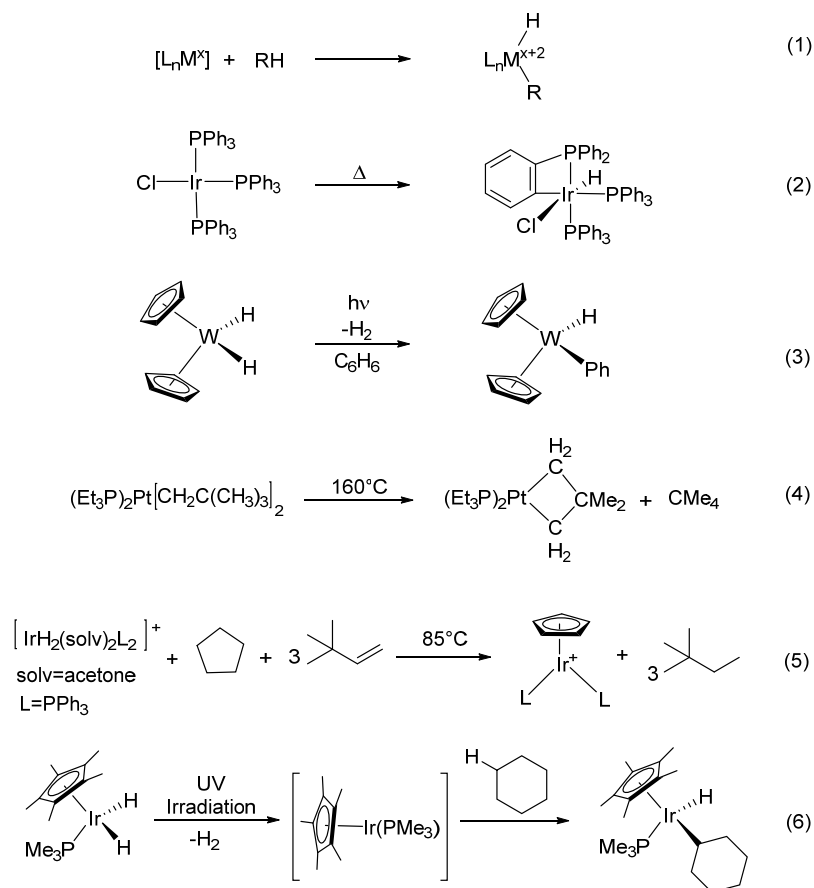
In recent past, this direct and selective replacement of inert and ubiquitous C-H bonds with new C-C or C-Y (Y=N, O) bonds is witnessing wide interest for bond breaking and bond forming processes.<sup>3</sup> Moreover, the concept of C-H bond activation allows the chemists to exploit organic compounds in previously unimaginable ways resulting ultimately a revolution in synthetic methodologies for the synthesis of complex natural products and pharmaceuticals.<sup>2,4</sup> The direct functionalization of C-H bond is associated with two fundamental challenges: 1) Reactivity - how to 'activate' single C-H bond in a molecule so that it becomes prone to chemical attack. 2) Selectivity - there is very little difference in reactivity between the various C-H bonds, therefore, targeting a specific C-H bond is difficult.<sup>3b</sup>

Historically, early approaches of selective functionalization of isolated alkyl C-H bond mostly relied on highly reactive intermediates (radical chemistry), for example, Hofmann-Löffler-Freytag<sup>5</sup> and Barton reaction<sup>6</sup> (Scheme 3). In these reactions, the critical regioselectivity was dictated by the proximity between the high energy radical species generated transiently in the reaction mixture and the C-H bond.<sup>7</sup>



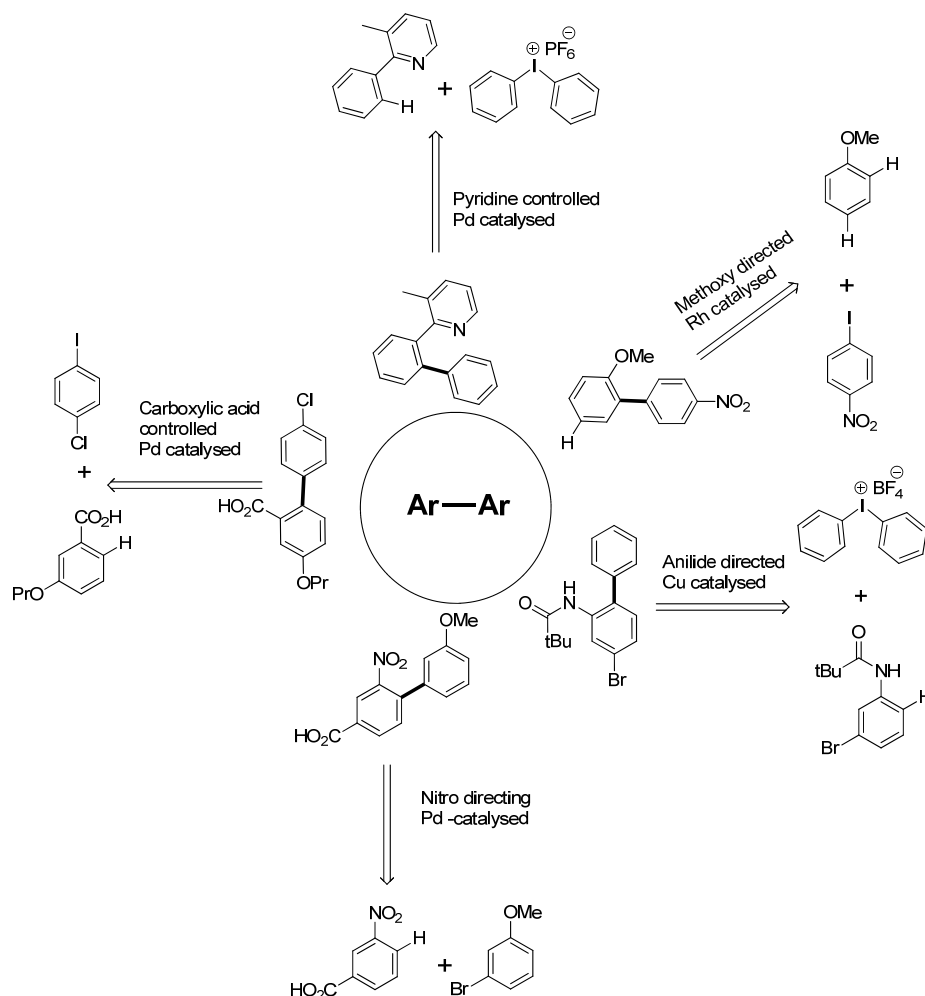
**Scheme 3:** Intramolecular radical reactions.

However, after late 1960s, a new kind of transition metal catalyzed reactions for C-H bond activation, so called oxidative addition (Scheme 4, eq. 1), where a metal from a soluble metal salt or complex insert itself between the atoms of C-H bond emerged. This strategy included both aromatic molecules (eq. 2, 3) as well as saturated hydrocarbons (eq. 4).<sup>8</sup> In addition, nearly at about the same time, it was observed that some metal complexes even catalyze alkane (generally unreactive) reactions such as hydrogen- deuterium (H-D) exchange or oxidation under relatively mild conditions.<sup>9</sup> However, in real sense this C-H activation field took off during the early 1980s, when two groups demonstrated intermolecular alkane activation<sup>10</sup> (eq. 5, 6). There afterwards, was a dramatic increase in the number of metal salts and complexes that were found to initiate direct C-H bond activation by oxidative addition. However, most of these transformations required stoichiometric amounts of the hydrocarbon and the metal salts and both partners were consumed during the reaction which limited their applications for large-scale chemical transformations, as the metals used were generally more expensive than the products.<sup>7</sup>



Scheme 4: Beginning of C-H activation.

In order to improve this chemistry, there has been an explosion of interest in developing catalytic C-H bond activation reaction by using transition metal catalysts.<sup>11</sup> In this perspective, direct  $sp^2$  C-H activation by the use of directing groups (DG), such as amides, pyridines, or acetanilides, have become the strategies of choice to allow site-selective arene functionalization<sup>12</sup> (Scheme 5).

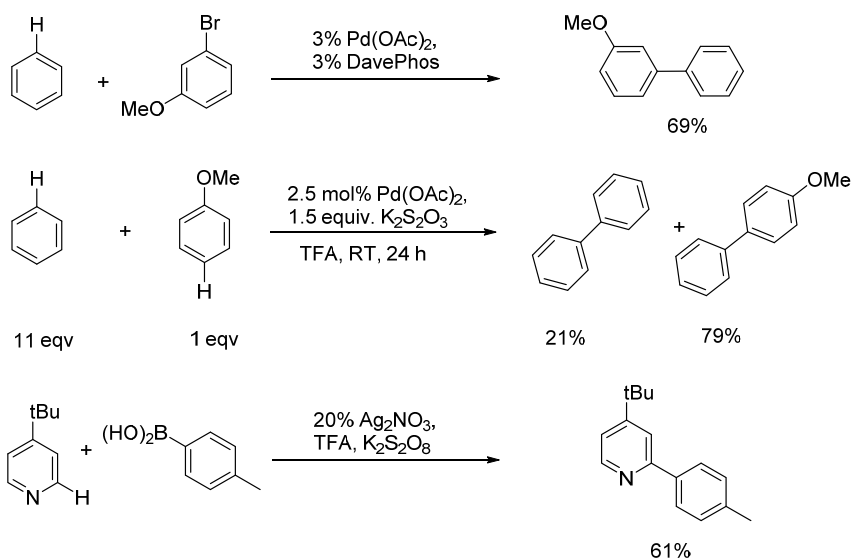


**Scheme 5:** Directed/Chelate assisted aryl C-H activation.

In these strategies, the coordination ability of the DG, brings the transition metal into close proximity of the C-H bond to be activated resulting in increased reactivity and regioselectivity owing to the higher effective concentration of the catalyst at the site of interest. However, despite these advantages, the use of DGs has certain limitations. For example, additional synthetic steps are often required to both install the DG into the starting material and to manipulate it after C-H functionalization. Besides this, in most cases, functionalization of the arenes occurs

only at the C–H bond *ortho* to the DG, thus, restricting the scope of accessible products.

Altogether, a more appealing strategy for  $sp^2$  C–H activation of benzene derivatives would be to avoid utilization of DGs. But to date, comparatively few examples of transition metal catalyzed regioselective  $sp^2$  C–H activation of benzene derivatives without the assistance of DGs have been reported. However, recent literature shows a rapidly growing interest in this class of transformation<sup>13</sup> (Scheme 6).<sup>7</sup>

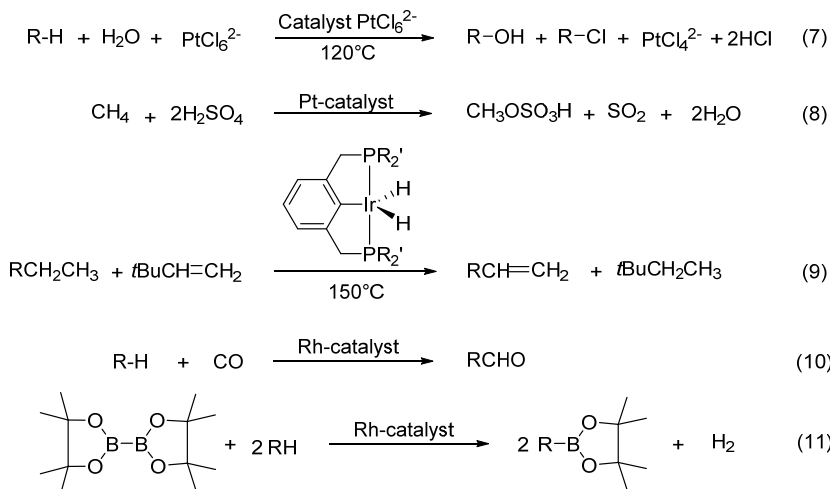


**Scheme 6:** Non-directed/Non-chelate assisted aryl C–H activation.

Although, intense research activities by several research groups have resulted in the development of useful strategies for directed/chelate-assisted and non-chelate-assisted, regioselective  $sp^2$  C–H activation through transition metal catalyses, the corresponding  $sp^3$  C–H activation is still in its infancy. The reason behind this deficiency is that most transition metal-catalyzed C–H activations involve cleavage of the C–H bond to form a C–M bond and this is generally more difficult to achieve with  $sp^3$  C–H bonds compared to  $sp^2$  C–H bond as the former are less acidic and lack proximal empty low–energy orbitals that readily interact with orbitals of the metal. Nevertheless, mechanistic insight into these fundamental processes, particularly in the development of catalysts, those are compatible with thermodynamic and economic constraints of the alkane activation lead to several promising examples in this field.

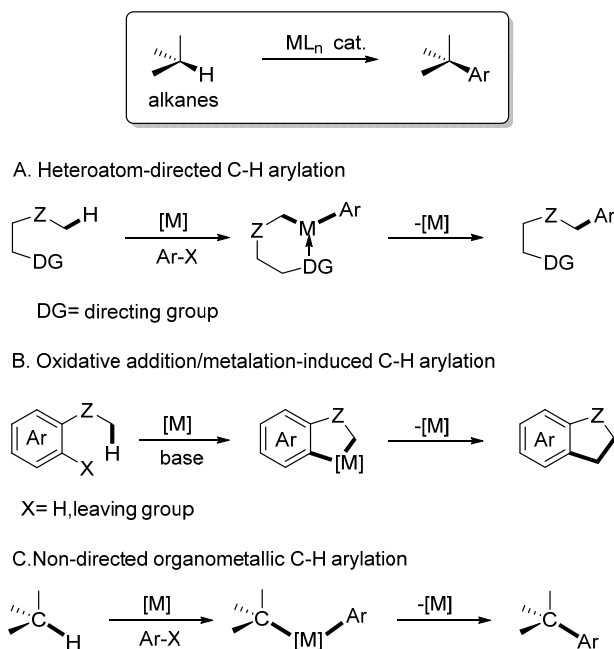
The earliest example in this area was the alkane oxidation through platinum chemistry discovered by Shilov and co-workers (Scheme 7, eq 7).<sup>11b</sup> Another

important example of alkane oxidation was the conversion of methane to methyl bisulphate by sulphuric acid catalysed by a Pt(II) complex (eq 8)<sup>14</sup> followed by several important C-H functionalization reactions of alkane such as dehydrogenation (eq 9),<sup>15</sup> carbonylation (eq 10),<sup>16</sup> borylation (eq 11)<sup>17</sup> etc.



**Scheme 7:** C-H activation of alkanes.

Furthermore, the C-H bond arylation reactions have emerged as a powerful tool for the functionalization of organic molecules that may complement or even replace traditional catalytic cross-couplings (Scheme 8).<sup>18</sup>



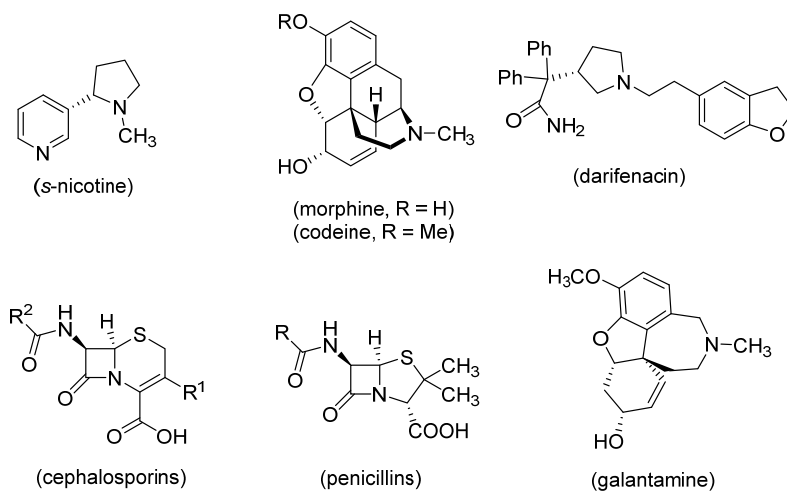
**Scheme 8:** C-H arylation reactions.



Importantly, the challenge for selective  $sp^3$  C-H bond activation in a molecule as a functional group can be surmounted by discerning the relative strength and stereo electronic properties of C-H bonds. For example, the presence of unsaturation (benzylic or allylic C-H bond) or heteroatom such as oxygen or nitrogen adjacent to  $sp^3$  C-H bonds make them “activated” owing to their lower thermodynamics strength and higher reactivity in comparison to isolated alkyl C-H bonds.<sup>19</sup> However, since this dissertation concerns with  $sp^3$  C-H activation of *t*-amines, it would be imperative to discuss first the nitrogen promoted C-H activation methodologies reported in this area to put work in proper perspectives.

## 1.2 $\alpha$ $sp^3$ C-H activation of *t*-amines:

Functionalized, nitrogen-containing heterocycles constitute a widespread structural motif in biologically active compounds (Scheme 9) and not surprisingly, efficient methods to synthesize these systems are of great significance. In this perspective, direct  $sp^3$  C-H activation in nitrogen atom containing framework is an important and



**Scheme 9:** Some biologically significant nitrogen containing compounds.

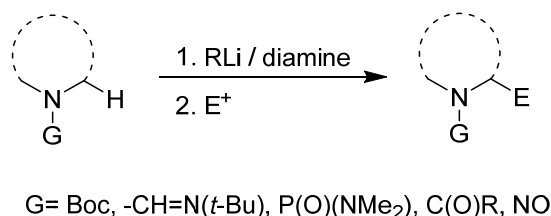
most attractive synthetic transformation for their syntheses, because it avoids long, impractical synthetic sequence. At the outset, few selected key examples of direct  $\alpha$   $sp^3$  C-H functionalization of nitrogen-containing heterocycles via non-photochemical (metal mediated and metal-catalyzed processes) and photochemical approaches are enlightened, which is meant to serve as a foundation for further exploration into this rapidly developing area of research.<sup>20</sup>

### 1.3 $\alpha$ $sp^3$ C-H activation of *t*-amines: Non-photochemical approaches

Activation of  $sp^3$  C-H bonds adjacent to nitrogen heterocycles is an attractive transformation in organic synthesis. In this endeavor, extensive research activities by several research groups have resulted in the development of many useful protocols for the direct  $\alpha$   $sp^3$  C-H functionalization of *t*-amines due to astonishing ability of nitrogen containing heterocycles to act either as nucleophile or electrophile under appropriate conditions.<sup>20</sup> Moreover, these non-photochemical  $\alpha$   $sp^3$  C-H functionalization reactions of *t*-amines can be broadly classified, according to the *in situ* formed:  $\alpha$ -amino anion, transition metal catalyzed,  $\alpha$ -amino alkyl radical and iminium cation intermediates.<sup>20</sup>

#### 1.3.1 $\alpha$ C-H functionalization of *t*-amines by $\alpha$ -lithiation reaction with alkyllithium/diamine:

Historically, one of the oldest reported methods for the direct functionalization of nitrogen-containing heterocycles is  $\alpha$ -lithiation with alkyllithium/diamine complexes (producing a dipole stabilized carbanion) followed by electrophilic substitution. The common dipole stabilizing group, including *tert*-butyl carbamate, formadine, amide, phosphoramidate, oxazoline, and nitroso functionalities are effective for the  $\alpha$ -lithiation of *t*-amines.<sup>20a</sup> This general methodology is depicted in Scheme 10 and has been extensively reviewed for achiral<sup>21</sup> as well as chiral<sup>22</sup> C-H functionalization of *t*-amines.



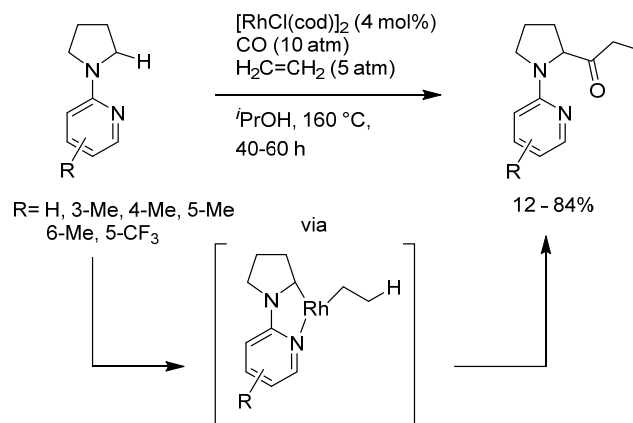
**Scheme 10:**  $\alpha$ -lithiation of *t*-amines.

#### 1.3.2 Transition metal-catalyzed $\alpha$ C-H activation of *t*-amines:

Although  $\alpha$ -lithiations of *t*-amines showed high reactivity and efficiency for their  $sp^3$  C-H activation, they all employed stoichiometric amounts of air and moisture sensitive alkyllithium reagents, further leading to the limitations for active groups

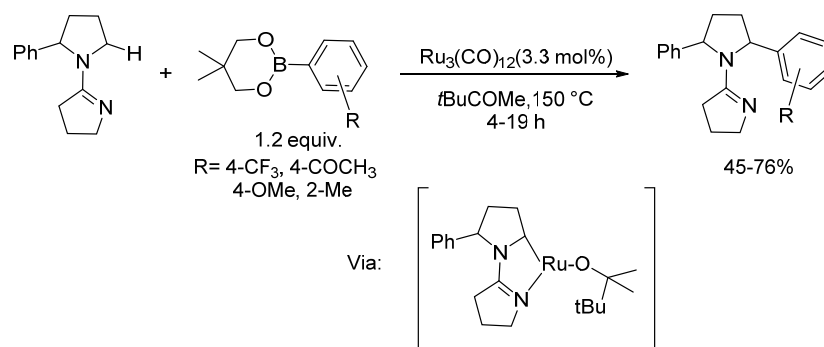
already present in the substrate. In order to solve these problems, transition metal catalyzed methodologies have been exploited for  $\alpha$   $sp^3$  C-H activation of *t*-amines.

Murai and co-workers in 2000, reported a pyridine-directed  $\alpha$   $sp^3$  C-H bond propionylation of the *t*-amines using rhodium complex  $[\text{RhCl}(\text{cod})]_2$  as a catalyst (Scheme 11).<sup>23</sup> The reaction was slow (40–60 h) and required rather harsh reaction conditions (160 °C, 10 atm CO, 5 atm ethylene), affording the desired ketone in 12 to 84 % yield depending on the nature of the pyridine substituents. Mechanistically, this reaction presumably involved a pyridine-directed C-H activation at the pyrrolidine ring to give alkyl Rh complex, subsequent ethylene insertion into the hydride–rhodium bond followed by CO insertion and reductive elimination.



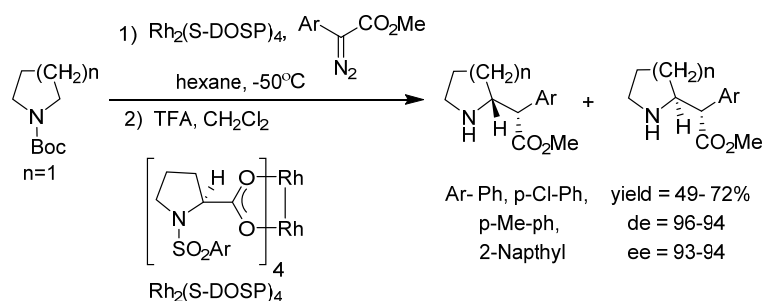
**Scheme 11:** Rh-catalyzed  $\alpha$   $sp^3$  C-H bond propionylation of *t*-amines.

Sames and co-workers reported  $\alpha$   $sp^3$  C-H arylation of tertiary amines with arylboronates in the presence of an amidine protecting group using  $\text{Ru}_3(\text{CO})_{12}$  catalyst (Scheme 12).<sup>24</sup> This catalytic method was compatible with a variety of arene donors containing both electron-donating and electron-withdrawing substituents. The proposed mechanism was nitrogen-directed C-H activation to generate a ruthenium hydride intermediate that was trapped by ketone followed by transmetalation with the arylboronate and reductive elimination to afford the coupling product.



**Scheme 12:**  $\text{Ru}_3(\text{CO})_{12}$ -catalyzed  $\alpha$   $\text{sp}^3$  C-H arylation of *t*-amines.

Another transition-metal-catalyzed approach, for the functionalization of *t*-amines involved metal carbene insertion into their  $\alpha$   $\text{sp}^3$  C-H bonds. In this context, as one of the most exceptional examples, Davies and co-workers reported the highly regio-, diastereo-, and enantioselective C-H insertion reactions of N-Boc-protected cyclic amines with methyl aryldiazoacetates, catalysed by the rhodium prolinato  $\text{Rh}_2(\text{S-DOSP})_4$  complex (Scheme 13).<sup>25</sup>

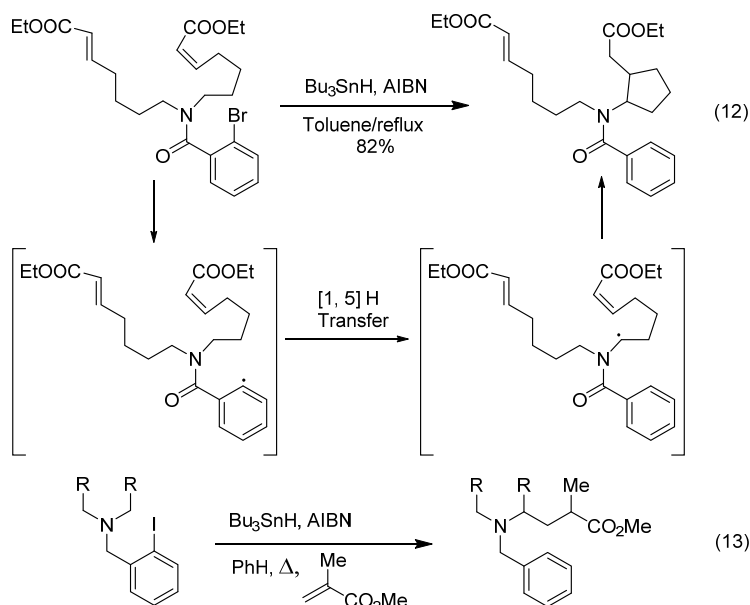


**Scheme 13:** Rh-catalyzed C-H insertion of Boc-protected cyclic amines.

### 1.3.3 $\alpha$ -aminoalkyl radical based C-H functionalization of *t*-amines:

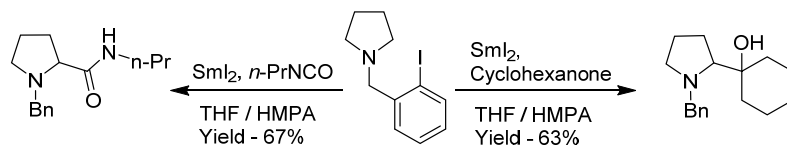
Several approaches have been reported for  $\alpha$   $\text{sp}^3$  C-H functionalizations of *t*-amines via the generation of  $\alpha$  aminoalkyl radical intermediates.<sup>20</sup>

Curran and Snieckus disclosed that radicals generated from ortho-halobenzamides by using  $\text{Bu}_3\text{SnH}/\text{AIBN}$  undergo a 1,5-hydrogen atom transfer producing an  $\alpha$ -aminoalkyl radical which could be subsequently inter or intramolecularly coupled to electrophiles, such as methyl or ethyl acrylate (Scheme 14, eq. 12).<sup>26</sup> Undheim and co-workers applied similar approach to *o*-iodo-benzyl-protected amine heterocycles, in generation and subsequent intermolecular addition of  $\alpha$ -aminoalkyl radical to methyl methacrylate electrophile (eq. 13)<sup>27</sup>.



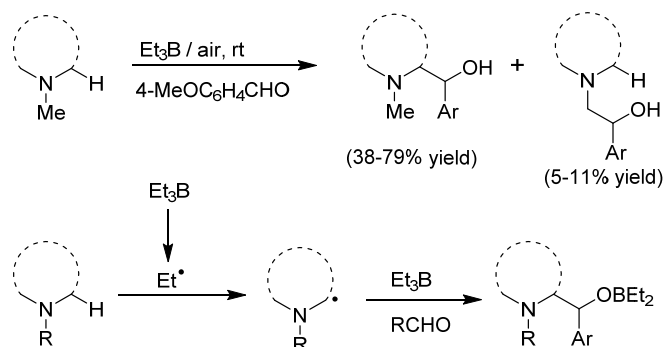
**Scheme 14:** Radical alkylation of  $\alpha$  C-H bond of *t*-amines.

Ito and co-workers have developed a process for  $\alpha$  C-H functionalization of nitrogen heterocycles by employing samarium diiodide as a reducing agent. In this reaction, authors proposed deiodination reaction by  $\text{SmI}_2$  to provide aryl radical, which undergoes 1,5-hydrogen atom translocation to generate  $\alpha$ -aminoalkyl radical. Single electron transfer by  $\text{SmI}_2$  to  $\alpha$ -aminoalkyl radical affords  $\alpha$ -aminoorganosamarium anion, which subsequently adds to a variety of electrophiles, such as, enolizable ketones, isocyanates, and isocyanides to deliver the addition product in good yield (Scheme 15).<sup>28</sup>



**Scheme 15:** Samarium-mediated  $\alpha$  C-H functionalization of *t*-amines.

Yoshimitsu and Nagaoka reported the radical hydroxyalkylation of  $\alpha$   $\text{sp}^3$  C-H bond of *t*-amines via intermediacy of  $\alpha$ -aminoalkyl radicals by using  $\text{Et}_3\text{B}/\text{air}$ . They proposed that an ethyl radical generated from  $\text{Et}_3\text{B}/\text{air}$  abstracts  $\alpha$ -hydrogen of *t*-amines to produce  $\alpha$ -aminoalkyl radical which further undergoes irreversible addition to aldehyde (Scheme 16).<sup>29</sup>



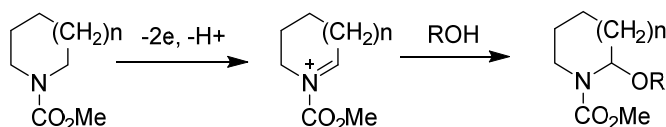
**Scheme 16:** Radical hydroxyalkylation of  $\alpha$  C-H bond of *t*-amines.

### 1.3.4 Iminium ion based $\alpha$ C-H functionalization of *t*-amines:

Various oxidative methods have been reported for  $\alpha$  C-H functionalization of *t*-amines via the generation of an iminium ion intermediate (an electrophilic species) that can be coupled with nucleophilic partner. The scope of applicable nucleophilic coupling partners is quite broad and their use is often referred to as variations of well-known name reactions, such as the oxidative aza-Henry reaction or the oxidative Mannich reaction or the oxidative Stecker reaction. The wide range of possible oxidation methods for the generation of an iminium ion intermediate represents a convenient mean to classify these C-H functionalization reactions.<sup>20</sup>

#### I) Electrochemical oxidation:

One of the earliest methods disclosed by Shono co-workers utilized anodic oxidation of cyclic amines to deliver the corresponding  $\alpha$ -aminals in good yield (Scheme 17).<sup>30</sup> The proposed reaction mechanism involved oxidation of *t*-amine to N-acyliminium



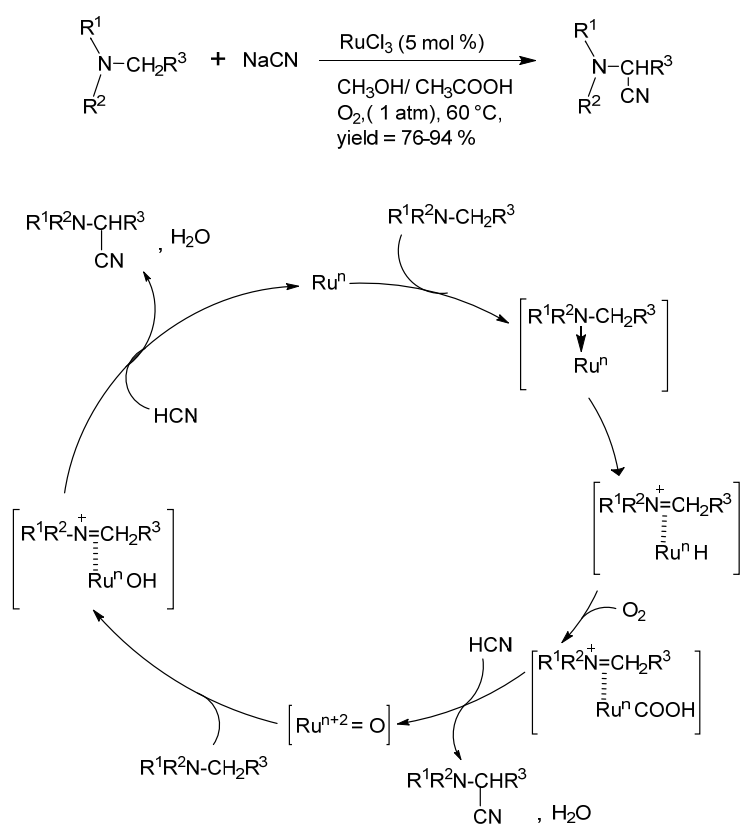
**Scheme 17:** Electrochemical oxidation of *t*-amines.

ion and its subsequent trapping with alcohol. The most common application of this methodology was utilized towards the practical synthesis of 2-alkoxy-N-heterocycles which are well-established stable precursors to N-acyliminium ions and valuable synthons in organic chemistry. Recently Yoshida and co-workers have reported the

expanded scope of N-acyliminium ion reactions with various nucleophilic species by “cation-pool” methods.<sup>31</sup>

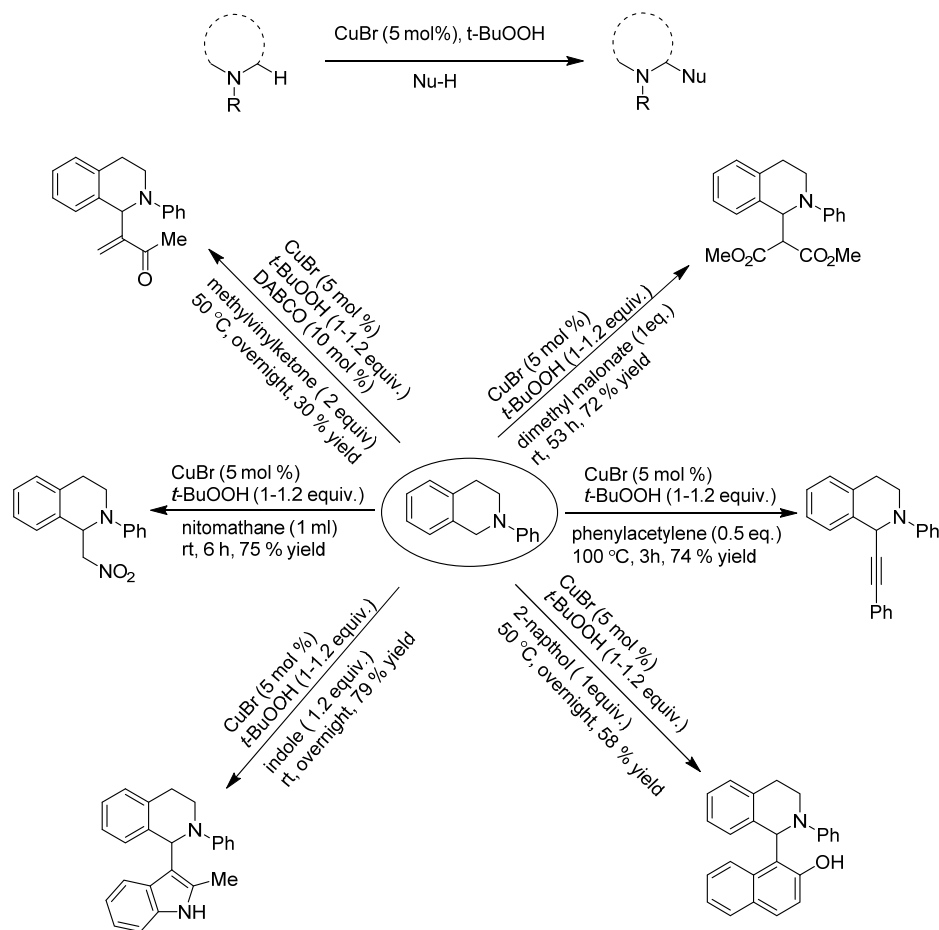
## II) Transition metal catalyzed oxidation:

In one of the earliest examples of transition metal catalyzed selective C–H bond functionalization of *t*-amines for C–C bond formation reaction, Murahashi and co-workers reported an oxidative cyanation of tertiary amines by using RuCl<sub>3</sub> as the catalyst and oxygen as the stoichiometric oxidant (Scheme 18). The products of these reactions i.e.  $\alpha$ -aminonitriles are useful for the synthesis of  $\alpha$ -amino acids and 1, 2-diamines. The proposed reaction mechanism of this reaction is shown in Scheme 18.<sup>32</sup>



**Scheme 18:** Aerobic Ru-catalyzed oxidative cyanation of *t*-amines.

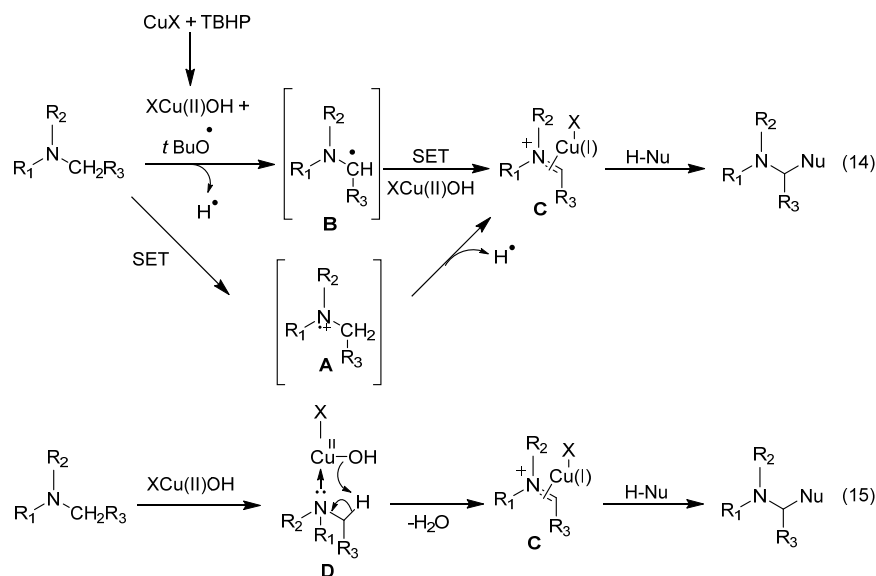
Li and co-workers broadened the scope of this oxidative C-H functionalization of *t*-amines through cross-dehydrogenative coupling (CDC) reactions<sup>19a,19c,33</sup> (in which none of the coupling components required prior functionalization) by utilization of copper catalysts. Using their Cu-catalyzed oxidative approach, they have been able to introduce many different functional groups into the  $\alpha$ -position of cyclic *t*-amines by using a vast array of reagents [(pro)nucleophilic coupling partners], such as alkynes,<sup>33a</sup> malonates and malononitrile,<sup>33b</sup> nitroalkanes,<sup>33c</sup> indoles,<sup>33d</sup> 2-naphthols and electron deficient alkenes<sup>33e</sup> (Scheme 19).



**Scheme 19:** Cu-catalyzed cross dehydrogenative coupling of *t*-amines.

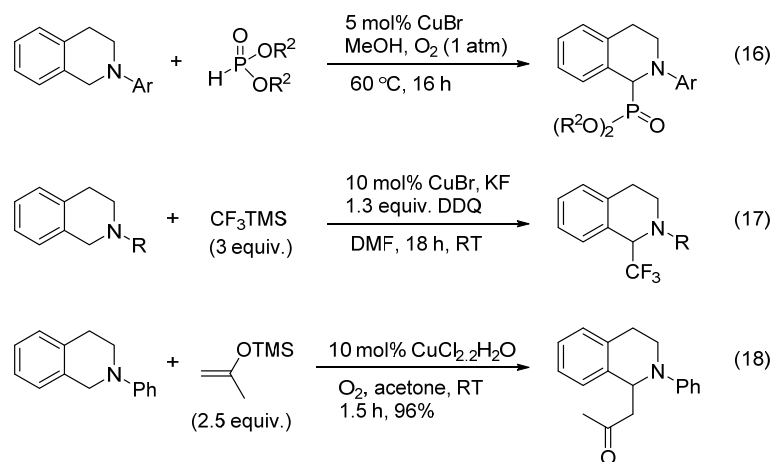
Based on the literature reports of the oxidation of *t*-amines to iminium species, authors proposed two possible CDC mechanisms: either a radical mechanism (eq 14) or an ionic mechanism (eq 15), as shown in Scheme 20.





**Scheme 20:** Proposed mechanism for CDC reactions of *t*-amines.

In recent past, a large number of reports have emerged on the oxidative Cu-catalyzed  $\alpha$ -functionalization of cyclic tertiary amines via trapping of the iminium ion intermediate by a variety of nucleophiles. For example, Basle and Li have reported a method for the coupling of *N*-aryltetrahydroisoquinolines and dialkyl phosphonates to yield biologically significant  $\alpha$ -aminophosphonates [Scheme 21, eq. (16)].<sup>34</sup> Li and Mitsudera described a highly efficient Cu-catalyzed protocol for the  $\alpha$ -trifluoromethylation of tetrahydroisoquinoline substrates using  $\text{CF}_3\text{TMS}$  as fluorine containing nucleophilic partner [eq. (17)].<sup>35</sup> Klussman and co-workers reported the introduction of 2-oxoalkyl functionality into the  $\alpha$ -position of tertiary amines to produce  $\beta$ -aminoketone derivatives [eq. (18)].<sup>36</sup>



**Scheme 21:** Oxidative Cu-catalyzed coupling of *t*-amines.

In transition metal catalyzed oxidative  $\alpha$  C-H functionalization reactions of cyclic tertiary amines, apart from broadening the scope of nucleophilic partners, substantial efforts have been made to develop methods that keep environmental concerns in mind. The use of oxygen as oxidant [as mentioned in above reactions (eq. 16, 18)] is becoming increasingly popular in this regard, not just as an environmentally benign reagent, but as one that is also safe and convenient. Further, efforts to achieve oxidative  $\alpha$ -functionalization of cyclic tertiary amines have by no means been limited to ruthenium and copper catalysis. Besides Ru and Cu, several methods using Fe, V, Au, Rh etc catalysis have also been developed, and comprehensively reviewed.<sup>20b</sup>

### 1.4 $\alpha$ sp<sup>3</sup> C-H activation of *t*-amines: Photochemical approaches

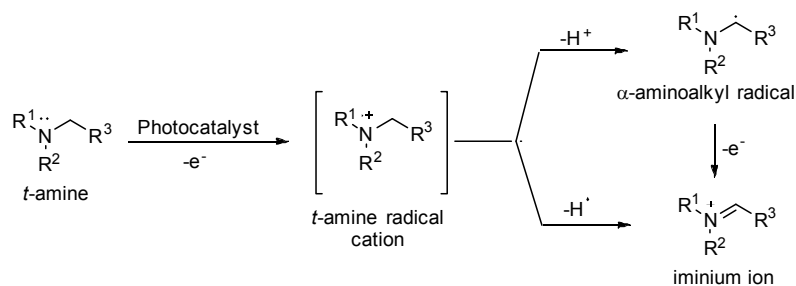
#### 1.4.1 Background:

In synthetic organic chemistry, a long term desire of organic chemists is to induce chemical transformations under mild and green condition using light as a reagent. After absorbing light, molecules reach to an electronically excited state. As a result, the distribution of electrons in the molecules is significantly different at these states as compared to their ground state. The chemical properties and more particularly the reactivity of molecules also change, and the reaction spectrum of a family of compounds is considerably broadened. Consequently, many useful reactions and fascinating transformations have been done using UV or visible light irradiation.<sup>37</sup>

Owing to low oxidation potential, tertiary amines act as potent electron donors in photoinduced electron transfer (PET) processes and generates potentially reactive intermediates i.e. amine radical cations. Single electron transfer (SET) occurs at near diffusion controlled rates from amines to acceptors which have excited state potentials that are higher than the oxidation potential of amines. Generally, in order to perform the PET reactions of *t*-amines via its single electron transfer (SET) oxidative pathway, three common methods have been used. These include (1) SET to the excited state of acceptors, which participate as substrate in photochemical reactions with amine (e.g.  $\alpha,\beta$ -unsaturated ketones); (2) SET to the excited-state acceptors, which serves as photocatalyst (e.g. Ru(II) complexes) or photosensitizers (e.g. cyanoarenes) for photochemical reactions occurring between amines and other substrates; and (3) SET

to preformed radical cations. The former two methods lead to direct formation of contact ion radical pairs (CIRP) or solvent separated ion radical pairs (SSIRP), whose lifetimes and behaviour depends on the polarity of the medium. Polar solvents facilitate cage escape of the ion radicals, leading to generation of fully solvated free ion radical intermediates, providing the basis for the development of many new and useful organic synthetic conversions.<sup>38</sup>

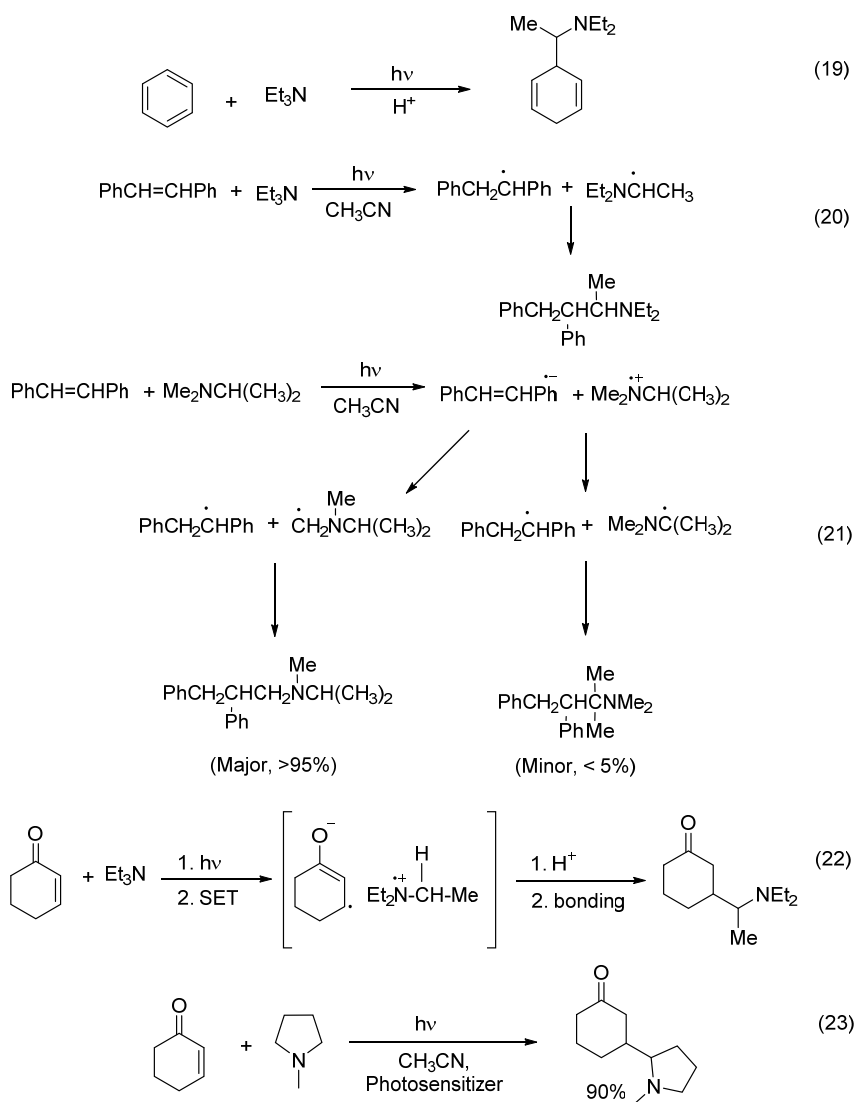
However, similar to most of the organic compounds, *t*-amines also do not absorb UV/visible light efficiently, unless they have a chromophore (e.g. highly conjugated  $\pi$ -bond systems). Hence, to initialize photoinduced electron transfer (PET) reactions of *t*-amines, a photocatalyst or photosensitizer is often required. Owing to the well defined differences in redox potentials, the single electron transfer (SET) occurs from *t*-amine to excited state of photocatalyst / photosensitizer producing planar amine radical cation (Figure 1), which in polar solvents, subject to kinetic acidity and stereoelectronic factors, undergo facile  $\alpha$ -deprotonation to produce  $\alpha$ -aminoalkyl radical (mainly due to stabilization of this  $\alpha$ -position radical by orbital overlap with the filled orbital on nitrogen). The rate of *t*-amine radical cation  $\alpha$ -deprotonation has been measured experimentally by several research groups.<sup>39</sup> Depending on the reaction conditions, the generated  $\alpha$ -aminoalkyl radical could either react as a nucleophile with a suitable substrate or could undergo further one-electron oxidation due to its reduced ionization potential to form iminium ion, thus serving as an electrophile. In literature in some cases, the second mode of reaction involves hydrogen abstraction from *t*-amine radical cation to produce iminium ion when a good hydrogen atom acceptors are present in the reaction.



**Figure 1:** Photochemical different modes of reactivity of *t*-amine radical cations.

1.4.2 UV photochemistry for  $\alpha$ -sp<sup>3</sup> C-H activation of *t*-amines:

Earlier, in the context of  $\alpha$ -sp<sup>3</sup> C-H functionalization of *t*-amines, our group<sup>40</sup> and others<sup>41</sup> have extensively reported the chemistry from both  $\alpha$ -aminoalkyl radical and iminium ion intermediates (Figure 1), via oxidative photoinduced electron transfer (PET) processes, mainly utilizing electron deficient aromatics as light absorbing electron acceptors. The product formation from PET reactions is dependant, among many other parameters, on the redox potentials of the donor-acceptor pairs and the solvent polarity and therefore, change in any one of these parameters has a significant influence on the reaction dynamics of the radical reactions.

Scheme 22: Photochemical coupling reactions of *t*-amines.

For example *t*-amine radical cations, produced from an excited arene-amine pair, are known to undergo  $H^+$  transfer from the  $\alpha$ -C-H bond to the geminal ion radical within the solvent cage, resulting in an arene-amine adduct through coupling of the resultant radical species (Scheme 22, eq. 19).<sup>42</sup> Further detailed mechanistic studies by Lewis and co-workers<sup>39a-b, 43</sup> of stilbene-amine photoaddition reactions have suggested predictive capabilities for the regioselectivity of unsymmetrical amine photoadditions (eq. 20, 21). Mariano and co-workers<sup>44</sup> reported the examples of direct photoaddition reactions between *t*-amine and enone via intermediacy of  $\alpha$ -amino alkyl radical (eq. 22). Much later, instead of direct irradiation, Hoffmann and co-workers<sup>45</sup> reported the similar type of coupling reaction between *t*-amine and enone by utilizing various photosensitizers (eq. 23).

However, in sharp contrast, it was reported that photoreaction<sup>46</sup> between cyanoarene, a potent electron acceptor, and *t*-amine in acetonitrile gives the addition product of acetonitrile to cyanoarene instead of amine, possibly due to the involvement of longer lived solvent separated ion pairs (SSIP) in these particular systems.<sup>40c,40g</sup> This difference in the reactivity pattern of the excited singlet cyanoarene with *t*-amines,<sup>46</sup> earlier led our group to explore further this fundamental reaction processes. It was argued that the SSIP formed between 1,4-dicyanonaphthalene (DCN) and *t*-amine after initial one electron exchange, in a solvent of high dielectric constant, would dissociate into free radical ion pair (FRIP) where the cyanoarene anion radical would be potentially less reactive towards the amino cation radical. Indeed, previously, our group observed that predominant deprotonation from these amino cation radicals in aqueous solvent results an  $\alpha$ -amino radical and molecular oxygen dissolved in the solvent would quench the cyanoarene anion radical to its original ground state, possibly making it available for a second oxidation step from  $\alpha$ -amino radical similar to the electrolytic oxidation of amines as shown in Figure 2.<sup>40c, 40g</sup>

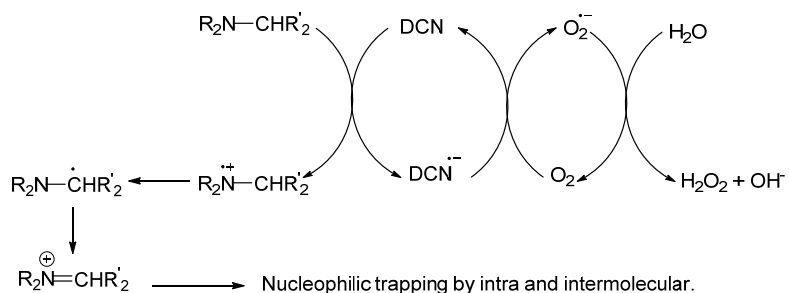
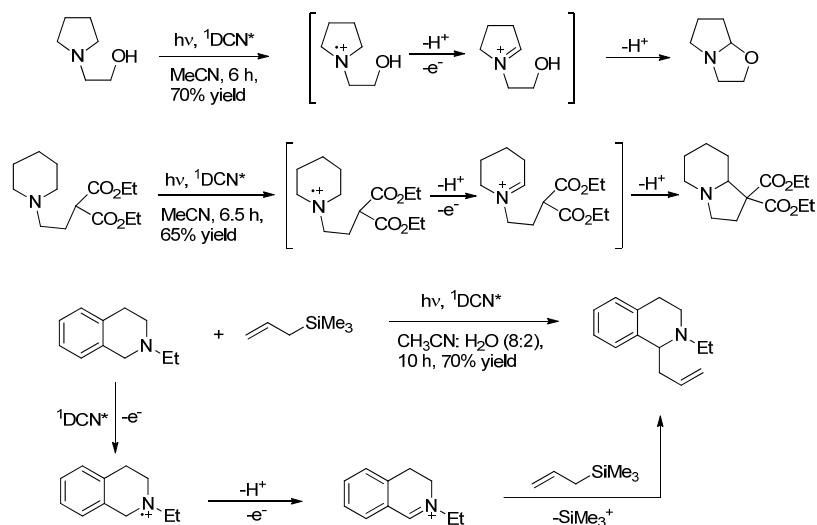


**Figure 2:** Our group's earlier approach for photochemical oxidation of *t*-amines.

In this manner, as one of the pioneering studies, our group reported  $sp^3$  C–H activation of *t*-amines via PET oxidation of tertiary amines by sequential electron-proton-electron (E-P-E) loss to generate iminium ion. The resultant iminium ion was *in situ* trapped both intra- as well as inter-molecularly by a variety of nucleophiles (Scheme 23).<sup>40</sup>



**Scheme 23:** PET Oxidative coupling of *t*-amines.

### 1.4.3 Visible light photoredox catalysis for $\alpha$ $sp^3$ C–H activation of *t*-amines:

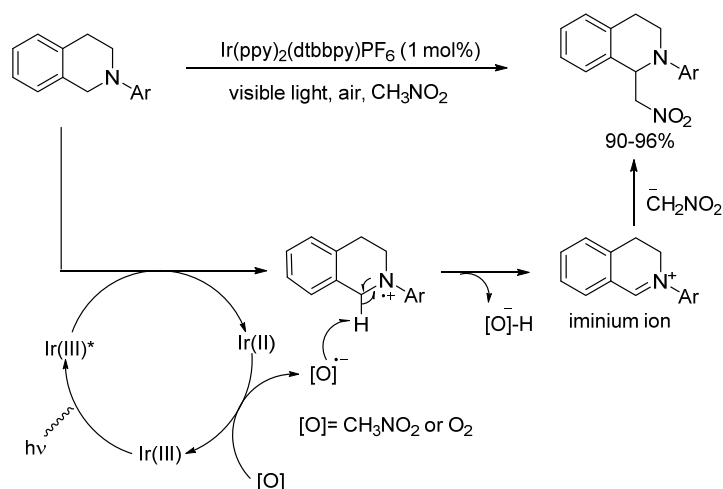
Since early of 20<sup>th</sup> century, chemical transformation induced by the use of visible light photochemistry and photocatalysis [via photoinduced electron-transfer (PET)] have been attracting attention of chemists.<sup>47</sup> However, the inability of most of the organic molecules to absorb visible light has limited the number of applications. In view of the fact that utilizing visible light absorbing photocatalyst and employing their electron/energy transfer process to sensitize organic molecules to carry out required photochemical reactions would serve as a valuable tool for overcoming this inadequacy.<sup>48</sup> This solution was inspired by research efforts to mimic nature's photosynthetic ability through the development of highly tunable photoredox catalyst. The underlying premise of this strategy is that solar energy from the visible light (about 46% in the solar spectrum reaching on earth) can be harnessed to chemical energy through the action of photoredox catalyst. Most commonly employed visible light photocatalysts are transition metal Ru(II) or Ir (III) polypyridine complexes, pigments and dyes e.g. methylene blue, Eosin Y, Rose Bengal.

Nevertheless, until the beginning of the 21<sup>st</sup> century, these visible light photoredox catalysts had been only sporadically employed in the area of organic synthesis.

A single electron oxidative chemistry of *t*-amines, generating the amine radical cation intermediates are of great utility in amine syntheses. As discussed earlier, this single electron oxidation process of *t*-amines has been attained by using electrochemistry, chemical oxidants, metal catalyzed oxidation, and UV light mediated photochemistry. However recently, visible light mediated photoredox catalyzed approach has become major focus in amine synthesis. The enthusiasm surrounding this approach is driven not only by its green transformation (i.e. using visible light as a reagent) but also by its unique ability to achieve unconventional bond formation.<sup>49,50</sup>

In early studies of  $\alpha$ -sp<sup>3</sup> C-H functionalization of *t*-amines by visible light photoredox catalysis, Whitten and co-workers<sup>51</sup> reported that irradiation of triethylamine with Ru (II) complexes produced iminium ion via initially produced amine radical cation which ultimately gave acetaldehyde, presumably formed by the hydrolysis of corresponding iminium ion. It is surprising to note that until 2010 such analogous research has been scarcely reported under visible light irradiation.

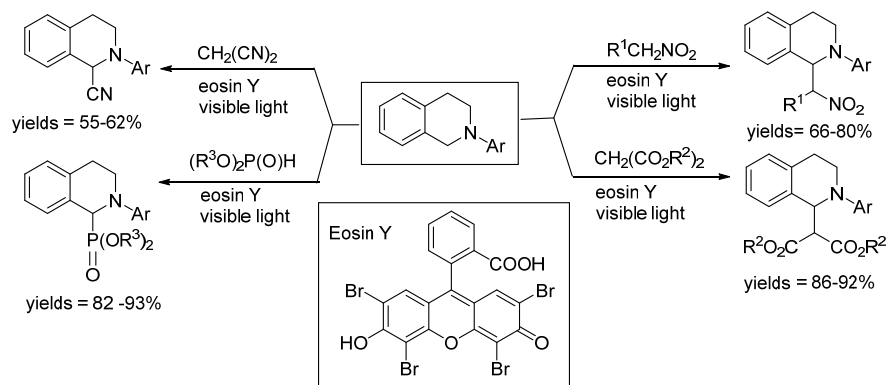
The first elegant example of C–H bond functionalization adjacent to a tertiary nitrogen atom under visible light irradiation appeared at the beginning of 2010 when Stephenson and co-workers<sup>52</sup> showed that the iminium ion, generated under photoredox conditions could be intercepted by nitroalkanes, providing aza-Henry products in excellent yields (Scheme 24). The mechanism of the reaction is shown



**Scheme 24:** Visible light mediated aza-Henry reaction.

in Scheme 24. Subsequently, Stephenson and co-workers<sup>53</sup> reported an improved protocol for the generation of the iminium intermediate by changing the stoichiometric oxidant to  $\text{BrCCl}_3$  which significantly decreased the rate and further allowed the successful utility of a broad range of appropriate nucleophiles. The reactions investigated in this report include Strecker, Cu-alkynylations, Mannich, Friedel–Crafts, Sakurai and aza-Henry reactions.<sup>50</sup>

Konig and co-worker reported similar type of visible light mediated, metal free, oxidative  $\alpha$ -coupling reactions of N-aryl tetrahydroisoquinolines with various pronucleophiles such as nitromethane, dialkyl malonates, malononitrile, and dialkyl phosphonates by using the organic dye Eosin Y (Scheme 25) as a photocatalyst.<sup>54</sup> It is important to note that, the detailed mechanistic studies of these metal free, Eosin Y-catalyzed coupling reactions was reported by Wu and co-workers.<sup>55</sup> Simultaneously, Tan and co-workers reported that another dye Rose Bengal (RB) also catalyzes the aza-Henry reaction<sup>56</sup> and a cocatalyst in combination with Rose Bengal and graphite oxide (GO) can be used for Strecker reaction.<sup>57</sup>

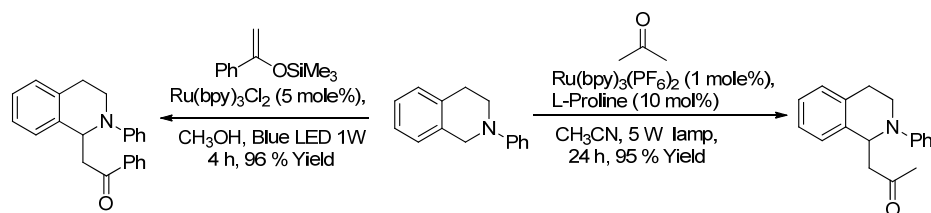


**Scheme 25:** Oxidative of  $\alpha$ -coupling reactions of N-aryl tetrahydroisoquinolines using Eosin Y.

In 2011, Rueping and co-workers reported a dual catalytic system combining photoredox and Lewis base catalysis for the Mannich-type reaction of tetrahydroisoquinoline derivatives with a large excess of ketones (Scheme 26).<sup>58</sup> Authors reported that, in absence of a Lewis base, the Mannich reaction was sluggish with the significant formation of oxidized isoquinoline, whereas in the presence of a Lewis base, a ketone was converted to enamine nucleophile *in situ* which was added to photochemically generated iminium ion yielding Mannich product. Xia and co-workers reported an alternative photoredox approach to this Mannich-type reaction by carrying out a coupling reaction between N-aryl tetrahydroisoquinolines and enol

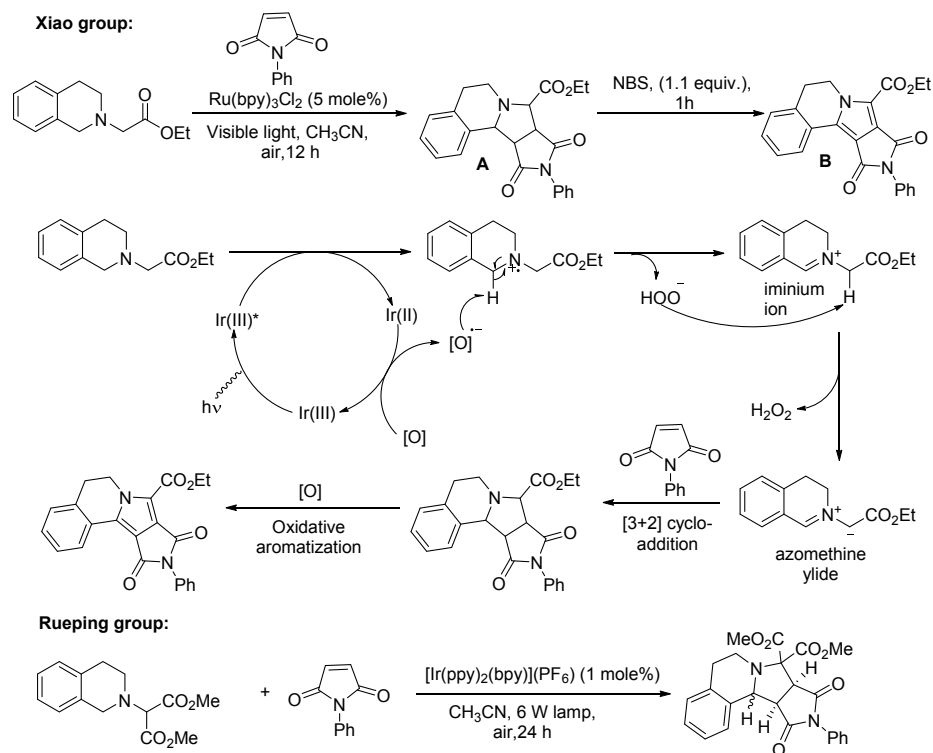


silanes (Scheme 26).<sup>59</sup> Further, the Rueping group extended the concept of dual catalysis by merging visible light photocatalysis with a metal-catalyzed process, for the alkylation reaction of tetrahydroisoquinoline derivatives.<sup>60</sup>



**Scheme 26:** Photooxidative Mannich reaction.

Xiao<sup>61</sup> and Rueping<sup>62</sup> groups independently reported visible light mediated [3+2] cycloaddition reaction of tetrahydroisoquinolines when they were substituted with a methylene group attached to one or two esters. In these reactions the initially formed iminium ions were readily converted to azomethine ylides which subsequently underwent 1,3-dipolar cycloaddition with a range of dipolarophiles to form fused pyrrolidines (Scheme 27). Xiao and co-workers further showed that the pyrrolidine ring (**A**) could be further oxidized to a fused pyrrole (**B**) under the same photoredox conditions or by treatment with NBS.<sup>49</sup>



**Scheme 27:** Photochemical [3+2] cycloaddition reaction.

### 1.5 Objective of present dissertation:

From Section 1.4.3 illustrations, it is evident that, recently,  $\alpha$   $sp^3$  C-H functionalization of *t*-amines via generation of iminium ions and its subsequent trapping with various nucleophiles, have been extensively studied by visible light photoredox catalysis. On the other hand, by this method, the  $\alpha$   $sp^3$  C-H functionalization of *t*-amines, via the use of  $\alpha$  aminoalkyl radical, as reactive intermediate is limited<sup>63</sup> because they are readily oxidized into iminium ions in the presence of a stoichiometric amount of oxidants.

Continuing with our group's interest to investigate new synthetic methodologies by photoredox catalysis in general<sup>64</sup> and our previous pioneering research contribution on PET reactions of *t*-amines<sup>40</sup> in particular, we sought to develop a new visible light mediated photoredox catalysed  $sp^3$  C-H activation of *t*-amines at its adjacent and distal position for C-C bond formation reaction. In this dissertation, we will present our results in the following order.

- i) Visible light photoredox catalysis:  $\alpha$   $sp^3$  C-H activation of *t*-amines.
- ii) Visible light photoredox catalysis: investigation of distal  $sp^3$  C-H activation of *t*-amines.

**1.6 References:**

1. Godula, K.; Sames, D. *Science* **2006**, *312*, 67-72.
2. Yamaguchi, J.; Yamaguchi, A. D.; Itami, K. *Angew. Chem. Int. Ed.* **2012**, *51*, 8960-9009.
3. (a) Labinger, J. A.; Bercaw, J. E. *Nature* **2002**, *417*, 507-514. (b) Bergman, R. G. *Nature* **2007**, *446*, 391-393. (c) White, M. C. *Synlett* **2012**, 2746-2748.
4. (a) Gutekunst, W.; Baran, P. *Chem. Soc. Rev.* **2011**, *40*, 1976-1991 (b) McMurray, L.; O'Hara, F.; Gaunt, M. J. *Chem. Soc. Rev.* **2011**, *40*, 1885-1898. (c) Chen, D. Y.-K.; Youn, S. W. *Chem. Eur. J.* **2012**, *18*, 9452-9474.
5. (a) Hofmann, A. W. *Berichte* **1885**, *18*, 109-131. (b) Löffler, K.; Kober, S. *Berichte* **1909**, *42*, 3431-3438.
6. Barton, D. H. R.; Beaton, J. M.; Geller, L. E.; Pechet, M. M. *J. Am. Chem. Soc.* **1961**, *83*, 4076-4083.
7. Pal, S. Ph. D. Thesis entitled, 'A non matallic approaches for C-H and C-Si bond activations'. submitted to University of Pune, Pune, India, 2013.
8. (a) Bennett, M. A.; Milner, D. L. *Chem. Commun.* **1967**, 581-582. (b) Green, M. L.; Knowles, P. J. *J. Chem. Soc. D: Chem. Commun.* **1970**, 1677. (c) Foley, P.; Whitesides, G. M. *J. Am. Chem. Soc.* **1979**, *101*, 2732-2733.
9. Shilov, A. E.; Shteinman, A. A. *Coord. Chem. Rev.* **1977**, *24*, 97-143.
10. (a) Hoyano, J. K.; Graham, W. A. G. *J. Am. Chem. Soc.* **1982**, *104*, 3723-3725. (b) Janowicz, A. H.; Bergman, R. G. *J. Am. Chem. Soc.* **1982**, *104*, 352-354.
11. (a) Jin-Quan Yu, Z. S., Springer: Berlin, Vol. 292. (b) Shilov, A. E.; Shul'pin, G. B. *Chem. Rev.* **1997**, *97*, 2879-2932. (c) Crabtree, R. H. *J. Chem. Soc., Dalton Trans.* **2001**, 2437-2450. (d) Lersch, M.; Tilset, M. *Chem. Rev.* **2005**, *105*, 2471-2526. (e) Wencel-Delord, J.; Dröge, T.; Liu, F.; Glorius, F. *Chem. Soc. Rev.* **2011**, *40*, 4740-4761.
12. (a) Arndtsen, B. A.; Bergman, R. G.; Mobley, T. A.; Peterson, T. H. *Acc. Chem. Res.* **1995**, *28*, 154-162. (b) Colby, D. A.; Bergman, R. G.; Ellman, J. A. *Chem. Rev.* **2009**, *110*, 624-655. (c) Daugulis, O.; Do, H.-Q.; Shabashov, D. *Acc. Chem. Res.* **2009**, *42*, 1074-1086. (d) Lyons, T. W.; Sanford, M. S. *Chem. Rev.* **2010**, *110*, 1147-1169. (e) Ackermann, L. *Chem. Rev.* **2011**, *111*, 1315-1345. (f) Arockiam, P. B.; Bruneau, C.; Dixneuf, P. H. *Chem. Rev.*

- 2012**, *112*, 5879-5918. (g) Zhu, C.; Wang, R.; Falck, J. R. *Chem. Asian J.* **2012**, *7*, 1502-1514.
13. (a) Campeau, L.-C.; Fagnou, K. *Chem. Comm.* **2006**, 1253-1264. (b) Do, H.-Q.; Khan, R. M. K.; Daugulis, O. *J. Am. Chem. Soc.* **2008**, *130*, 15185-15192. (c) Bellina, F.; Rossi, R. *Tetrahedron* **2009**, *65*, 10269-10310. (d) Ashenhurst, J. A. *Chem. Soc. Rev.* **2010**, *39*, 540-548. (e) Lei, A.; Liu, W.; Liu, C.; Chen, M. *Dalton Trans.* **2010**, *39*, 10352-10361. (f) Kuhl, N.; Hopkinson, M. N.; Wencel-Delord, J.; Glorius, F. *Angew. Chem. Int. Ed.* **2012**, *51*, 10236-10254.
14. Periana, R. A.; Taube, D. J.; Gamble, S.; Taube, H.; Satoh, T.; Fujii, H. *Science* **1998**, *280*, 560-564.
15. (a) Crabtree, R. H.; Mihelcic, J. M.; Quirk, J. M. *J. Am. Chem. Soc.* **1979**, *101*, 7738-7740. (b) Jensen, C. M. *Chem. Commun.* **1999**, 2443-2449.
16. Sakakura, T.; Sodeyama, T.; Sasaki, K.; Wada, K.; Tanaka, M. *J. Am. Chem. Soc.* **1990**, *112*, 7221-7229.
17. (a) Waltz, K. M.; Hartwig, J. F. *Science* **1997**, *277*, 211-213. (b) Chen, H.; Hartwig, J. F. *Angew. Chem. Int. Ed.* **1999**, *38*, 3391-3393.
18. (a) Bellina, F.; Rossi, R. *Chem. Rev.* **2009**, *110*, 1082-1146. (b) Baudoin, O. *Chem. Soc. Rev.* **2011**, *40*, 4902-4911.
19. (a) Li, C.-J. *Acc. Chem. Res.* **2008**, *42*, 335-344. (b) Jazzar, R.; Hitce, J.; Renaudat, A.; Sofack-Kreutzer, J.; Baudoin, O. *Chem. Eur. J.* **2010**, *16*, 2654-2672. (c) Yoo, W.-J.; Li, C.-J. *Top. Curr. Chem.* **2010**, *292*, 281-302. (d) Hu, L.; Bi-Jie, L.; Zhang-Jie, S. *Catal. Sci. Technol.* **2011**, *1*, 191-206.
20. (a) Campos, K. R. *Chem. Soc. Rev.* **2007**, *36*, 1069-1084. (b) Mitchell, E. A.; Peschiulli, A.; Lefevre, N.; Meerpoel, L.; Maes, B. U. W. *Chem. Eur. J.* **2012**, *18*, 10092-10142.
21. (a) Beak, P.; Zajdel, W. J.; Reitz, D. B. *Chem. Rev.* **1984**, *84*, 471-523. (b) Beak, P.; Lee, W.-K. *Tetrahedron Lett.* **1989**, *30*, 1197-1200.
22. (a) Beak, P.; Basu, A.; Gallagher, D. J.; Park, Y. S.; Thayumanavan, S. *Acc. Chem. Res.* **1996**, *29*, 552-560. (b) Hoppe, D.; Hense, T. *Angew. Chem. Int. Ed.* **1997**, *36*, 2282-2316.
23. Chatani, N.; Asaumi, T.; Ikeda, T.; Yorimitsu, S.; Ishii, Y.; Kakiuchi, F.; Murai, S. *J. Am. Chem. Soc.* **2000**, *122*, 12882-12883.

24. Pastine, S. J.; Gribkov, D. V.; Sames, D. *J. Am. Chem. Soc.* **2006**, *128*, 14220-14221.
25. (a) Davies, H. M. L.; Hansen, T.; Hopper, D. W.; Panaro, S. A. *J. Am. Chem. Soc.* **1999**, *121*, 6509-6510. (b) Davies, H. M. L.; Venkataramani, C. *Org. Lett.* **2001**, *3*, 1773-1775. (c) Davies, H. M. L.; Venkataramani, C.; Hansen, T.; Hopper, D. W. *J. Am. Chem. Soc.* **2003**, *125*, 6462-6468.
26. Snieckus, V.; Cuevas, J. C.; Sloan, C. P.; Liu, H.; Curran, D. P. *J. Am. Chem. Soc.* **1990**, *112*, 896-898.
27. Williams, L.; Booth, S. E.; Undheim, K. *Tetrahedron* **1994**, *50*, 13697-13708.
28. Murakami, M.; Hayashi, M.; Ito, Y. *Appl. Organomet. Chem.* **1995**, *9*, 385-397.
29. Yoshimitsu, T.; Arano, Y.; Nagaoka, H. *J. Am. Chem. Soc.* **2005**, *127*, 11610-11611.
30. (a) Shono, T. *Tetrahedron* **1984**, *40*, 811-850. (b) T. Shono; Y. Matsumura, a.; Tsubata, K. *Org. Synth.* **1985**, 206-211.
31. (a) Maruyama, T.; Suga, S.; Yoshida, J.-i. *J. Am. Chem. Soc.* **2005**, *127*, 7324-7325. (b) Maruyama, T.; Mizuno, Y.; Shimizu, I.; Suga, S.; Yoshida, J.-i. *J. Am. Chem. Soc.* **2007**, *129*, 1902-1903.
32. Murahashi, S.-I.; Komiya, N.; Terai, H.; Nakae, T. *J. Am. Chem. Soc.* **2003**, *125*, 15312-15313.
33. (a) Li, Z.; Li, C.-J. *J. Am. Chem. Soc.* **2004**, *126*, 11810-11811. (b) Li, Z.; Li, C.-J. *Eur. J. Org. Chem.* **2005**, *2005*, 3173-3176. (c) Li, Z.; Li, C.-J. *J. Am. Chem. Soc.* **2005**, *127*, 3672-3673. (d) Li, Z.; Li, C.-J. *J. Am. Chem. Soc.* **2005**, *127*, 6968-6969. (e) Li, Z.; Bohle, D. S.; Li, C.-J. *Proc. Natl. Acad. Sci. U. S. A.* **2006**, *103*, 8928-8933.
34. Basle, O.; Li, C.-J. *Chem. Commun.* **2009**, 4124-4126.
35. Mitsudera, H.; Li, C.-J. *Tetrahedron Lett.* **2011**, *52*, 1898-1900.
36. (a) Sureshkumar, D.; Sud, A.; Klussmann, M. *Synlett* **2009**, *2009*, 1558-1561. (b) Boess, E.; Sureshkumar, D.; Sud, A.; Wirtz, C.; Farès, C.; Klussmann, M. *J. Am. Chem. Soc.* **2011**, *133*, 8106-8109.
37. Hoffmann, N. *Chem. Rev.* **2008**, *108*, 1052-1103.
38. Horspool, W.; Lenci, F., CRC HANDBOOK OF Organic Photochemistry and Photobiology. (The Dynamics and Photochemical Consequences of

- Aminium Radical Reactions by Ung Chan Yoon, Z. S., and Patrick S. Mariano), Ed. CRC press: Vol. 2, p 101.
39. (a) Lewis, F. D.; Ho, T.-I.; Simpson, J. T. *J.Org.Chem.* **1981**, *46*, 1077-1082. (b) Lewis, F. D. *Acc. Chem. Res.* **1986**, *19*, 401-405. (c) Nelsen, S. F.; Ippoliti, J. T. *J. Am. Chem. Soc.* **1986**, *108*, 4879-4881.
40. (a) Pandey, G.; Kumaraswamy, G. *Tetrahedron Lett.* **1988**, *29*, 4153-4156. (b) Pandey, G.; Kumaraswamy, G.; Bhalerao, U. T. *Tetrahedron Lett.* **1989**, *30*, 6059-6062. (c) Pandey, G. *Synlett* **1992**, 546-552. (d) Pandey, G.; Kumaraswamy, G.; Reddy, P. Y. *Tetrahedron* **1992**, *48*, 8295-8308. (e) Pandey, G.; Rani, K. S.; Lakshmaiah, G. *Tetrahedron Lett.* **1992**, *33*, 5107-5110. (f) Pandey, G.; Devi Reddy, G.; Kumaraswamy, G. *Tetrahedron* **1994**, *50*, 8185-8194. (g) Pandey, G.; Gadre, S. R. *Arkivoc* **2003**, 45-54.
41. (a) Dileep Kumar, J. S.; Das, S. *Res. Chem. Intermed.* **1997**, *23*, 755-800. (b) Das, S.; Suresh, V., Electron-transfer Reactions of Amines. In *Electron Transfer in Chemistry*, Balzani, V., Ed. Wiley-VCH Verlag GmbH: Weinheim, Germany, 2008; pp 379-456.
42. (a) Bryce-Smith, D.; Clarke, M. T.; Gilbert, A.; Klunklin, G.; Manning, C. *J. Chem. Soc. Chem. Commun.* **1971**, 916-918. (b) Barltrop, J. A. *Pure and Appl. Chem.* **1973**, *33*, 179-195. (c) Yang, N. C.; Shold, D. M.; Kim, B. *J. Am. Chem. Soc.* **1976**, *98*, 6587-6596. (d) Bellas, M.; Bryce-Smith, D.; Clarke, M. T.; Gilbert, A.; Klunkin, G.; Krestonosich, S.; Manning, C.; Wilson, S. *J. Chem.Soc. Perkin Trans 1* **1977**, 2571-2580.
43. (a) Hub, W.; Schneider, S.; Doerr, F.; Simpson, J. T.; Oxman, J. D.; Lewis, F. D. *J. Am. Chem. Soc.* **1982**, *104*, 2044-2045. (b) Hub, W.; Schneider, S.; Doerr, F.; Oxman, J. D.; Lewis, F. D. *J. Am. Chem. Soc.* **1984**, *106*, 708-715.
44. (a) Hasegawa, E.; Xu, W.; Mariano, P. S.; Yoon, U. C.; Kim, J. U. *J. Am. Chem. Soc.* **1988**, *110*, 8099-8111. (b) Jeon, Y. T.; Lee, C. P.; Mariano, P. S. *J. Am. Chem. Soc.* **1991**, *113*, 8847-8863. (c) Xu, W.; Zhang, X. M.; Mariano, P. S. *J. Am. Chem. Soc.* **1991**, *113*, 8863-8878. (d) Yoon, U. C.; Mariano, P. S. *Acc. Chem. Res.* **1992**, *25*, 233-240.
45. (a) Bertrand, S.; Glapski, C.; Hoffmann, N.; Pete, J.-P. *Tetrahedron Lett.* **1999**, *40*, 3169-3172. (b) Bertrand, S.; Hoffmann, N.; Pete, J.-P. *Eur. J. Org. Chem* **2000**, *2000*, 2227-2238. (c) Harakat, D.; Pesch, J.; Marinkovic, S.; Hoffmann, N. *Org. Biomol. Chem.* **2006**, *4*, 1202-1205.

46. Ohashi, M.; Kudo, H.; Yamada, S. *J. Am. Chem. Soc.* **1979**, *101*, 2201-2202.
47. Ciamician, G. *Science* **1912**, *36*, 385-394.
48. Narayanam, J. M. R.; Stephenson, C. R. J. *Chem. Soc. Rev.* **2011**, *40*, 102-113.
49. Hu, J.; Wang, J.; Nguyen, T. H.; Zheng, N. *Beilstein J. Org. Chem.* **2013**, *9*, 1977-2001.
50. Shi, L.; Xia, W. *Chem. Soc. Rev.* **2012**, *41*, 7687-7697.
51. (a) DeLaive, P. J.; Lee, J. T.; Sprintschnik, H. W.; Abruna, H.; Meyer, T. J.; Whitten, D. G. *J. Am. Chem. Soc.* **1977**, *99*, 7094-7097. (b) DeLaive, P. J.; Foreman, T. K.; Giannotti, C.; Whitten, D. G. *J. Am. Chem. Soc.* **1980**, *102*, 5627-5631.
52. Condie, A. G.; González-Gómez, J. C.; Stephenson, C. R. J. *J. Am. Chem. Soc.* **2010**, *132*, 1464-1465.
53. Freeman, D. B.; Furst, L.; Condie, A. G.; Stephenson, C. R. J. *Org. Lett.* **2012**, *14*, 94-97.
54. Hari, D. P.; König, B. *Org. Lett.* **2011**, *13*, 3852-3855.
55. Liu, Q.; Li, Y.-N.; Zhang, H.-H.; Chen, B.; Tung, C.-H.; Wu, L.-Z. *Chem. Eur. J.* **2012**, *18*, 620-627.
56. Pan, Y.; Kee, C. W.; Chen, L.; Tan, C.-H. *Green Chem.* **2011**, *13*, 2682-2685.
57. Pan, Y.; Wang, S.; Kee, C. W.; Dubuisson, E.; Yang, Y.; Loh, K. P.; Tan, C.-H. *Green Chem.* **2011**, *13*, 3341-3344.
58. Rueping, M.; Vila, C.; Koenigs, R.; Poscharny, K.; Fabry, D. *Chem. Commun.* **2011**, *47*, 2360-2362.
59. Zhao, G.; Yang, C.; Guo, L.; Sun, H.; Chen, C.; Xia, W. *Chem. Commun.* **2012**, *48*, 2337-2339.
60. Rueping, M.; Koenigs, R. M.; Poscharny, K.; Fabry, D. C.; Leonori, D.; Vila, C. *Chem. Eur. J.* **2012**, *18*, 5170-5174.
61. Zou, Y.-Q.; Lu, L.-Q.; Fu, L.; Chang, N.-J.; Rong, J.; Chen, J.-R.; Xiao, W. *J. Angew. Chem. Int. Ed.* **2011**, *50*, 7171-7175.
62. Rueping, M.; Leonori, D.; Poisson, T. *Chem. Commun.* **2011**, *47*, 9615-9617.
63. McNally, A.; Prier, C.; MacMillan, D. W. C. *Science* **2011**, *334*, 1114-1117.
64. Pandey, G. *Top. Curr. Chem.* **1993**, *168*, 175-221.



## *Chapter 2*

### **Visible Light Photoredox Catalysis: $\alpha$ $sp^3$ C-H Activation of *t*-Amines**



## 2.1 Introduction:

The ability of  $\text{Ru}(\text{bpy})_3^{2+}$  and related complexes to function as visible light photocatalysts have been extensively investigated for applications in inorganic and materials chemistry. In particular, photoredox catalysts have been utilized to accomplish the splitting of water into hydrogen and oxygen and the reduction of carbon dioxide to methane. Also  $\text{Ru}(\text{bpy})_3^{2+}$  and its analogues have been used (i) as components of dye-sensitized solar cells and organic light-emitting diodes and (ii) to initiate polymerization reactions.<sup>1</sup>

Nevertheless, until the beginning of the 21<sup>st</sup> century, these visible light photoredox catalysts had been only sporadically employed in the area of organic synthesis. Remarkably, since 2008 seminal studies by Macmillan,<sup>1</sup> Stephenson,<sup>2</sup> Yoon<sup>3</sup> followed by several other groups have dramatically highlighted the importance of visible light mediated bond forming strategy for organic synthesis utilizing transition metal Ru(II) or Ir(III) polypyridine complexes, pigments and dyes as photoredox catalyst. With remarkable rejuvenated interest in this organic transformation, recently significant volume of research work has been done for C-C bond formation reaction which is articulated in several reviews.<sup>1-7</sup>

Importantly, among the several visible light photoredox catalysts, Ru(II) polypyridine complexes are deeply investigated due to their ease of synthesis, stability at room temperature, and excellent redox properties (excited-state reactivity, luminescence emission, and excited-state lifetime).<sup>8</sup> In particular, a commercially available complex  $\text{Ru}(\text{bpy})_3\text{Cl}_2$ , is one of the most widely employed photoredox catalyst. Before we discuss  $\text{sp}^3$  C-H functionalization of *t*-amines enabled by visible light photoredox catalysis, it is instructive to consider the photochemistry of the prototypical photoredox catalyst  $\text{Ru}(\text{bpy})_3^{2+}$  as a foundation of our research work done.

### Photoredox properties of $\text{Ru}(\text{bpy})_3^{2+}$ :

Irradiation of  $\text{Ru}(\text{bpy})_3\text{Cl}_2$  with visible light (~452 nm) gives the lowest singlet excited state ( $^1\text{Ru}^{2+*}$  or  $^1\text{MLCT}$ ) via excitation of an electron from a metal centered ( $t_{2g}$ ) orbitals to ligand centred ( $\pi^*$ ) orbital. This initially generated singlet ( $^1\text{Ru}^{2+*}$  or  $^1\text{MLCT}$ ) state undergoes rapid intersystem crossing (ISC) yielding a long lived luminescent triplet excited state ( $^3\text{Ru}^{2+*}$  or  $^3\text{MLCT}$ ), which engages in single-electron

transfer.<sup>1</sup> Relative to ground state, this triplet excited state acts as a better oxidizing or reducing agent. This can be explained on the basis of their standard reduction potential. For instance reduction potential of the excited state ( $E_{1/2}^{\text{III}^*/\text{II}} = -0.81\text{ V}$  vs SCE in  $\text{CH}_3\text{CN}$ ) signifies that it is more potent reductant compared to its ground state  $\text{Ru}(\text{bpy})_3^{2+}$  ( $E_{1/2}^{\text{III}/\text{II}} = +1.29$  vs SCE in  $\text{CH}_3\text{CN}$ ). At the same time, the reduction potential of the excited state ( $E_{1/2}^{*\text{II}/\text{I}} = +0.77\text{ V}$  vs SCE in  $\text{CH}_3\text{CN}$ ) indicates that this species is a much stronger oxidant than the ground state ( $E_{1/2}^{\text{III}/\text{I}} = -1.33\text{ V}$  vs SCE in  $\text{CH}_3\text{CN}$ ).

As a result of unique property (acting as both oxidant and reductant) of the  $\text{Ru}(\text{bpy})_3^{2+}$  photoexcited state, several oxidative quencher (a compound that accepts an electron from  $\text{Ru}(\text{bpy})_3^{2+*}$ ) and reductive quenchers (a compound that donates an electron to  $\text{Ru}(\text{bpy})_3^{2+*}$ ) are known and some of them are shown in Figure 1. In oxidative quenching cycle  $\text{Ru}(\text{bpy})_3^{2+*}$  function as a reductant where as in reductive quenching cycle it works as an oxidant. Commonly fluorescence quenching (or Stern-Volmer) studies are employed in order to determine whether a reductive or oxidative quenching cycle is operative in a particular reaction. In recent past, by utilizing the oxidative and reductive quenching concept of visible light photoredox catalysis, a plethora of research is reported in organic synthesis for a wide range of chemical transformations. In some reactions, in addition to the single electron transfer pathways,  $\text{Ru}(\text{bpy})_3^{2+}$  photoexcited state may also engage in energy transfer with organic substrates.

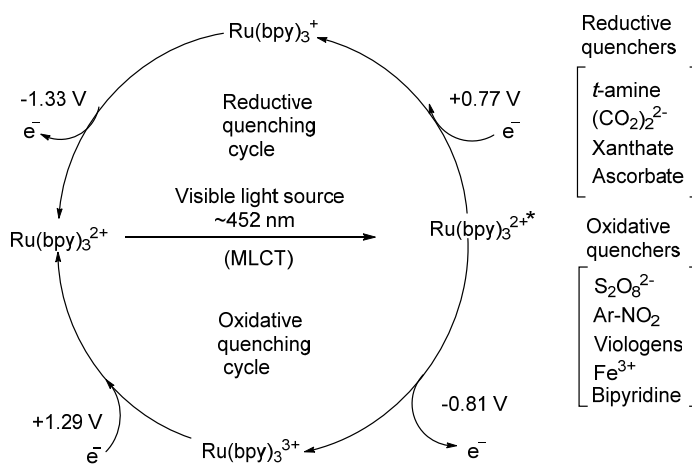


**Figure 1:** Photophysical properties of  $\text{Ru}(\text{bpy})_3^{2+}$ .

## 2.2 Background of our concept:

From the Chapter 1, Section 1.4.1 illustrations, it is evident that in photoinduced electron transfer (PET) processes between a *t*-amines (**1**) and a photocatalyst, amine reductively quenches the photoexcited state of catalyst owing to the low oxidation potential and results in the formation of amine radical cation (Figure 2) which in polar solvents, subject to kinetic acidity and stereoelectronic factors, undergoes facile  $\alpha$ -deprotonation to produce  $\alpha$ -amine alkyl radical (**3**). Depending upon the reaction conditions, the generated  $\alpha$ -amine alkyl radical could either react as a nucleophile with a suitable substrate or could undergo further one-electron oxidation due to its reduced ionization potential to form iminium ion (**4**), thus serving as an electrophile.<sup>9</sup> In Chapter 1, the generation and exploitation of iminium ion photochemistry for the  $\alpha$  sp<sup>3</sup> C-H functionalization of *t*-amines have been discussed in Section 1.4.2 and 1.4.3 by UV and visible light photoredox catalysis, respectively. Although, some examples of  $\alpha$ -amino alkyl radicals being utilized as synthetic intermediates are known, they are generated using high-energy UV light (Chapter 1, Section 1.4.2).<sup>10-14</sup> Until recently there was hardly any example of the generation and use of  $\alpha$ -amino alkyl radical by visible light photoredox catalysis, therefore, synthetic applications of this reactive intermediate largely remained unexplored.

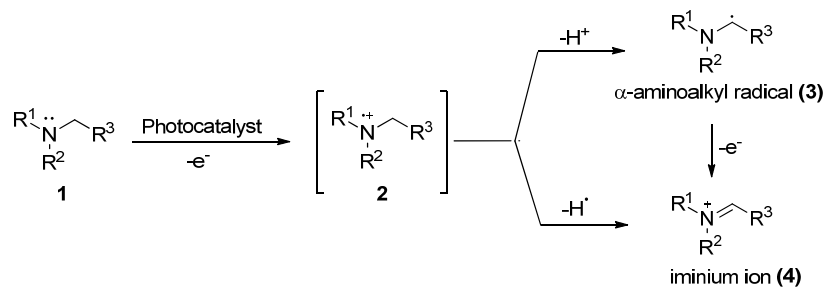


**Figure 2:** Photochemical different modes of reactivity of *t*-amines.

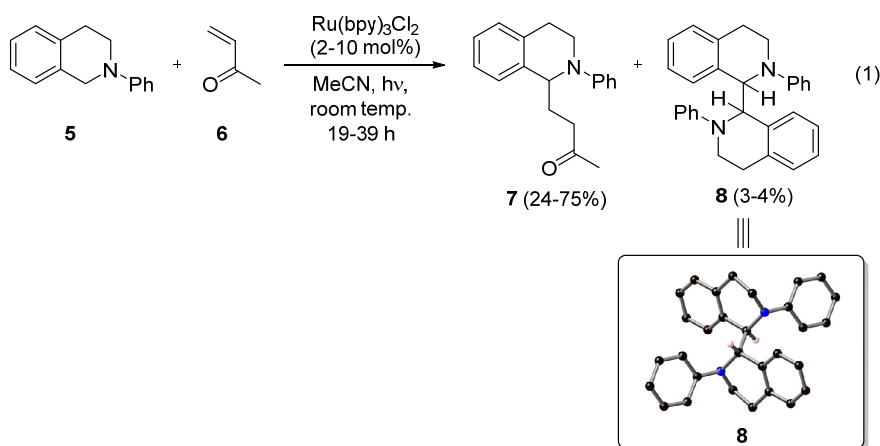
Given our group's interest in photoredox processes for sp<sup>3</sup> C-H activation of *t*-amines,<sup>15</sup> we decided to explore opportunity of generating  $\alpha$ -amine alkyl radicals by visible light photoredox catalysis and also to evaluate their synthetic utility. It was anticipated that  $\alpha$ -amine alkyl radical may undergo 1, 4-addition with various Michael acceptors resulting in the novel C-C bond formation reaction. The rationale behind conceiving this strategy emanated from the idea that photoirradiation between excited state Ru(bpy)<sub>2</sub><sup>2+</sup> and *t*-amine could lead to efficient single electron transfer giving rise

to  $\text{Ru}(\text{bpy})_2^+$  and amine radical cation. In polar solvent this amine radical cation will undergo  $\alpha$ -deprotonation to form  $\alpha$ -aminoalkyl radical. Since in absence of an oxidant its further oxidation to iminium ion would not be possible, this  $\alpha$ -amino alkyl radical would undergo conjugate addition reactions with Michael acceptor. Finally, the ultimate reduction of conjugate adduct radical followed by protonation would complete the catalytic cycle along with regeneration of  $\text{Ru}(\text{bpy})_2^{2+}$  catalyst. Hence, in general, these coupling reactions will be overall redox neutral.

### 2.3 Results and discussion:

#### 2.3.1 $\alpha$ $\text{sp}^3$ C-H activation reaction of *t*-amines with electron deficient alkenes:

Initially to test the feasibility of the proposed concept (Section 2.2), we irradiated a mixture of *N*-phenyltetrahydroisoquinoline (**5**, 1 equiv) and methyl vinyl ketone (**6**, 1 equiv) in the presence of catalytic amounts of  $\text{Ru}(\text{bpy})_3\text{Cl}_2 \cdot 6\text{H}_2\text{O}$  (2 mol%) in degassed acetonitrile with a blue light emitting diode (LED;  $\lambda_{\text{max}} \sim 452$  nm) which gave rise to the conjugate addition product **7** in 24% yield along with dimeric **8** (3%) (Scheme 1). These products were characterized by NMR and mass spectral analyses. The structure of compound **8** was also ambiguously established by X-ray analysis.



**Scheme 1:** Photoredox  $\alpha$  C-H functionalization of **5** with MVK (**6**).

With the aim to improve the yield and to optimize the reaction conditions several parameters were investigated and the results are summarized in Table 1. It was observed that there is slight improvement in the yield (38%) when 2 equiv. of MVK (**6**) was used (entry 2). Comparatively little low yield was observed when similar

reaction was performed in dry DMF or DCM (entries 3-4). However, a noticeable improvement in the yield and was observed when 3 equiv. of MVK (**6**) was used in presence of 2 mol% (58%) and 5 mol% (60%) of Ru(bpy)<sub>3</sub>Cl<sub>2</sub> (entries 5-6). For this reaction, highest yield (75%) was observed when 10 equiv. of MVK (**6**) and 10 mol% of Ru(bpy)<sub>3</sub>Cl<sub>2</sub> catalyst was used. Due to competing self-polymerisation reaction of MVK (**6**), its excess use (either 3 or 10 equiv.) was helpful in improvising the yield. The use of Lewis acid additives such as LiBF<sub>4</sub> (2 equiv.) or NaBF<sub>4</sub> (2 equiv.) did not help in the improvement of the yield of coupling product (**7**).

**Table 1:** Photoredox  $\alpha$  C-H functionalization of **5** with MVK (**6**).<sup>[a]</sup>

| Entry | <b>5</b> (equiv.) | <b>6</b> (equiv.) | Ru(bpy) <sub>3</sub> Cl <sub>2</sub><br>(mol%) | Time (h) | Solvent | Yield (%) |
|-------|-------------------|-------------------|--|----------|---------|-----------|
| 1     | 1                 | 1                 | 2  | 39       | MeCN    | 24        |
| 2     | 1                 | 2                 | 2  | 19       | MeCN    | 38        |
| 3     | 1                 | 2                 | 2  | 19       | DMF     | 35        |
| 4     | 1                 | 2                 | 2  | 19       | DCM     | 15        |
| 5     | 1                 | 3                 | 2  | 24       | MeCN    | 58        |
| 6     | 1                 | 3                 | 5  | 23       | MeCN    | 60        |
| 7     | 1                 | 10                | 10   | 23       | MeCN    | 75        |

<sup>[a]</sup> Reaction condition: **5** (0.48 mmol), **6** (0.48-4.8 mmol), Ru(bpy)<sub>3</sub>Cl<sub>2</sub> (2-10 mol%), Blue LED light irradiation, Solvent (2 mL), 19-39 h.

### 2.3.2 Control experiments:

In order to test the whether photocatalyst and visible light is necessary for above mentioned reaction (eq. 1), two independent control experiments were conducted. When photoirradiation between **5** (1 equiv.) and MVK (**6**, 3 equiv.) was carried out in the absence of Ru(bpy)<sub>3</sub>Cl<sub>2</sub> catalyst in degassed acetonitrile with blue LED, there was no observable product even after prolonged irradiation (48 h). Similarly, when the mixture of **5** (1 equiv.), MVK (**6**, 3 equiv.) and Ru(bpy)<sub>3</sub>Cl<sub>2</sub> (5 mol%) in degassed acetonitrile was kept for 48 h in dark at room temperature, there was no reaction observed. These two appropriate control experiments showed that for the formation of **7** by reaction between **5** and **6**, both Ru(bpy)<sub>3</sub>Cl<sub>2</sub> catalyst and visible light (blue LED) were necessary.

### 2.3.3 Experimental set-up:

The experimental set-up used for this reaction was very simple. It utilized blue light emitting diode (LED;  $\lambda_{\text{max}} \sim 452 \text{ nm}$ , 3 W) as a source of light (Figure 3). Further in order to avoid loss of light by scattering, more focused light in Schlenk flask with slightly modified experimental set-up as shown in Figure 3 was used.

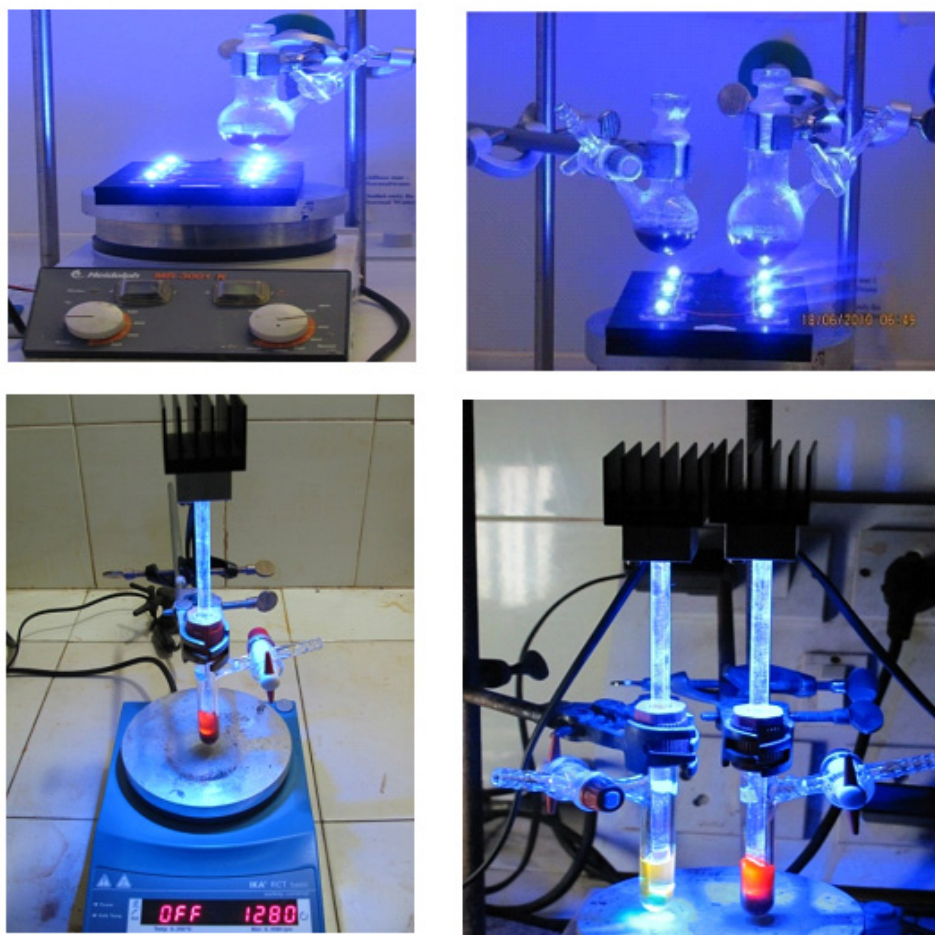


**Figure 3:** Experimental set-up.

### 2.3.4 Proposed reaction mechanism:

In order to rationalize the photoreaction (eq. 1), a plausible reaction mechanism is proposed as shown in Figure 4. The excited  $\text{Ru}(\text{bpy})_3^{2+}$  is quenched by single electron transfer from *N*-phenyltetrahydroisoquinoline (**5**) producing corresponding amine radical cation **9** and a  $\text{Ru}(\text{bpy})_3^+$ . The amine radical cation **9** undergoes  $\alpha$ -deprotonation to generate  $\alpha$ -amino alkyl radical **10** which upon addition to activated alkenes forms  $\alpha$ -carbonyl radical **11**. Reduction of **11** by  $\text{Ru}(\text{bpy})_3^+$  followed by

protonation provides conjugate addition product **7** along with the regeneration of the Ru catalyst.<sup>9</sup>

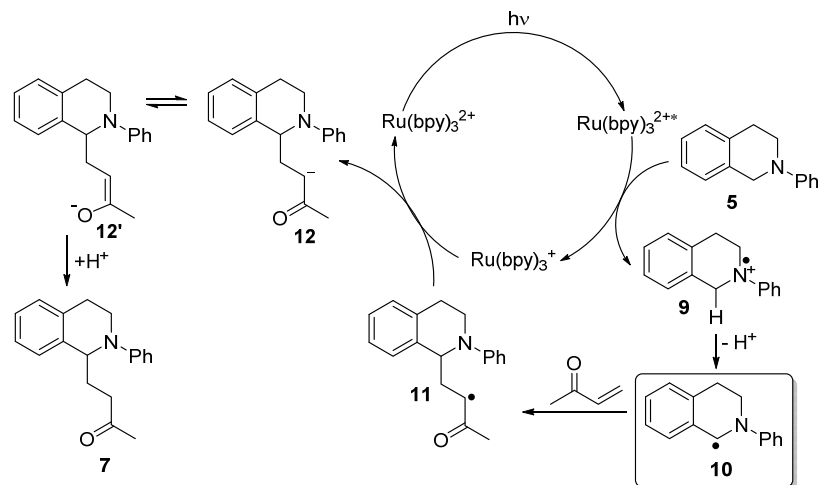
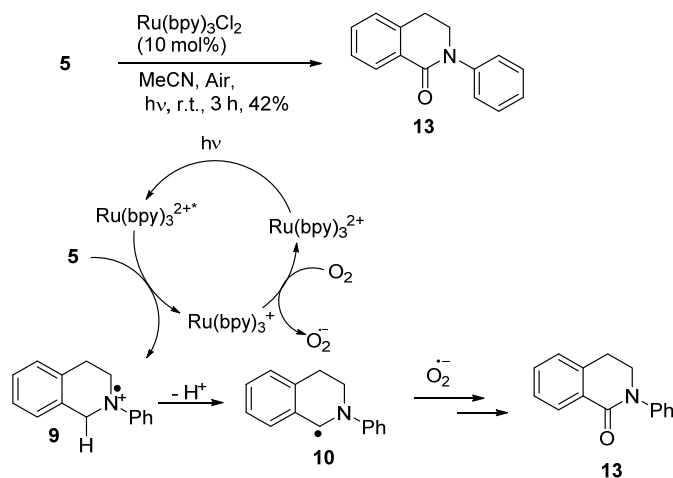


**Figure 4:** Proposed reaction mechanism.

The involvement of  $\alpha$ -amino alkyl radical **10** intermediacy in this reaction (eq. 1) is established by observing the formation of **8**. Furthermore, in order to substantiate the involvement of **10**, a controlled experiments by irradiating **5** in acetonitrile in presence of air was carried out which produced **13** (42%) (Scheme 2). The formation of **13** can be explained by initial coupling of **10** with ground-state oxygen or by reaction with  $\text{O}_2^-$  generated through regeneration of  $\text{Ru}(\text{bpy})_3^{2+}$  via an electron transfer by  $\text{Ru}(\text{bpy})_3^+$  to dissolved air in the solvent.<sup>16</sup> Very recently, compelling evidence for the formation of  $\alpha$ -amino alkyl radical **10** from the deprotonation of corresponding radical cation **9** was also reported.<sup>17</sup>



**Scheme 2:** Photocatalyzed reaction of **5** in the presence of oxygen.

### 2.3.5 Evaluation of the generality of the reactions:

In order to generalise this photoreaction (eq. 1), irradiation of *N*-aryltetrahydroisoquinolines with various electron deficient alkenes in an identical reaction conditions were studied by using catalytic amount of Ru(bpy)<sub>3</sub>Cl<sub>2</sub> (5 mol%) and the results are shown in Table 2. For example, photoirradiation of **5** (1 equiv.) with chalcone (**15**) (1 equiv.) produced **19** (61% yield) as a diastereomeric mixture (70:30 ratio, determined by NMR spectroscopy) (entry 1). The major diastereomer was obtained in pure form by fractional crystallization and its relative configuration was assigned on the basis of the X-ray-structure (Figure 5).<sup>9</sup>

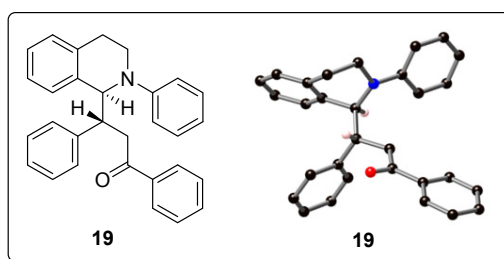
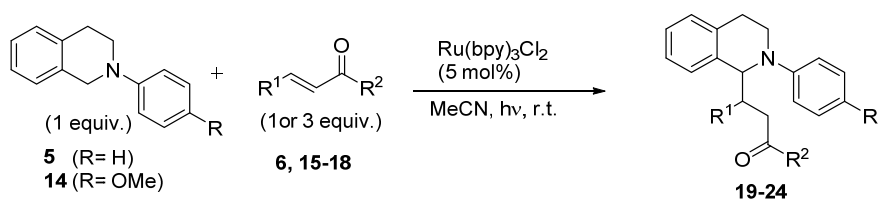


Figure 5: X-ray analysis of **19**.

In another experiment, photoirradiation of **5** (1 equiv.) with methacrylaldehyde (**16**) (3 equiv.) gave corresponding **20** (50% yield, *dr* = 60:40, entry 2). Similar to chalcone (**15**), the coupling of 4-methoxychalcone (**17**) proceeded smoothly to give the corresponding coupling product **21** (56% yield, *dr* = 60:40, entry 3). The scope of this reaction was also evaluated with (1-furyl)alkene framework **18** and the corresponding coupling product **22** was formed in (53% yield, *dr* = 50:50, entry 4). With the aim to study another example of *N*-aryltetrahydroisoquinoline, a similar type of photoirradiation reactions were carried out between 2-(4-methoxyphenyl)-1,2,3,4-tetrahydroisoquinoline (**14**) and enones (**6** and **15**). It was observed that irradiation of **14** with **6** gave **23** in 63% yield whereas its irradiation with **15** forms **24** in slightly low yield (43%, *dr* = 66:34) (entries 5-6). The yield reported herein refers to actual yield obtained after column chromatographic purification and the diastereomeric ratio were determined by NMR spectroscopy. In case of entry 2 and 5, excess of electron deficient alkenes (**6** and **16**) (3 equiv.) were used due to their competing self-polymerization reactions.<sup>9</sup>

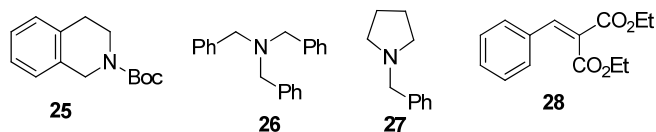



**Table 2:** Photoredox  $\alpha$  C-H functionalization of **5/14** with electron deficient alkenes <sup>[a]</sup>

| Entry | <i>t</i> -Amines         | Alkenes                   | Product       | Time (h) | Yield (%) <sup>[b]</sup> | dr <sup>[c]</sup> |
|-------|--------------------------|---------------------------|---------------|----------|--------------------------|-------------------|
| 1     | <b>5</b><br>(0.48 mmol)  | <br><b>15</b> (0.48 mmol) | <br><b>19</b> | 20       | 61                       | 70:30             |
| 2     | <b>5</b><br>(0.3 mmol)   | <br><b>16</b> (0.9 mmol)  | <br><b>20</b> | 21       | 50                       | 60:40             |
| 3     | <b>5</b><br>(0.33 mmol)  | <br><b>17</b> (0.33 mmol) | <br><b>21</b> | 48       | 56                       | 60:40             |
| 4     | <b>5</b><br>(0.33 mmol)  | <br><b>18</b> (0.33 mmol) | <br><b>22</b> | 21       | 53                       | 50:50             |
| 5     | <b>14</b><br>(0.3 mmol)  | <br><b>6</b> (0.9 mmol)   | <br><b>23</b> | 24       | 63                       | -                 |
| 6     | <b>14</b><br>(0.42 mmol) | <br><b>15</b> (0.42 mmol) | <br><b>24</b> | 48       | 43                       | 66:34             |

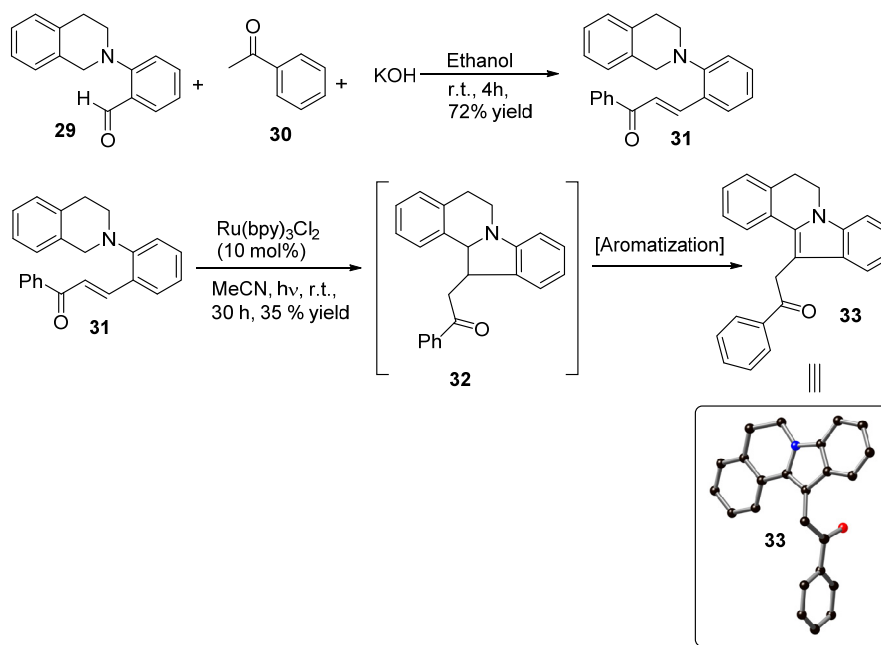
<sup>[a]</sup> Reaction condition: **5** or **14** (1 equiv.), **6, 15-18** (1 or 3 equiv.), Ru(bpy)<sub>3</sub>Cl<sub>2</sub> (5 mol%), Blue LED light irradiation, MeCN (2 mL), 21-48 h. <sup>[b]</sup> Isolated yield, after column chromatographic purification. <sup>[c]</sup> Diastereomeric ratio determined by NMR.

It should be noted that under our optimized reaction condition, identical irradiation of *t*-amines of type (**25-27**) with enones (**6** and **15**) and of *t*-amine (**5**) with different type electron deficient alkene (**28**) did not give any desired products, may be due to their mismatched redox potential with Ru(bpy)<sub>3</sub>Cl<sub>2</sub> catalyst.



### 2.3.6 Intramolecular coupling reaction:

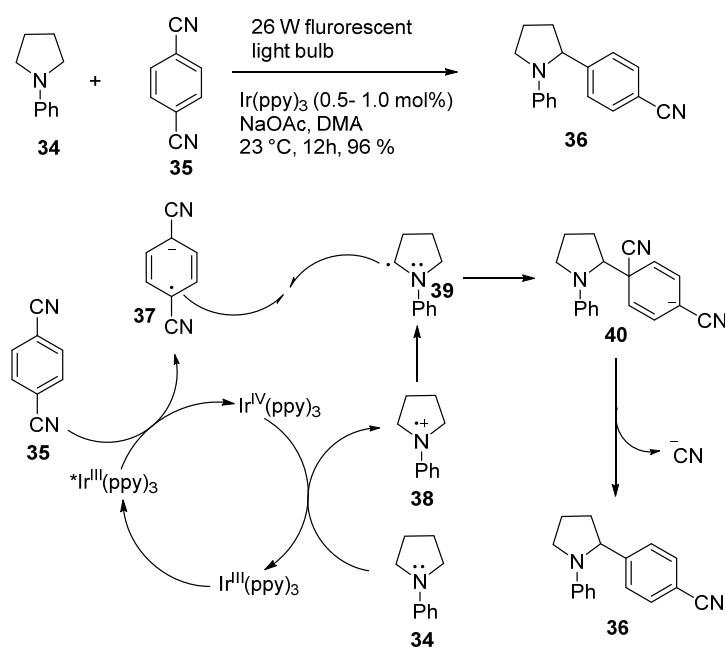
After above successful demonstration that  $\alpha$  amino radical, generated by visible light photoredox reaction between a *t*-amine and Ru(bpy)<sub>3</sub>Cl<sub>2</sub>, undergoes conjugate addition with activated olefins, it encouraged us to evaluate the scope of this work for the synthesis of important heterocyclic scaffold by carrying out intramolecular reaction. In this regard, identical photoredox reaction was carried out with **31**, readily synthesizable by aldol reaction of **29** with acetophenone (**30**), produced 5,6-dihydroindolo[2,1-a]- tetrahydroisoquinoline **33** (35%) (Scheme 3). Compound **33** have obviously been formed by the aromatization of **32**. Moreover, this **33** class of compounds have been found to exhibit significant immunosuppressive activity against IL-2, IL-10, and IFN- $\gamma$ .<sup>18</sup>



**Scheme 3:** Synthesis of 5,6-dihydroindolo[2,1-a]-tetrahydroisoquinoline (**33**).

It is noteworthy to mention that above mentioned reactions was also performed by using another photoredox catalyst  $[\text{Ir}(\text{ppy})_2(\text{dtb-bpy})]\text{PF}_6$ , however, except one or two cases, there was no marked difference observed either in yields or rate of the reaction.\*

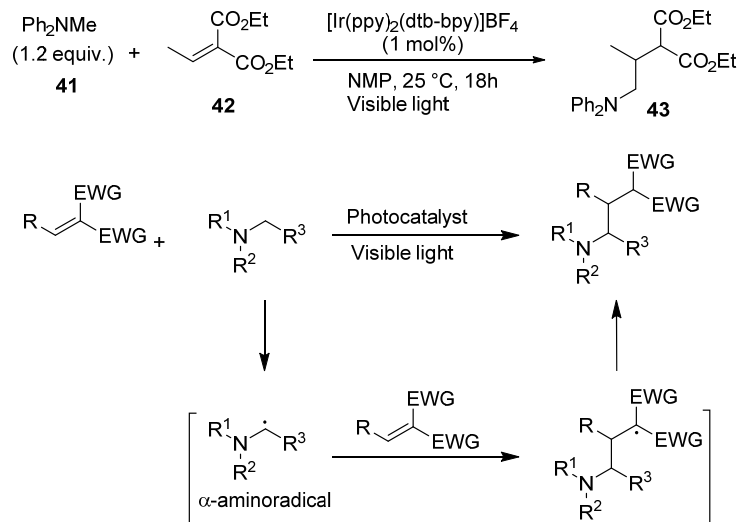
While our research work was under progress, MacMillan and co-workers reported  $\alpha$   $\text{sp}^3$  C-H arylation reaction of *t*-amines<sup>19</sup> by visible light photoredox catalysis. In their reaction, photoirradiation of N-phenylpyrrolidine (**34**) in the presence of 1,4-dicyanobenzene (**35**) and photocatalyst  $\text{Ir}(\text{ppy})_3$  produced **36**. The mechanism of the reaction is shown in Scheme 4.



**Scheme 4:** Photoredox  $\alpha$   $\text{sp}^3$  C-H arylation of *t*-amines.

\* This study was carried out by me along with Paul Kohls from Reiser's group, at the University of Regensburg as a part of INDIGO programme.<sup>9</sup>

It was gratifying to see that soon after our results<sup>9</sup>; a similar report appeared independently from Nishibayashi's group as shown in Scheme 5<sup>20</sup>.



**Scheme 5:** Photocatalytic reaction of *t*-amine **41** with alkene **42**

#### 2.4 Summary:

In conclusion, we have successfully developed a new visible light mediated photoredox catalyzed strategy of  $\alpha$   $\text{sp}^3$  C-H activation of *t*-amines for C-C bond formation reaction. In this strategy, the photoredox catalyzed generation and addition of N-aryltetrahydroisoquinoline derived  $\alpha$ -amine radicals to electron deficient alkenes were achieved using  $\text{Ru}(\text{bpy})_3\text{Cl}_2$  in combination with visible light at 452 nm generated by a blue LED. This reaction demonstrated the unprecedented trapping of photochemically generated  $\alpha$ -amino radicals. Furthermore, intramolecular variant of this reaction produced directly to 5,6-dihydroindolo[2,1-a]isoquinoline which is a privilege scaffold in biologically active immunosuppressive agent.

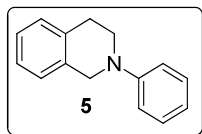
## 2.5 Experimental section:

### 2.5.1 General procedure for synthesis of starting material:

#### 2-aryl-1,2,3,4-tetrahydroisoquinoline **5** and **14**<sup>21</sup>:

Copper (I) iodide (200 mg, 1.0 mmol, 0.1 equiv.) and potassium phosphate (4.25 g, 20.0 mmol, 2 equiv.) were put into a Schlenk tube. The tube was evacuated and back filled with nitrogen. 2-Propanol (10.0 mL), ethylene glycol (1.11 mL, 20.0 mmol, 2 equiv.), 1,2,3,4- tetrahydroisoquinoline (2.0 mL, 15 mmol, 1.5 equiv.) and iodobenzene (1.12 mL, 10.0 mmol, 1 equiv.) or 1-iodo-4-methoxybenzene (2.34 g, 10.0 mmol, 1 equiv.) were added. The reaction mixture was heated to 90 °C and kept for 24 h and then allowed to cool to room temperature. Diethyl ether (20 mL) and water (20 mL) were then added to the reaction mixture. The aqueous layer was extracted by diethyl ether (2 × 20 mL). The combined organic phases were washed with brine and dried over magnesium sulfate. The solvent was removed by rotary evaporation and purified by column chromatography on silica gel (hexane/ethyl acetate=20:1), to give the desired product **5** or **14** with 63 % and 58% isolated yields respectively.

#### 2-phenyl-1,2,3,4-tetrahydroisoquinoline (**5**)<sup>21</sup>:



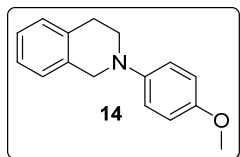
**Yield:** 63 % (light yellow solid)

**R<sub>f</sub>** (19:1 Hexanes : EtOAc) = 0.7

**<sup>1</sup>H NMR** (300 MHz, CHCl<sub>3</sub>) δ 7.34 - 7.25 (m, 2 H), 7.23 - 7.14 (m, 4 H), 7.00 (d, *J* = 8.0 Hz, 2 H), 6.84 (t, *J* = 7.3 Hz, 1 H), 4.43 (s, 2 H), 3.58 (t, *J* = 5.8 Hz, 2 H), 3.00 (t, *J* = 5.8 Hz, 2 H)

**<sup>13</sup>C NMR** (75 MHz, CHCl<sub>3</sub>) δ 150.5, 134.8, 134.4, 129.2, 128.5, 126.5, 126.3, 126.0, 118.6, 115.1, 50.7, 46.5, 29.1

**2-(4-methoxyphenyl)-1,2,3,4-tetrahydroisoquinoline (14)**<sup>21</sup>:



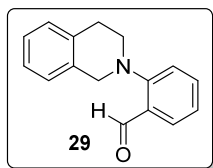
**Yield:** 58 % (light yellow solid)

**R<sub>f</sub>** (19:1 Hexanes : EtOAc) = 0.45

**<sup>1</sup>H NMR** (300 MHz, CHCl<sub>3</sub>) δ 7.23 - 7.12 (m, 4 H), 7.05 - 6.97 (m, 2 H), 6.93 - 6.85 (m, 2 H), 4.32 (s, 2 H), 3.80 (s, 3 H), 3.47 (t, *J* = 5.8 Hz, 2 H), 3.01 (t, *J* = 5.8 Hz, 2 H).

**<sup>13</sup>C NMR** (75MHz, CHCl<sub>3</sub>) δ 153.5, 145.3, 134.6, 134.5, 128.7, 126.5, 126.2, 125.9, 118.0, 114.5, 55.6, 52.6, 48.4, 29.1

**2-(3,4-dihydroisoquinolin-2(1H)-yl)benzaldehyde (29)**<sup>18</sup>:



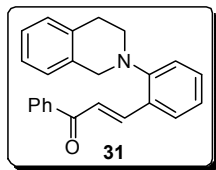
To a solution of 1,2,3,4-tetrahydroisoquinoline (540 μL, 4.5 mmol, 1.05 equiv.) in dry DMF (6 mL), dry K<sub>2</sub>CO<sub>3</sub> (558 mg, 4 mmol, 1 equiv.) was added, followed by a solution of 2-fluorobenzaldehyde (420 μL, 4 mmol, 1 equiv.) in dry DMF (4 mL) at ambient temperatures. Reaction mixture was heated to reflux for 20 h, under nitrogen atmosphere. After the completion, reaction mixture was cooled to rt, diluted with water (10 mL) and extracted with ethyl acetate (3 x 15 mL). The combined organic phases were washed once with water (15 mL) and brine (2 x 15 mL) and dried over MgSO<sub>4</sub>. The pure product was obtained as yellow oil (491 mg, 2.1 mmol, 49%) after purification on silica gel (9:1 hexanes : EtOAc).

**R<sub>f</sub>** (9:1 Hexanes : EtOAc) = 0.40.

**<sup>1</sup>H NMR** (300 MHz, CDCl<sub>3</sub>) δ 10.33 (s, 1H), 7.85 (dd, *J* = 7.7, 1.7 Hz, 1H), 7.60 – 7.47 (m, 1H), 7.29 – 6.99 (m, 6H), 4.34 (s, 2H), 3.46 (t, *J* = 5.8 Hz, 2H), 3.07 (t, *J* = 5.8 Hz, 2H).

$^{13}\text{C}$  NMR (75 MHz,  $\text{CDCl}_3$ )  $\delta$  191.4, 173.4, 155.2, 148.3, 134.9, 134.1, 130.0, 129.0, 126.6, 126.3, 126.1, 122.3, 119.0, 54.8, 53.5, 29.0.

**(E)-3-(2-(3,4-dihydroisoquinolin-2(1H)-yl)phenyl)-1-phenylprop-2-en-1-one (31):**



To a solution of acetophenone (0.5 g, 4.2 mmol, 1 equiv.) and KOH (0.4 g, 7.1 mmol, 1.7 equiv.) in absolute ethanol (25 mL) a solution of 2-(3,4-dihydroisoquinolin-2(1H)-yl)benzaldehyde (**29**) (1 g, 4.2 mmol, 1 equiv.) in absolute ethanol (25 mL) was added dropwise at 0 °C. The reaction mixture was stirred for 4 h at room temperature. After completion of reaction, as monitored by TLC analysis, the solvent was removed under reduced pressure, the residue was dissolved in diethyl ether (50 mL) and washed with water (30 mL). The aqueous layer was extracted with diethyl ether (3  $\times$  40 mL). The combined organic phases were washed with brine (25 mL) and dried with sodium sulfate. The solvent was evaporated and the crude product was purified by column chromatography (19:1 hexanes : EtOAc) to afford the desired product as red oil (1.03 g, 3.03 mmol, 72%).

$R_f$  (9:1 Hexanes : EtOAc) = 0.7.

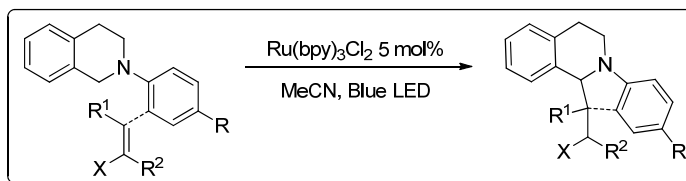
IR (neat): 1659, 1590, 1485, 1211, 1016, 740, 695  $\text{cm}^{-1}$ .

$^1\text{H}$  NMR (300 MHz,  $\text{CDCl}_3$ )  $\delta$  8.18 (d,  $J$  = 15.9 Hz, 1 H), 7.95-7.91 (m, 2 H), 7.71 (dd,  $J$  = 7.7, 1.5 Hz, 1 H), 7.59 (d,  $J$  = 15.9 Hz, 1 H), 7.53 (td,  $J$  = 2.6, 1.7 Hz, 1 H), 7.44-7.37 (m, 3 H), 7.22-7.08 (m, 6 H), 4.26 (s, 2 H), 3.33 (t,  $J$  = 5.8 Hz, 2 H), 3.05 (t,  $J$  = 5.8 Hz, 2 H).

$^{13}\text{C}$  NMR (75 MHz,  $\text{CDCl}_3$ )  $\delta$  191.1, 152.9, 142.8, 138.3, 134.6, 134.5, 132.5, 131.1, 129.1, 129.0, 128.8, 128.5 (2 C), 128.4 (2 C), 126.4, 126.3, 125.9, 122.8, 122.2, 119.3, 54.2, 52.0, 29.3.

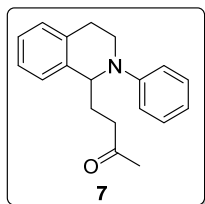
HRMS: (EI-MS)  $m/z$  calculated for  $\text{C}_{24}\text{H}_{21}\text{NO}$  [ $\text{M}^{++}$ ]: 339.1623, found 339.1618.

### 2.5.2 General procedure<sup>9</sup> for photoinduced conjugate addition of tetrahydroisoquinoline derivatives to enone systems with $\text{Ru}(\text{bpy})_3^{2+}$ :



A dry 25 mL Schlenk flask or round bottom flask equipped with a magnetic stir bar was charged with a 1,2,3,4-tetrahydroisoquinoline derivative (1 equiv.), enone (1 or 3 equiv.) and  $\text{Ru}(\text{bpy})_3\text{Cl}_2 \cdot 6\text{H}_2\text{O}$  (5 mol%) in acetonitrile (2 mL). The solution was degassed using three freeze-pump-thaw cycles and stirred at room temperature at a distance of approximately 3 cm from a blue light emitting diode (LED) ( $\lambda_{\text{max}} \sim 452$  nm). The photochemical reaction was monitored by TLC analysis. After completion the solvent was removed under reduced pressure. The residue was purified by silica gel column chromatography using hexane : ethyl acetate solvent systems to yield the desired 1,4 addition product<sup>9</sup> (The details of reaction conditions are summarized in Table 1, 2).

#### 4-(2-phenyl-1,2,3,4-tetrahydroisoquinolin-1-yl)butan-2-one (7) :



**Yield:** 75% (brown oil)

**R<sub>f</sub>** (9:1 Hexanes : EtOAc)= 0.31.

**IR** (neat): 1712, 1597, 1503, 1394, 1364, 1159, 947, 817, 751, 694, 633, 551, 534  $\text{cm}^{-1}$ .

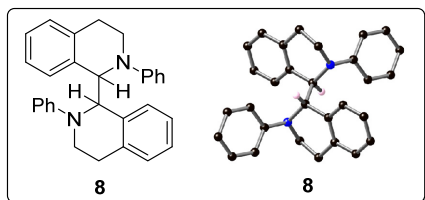
**<sup>1</sup>H NMR** (400 MHz,  $\text{CDCl}_3$ )  $\delta$  7.29 – 7.23 (m, 2 H), 7.21 – 7.10 (m, 4 H), 6.92 (d,  $J$  = 8.1 Hz, 2 H), 6.77 (t,  $J$  = 7.3 Hz, 1 H), 4.77 (dd,  $J$  = 9.1, 5.7 Hz, 1 H), 3.72 – 3.51 (m, 2 H), 3.03 (ddd,  $J$  = 15.4, 9.3, 5.7 Hz, 1 H), 2.78 (dt,  $J$  = 16.1, 4.5 Hz, 1 H), 2.60 (t,  $J$  = 6.9 Hz, 2 H), 2.26 (ddt,  $J$  = 18.9, 9.2, 6.7 Hz, 1 H), 2.18 – 2.01 (m, 4 H).



$^{13}\text{C}$  NMR (75 MHz,  $\text{CDCl}_3$ )  $\delta$  208.6, 149.8, 138.3, 134.9, 129.3 (2 C), 128.7, 127.2, 126.5, 125.9, 117.7, 114.5 (2 C), 57.9, 41.4, 40.3, 30.3, 30.2, 26.3.

**HRMS:** (EI-MS)  $m/z$  calculated for  $\text{C}_{19}\text{H}_{21}\text{NO}$  [ $\text{M}^{++}$ ]: 279.1623, found: 279.1621.

**2,2'-diphenyl-1,1',2,2',3,3',4,4'-octahydro-1,1'-biisoquinoline (8):**



**Yield:** 10% (white crystalline solid)

$R_f$  (9.8:0.2 Hexanes : EtOAc) = 0.4.

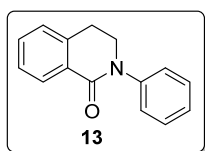
**IR** (neat): 1597, 1503, 1339, 1325, 746, 691  $\text{cm}^{-1}$ .

$^1\text{H}$  NMR (300 MHz,  $\text{CDCl}_3$ )  $\delta$  7.23-7.14 (m, 6 H), 7.09-7.04 (m, 4 H), 6.96 (d,  $J$  = 7.7 Hz, 2 H), 6.86 (d,  $J$  = 8.2 Hz, 4 H), 6.72 (t,  $J$  = 7.2 Hz, 2 H), 5.34 (s, 2 H), 3.34-3.25 (m, 4 H), 2.82 (td,  $J$  = 15.6, 5.8 Hz, 2 H), 2.63-2.54 (m, 2 H).

$^{13}\text{C}$  NMR (75 MHz,  $\text{CDCl}_3$ )  $\delta$  149.5 (2 C), 136.5 (2 C), 135.6 (2 C), 129.3 (4 C), 128.1 (2 C), 127.6 (2 C), 127.0 (2 C), 125.7 (2 C), 117.1 (2 C), 112.8 (4 C), 64.4 (2 C), 43.0 (2 C), 27.3 (2 C).

**HRMS:** (LSI-MS)  $m/z$  calculated for  $\text{C}_{30}\text{H}_{29}\text{N}_2$  [ $\text{M} + \text{H}$ ] $^+$ : 417.2325, found 417.2327.

**2-phenyl-3,4-dihydroisoquinolin-1(2H)-one (13):**



**Yield:** 42% (white solid)

$R_f$  (9:1 Hexanes : EtOAc) = 0.2.

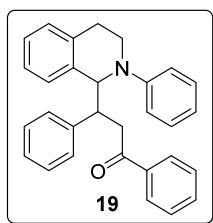
**IR** (neat): 1652, 1595, 1493, 1470, 1408, 1319, 1256, 1224, 742, 694  $\text{cm}^{-1}$ .

<sup>1</sup>H NMR (300 MHz, CDCl<sub>3</sub>) δ 8.17 (dd, *J* = 7.7, 1.3 Hz, 1 H), 7.50-7.35 (m, 6 H), 7.28-7.23 (m, 2 H), 4.00 (t, *J* = 6.5 Hz, 2 H), 3.15 (t, *J* = 6.5 Hz, 2 H).

<sup>13</sup>C NMR (75 MHz, CDCl<sub>3</sub>) δ 164.1, 143.1, 138.3, 132.0, 129.7, 128.9 (2 C), 128.7, 127.1, 126.9, 126.2, 125.3 (2 C), 49.3, 28.6.

HRMS: (EI-MS) *m/z* calculated for C<sub>15</sub>H<sub>13</sub>NO [M<sup>+</sup>]: 223.0997, found 223.0994.

**1,3-diphenyl-3-(2-phenyl-1,2,3,4-tetrahydroisoquinolin-1-yl)propan-1-one (19):**



**Yield:** 61% (white crystalline solid, Diastereomeric ratio: 7:3)

**R<sub>f</sub>** (9:1 Hexanes : EtOAc) = 0.7.

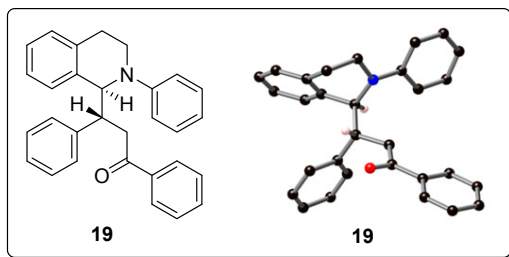
**IR** (neat): 1682, 1597, 1503, 1449, 747, 698 cm<sup>-1</sup>.

<sup>1</sup>H-NMR (300 MHz, CDCl<sub>3</sub>, major diastereomer marked with \*) δ 7.85-7.82 (m, 2 H), 7.55-7.46 (m, 1 H), 7.43-7.33 (m, 2 H), 7.25-7.16 (m, 5 H), 7.12-7.04 (m, 4 H), 6.89-6.62 (m, 4 H), 6.29 (d, *J* = 7.6 Hz, 1 H), 5.20 (d, *J* = 5.2 Hz) / 4.95\* (d, *J* = 8.9 Hz) (1 H), 4.23-4.17 / 4.09-4.02\* (m, 1 H), 3.82\* (dd, *J* = 16.6, 7.4 Hz) / 3.73 (dd, *J* = 17.5, 7.7 Hz) (1 H), 3.61-3.11 (m, 3 H), 2.89-2.72 (m, 1 H), 2.59-2.45 (m, 1 H).

<sup>13</sup>C NMR (75 MHz, CDCl<sub>3</sub>, major diastereomer marked with \*) δ 199.1 / 198.2\*, 150.5 / 149.5\*, 142.2\* / 141.4, 137.2\* / 136.8, 135.7 (2 C), 132.9 / 132.6\*, 129.2 (2 C), 129.1 (2 C), 128.5 / 128.4\* (2 C), 128.3, 128.2 (2 C), 128.0\* / 127.9 (3 C), 126.8\* / 126.6 (2 C), 125.6 / 124.9\*, 117.6 / 117.4\*, 114.8 / 113.7\* (2 C), 63.2\* / 62.2, 48.0\* / 46.8, 43.6\* / 43.2, 41.6\* / 41.2, 26.7\* / 26.5.

HRMS: (EI-MS) *m/z* calculated for C<sub>30</sub>H<sub>27</sub>NO [M<sup>+</sup>]: 417.2093, found: 417.2083.

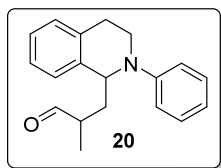
**1,3-diphenyl-3-(2-phenyl-1,2,3,4-tetrahydroisoquinolin-1-yl)propan-1-one (major isomer) (19):**



**<sup>1</sup>H-NMR** (300 MHz, CDCl<sub>3</sub>) δ 7.84-7.81 (m, 2 H), 7.51-7.45 (m, 1 H), 7.38-7.33 (m, 2 H), 7.23-7.16 (m, 5 H), 7.09-7.03 (m, 4 H), 6.88-6.70 (m, 4 H), 6.27 (d, *J* = 7.6 Hz, 1 H), 4.93 (d, *J* = 8.9 Hz, 1 H), 4.07- 4.00 ( m, 1 H ), 3.80 (dd, *J* = 16.6, 7.4 Hz, 1 H), 3.55(td, *J* = 12.1, 6.1 Hz, 1 H), 3.29-3.16 (m, 2 H), 2.75 (td, *J* = 16.0, 6.0 Hz, 1 H), 2.54-2.44 (m, 1 H).

**<sup>13</sup>C NMR** (75 MHz, CDCl<sub>3</sub>) δ 198.2, 149.5, 142.2, 137.2, 135.7 (2 C), 132.6, 129.2 (2 C), 129.1 (2 C), 128.4 (2 C), 128.3, 128.2 (2 C), 128.0 (3 C), 126.8 (2 C), 124.9, 117.4, 113.7 (2 C), 63.2, 48.0, 43.6, 41.6, 26.7.

**2-methyl-3-(2-phenyl-1,2,3,4-tetrahydroisoquinolin-1-yl)propanal (20):**



**Yield:** 50% (Yellow oil, Diastereomeric ratio: 6:4)

**R<sub>f</sub>** (9:1 Hexanes : EtOAc) = 0.70.

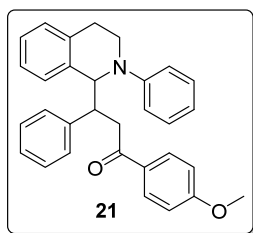
**IR** (neat): 2962, 2928, 2715, 1718, 1597, 1503, 1392, 1216, 750, 693 cm<sup>-1</sup>.

**<sup>1</sup>H NMR** (300 MHz, CDCl<sub>3</sub>, major diastereomer marked with \*) δ 9.62\* / 9.61 (s, 1 H), 7.28 – 7.21 (m, 2 H), 7.20 – 7.07 (m, 4 H), 6.90 (m, 2 H), 6.85 – 6.76 (m, 1 H), 4.80 (t, *J* = 7.4 Hz) / 4.72 (dd, *J* = 10.2, 5.0 Hz)\* (1 H), 3.72 – 3.46 (m, 2 H), 3.04 – 2.85 (m, 1 H), 2.75 – 2.59 (m, 1 H), 2.58 – 2.43 (m, 1 H), 2.20 (t, *J* = 6.6 Hz, 1 H), 1.79\* / 1.75 (d, *J* = 5.1 Hz, 1 H), 1.19 / 1.15\* (d, *J* = 6.9 Hz, 3 H).

<sup>13</sup>C NMR (75 MHz, CDCl<sub>3</sub>, major diastereomer marked with \*) δ 204.1 / 203.7\*, 149.8, 138.0 / 137.8\*, 135.0 / 134.9\*, 129.3 / 129.3\* (2C), 129.1\* / 129.0, 127.3, 126.6\* / 126.6, 126.1 / 126.1\*, 119.1\* / 119.0, 116.5\* / 116.3 (2C), 57.3\* / 55.7, 44.7\* / 43.5, 42.5 / 42.1\*, 39.5\* / 38.3, 25.8 / 25.5\*, 14.6\* / 13.8.

**HRMS:** (EI-MS) *m/z* calculated for C<sub>19</sub>H<sub>21</sub>NO [M<sup>+</sup>]: 279.1623, found: 279.1623.

**1-(4-methoxyphenyl)-3-phenyl-3-(2-phenyl-1,2,3,4-tetrahydroisoquinolin-1-yl)propan-1-one (21):**



**Yield:** 56% (pale brown solid, Diastereomeric ratio: 6:4).

**R<sub>f</sub>** (9:1 Hexanes : EtOAc) = 0.5.

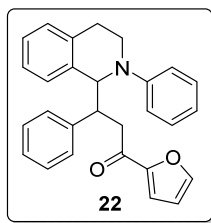
**IR** (neat): 1673, 1598, 1503, 1259, 1169, 750, 699 cm<sup>-1</sup>.

<sup>1</sup>H NMR (300 MHz, CDCl<sub>3</sub> major diastereomer marked with \*) δ 7.84-7.80 (m, 2 H), 7.24-7.01 (m, 10 H), 6.90-6.29 (m, 6 H), 5.18 (d, *J* = 5.0 Hz) / 4.94\* (d, *J* = 8.7 Hz) (1 H), 4.17 (dd, *J* = 12.8, 6.2 Hz) / 4.03\* (dd, *J* = 15.5, 7.0 Hz) (1 H), 3.85 / 3.84\* (s, 3 H), 3.77-3.63 (m, 1 H), 3.59-3.05 (m, 3 H), 2.87-2.69 (m, 1 H), 2.54-2.39 (m, 1 H).

<sup>13</sup>C NMR (75 MHz, CDCl<sub>3</sub>, major diastereomer marked with \*) δ 197.5 / 196.8\*, 163.3 / 163.1\*, 149.4, 142.3\* / 141.4, 135.7\* / 135.6 (2 C), 130.2 (3 C), 129.2 (2 C), 129.1(3 C), 128.7\* / 128.5, 128.3 / 128.1\* (2 C), 127.9 (2 C), 126.7, 126.6 / 126.5\*, 125.6 / 124.9\*, 117.2, 113.6 / 113.5\* (2 C), 63.1, 55.4, 47.8\* / 46.9, 43.7, 41.1\* / 40.7, 26.7\* / 26.4.

**HRMS:** (EI-MS) *m/z* calculated for C<sub>31</sub>H<sub>29</sub>NO<sub>2</sub> [M<sup>+</sup>]: 447.2198, found 447.2185.

**1-(furan-2-yl)-3-phenyl-3-(2-phenyl-1,2,3,4-tetrahydroisoquinolin-1-yl)propan-1-one (22):**



**Yield:** 53% (white solid, Diastereomeric ratio: 1:1).

**R<sub>f</sub>** (9:1 Hexanes : EtOAc) = 0.4.

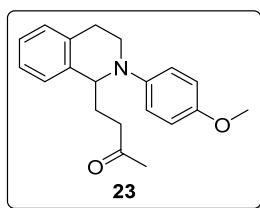
**IR** (neat): 1663, 1597, 1568, 1502, 1467, 1394, 1032, 750, 700 cm<sup>-1</sup>.

**<sup>1</sup>H NMR** (300 MHz, CDCl<sub>3</sub>) δ 7.50-7.29 (m, 2 H), 7.24-7.11 (m, 6 H), 7.08-6.94 (m, 4 H), 6.83-6.44 (m, 4 H), 6.36 (dd, *J* = 3.5, 1.7 Hz) / 6.20 (d, *J* = 7.6 Hz) (1 H), 5.13 (d, *J* = 5.7 Hz) / 4.89 (d, *J* = 9.3 Hz) (1 H), 4.17- 3.95 ( m, 1 H ), 3.71-3.34 (m, 2 H), 3.30-2.90 (m, 2 H), 2.87-2.73 (m, 1 H), 2.69-2.55 (m, 1 H).

**<sup>13</sup>C NMR** (75 MHz, CDCl<sub>3</sub>) δ 188.0 / 186.8, 152.8, 150.5 / 149.5, 146.1 / 146.0, 142.1 / 141.2 136.6 / 135.8, 135.6, 129.1 / 129.0 (2 C), 128.6 (2 C), 128.3 (2 C), 128.0 / 127.9 (2 C), 126.9 / 126.8, 126.7 / 126.6, 125.5 / 124.8, 117.6 / 117.5, 116.9 / 116.5, 115.0, 113.9, 112.1 / 112.0, 63.2 / 62.5, 48.6 / 46.6, 43.8 / 43.2, 41.6 / 41.0, 26.6 / 26.5.

**HRMS:** (EI-MS) *m/z* calculated for C<sub>28</sub>H<sub>25</sub>NO<sub>2</sub> [M<sup>+</sup>]: 407.1885, found 407.1880.

**4-(2-(4-methoxyphenyl)-1,2,3,4-tetrahydroisoquinolin-1-yl)butan-2-one (23):**



**Yield:** 63% (brown oil)

**R<sub>f</sub>** (9:1 Hexanes : EtOAc)= 0.11.

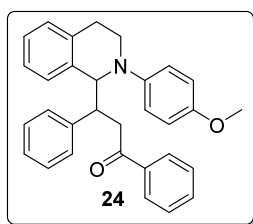
**IR** (neat): 1710, 1509, 1243, 1036, 816, 590, 454, 425, 411 cm<sup>-1</sup>.

<sup>1</sup>H NMR (400 MHz, CDCl<sub>3</sub>) δ 7.23 – 7.02 (m, 4 H), 6.90 – 6.76 (m, 4 H), 4.53 (dd, *J* = 9.4, 5.0 Hz, 1 H), 3.83 – 3.72 (m, 3 H), 3.51 (dd, *J* = 8.0, 4.1 Hz, 2 H), 2.91 (dt, *J* = 16.0, 7.9 Hz, 1 H), 2.73 – 2.52 (m, 3 H), 2.33 – 1.96 (m, 5 H).

<sup>13</sup>C NMR (100 MHz, CDCl<sub>3</sub>) δ 208.8, 153.0, 144.6, 138.5, 135.0, 128.9, 127.3, 126.4, 126.0, 118.2 (2 C), 114.7 (2 C), 58.8, 55.7, 43.1, 40.5, 30.7, 30.4, 25.9.

HRMS: (EI-MS) *m/z* calculated for C<sub>20</sub>H<sub>23</sub>NO<sub>2</sub> [M<sup>+</sup>]: 309.1729, found: 309.1727.

**3-(2-(4-methoxyphenyl)-1,2,3,4-tetrahydroisoquinolin-1-yl)-1,3-diphenylpropan-1-one (24):**



**Yield:** 43% (white solid, Diastereomeric ratio: 6.6:3.4)

**R<sub>f</sub>** (9:1 Hexanes : EtOAc) = 0.65.

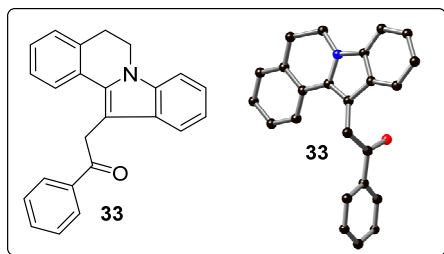
**IR** (neat): 1680, 1597, 1508, 1448, 1242, 1036, 747, 699 cm<sup>-1</sup>.

<sup>1</sup>H NMR (300 MHz, CDCl<sub>3</sub>, major diastereomer marked with \*) δ 7.88-7.78 (m, 2 H), 7.53-7.47 (m, 1 H), 7.40-7.35 (m, 2 H), 7.24 (d, *J* = 1.6 Hz) / 7.23 (d, *J* = 1.9 Hz)\* (2 H), 7.18-7.15 (m, 2 H), 7.09-7.02 (m, 3 H), 6.83-6.65 (m, 5 H), 6.14 (d, *J* = 7.6 Hz, 1 H), 5.01 (d, *J* = 4.8 Hz) / 4.68 (d, *J* = 9.3 Hz)\* (1 H), 4.13-3.97 (m, 1 H), 3.97-3.76 (m, 1 H), 3.73\* / 3.69 (s, 3 H), 3.59-3.02 (m, 3 H), 2.77-2.66 (m, 1 H), 2.51-2.38 (m, 1 H).

<sup>13</sup>C NMR (75 MHz, CDCl<sub>3</sub>, major diastereomer marked with \*) δ 199.3 / 197.9\*, 153.0 / 152.5\*, 145.8 / 144.2\*, 142.5\* / 141.6, 137.5\* / 137.3, 136.9\* / 136.1, 135.7\* / 135.6, 132.9 / 132.6\*, 129.2\* / 128.8, 128.6 / 128.5\*, 128.4 / 128.3\* (3 C), 128.2 / 128.1 (2 C)\*, 127.9, 126.8 / 126.6\*, 126.4, 125.6, 124.7, 119.2, 116.9 (2 C), 114.5 (2 C), 64.1\* / 63.2, 55.7\* / 55.6, 48.5\* / 47.1, 45.6 / 44.2\*, 42.2\* / 41.0, 26.7 / 26.0\*.

HRMS: (EI-MS) *m/z* calculated for C<sub>31</sub>H<sub>29</sub>NO<sub>2</sub> [M<sup>+</sup>]: 447.2198, found 447.2190.

**2-(5,6-dihydroindolo[2,1-a]isoquinolin-12-yl)-1-phenylethanone (33):**



After degassing using three freeze-pump-thaw cycles, (E)-3-(2-(3,4-dihydroisoquinolin-2(1H)-yl)phenyl)-1-phenylprop-2-en-1-one (**31**) (320 mg, 0.94 mmol, 1.0 equiv.) and tris(2,2'-bipyridyl)ruthenium(II)chloride hexahydrate (70 mg, 94.0  $\mu$ mol, 10 mol%) were irradiated by blue LED's in 3 mL acetonitrile for 30 h. The pure product **33** was obtained as white crystals (110 mg, 0.33 mmol, 35 %) after purification on silica gel (19:1 hexanes : EtOAc).

$R_f$  (9:1 Hexanes : EtOAc) = 0.5.

**IR** (neat): 1686, 1596, 1457, 1328, 1211, 735, 690  $\text{cm}^{-1}$ .

**$^1\text{H-NMR}$**  (300 MHz,  $\text{CDCl}_3$ )  $\delta$  8.13-8.10 (m, 2 H), 7.62-7.56 (m, 2 H), 7.51-7.46 (m, 3 H) 7.34-7.19 (m, 5 H), 7.08 (ddd,  $J$  = 1.0, 7.0, 7.9 Hz, 1 H), 4.77 (s, 2 H), 4.27 (t,  $J$  = 6.3 Hz, 2 H), 3.13 (t,  $J$  = 6.3 Hz, 2 H).

**$^{13}\text{C NMR}$**  (75 MHz,  $\text{CDCl}_3$ )  $\delta$  197.6, 136.9, 135.5, 133.9, 133.1, 132.4, 129.4, 129.0, 128.6 (2 C), 128.4 (3 C), 127.3, 127.2, 125.2, 122.1, 119.5, 118.7, 108.8, 104.0, 40.1, 36.1, 30.2.

**HRMS:** (EI-MS)  $m/z$  calculated for  $\text{C}_{24}\text{H}_{19}\text{NO}$  [ $\text{M}^+$ ]: 337.1467, found 337.1463.

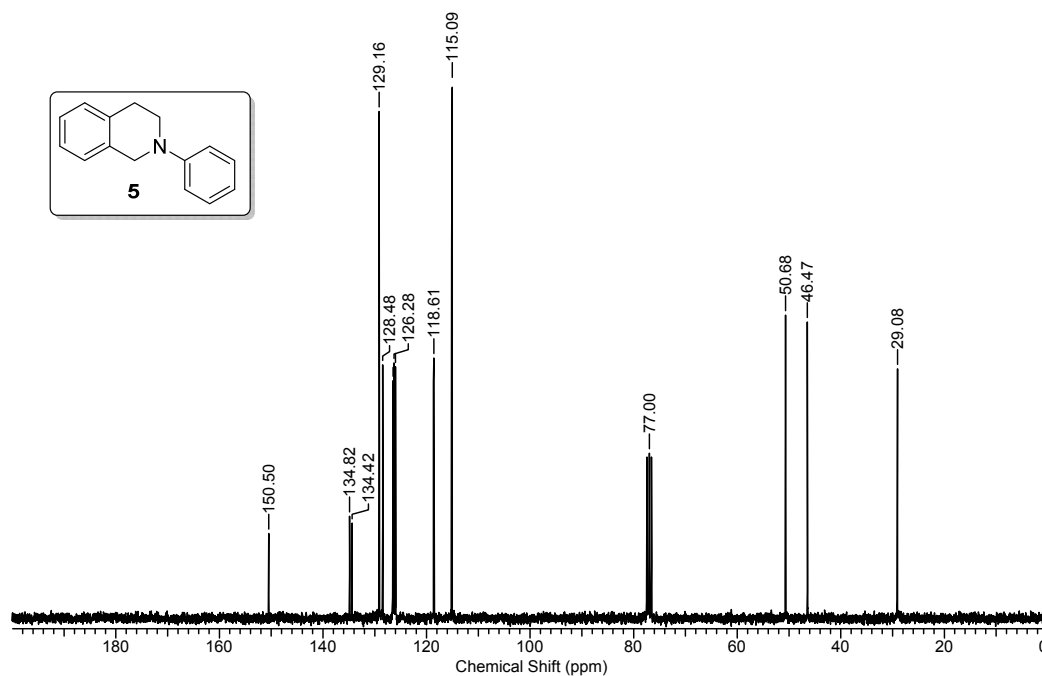
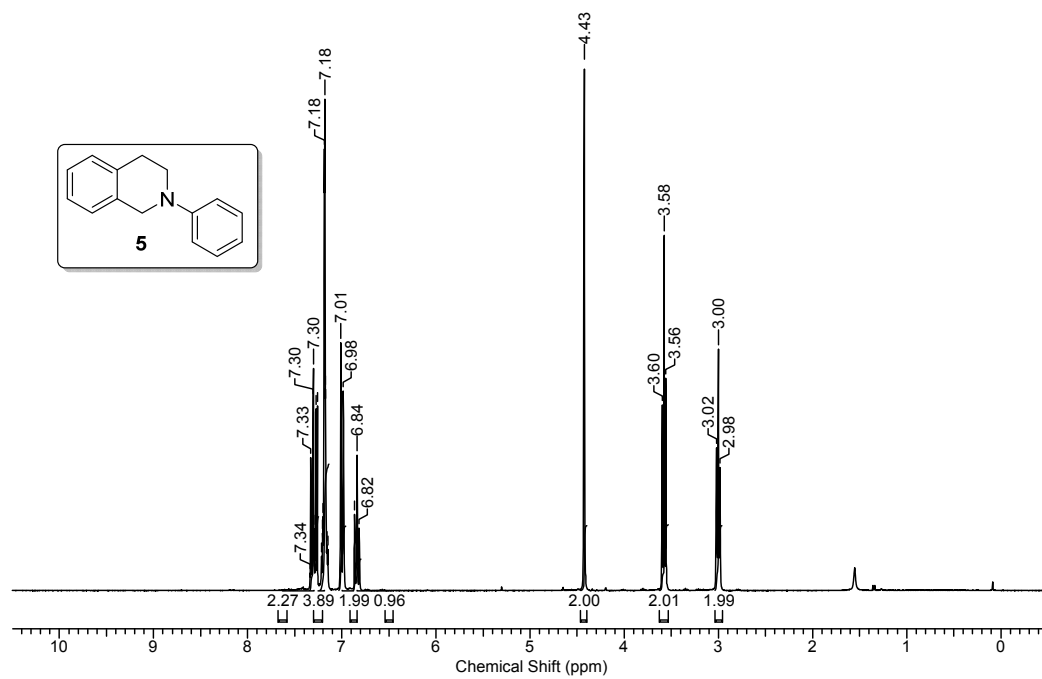
**2.6 References:**

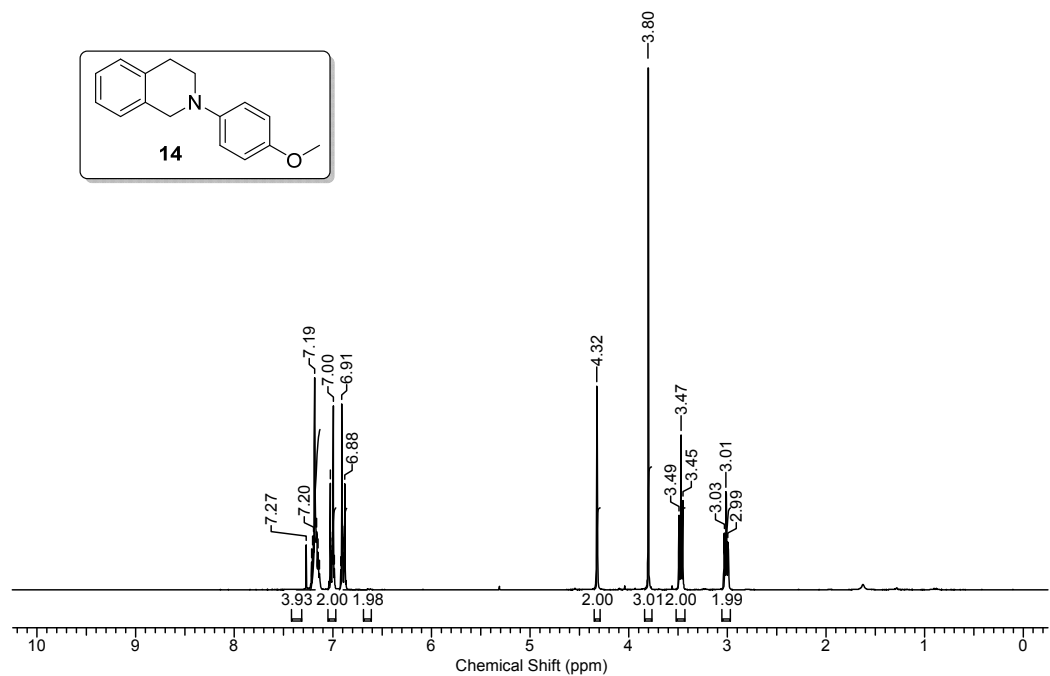
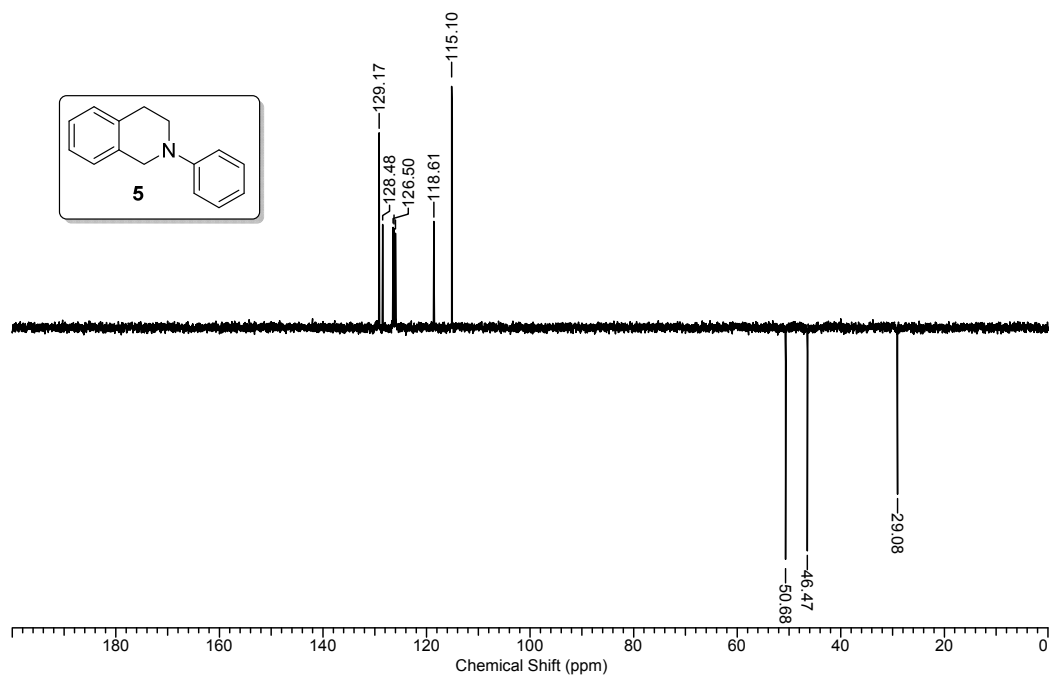
1. Prier, C. K.; Rankic, D. A.; MacMillan, D. W. C. *Chem. Rev.* **2013**, *113*, 5322-5363.
2. Narayanam, J. M. R.; Stephenson, C. R. J. *Chem. Soc. Rev.* **2011**, *40*, 102-113.
3. Yoon, T. P.; Ischay, M. A.; Du, J. *Nat. Chem.* **2010**, *2*, 527-532.
4. Filip, T. *Collect. Czech. Chem. Commun.* **2011**, *76*, 859-917.
5. Xuan, J.; Xiao, W.-J. *Angew. Chem. Int. Ed.* **2012**, *51*, 6828-6838.
6. Hari, D. P.; König, B. *Angew. Chem. Int. Ed.* **2013**, *52*, 4734-4743.
7. Xi, Y.; Yi, H.; Lei, A. *Org. Biomol. Chem.* **2013**, *11*, 2387-2403.
8. (a) Kalyanasundaram, K. *Coord. Chem. Rev.* **1982**, *46*, 159-244. (b) Juris, A.; Balzani, V.; Barigelletti, F.; Campagna, S.; Belser, P.; von Zelewsky, A. *Coord. Chem. Rev.* **1988**, *84*, 85-277. (c) Campagna, S.; Puntoriero, F.; Nastasi, F.; Bergamini, G.; Balzani, V. *Top. Curr. Chem.* **2007**, *280*, 117-214.
9. Kohls, P.; Jadhav, D.; Pandey, G.; Reiser, O. *Org. Lett.* **2012**, *14*, 672-675.
10. (a) Bryce-Smith, D.; Clarke, M. T.; Gilbert, A.; Klunklin, G.; Manning, C. *J. Chem. Soc. Chem. Commun.* **1971**, 916-918. (b) Barltrop, J. A. *Pure and Appl. Chem.* **1973**, *33*, 179-195. (c) Yang, N. C.; Shold, D. M.; Kim, B. *J. Am. Chem. Soc.* **1976**, *98*, 6587-6596. (d) Bellas, M.; Bryce-Smith, D.; Clarke, M. T.; Gilbert, A.; Klunkin, G.; Krestonosich, S.; Manning, C.; Wilson, S. *J. Chem. Soc. Perkin Trans 1* **1977**, 2571-2580.
11. (a) Lewis, F. D.; Ho, T.-I.; Simpson, J. T. *J. Org. Chem.* **1981**, *46*, 1077-1082. (b) Lewis, F. D. *Acc. Chem. Res.* **1986**, *19*, 401-405.
12. (a) Hasegawa, E.; Xu, W.; Mariano, P. S.; Yoon, U. C.; Kim, J. U. *J. Am. Chem. Soc.* **1988**, *110*, 8099-8111. (b) Jeon, Y. T.; Lee, C. P.; Mariano, P. S. *J. Am. Chem. Soc.* **1991**, *113*, 8847-8863. (c) Xu, W.; Zhang, X. M.; Mariano, P. S. *J. Am. Chem. Soc.* **1991**, *113*, 8863-8878. (d) Yoon, U. C.; Mariano, P. S. *Acc. Chem. Res.* **1992**, *25*, 233-240.
13. (a) Bertrand, S.; Glapski, C.; Hoffmann, N.; Pete, J.-P. *Tetrahedron Lett.* **1999**, *40*, 3169-3172. (b) Bertrand, S.; Hoffmann, N.; Pete, J.-P. *Eur. J. Org. Chem.* **2000**, *2000*, 2227-2238. (c) Harakat, D.; Pesch, J.; Marinkovic, S.; Hoffmann, N. *Org. Biomol. Chem.* **2006**, *4*, 1202-1205.
14. (a) Cookson, R. C.; De B. Costa, S. M.; Hudec, J. *J. Chem. Soc. D: Chem. Commun.* **1969**, 753-754. (b) Das, S.; Kumar, J. S. D.; Thomas, K. G.;

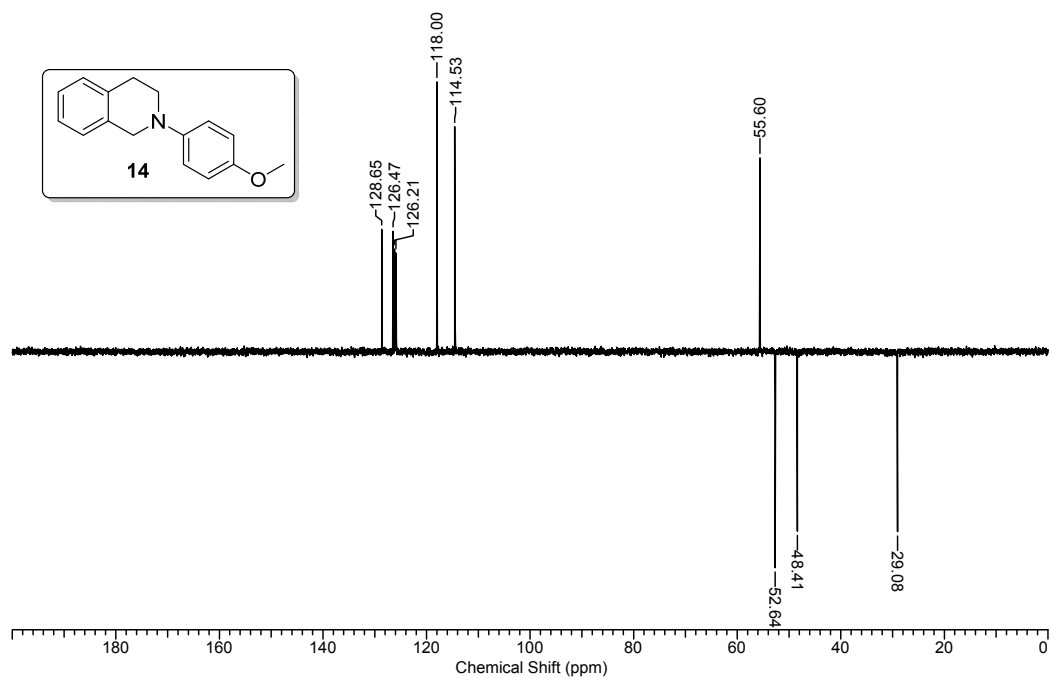
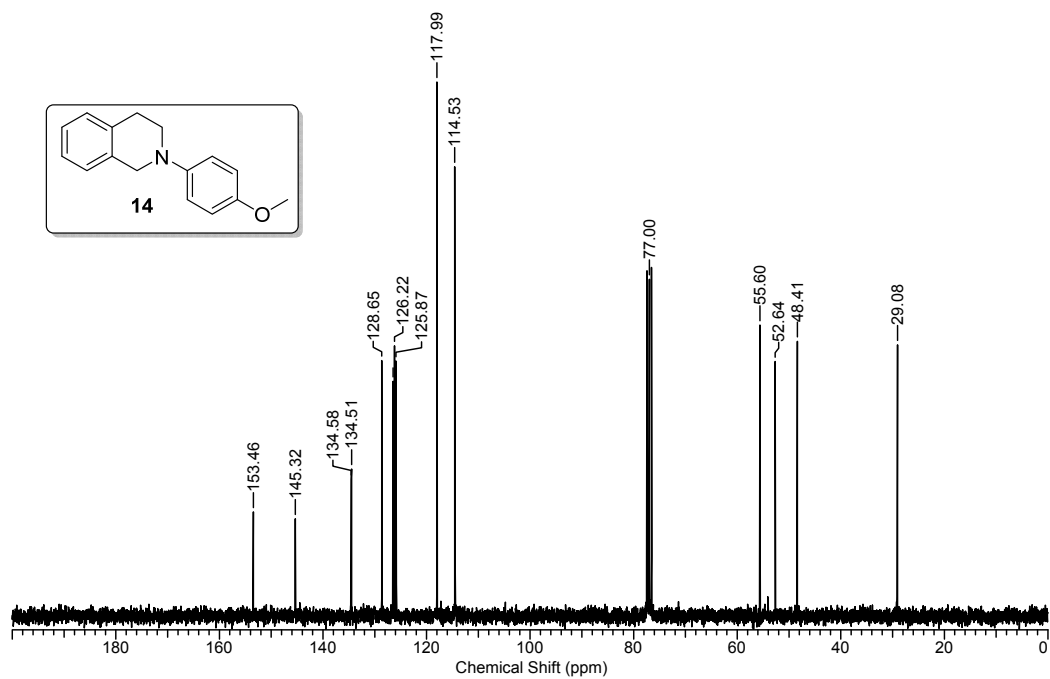


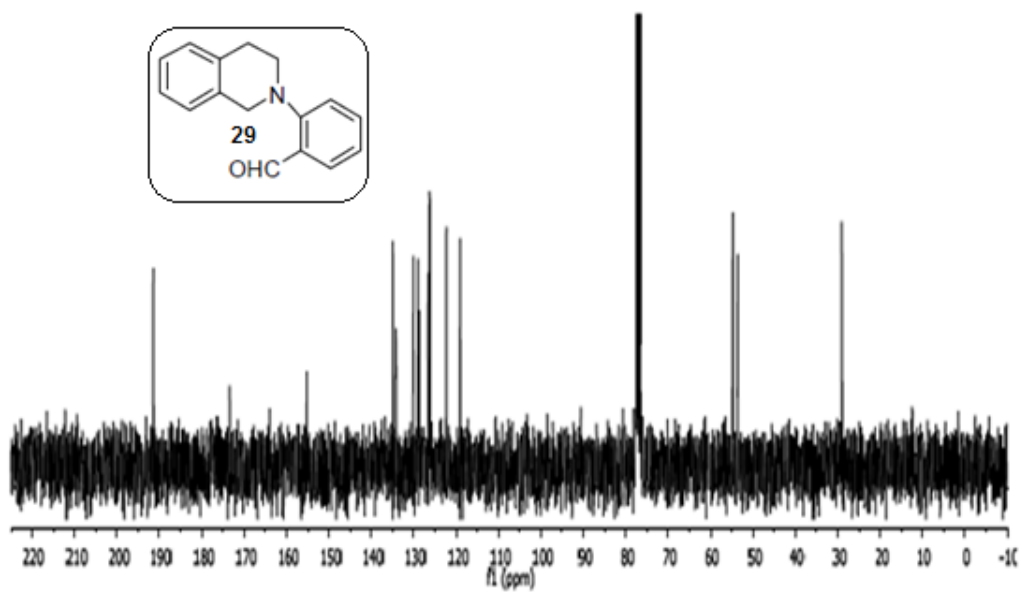
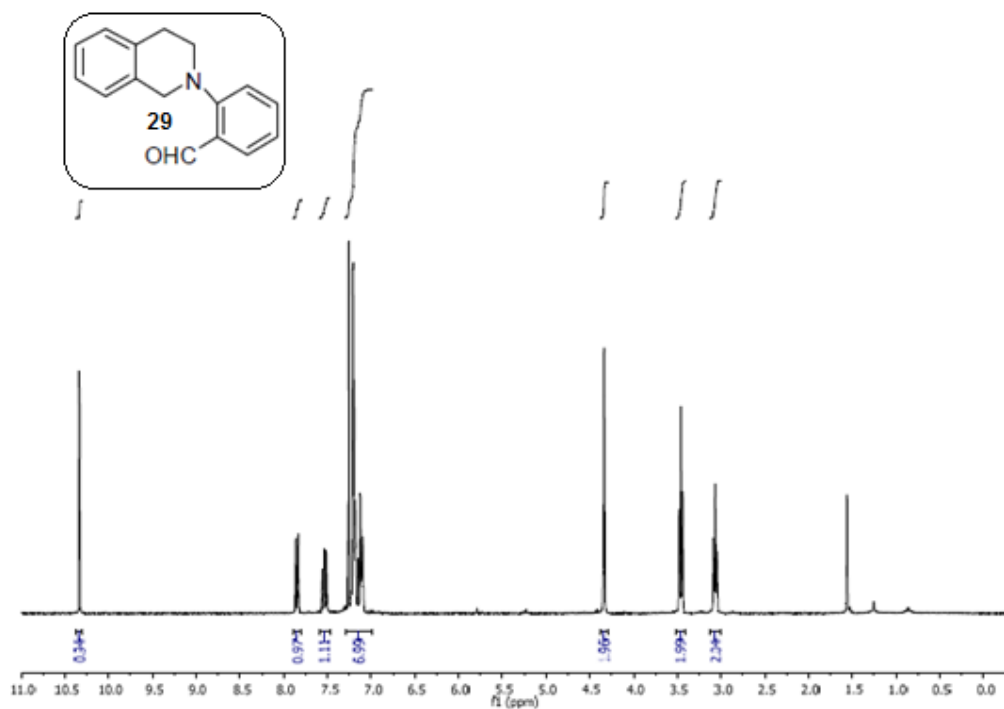
- Shivaramayya, K.; George, M. V. *J.Org.Chem.* **1994**, *59*, 628-634. (c)  
Alvarenga, E. S. d.; Cardin, C. J.; Mann, J. *Tetrahedron* **1997**, *53*, 1457-1466.  
(d) Bauer, A.; Westkamper, F.; Grimme, S.; Bach, T. *Nature* **2005**, *436*, 1139-1140.
15. (a) Pandey, G.; Kumaraswamy, G. *Tetrahedron Lett.* **1988**, *29*, 4153-4156. (b) Pandey, G.; Kumaraswamy, G.; Bhalerao, U. T. *Tetrahedron Lett.* **1989**, *30*, 6059-6062. (c) Pandey, G. *Synlett* **1992**, 546-552. (d) Pandey, G.; Kumaraswamy, G.; Reddy, P. Y. *Tetrahedron* **1992**, *48*, 8295-8308. (e) Pandey, G.; Rani, K. S.; Lakshmaiah, G. *Tetrahedron Lett.* **1992**, *33*, 5107-5110. (f) Pandey, G.; Devi Reddy, G.; Kumaraswamy, G. *Tetrahedron* **1994**, *50*, 8185-8194. (g) Pandey, G.; Gadre, S. R. *Arkivoc* **2003**, 45-54.
16. Anderson, C. P.; Salmon, D. J.; Meyer, T. J.; Young, R. C. *J. Am. Chem. Soc.* **1977**, *99*, 1980-1982.
17. Liu, Q.; Li, Y.-N.; Zhang, H.-H.; Chen, B.; Tung, C.-H.; Wu, L.-Z. *Chem. Eur. J.* **2012**, *18*, 620-627.
18. Kraus, G. A.; Gupta, V.; Kohut, M.; Singh, N. *Biorg. Med. Chem. Lett.* **2009**, *19*, 5539-5542.
19. McNally, A.; Prier, C.; MacMillan, D. *Science* **2011**, *334*, 1114-1117.
20. Miyake, Y.; Nakajima, K.; Nishibayashi, Y. *J. Am. Chem. Soc.* **2012**, *134*, 3338-3341.
21. Li, Z.; Li, C.-J. *J. Am. Chem. Soc.* **2005**, *127*, 6968-6969.
22. Cheng, C.-Y.; Tsai, H.-B.; Lin, M.-S. *J. Heterocyclic Chem.* **1995**, *32*, 73-77

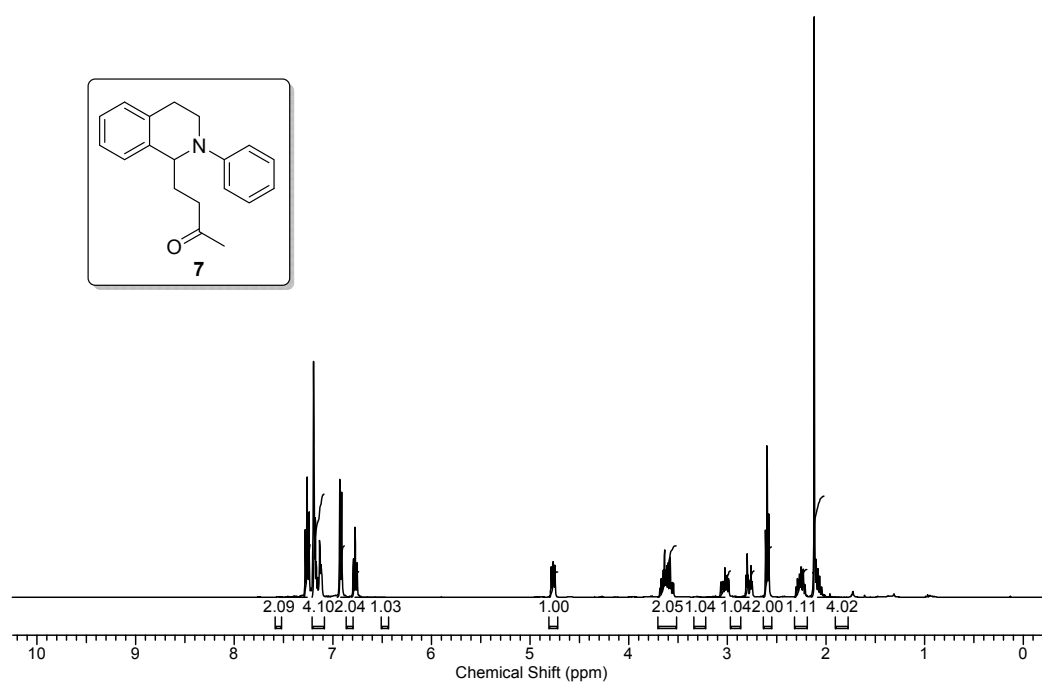
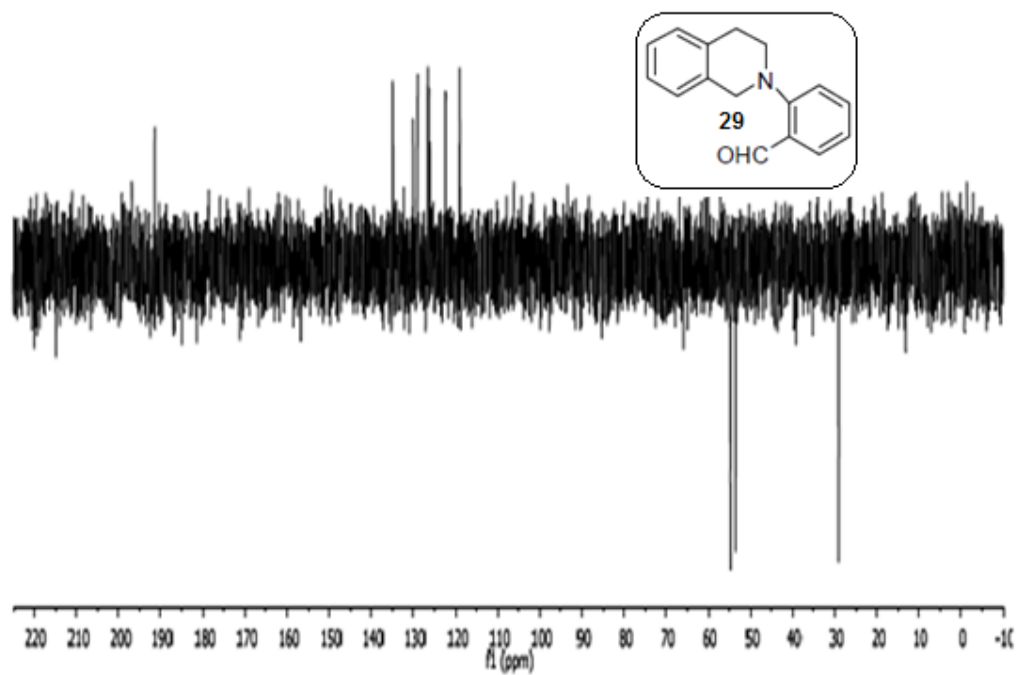
2.7 Spectra:

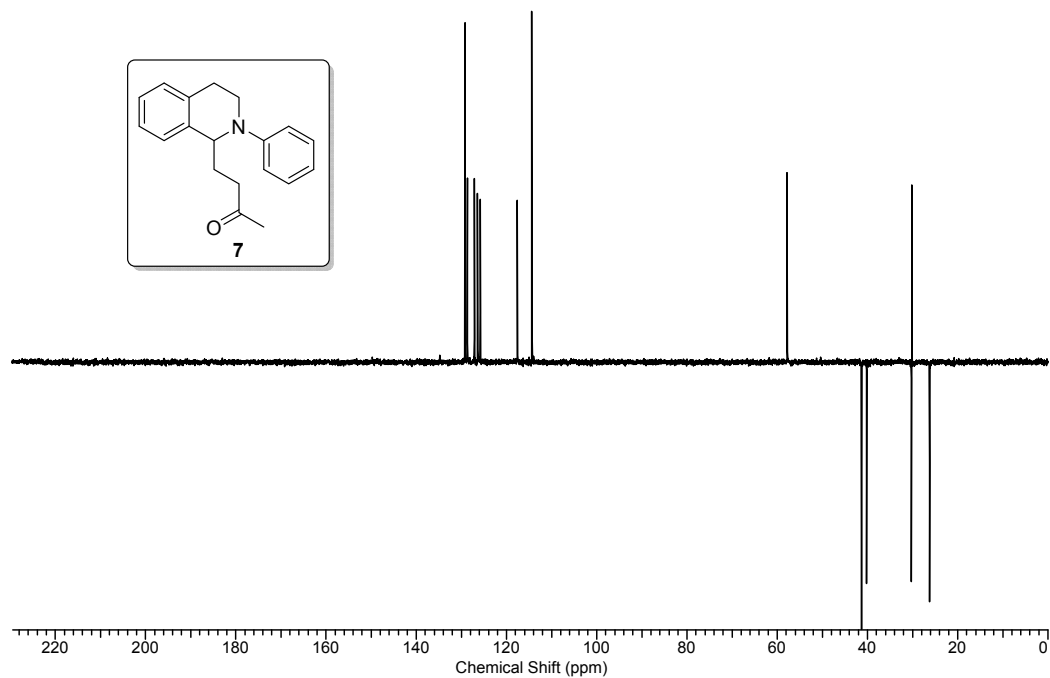
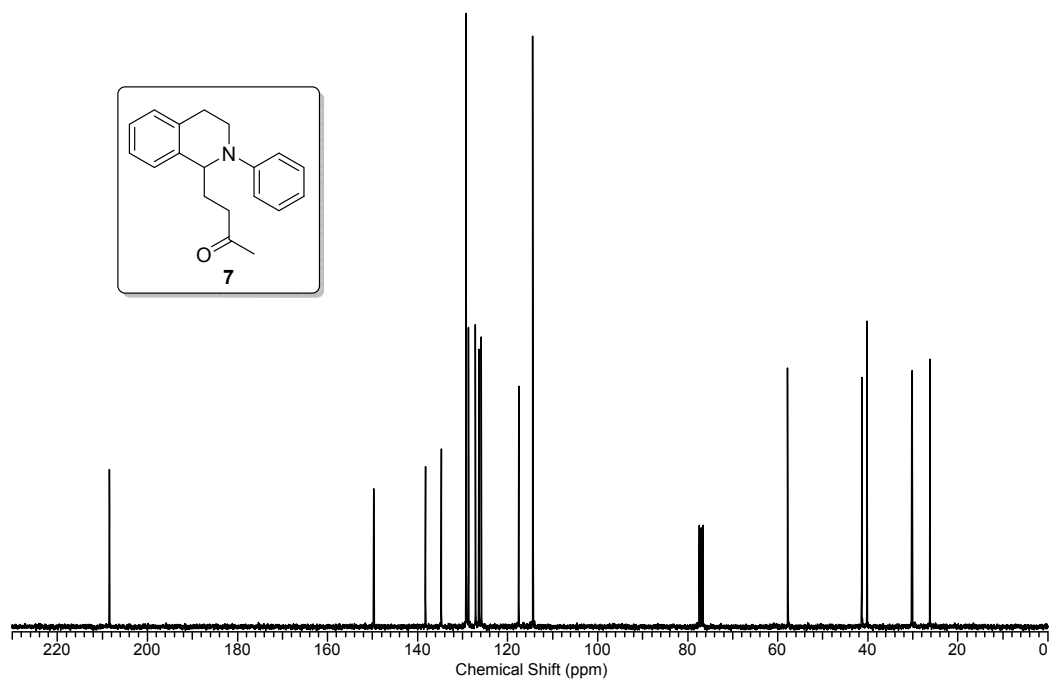


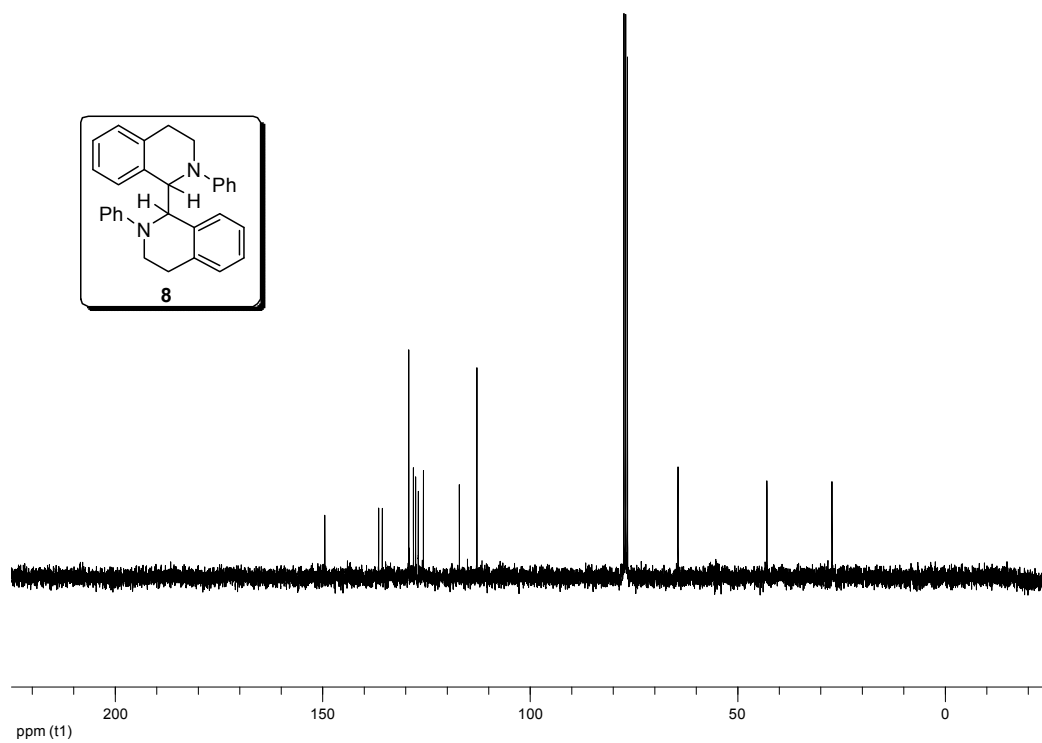
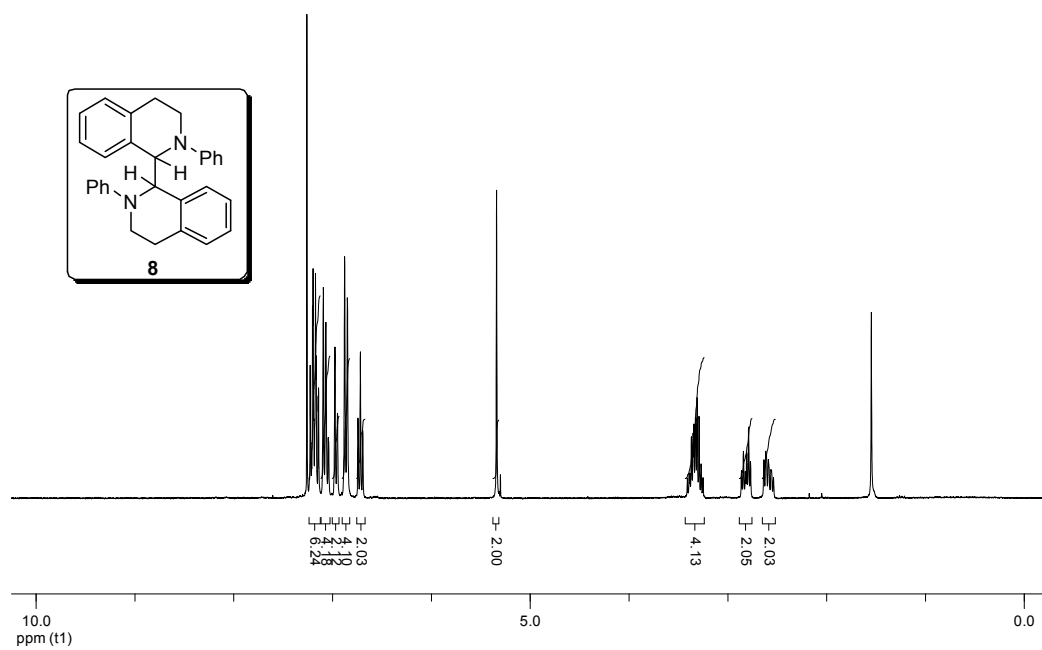




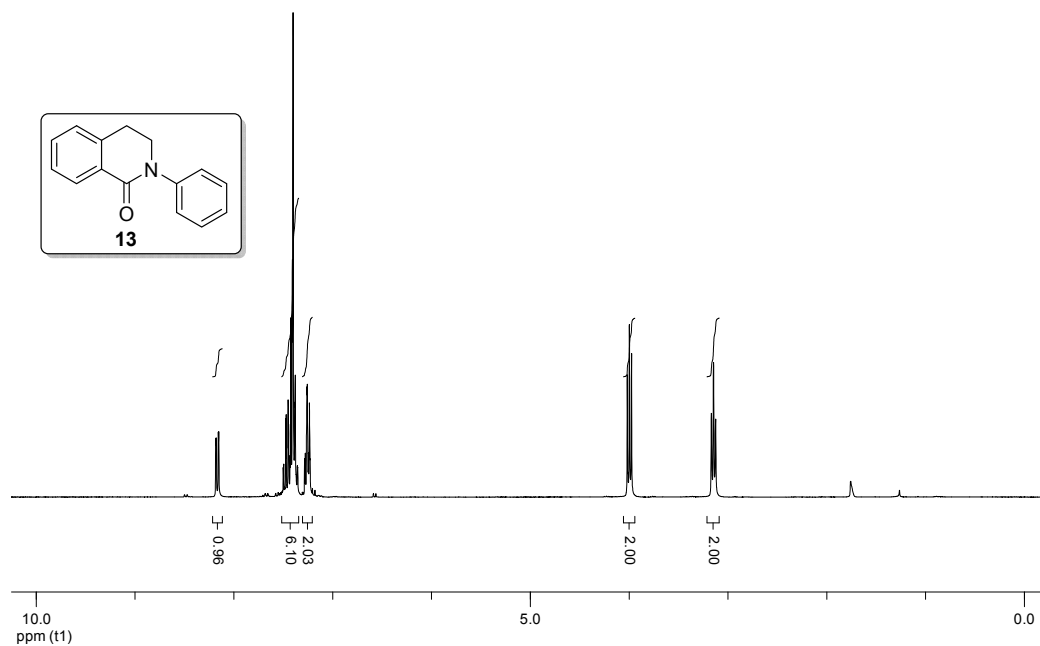
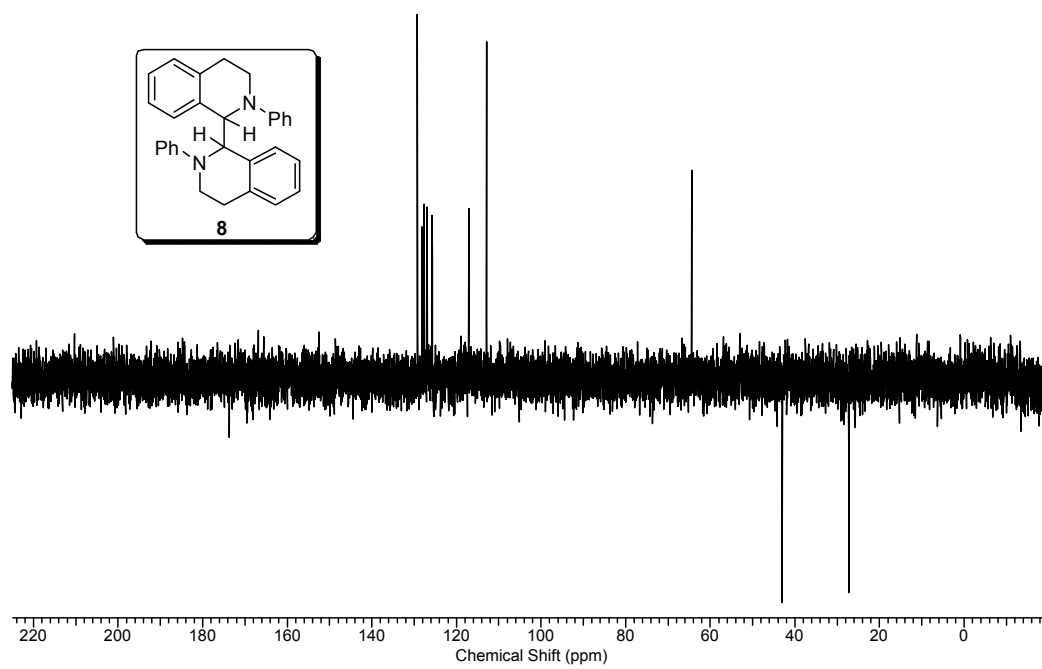


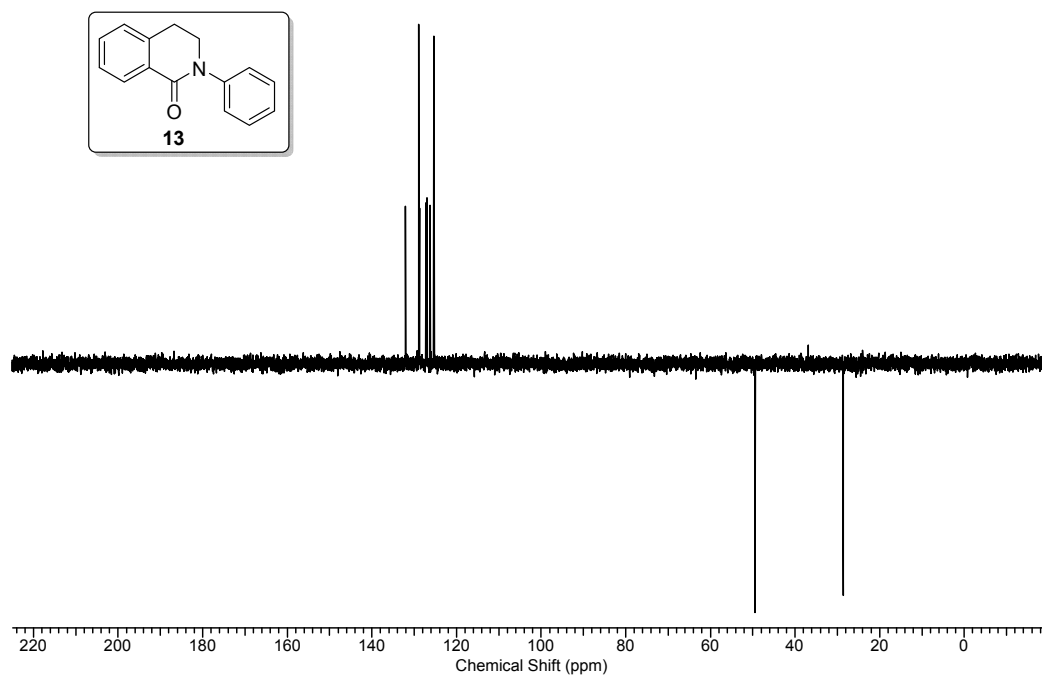
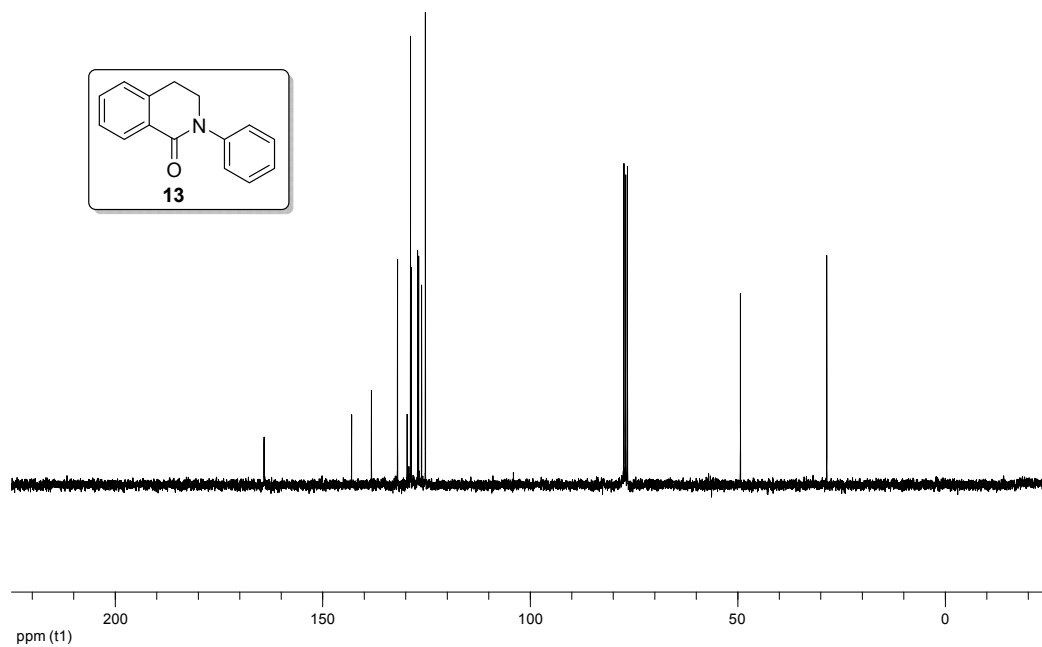


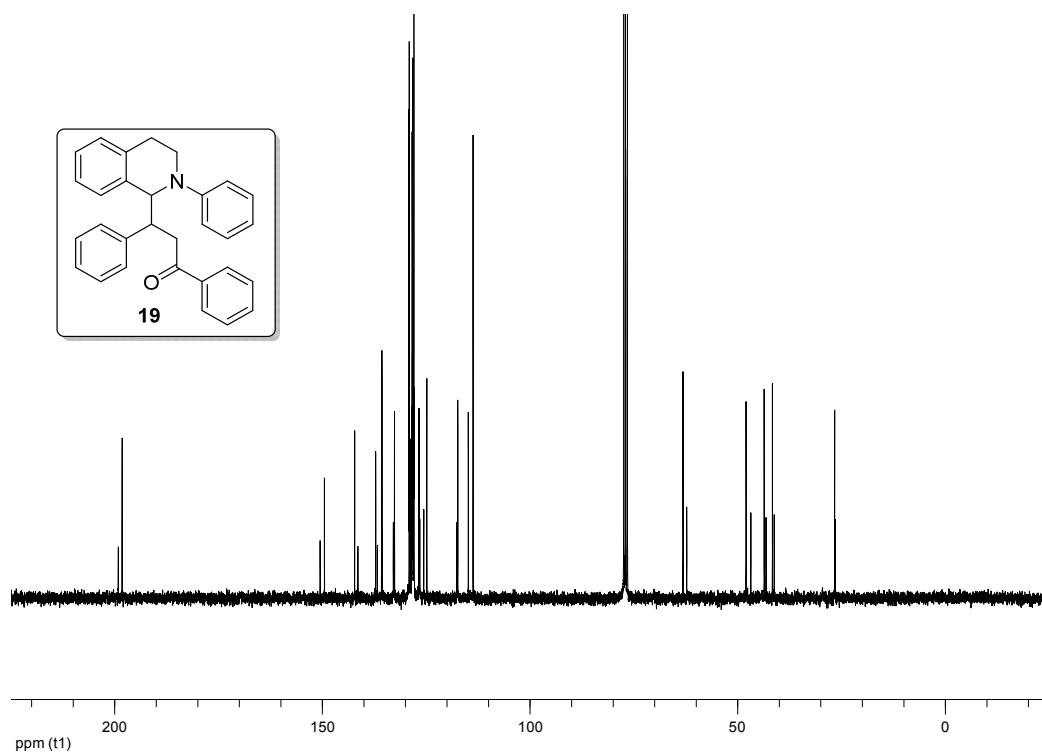
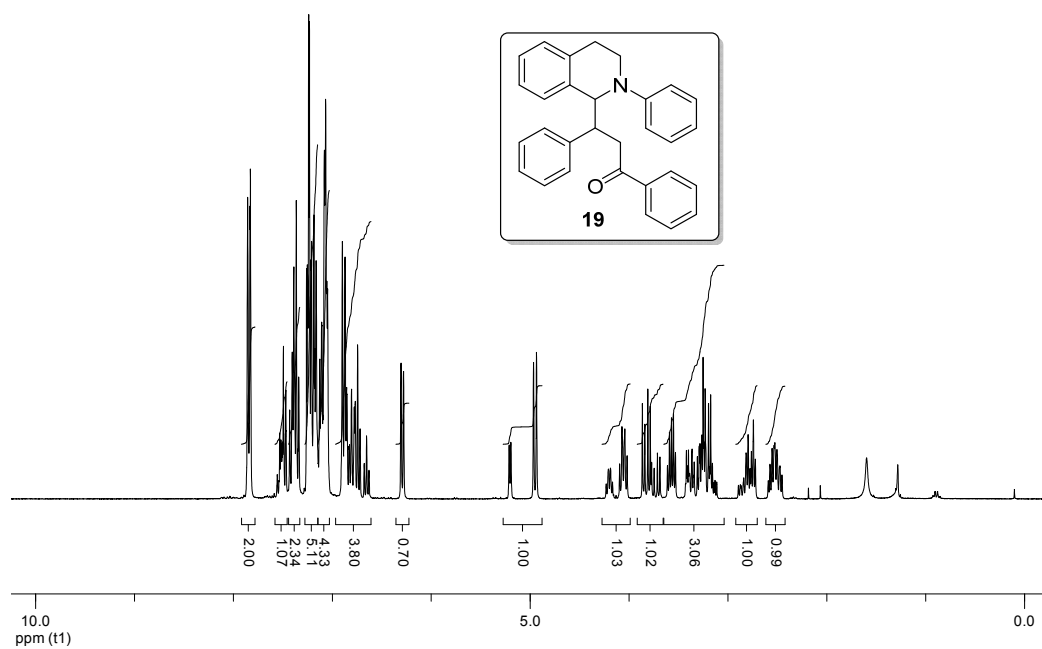


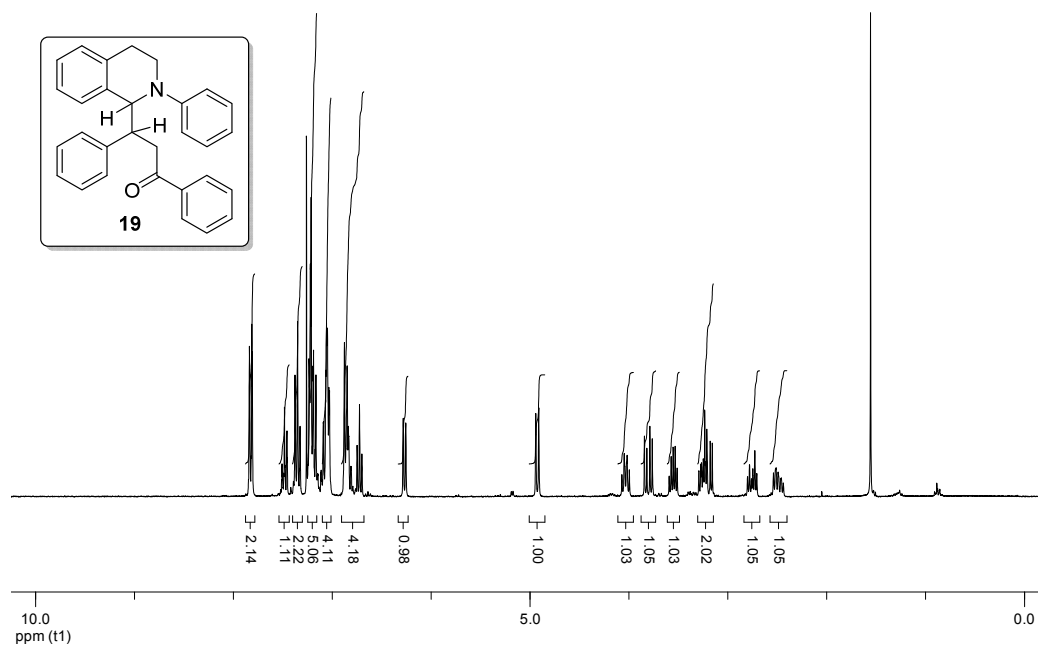
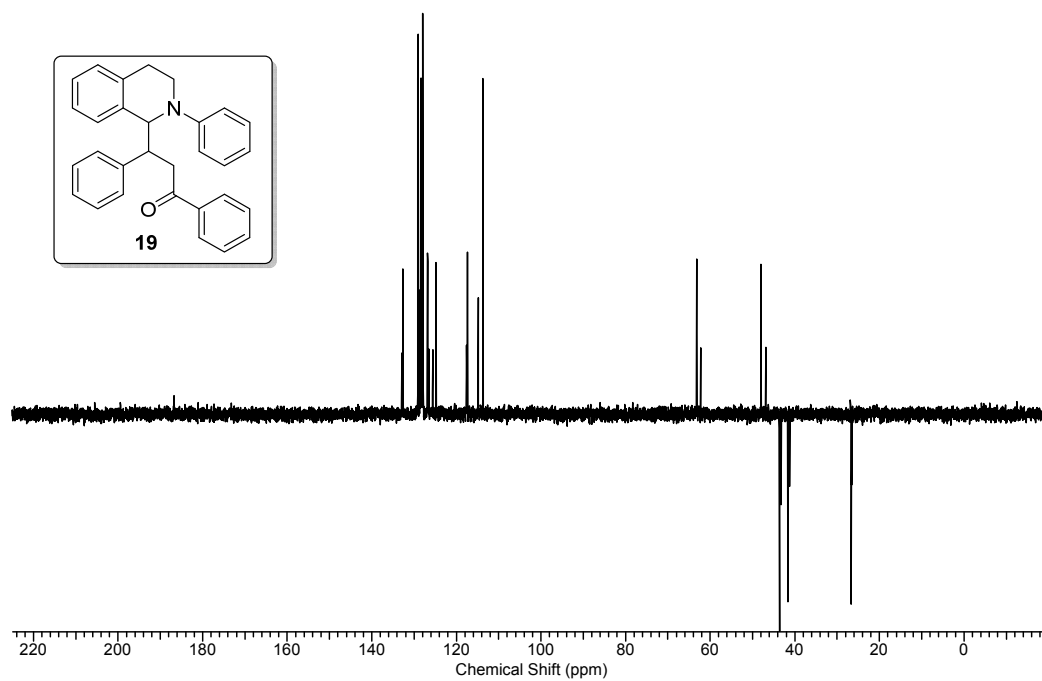


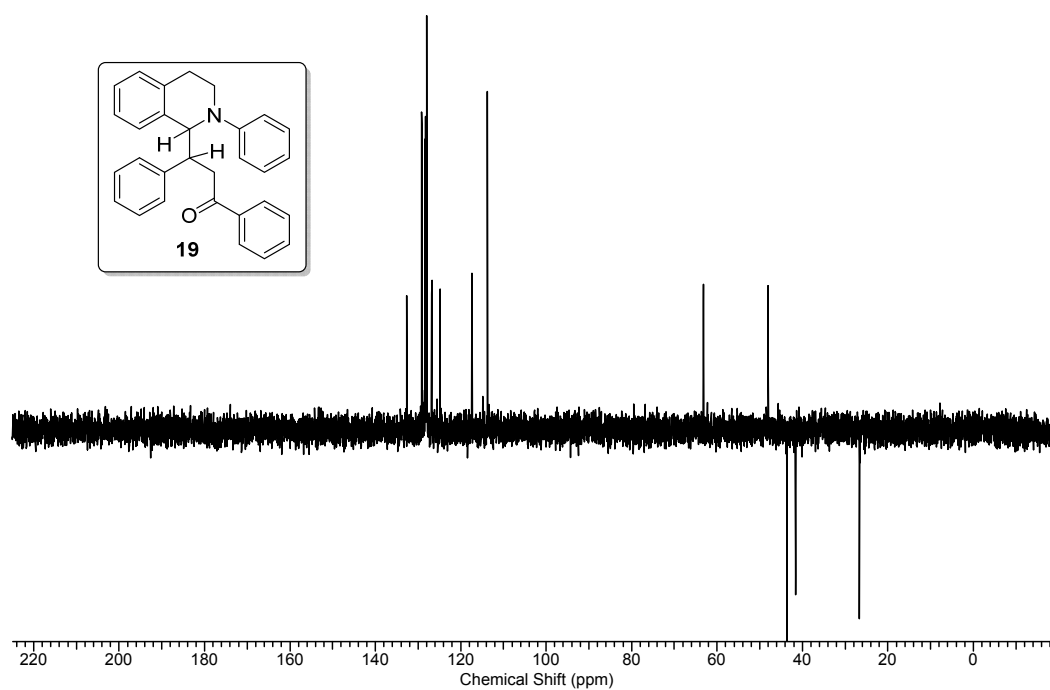
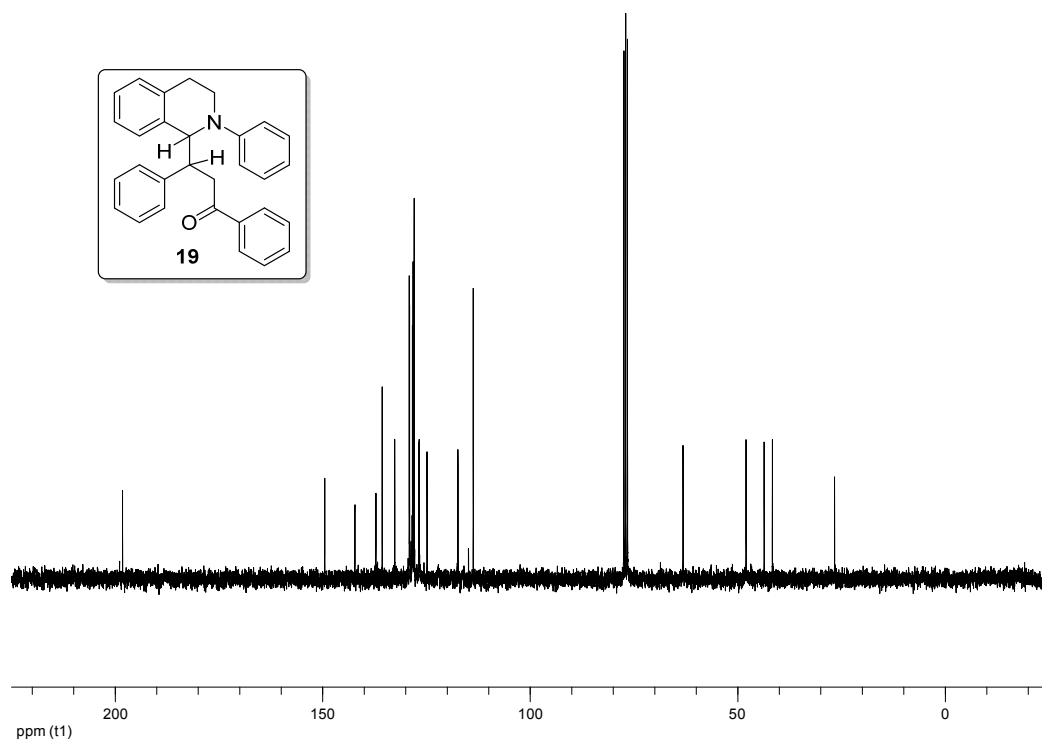


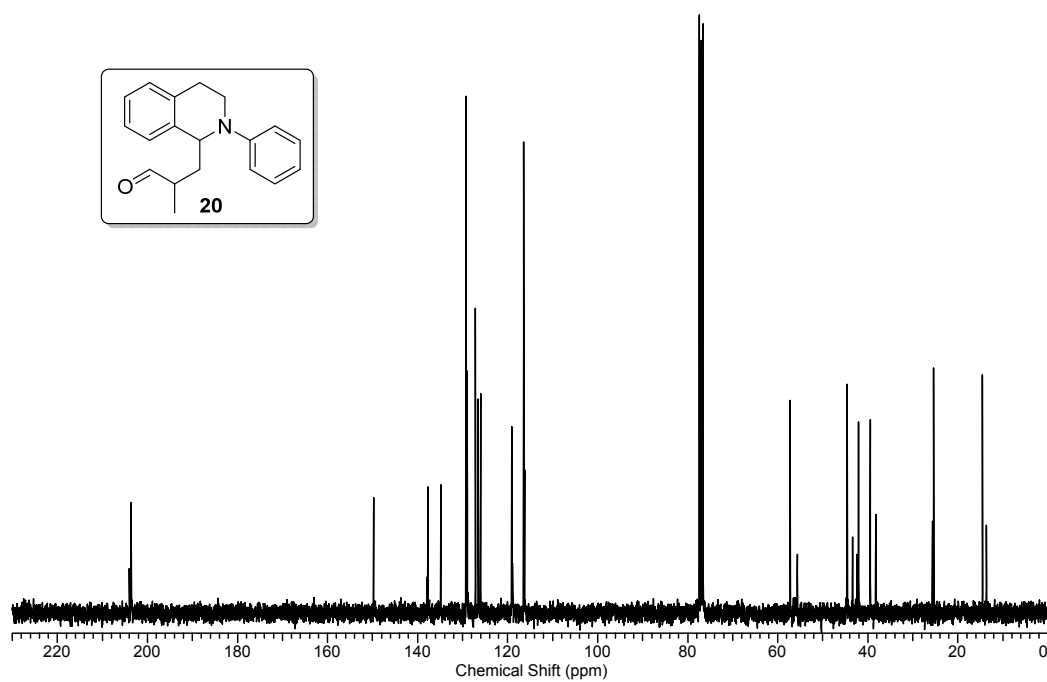
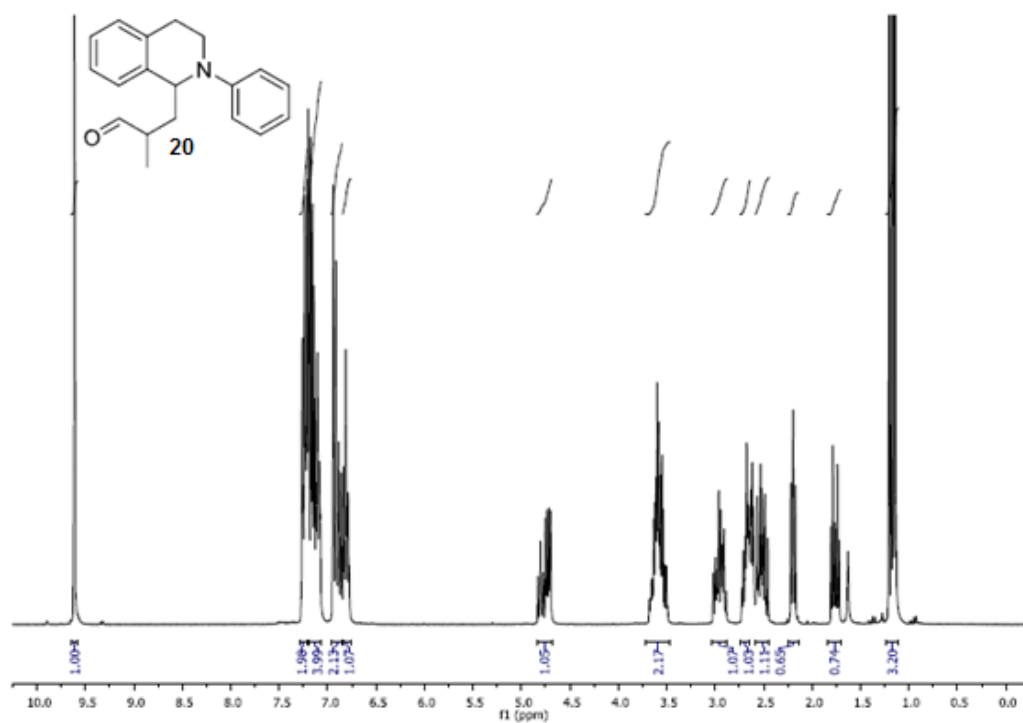


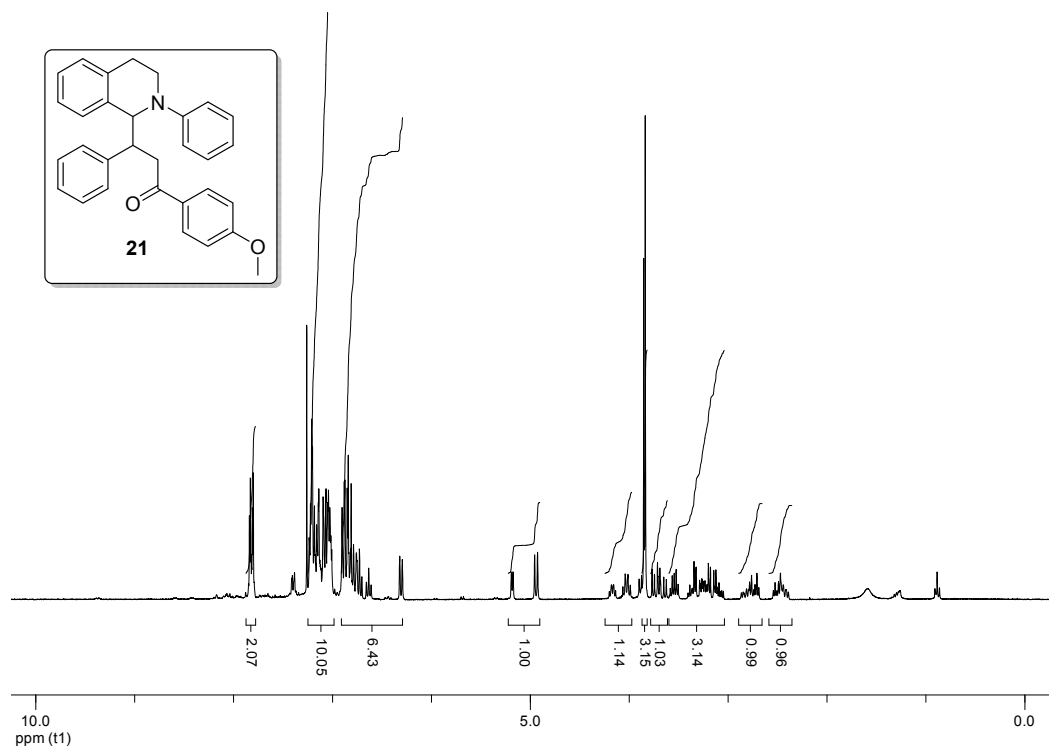
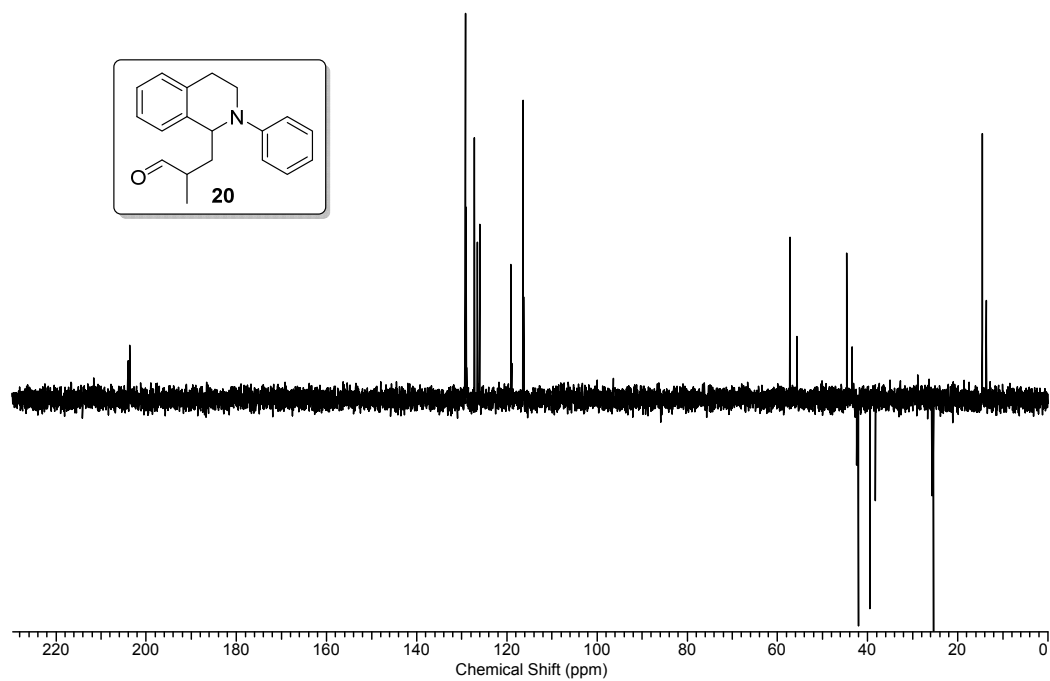


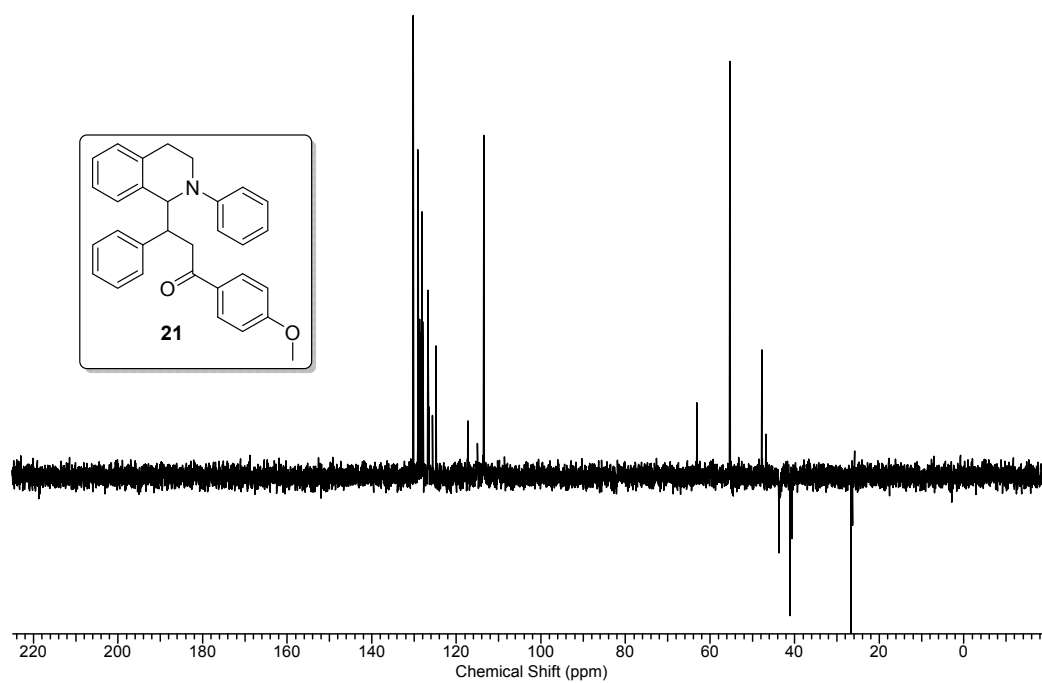
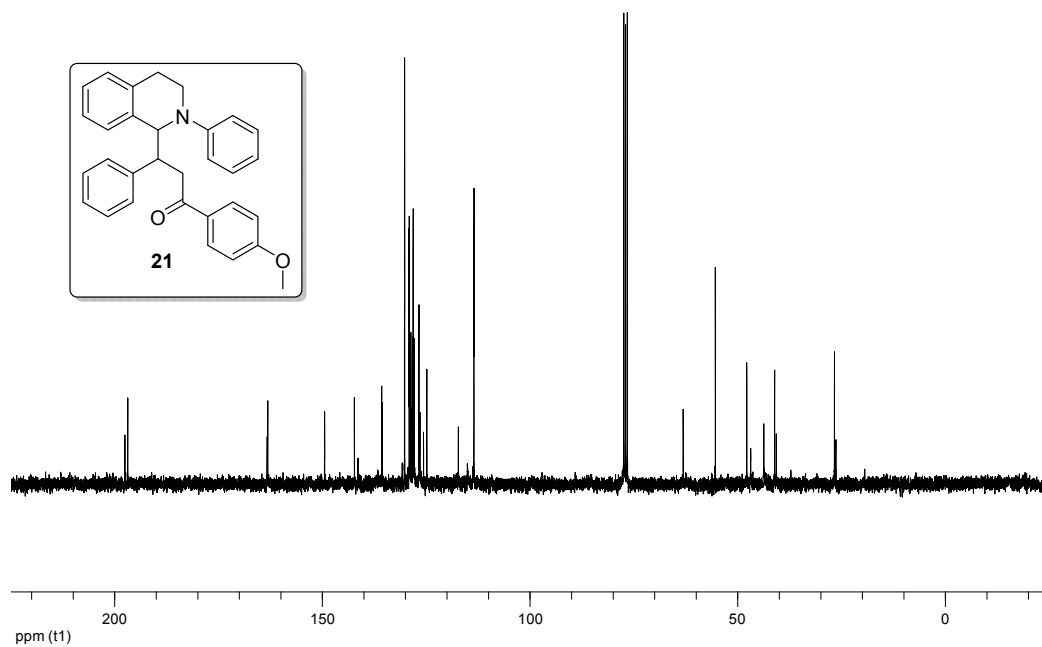




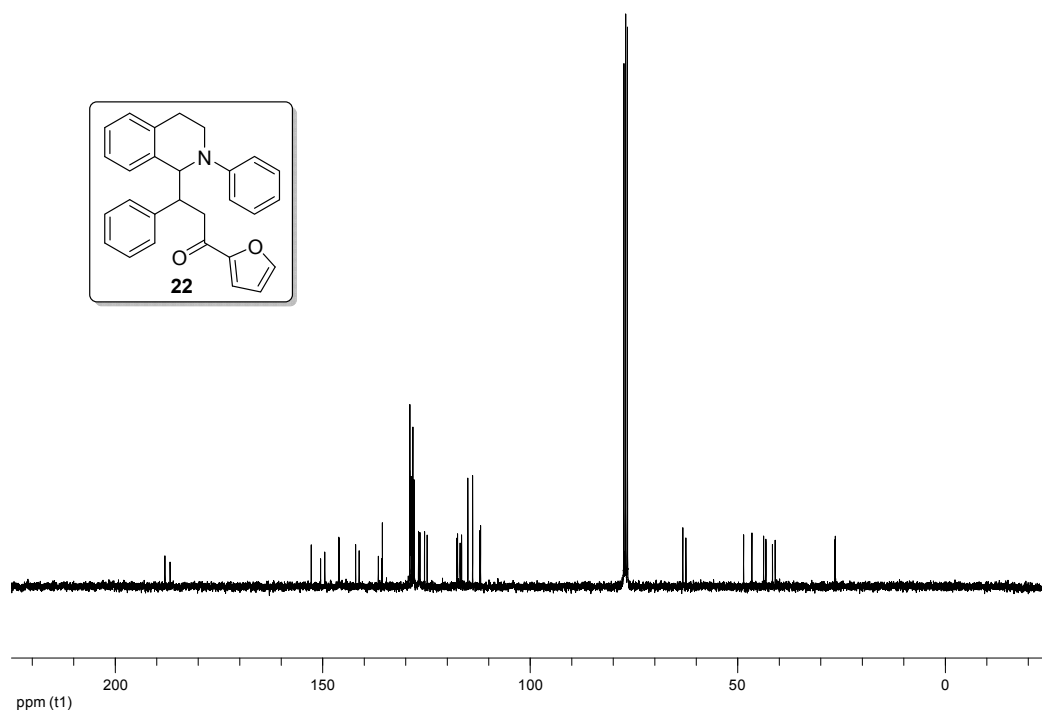
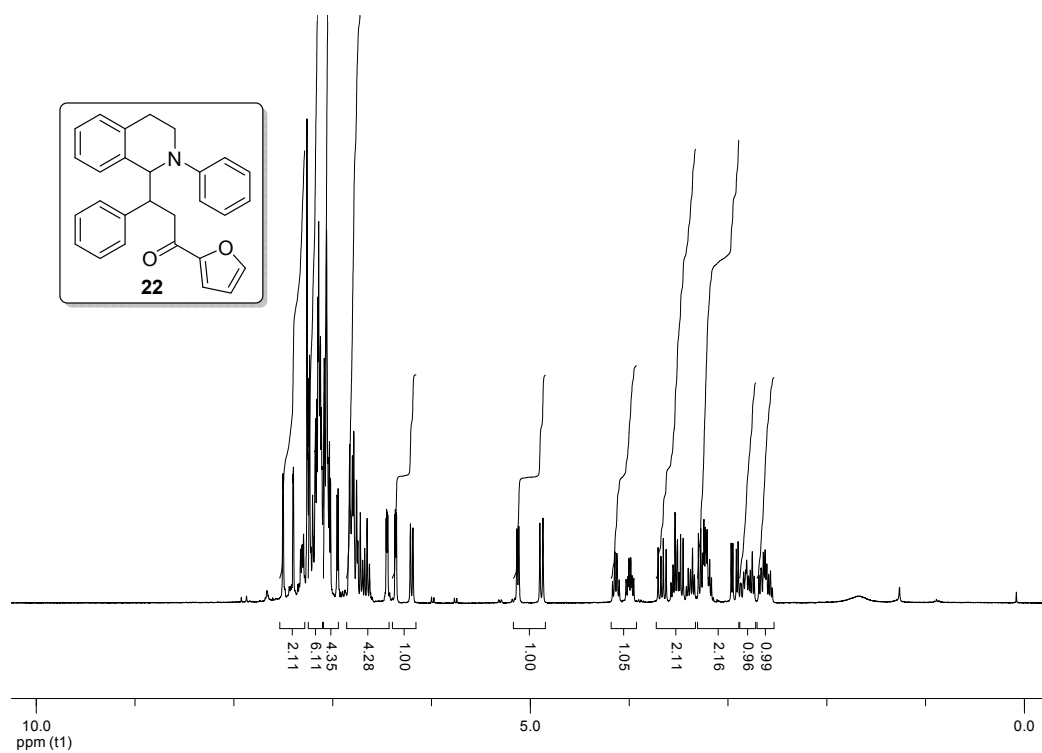


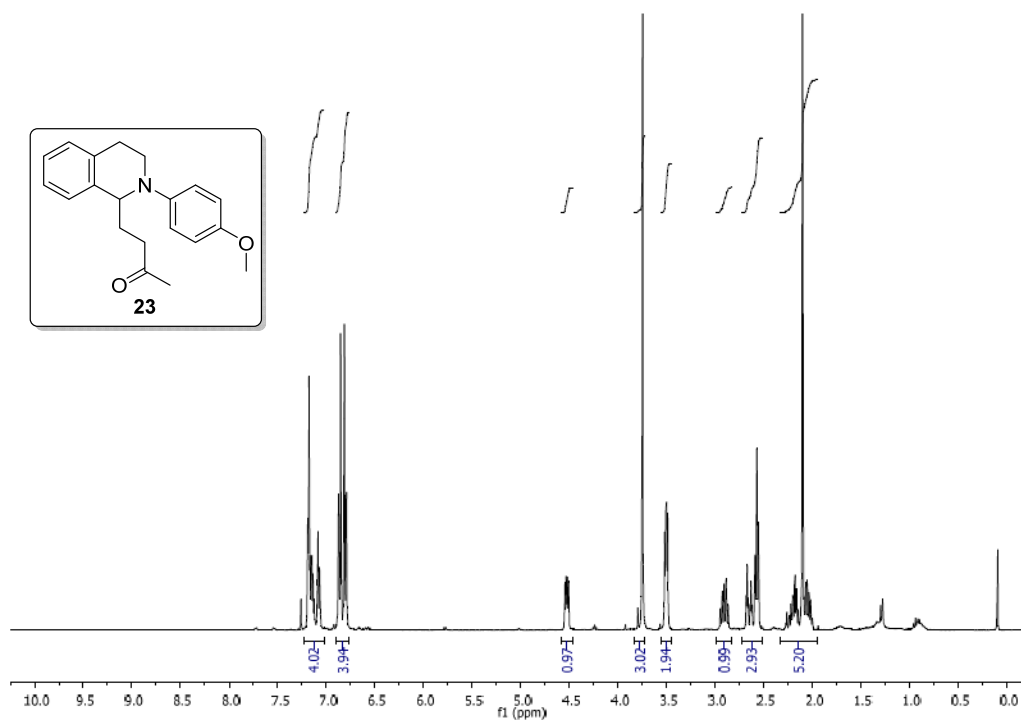
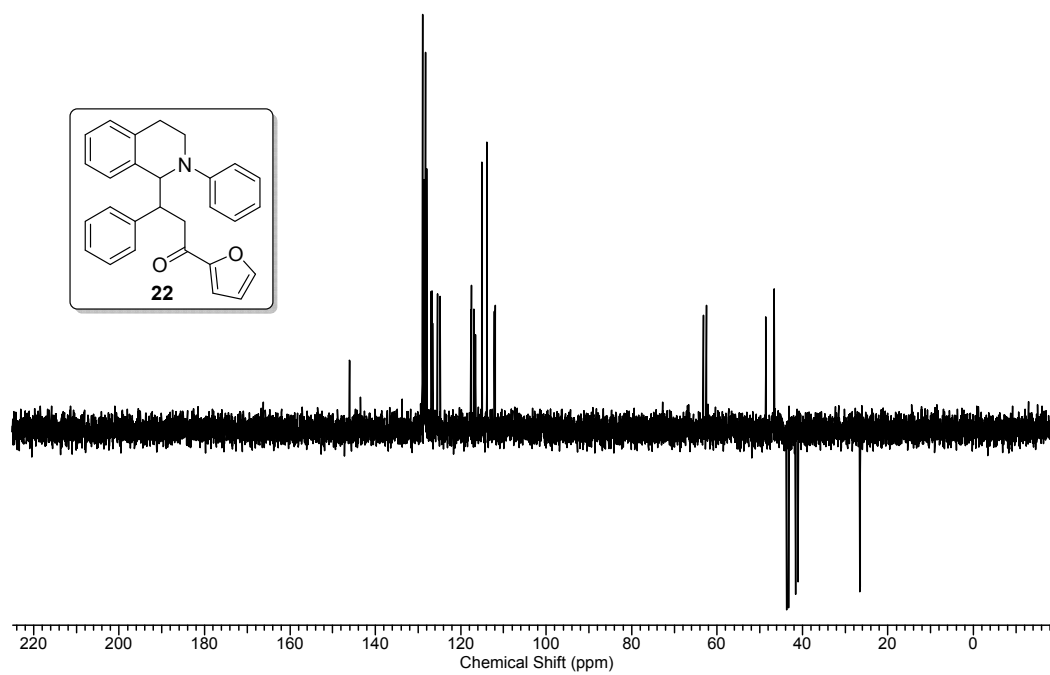


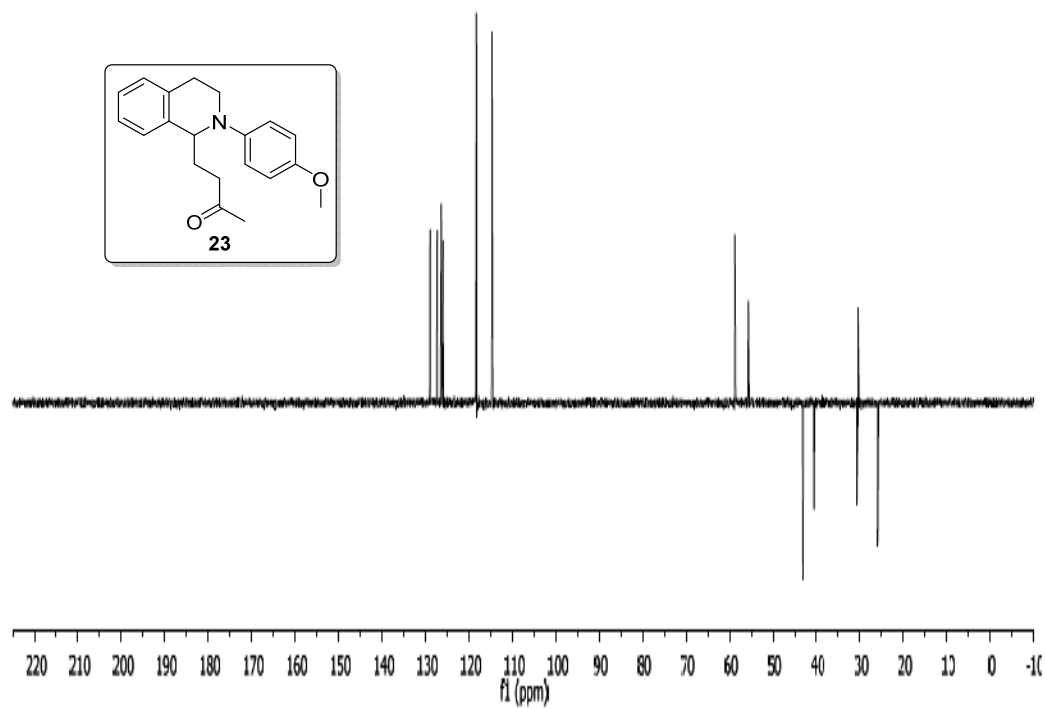
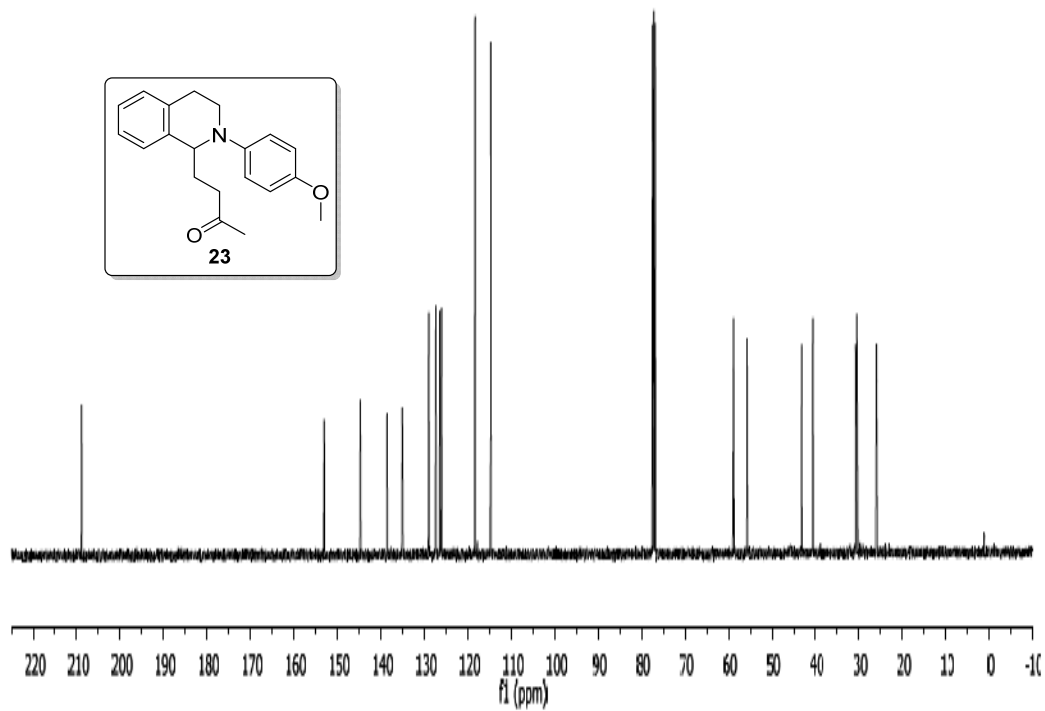


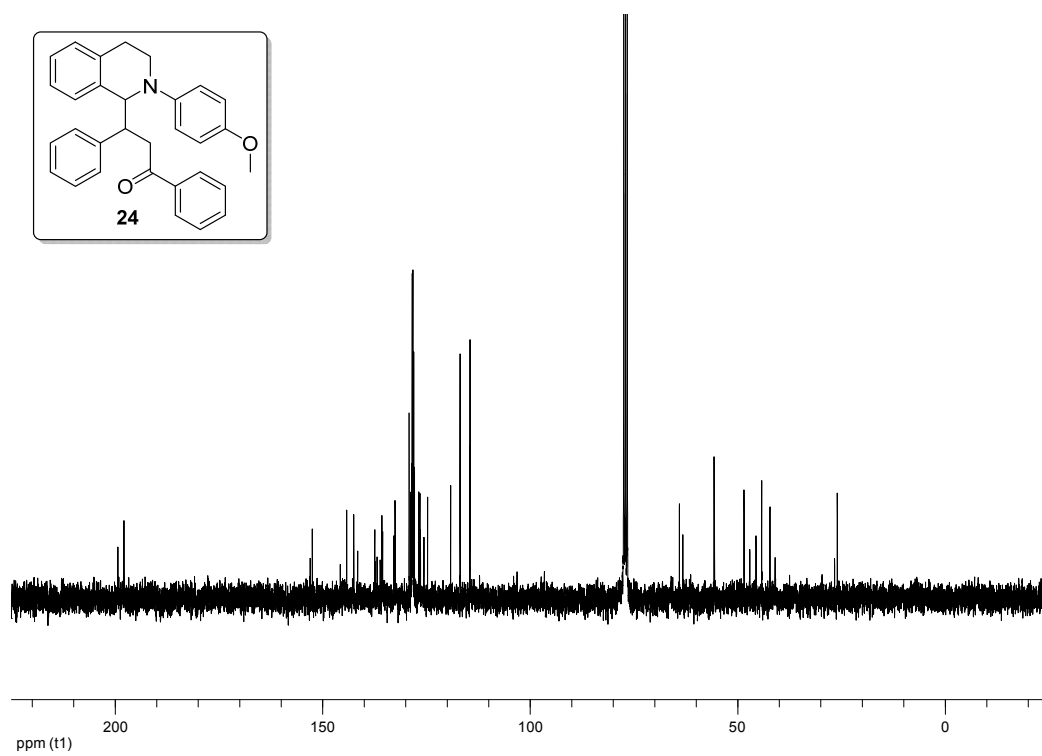
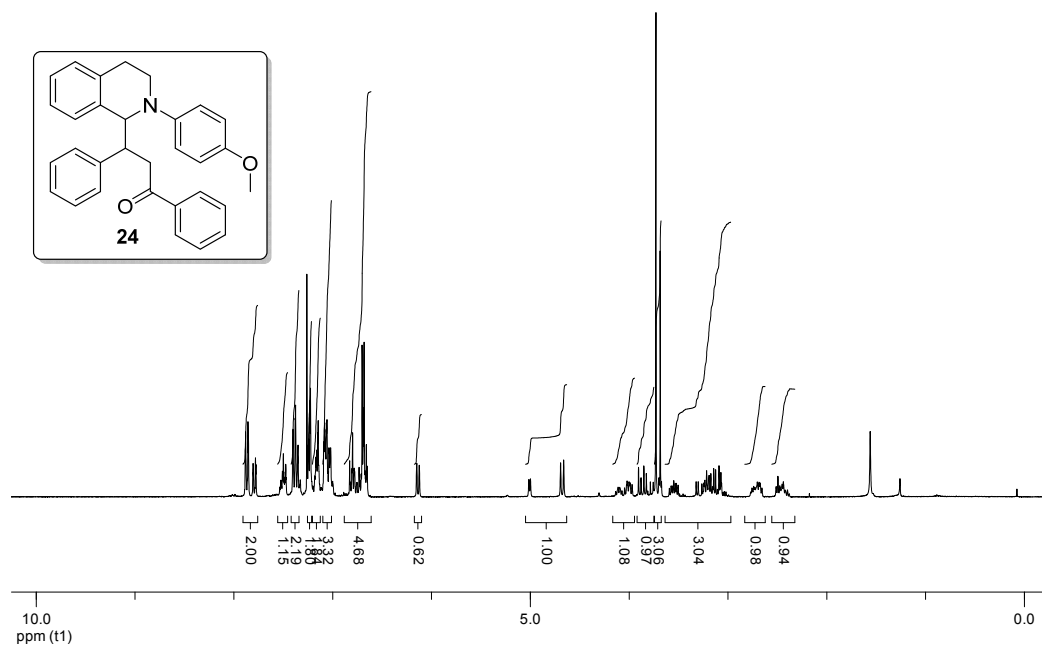


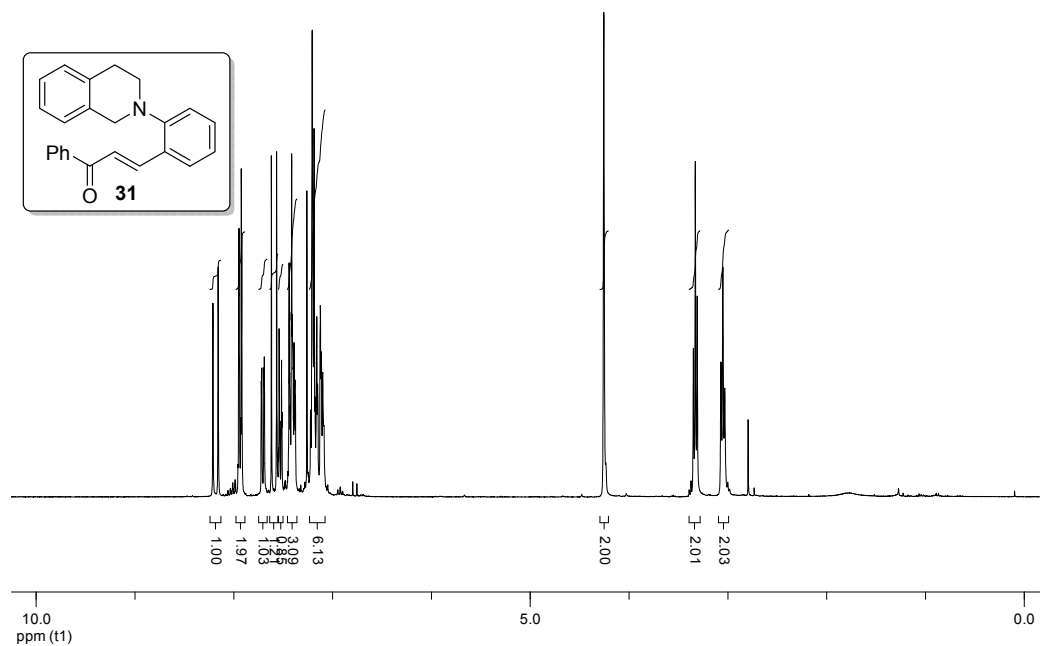
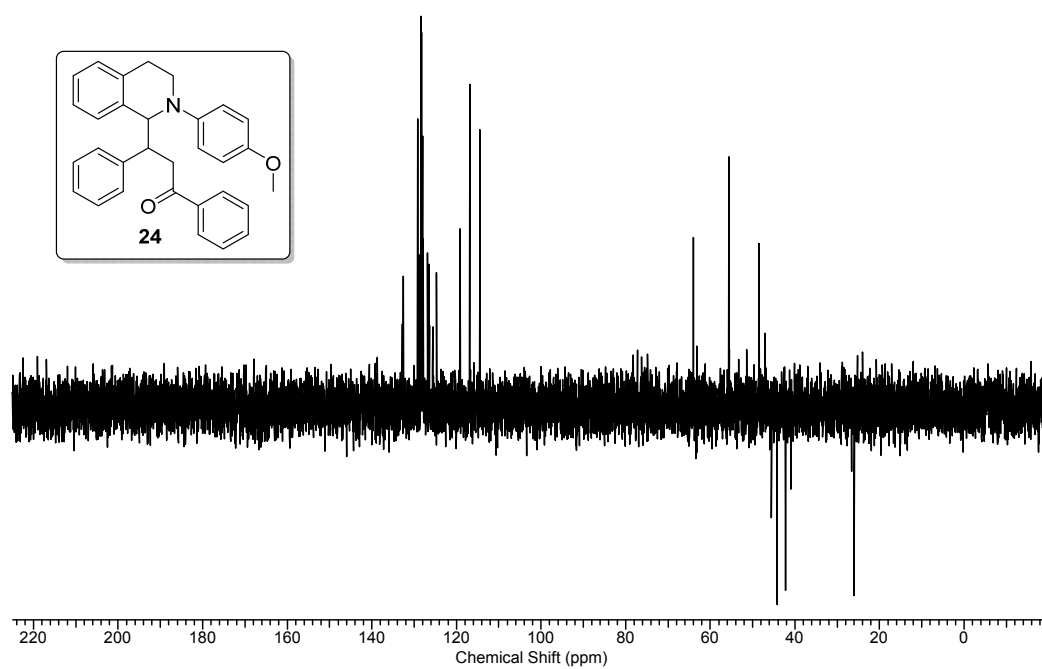


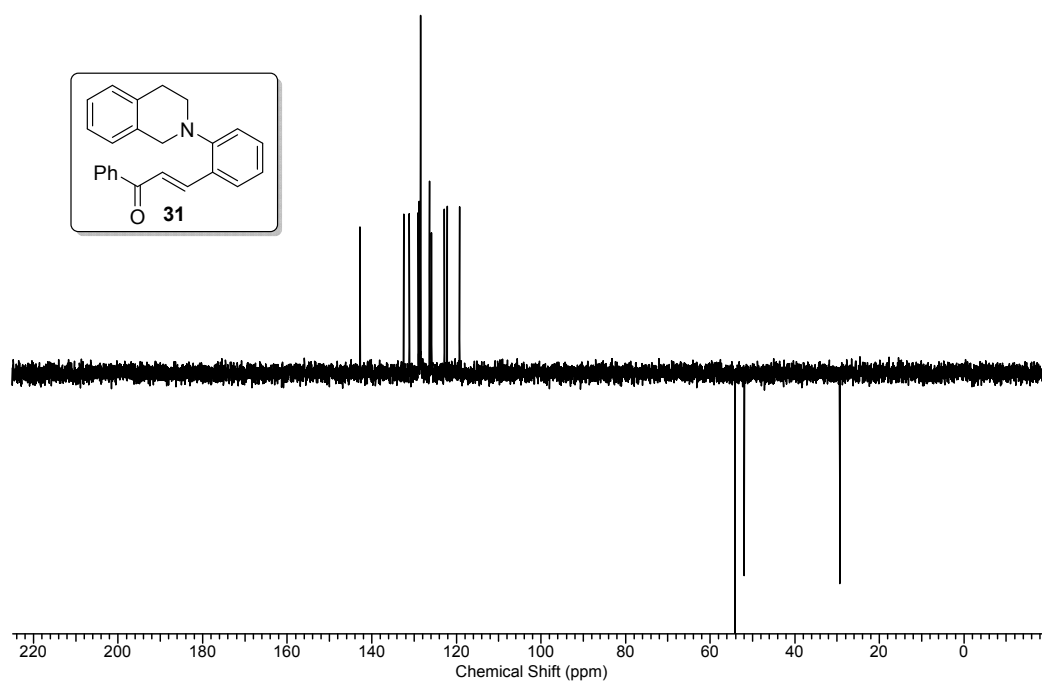
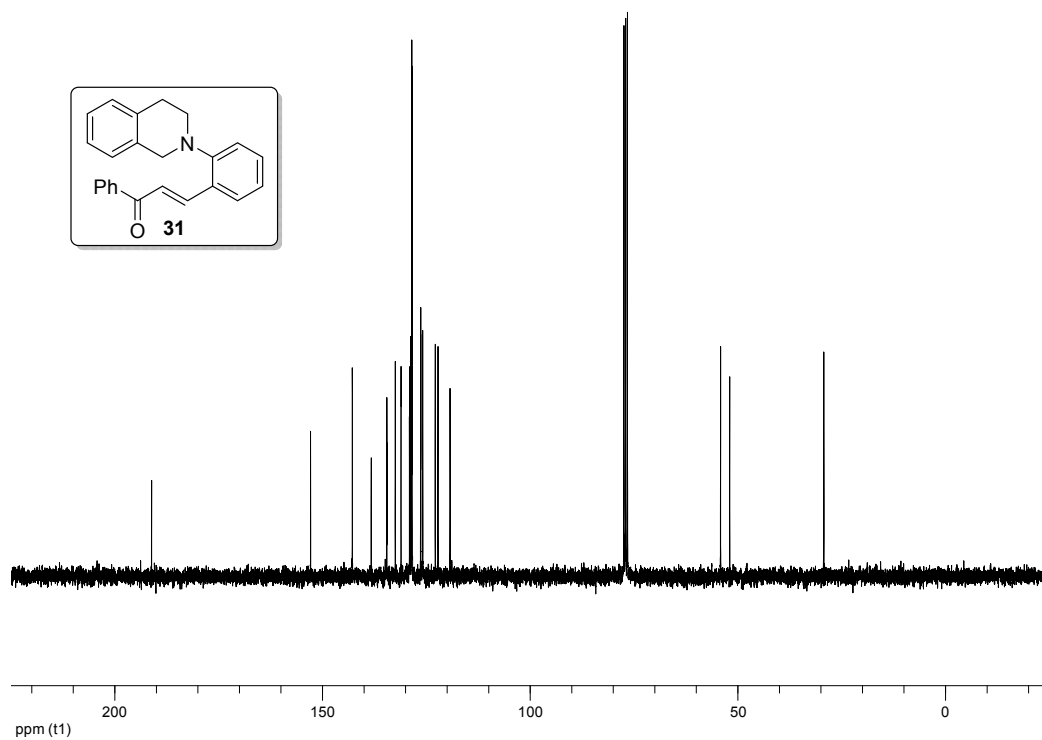


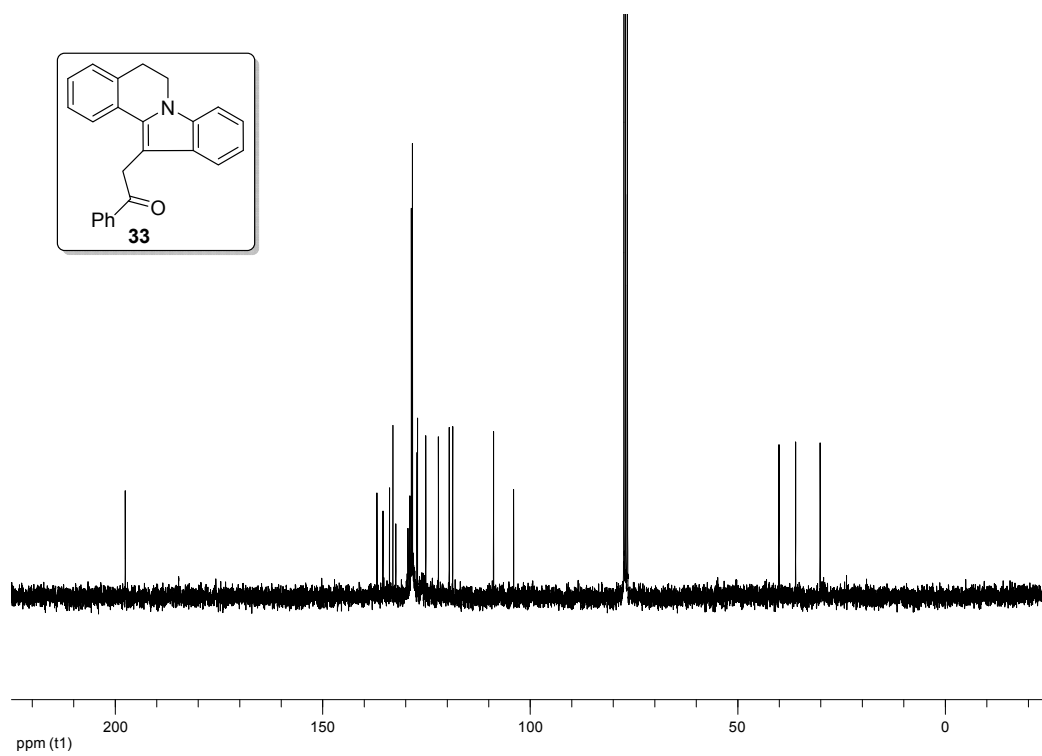
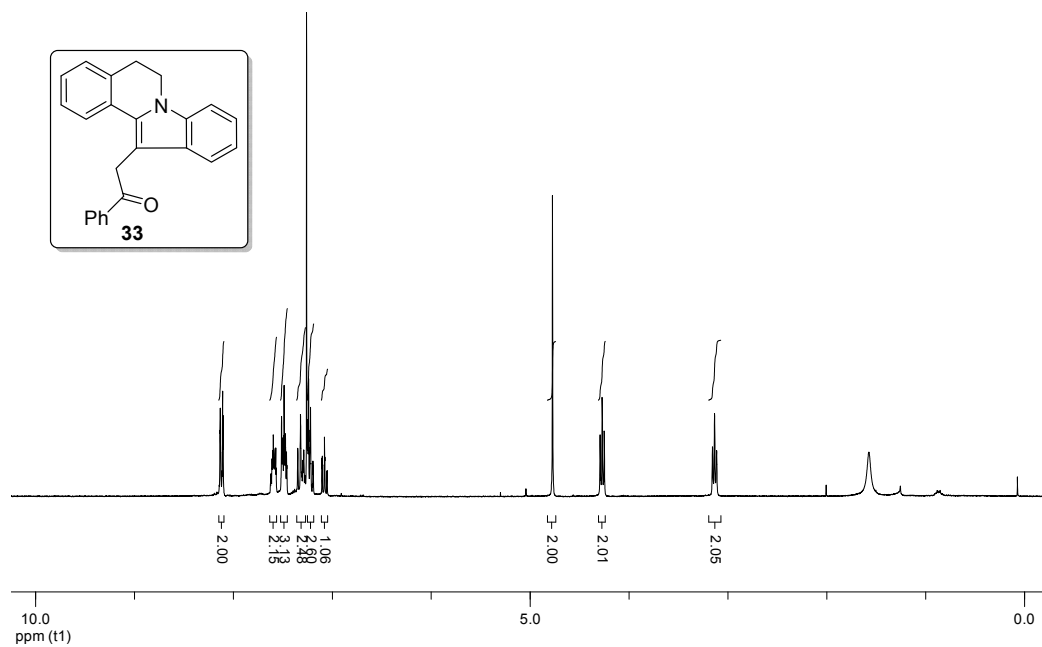


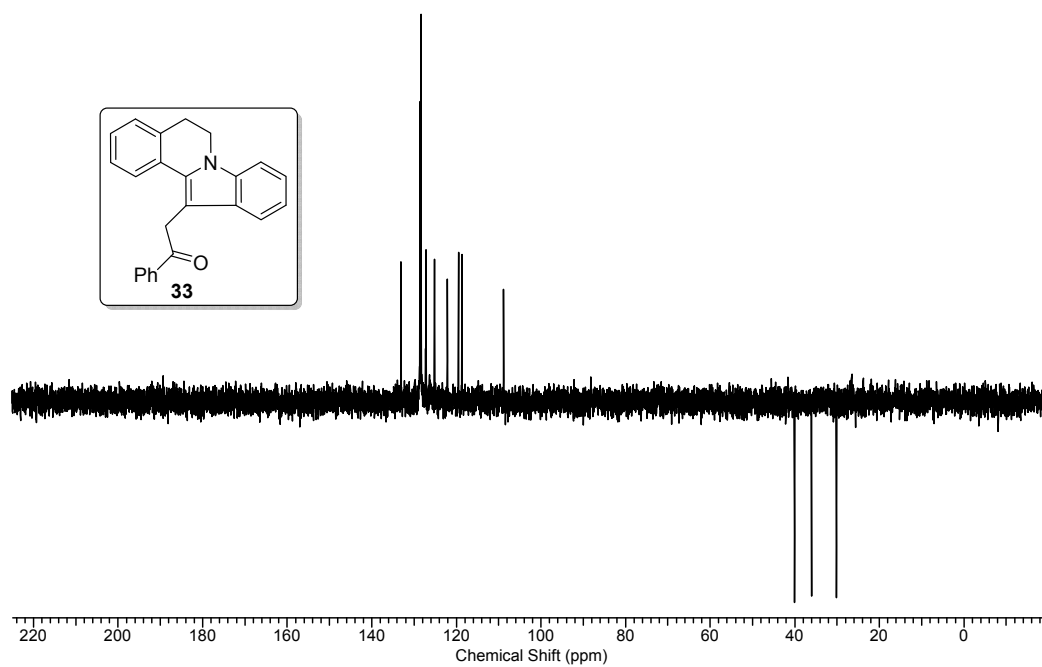














## 2.8 Single crystal structure analysis:

Crystal structure of 2,2'-diphenyl-1,1',2,2',3,3',4,4'-octahydro-1,1'-biisoquinoline (8):

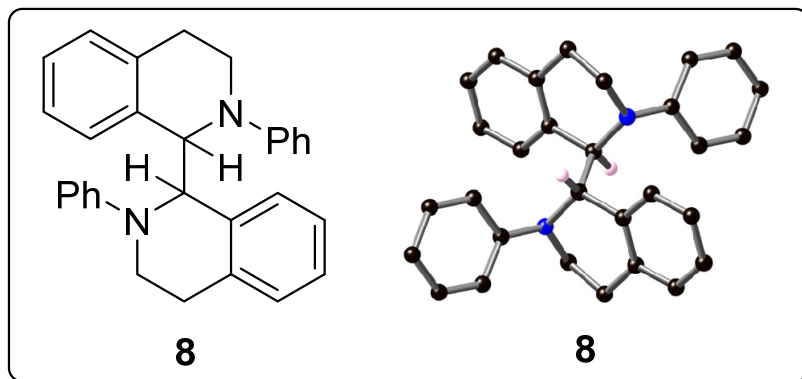


**Table 3:** Crystal data and structural refinement for 8.

| Crystal Data                       |  |
|------------------------------------|--|
| Empirical formula                  | C <sub>30</sub> H <sub>28</sub> N <sub>2</sub> |
| Formula weight                     | 416.54   |
| Temperature/K                      | 123.15   |
| Crystal system                     | triclinic                                      |
| Space group                        | P-1  |
| a/Å                                | 7.5553(7)                                      |
| b/Å                                | 10.2402(8)                                     |
| c/Å                                | 14.3883(15)                                    |
| α/°                                | 94.865(8)                                      |
| β/°                                | 90.429(8)                                      |
| γ/°                                | 101.756(7)                                     |
| Volume/Å <sup>3</sup>              | 1085.56(18)                                    |
| Z                                  | 4  |
| ρ <sub>calc</sub> /mm <sup>3</sup> | 1.274  |
| m/mm <sup>-1</sup>                 | 0.564  |
| F(000)                             | 444.0  |
| Data Collection                    |  |
| Crystal size/mm <sup>3</sup>       | 0.4241 × 0.2575 × 0.0764                       |

|   |   |
|---|---|
| 2 $\theta$ range for data collection        | 6.16 to 133.4°                                    |
| Index ranges                                | -8 ≤ h ≤ 8, -11 ≤ k ≤ 9, -16 ≤ l ≤ 16             |
| Reflections collected                       | 7066  |
| Independent reflections                     | 3225[R(int) = 0.0310]                             |
| Data/restraints/parameters                  | 3225/0/289  |
| Goodness-of-fit on F <sup>2</sup>           | 1.080   |
| Final R indexes [I ≥ 2σ (I)]                | R <sub>1</sub> = 0.0504, wR <sub>2</sub> = 0.1295 |
| Final R indexes [all data]                  | R <sub>1</sub> = 0.0577, wR <sub>2</sub> = 0.1333 |
| Largest diff. peak/hole / e Å <sup>-3</sup> | 0.19/-0.20  |

**Crystal structure of 1,3-diphenyl-3-(2-phenyl-1,2,3,4-tetrahydroisoquinolin-1-yl)propan-1-one (19):**

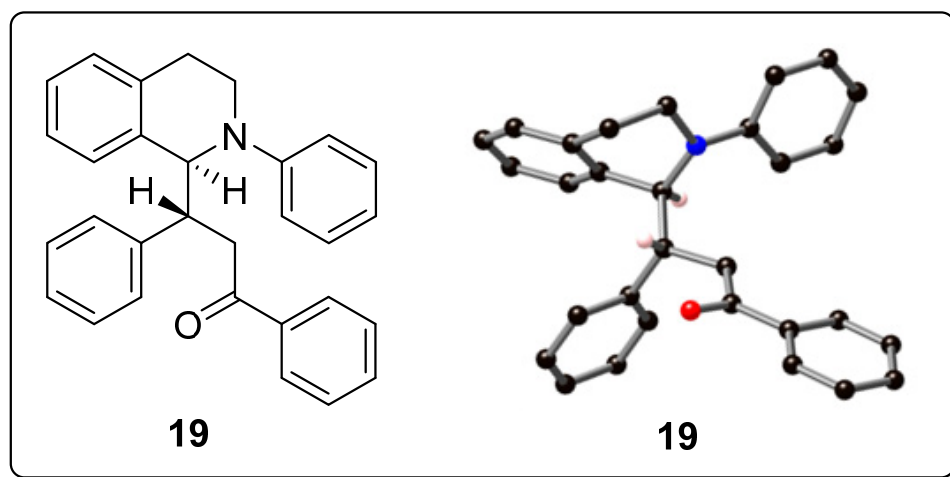


**Table 4:** Crystal data and structural refinement for **19**.

| Crystal Data      |                                    |
|-------------------|------------------------------------|
| Empirical formula | C <sub>30</sub> H <sub>27</sub> NO |
| Formula weight    | 417.53                             |
| Temperature/K     | 123.15                             |
| Crystal system    | monoclinic                         |
| Space group       | P2 <sub>1</sub> /c                 |
| a/Å               | 12.70110(15)                       |
| b/Å               | 5.87973(7)                         |
| c/Å               | 29.5998(4)                         |

## Chapter 2:

|  |             |
|--|-------------|
| $\alpha/^\circ$                            | 90          |
| $\beta/^\circ$                             | 91.6291(11) |
| $\gamma/^\circ$                            | 90          |
| Volume/ $\text{\AA}^3$                     | 2209.59(5)  |
| Z  | 4           |
| $\rho_{\text{calc}}/\text{mg}/\text{mm}^3$ | 1.255       |
| $\text{m}/\text{mm}^{-1}$                  | 0.578       |
| F(000)                                     | 888.0       |

### Data Collection

|   |  |
|---|--|
| Crystal size/ $\text{mm}^3$                   | $0.5163 \times 0.0836 \times 0.0264$                             |
| $2\Theta$ range for data collection           | 6.96 to $134.46^\circ$   |
| Index ranges                                  | $-14 \leq h \leq 15$ , $-6 \leq k \leq 7$ , $-34 \leq l \leq 34$ |
| Reflections collected                         | 19906  |
| Independent reflections                       | 3896 [R(int) = 0.0337]   |
| Data/restraints/parameters                    | 3896/0/289   |
| Goodness-of-fit on $F^2$                      | 1.059  |
| Final R indexes [ $I \geq 2\sigma(I)$ ]       | $R_1 = 0.0357$ , $wR_2 = 0.0968$                                 |
| Final R indexes [all data]                    | $R_1 = 0.0413$ , $wR_2 = 0.1002$                                 |
| Largest diff. peak/hole / $e \text{\AA}^{-3}$ | 0.16/-0.20   |

### Crystal structure of 2-(5,6-dihydroindolo[2,1-a]isoquinolin-12-yl)-1-phenylethanone (33):

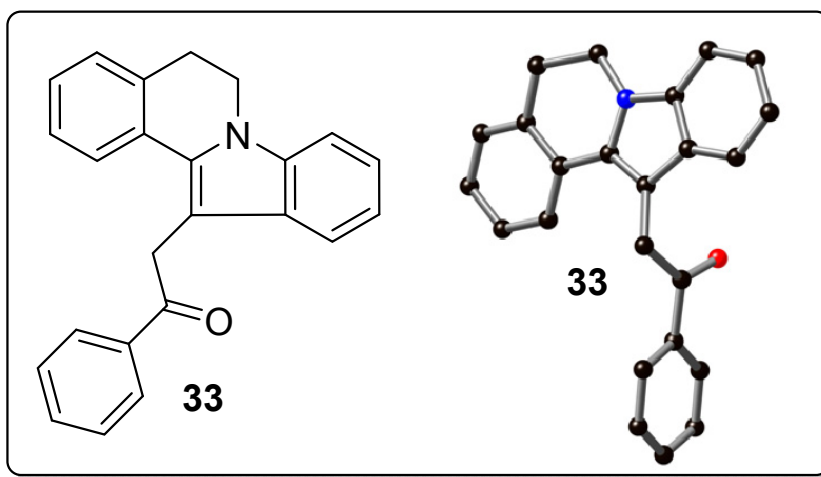


**Table 5:** Crystal data and structural refinement for **33**.

| <b>Crystal Data</b>                         |   |
|---|---|
| Empirical formula                           | C <sub>24</sub> H <sub>19</sub> NO                |
| Formula weight                              | 337.40  |
| Temperature/K                               | 123.15  |
| Crystal system                              | monoclinic  |
| Space group                                 | P2 <sub>1</sub> /c                                |
| a/Å   | 9.1545(5)   |
| b/Å   | 21.6152(10)                                       |
| c/Å   | 8.6185(3)   |
| α/°   | 90  |
| β/°   | 98.632(4)   |
| γ/°   | 90  |
| Volume/Å <sup>3</sup>                       | 1686.08(14)                                       |
| Z   | 4   |
| ρ <sub>calc</sub> /mg/mm <sup>3</sup>       | 1.329   |
| m/mm <sup>-1</sup>                          | 0.628   |
| F(000)                                      | 712.0   |
| <b>Data Collection</b>                      |   |
| Crystal size/mm <sup>3</sup>                | 0.5475 × 0.0566 × 0.0185                          |
| 2θ range for data collection                | 8.18 to 134.54°                                   |
| Index ranges                                | -8 ≤ h ≤ 10, -24 ≤ k ≤ 25, -10 ≤ l ≤ 6            |
| Reflections collected                       | 5394  |
| Independent reflections                     | 2848[R(int) = 0.0369]                             |
| Data/restraints/parameters                  | 2848/0/235  |
| Goodness-of-fit on F <sup>2</sup>           | 0.923   |
| Final R indexes [I ≥ 2σ (I)]                | R <sub>1</sub> = 0.0501, wR <sub>2</sub> = 0.1233 |
| Final R indexes [all data]                  | R <sub>1</sub> = 0.0767, wR <sub>2</sub> = 0.1373 |
| Largest diff. peak/hole / e Å <sup>-3</sup> | 0.24/-0.30  |



## *Chapter 3*

### **Visible Light Photoredox Catalysis: Investigation of Distal $\text{sp}^3$ C-H Activation of *t*-Amines**

### 3.1 Introduction / Background of our concept:

Recently, C-H functionalization using visible light photoredox catalysis<sup>1</sup> have emerged as a novel concept in organic synthesis mainly due to environmental concern. As discussed in Chapter 1 (Section 1.4.3) and 2, in the context of  $\alpha$ -sp<sup>3</sup> C-H functionalization of *t*-amines (an important synthetic transformation in the synthesis of many biologically active compounds), chemistry from both  $\alpha$ -amino alkyl radical<sup>2,3</sup> and iminium ion<sup>2,4</sup> have been explored mainly employing Ru(bpy)<sub>3</sub>Cl<sub>2</sub> or [Ir(ppy)<sub>2</sub>(dtb-bpy)]PF<sub>6</sub> complex as visible light absorbing photocatalyst, (Figure 1), though such transformations were reported earlier via oxidative photoinduced electron transfer (PET) processes<sup>5</sup> utilizing electron deficient aromatics as an electron acceptors.

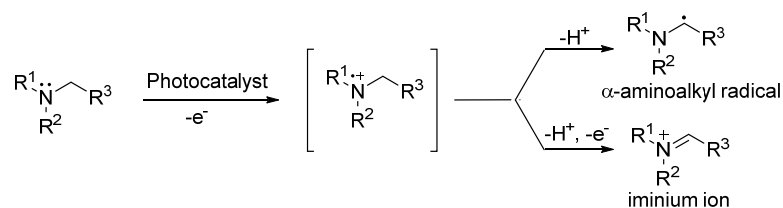


**Figure 1.** Photoredox oxidation of *t*-amines.

Importantly, although  $\alpha$ -sp<sup>3</sup> C-H functionalization of *t*-amines by photoredox catalyses abound, distal sp<sup>3</sup> C-H functionalization of *t*-amines is an infrequent observation.<sup>6,7</sup> Continuing with our interest to investigate new synthetic methodologies by photoredox catalysis in general<sup>8</sup> and *t*-amines in particular,<sup>5a,9,10</sup> we got interested to explore visible light (blue LED) mediated photoredox catalyzed one electron oxidation of *t*-amines where two possible sp<sup>3</sup> C-H sites are available for deprotonation (Figure 2). In this context, we selected 10-methyl-9,10-dihydroacridine (AcrH<sub>2</sub>, **1**) and 4-alkyl-*N,N* dimethyl anilines (**2-3**) for our study and disclose herein a mechanistically interesting and synthetically useful chemistry.

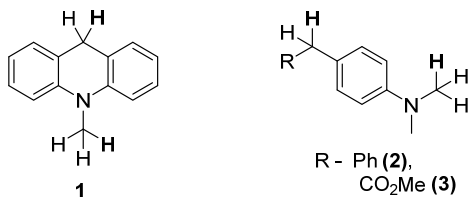


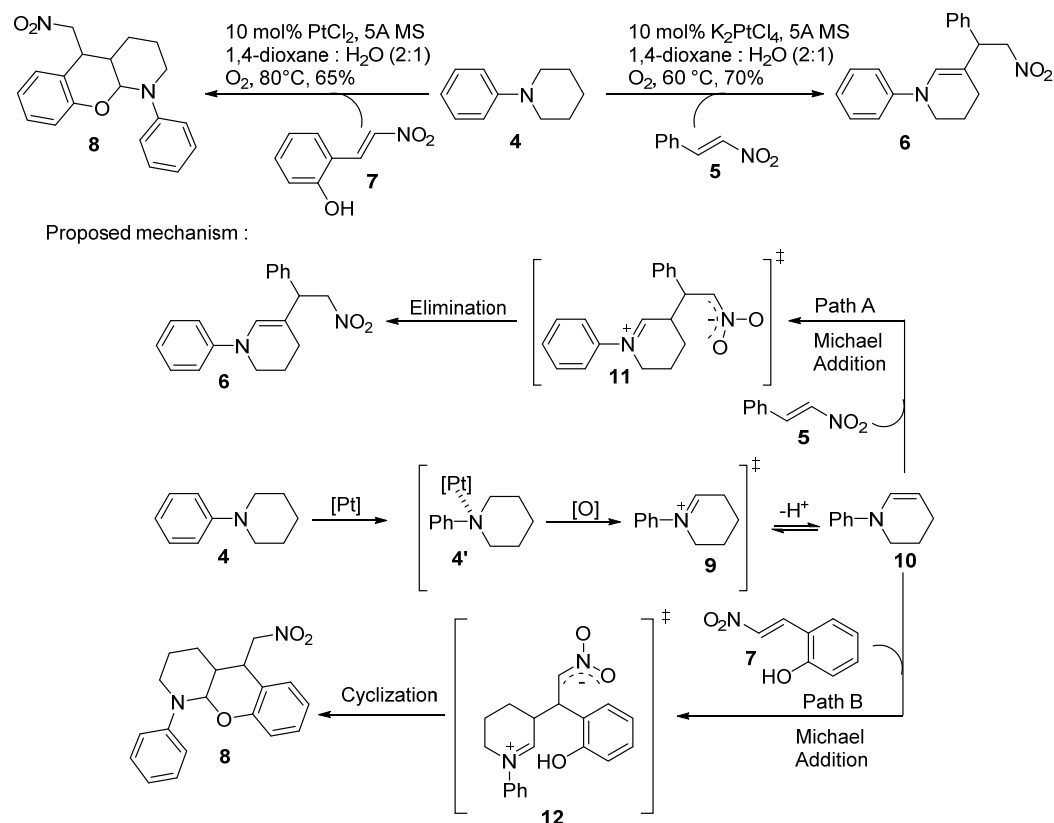
**Figure 2.** *t*-Amines having two possible deprotonation sites.

However, in order to put our work in proper perspective, it would be appropriate to highlight few important literature methodologies pertaining to distal ( $\beta/\text{C}3$  or  $\gamma/\text{C}4$ )  $\text{sp}^3$  C-H activation of *t*-amines for C-C bond formation reactions.

### 3.2 Earlier reports:

#### 3.2.1 Non-photochemical approaches:

Liang and co-workers have reported a mild platinum-catalyzed oxidative dehydrogenation of  $\alpha,\beta\text{-C}(\text{sp}^3)\text{-H}$  bonds of *t*-amines for *in situ* generation of enamine intermediate, which reacted with various nitroolefins to produce corresponding addition product (Scheme 1).<sup>11</sup>

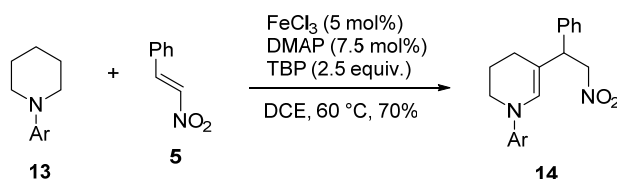


**Scheme 1:** Platinum-catalyzed reaction of *t*-amines with nitroolefins.

Mechanistically, platinum catalyst [Pt] coordinates to nitrogen, which upon oxidation produces an iminium ion intermediate **9** through the activation of  $\alpha$   $\text{sp}^3$  C-H bond. Subsequent  $\beta$ -hydrogen elimination produces enamine **10**, which undergoes

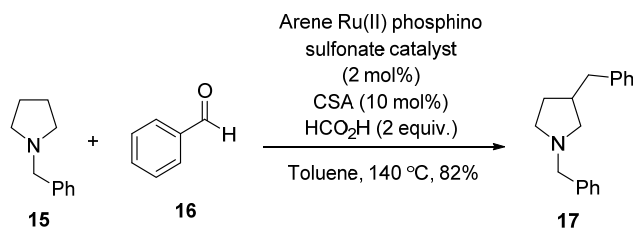
Michael addition with nitroolefins **5** and **7** to give the Michael adduct intermediates **11** (path A) and **12** (path B), respectively. Afterward, hydrogen elimination from **11** produces **6** readily. In contrast, **12** reacts intramolecularly by the nucleophilic hydroxyl group giving rise to a structurally different product **8**.<sup>11</sup>

Similar reaction as mentioned above by using more ubiquitous Fe metal catalyst in presence of di-*tert*-butyl peroxide (TBP) as an oxidant (Scheme 2) is also reported.<sup>12</sup>



**Scheme 2:** Iron-catalyzed reaction of *t*-amines with nitroolefins.

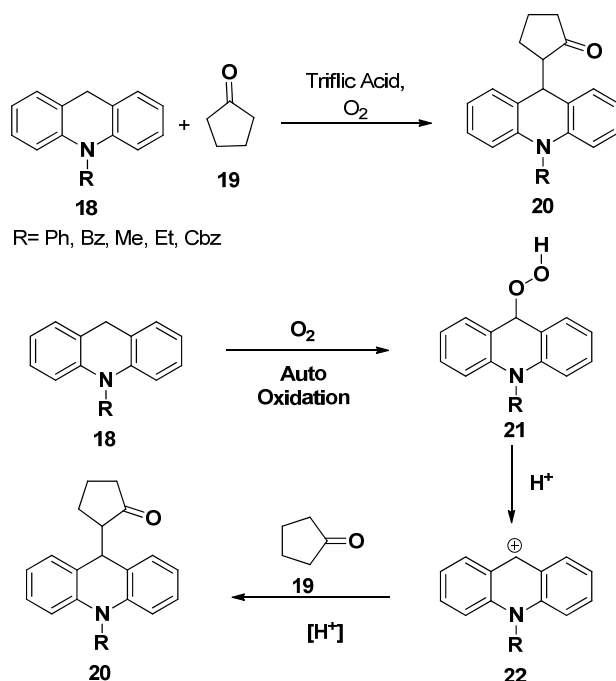
Bruneau and co-workers have reported ruthenium catalysed regioselective C(3) alkylation of **15** via dehydrogenation (under nonoxidative conditions), C-C bond formation followed by transfer hydrogenation reaction sequence as shown in Scheme 3.<sup>13</sup>



**Scheme 3:** C3 alkylation of *t*-amines with aldehyde.

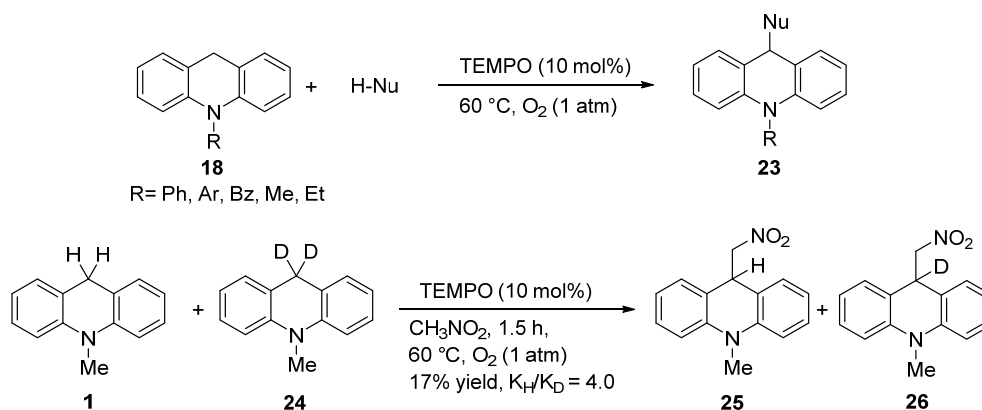
In the context of direct  $\gamma$   $sp^3$  C-H bond activation of *t*-amines, Klusmann and co-workers have reported an oxidative cross-coupling reaction of *N*-substituted acridanes (**18**) with ketones (**19**) in presence of catalytic amount of triflic acid and elemental oxygen.<sup>14</sup> Mechanistically this reaction involved a radical pathway intermediated-autoxidative formation of *N*-substituted acridane hydroperoxide (**21**), which through  $H^+$  catalysis generated carbocationic intermediate **22** and reaction of this intermediate with the enolate produced **20** (Scheme 4).





**Scheme 4:** Acid catalyzed aerobic coupling of *N*-substituted acridane with ketone.

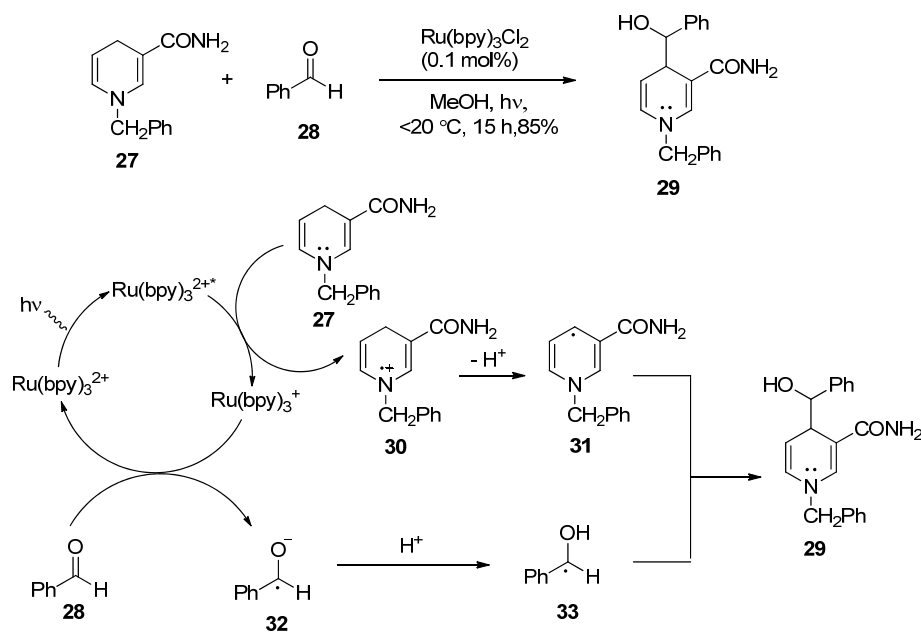
Similar type of reaction is also reported by TEMPO-catalysed coupling of *N*-substituted acridanes **18** with various nucleophiles, such as nitromethane, malonate and malononitrile (Scheme 5).<sup>15</sup> Although in this report, on the basis of kinetic isotopic effect ( $K_{\text{H}}/K_{\text{D}} = 4.0$ ), the cleavage of benzylic C-H bond ( $\gamma$   $\text{sp}^3$  C-H) was involved as the rate-determining step, more detailed mechanistic studies were suggested in order to unravel this hypothesis.



**Scheme 5:** TEMPO catalyzed aerobic coupling of *N*-substituted acridanes with various nucleophiles.

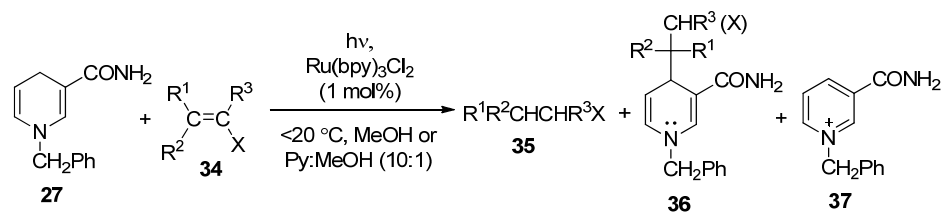
## 3.2.2 Photochemical approaches:

Photoinduced electron-proton-electron loss reaction sequence of  $\text{NADH}^{16}$  and their analogues such as 10-methyl-9,10-dihydroacridine<sup>17</sup>(AcrH<sub>2</sub>, **1**) and 1-benzyl-1,4-dihydronicotinamide (BNAH, **27**)<sup>6a</sup> have been extensively studied to understand the mechanistic pathways involved in biological oxidation-reduction reactions and for the reduction of various organic substrates. However, in rare transformations Pac and co-workers reported the  $\text{Ru}(\text{bpy})_3\text{Cl}_2$  photocatalysed reaction of BNAH (**27**) with several aromatic carbonyl compounds to obtain 1:1 coupling adducts of kind **29** in moderate to good yields along with corresponding less efficient or no reduction products of carbonyl compounds. The mechanism of this reaction is shown in Scheme 6.



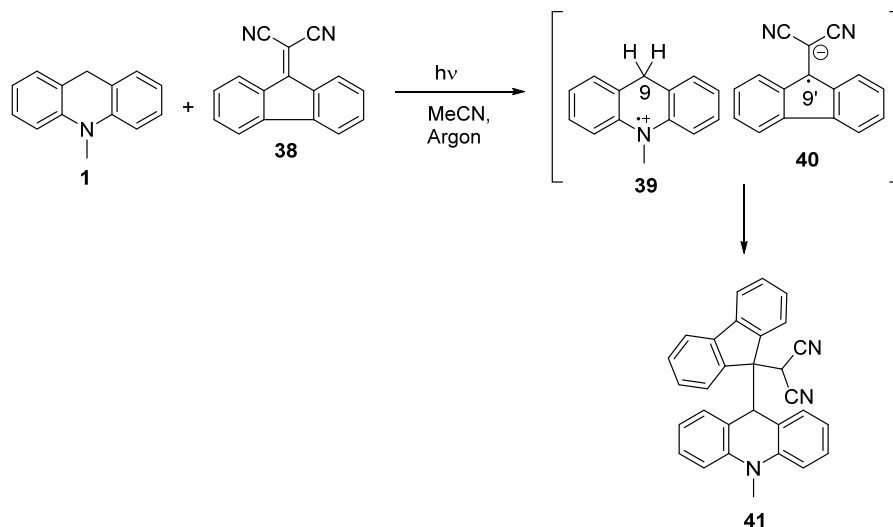
**Scheme 6:** Coupling reactions of BNAH with carbonyl compounds.

However, it is important to note that Pac and co-workers in their earlier report demonstrated that the  $\text{Ru}(\text{bpy})_3\text{Cl}_2$  photocatalysed reaction of BNAH (**27**) with electron deficient olefin **34** mainly gave reduced product **35** along with some minor coupling adduct **36** in exceptional cases (Scheme 7).<sup>6a</sup> Furthermore, in an elaborate mechanistic study, it was pointed out that **34** which possessed one aryl substituent with no extra electron-withdrawing group at  $\beta$  position gave coupling adduct **36** in low to moderate yield (4-37%) along with traces of dimers of **27** and **34**.<sup>6b</sup>



**Scheme 7:** Photochemical reactions of BNAH with electron deficient alkenes

It may be worthy of mention that Mak and co-workers reported the direct irradiation between **1** and more activated 9-fluorenylidene malononitrile (**38**) in deaerated acetonitrile, using high-pressure Hg lamp produced coupling product (**41**), as shown in Scheme 8.<sup>18</sup>



**Scheme 8:** Photochemical coupling of **1** with 9-fluorenylidene malononitrile (**38**).

From above discussion, it is evident that compared to  $\alpha/\text{C}2$   $\text{sp}^3$  C-H activation of *t*-amines (Chapter 1, 2), very limited studies are available for distal  $\text{sp}^3$  C-H activation of *t*-amines. Considering the demand for further exploration in this field and our interest in developing photoinduced electron processes, we decided to take this challenge of investigating distal  $\text{sp}^3$  C-H functionalization of *t*-amines for alkylation reaction by visible light photoredox catalysis.

### 3.3 Results and discussion:

#### 3.3.1 $\gamma$ $sp^3$ C-H activation reaction of *t*-amines with electron deficient alkenes:

We began our investigation by irradiating a mixture of **1** (AcrH<sub>2</sub>, 1 equiv.), methyl vinyl ketone (**42**, 3 equiv.) and catalytic amount of Ru(bpy)<sub>3</sub>Cl<sub>2</sub>·6H<sub>2</sub>O (5 mol%) in degassed acetonitrile utilizing a blue LED (light emitting diode) (eq 1). Progress of reaction was monitored by following the disappearance of **1** on TLC. After 20 h of photoirradiation, when almost all of the **1** was consumed, solvent was removed and the product was purified by column chromatography to obtain **43** in 70% yield. In order to study the effect of solvent on this reaction, irradiations were carried out in different solvents and the results are summarized in Table 1. It was observed that there is no reaction either in dry toluene or dry THF (entries 2-3) and comparatively low yield was observed in dry CH<sub>2</sub>Cl<sub>2</sub>, MeOH, DMSO and DMF (entries 4-7). Almost similar results were observed employing [Ir(ppy)<sub>2</sub>(dtb-bpy)]PF<sub>6</sub> (5 mol%) as a photoredox catalyst (entry 8).<sup>19</sup>

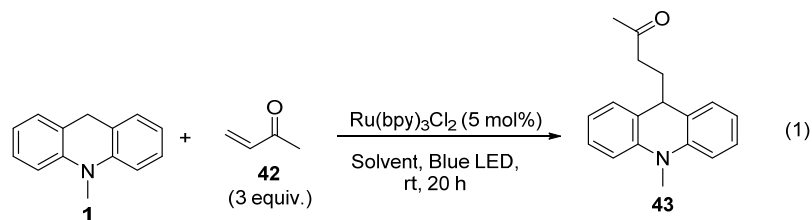


**Table 1:** Photocatalyzed  $\gamma$   $sp^3$  C-H alkylation of **1** with MVK (**42**).<sup>[a]</sup>

| Entry | Solvent                         | Yield [%]         |
|-------|---------------------------------|-------------------|
| 1     | MeCN                            | 70                |
| 2     | Toluene                         | -                 |
| 3     | THF                             | -                 |
| 4     | CH <sub>2</sub> Cl <sub>2</sub> | 09                |
| 5     | MeOH                            | 12                |
| 6     | DMSO                            | 26                |
| 7     | DMF                             | 40                |
| 8     | MeCN                            | 72 <sup>[b]</sup> |

<sup>[a]</sup> Reaction condition: **1** (0.51 mmol), **42** (1.53 mmol), Ru(bpy)<sub>3</sub>Cl<sub>2</sub> catalyst (5 mol%), Blue LED light irradiation, Solvent (2 mL), 20 h. <sup>[b]</sup> Reaction using [Ir(ppy)<sub>2</sub>(dtb-bpy)]PF<sub>6</sub> catalyst (5 mol%).

**Control experiments:**

When photoirradiation between **1** (1 equiv.) and MVK (**42**, 3 equiv.) was carried out in the absence of Ru(bpy)<sub>3</sub>Cl<sub>2</sub> catalyst in degassed acetonitrile with blue LED, there was no observable product even after prolonged irradiation (48 h). Similarly, when the mixture of **1** (1 equiv.), MVK (**42**, 3 equiv.) and Ru(bpy)<sub>3</sub>Cl<sub>2</sub> (5 mol%) in degassed acetonitrile was kept for 48 h in dark at room temperature, there was no reaction observed. These two appropriate control experiments showed that both Ru(bpy)<sub>3</sub>Cl<sub>2</sub> catalyst and visible light (blue LED) were needed for the formation of **43**.

**Experimental set-up:**

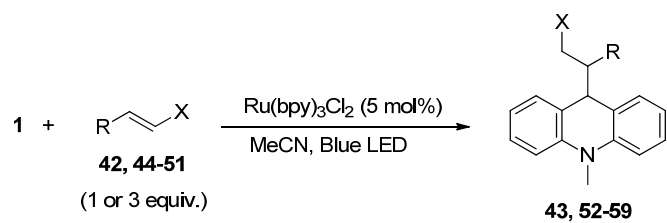
Identical experimental set-up, as portrayed in chapter 2, section 2.3.3 was utilized to perform these photolytic reactions.

**3.3.2 Evaluation of the generality of the reaction:**

After our initial successful results, in order to broaden the substrate scope of the reaction (eq. 1), a wide variety of electron deficient alkenes bearing non-aromatic as well as aromatic groups particularly at  $\beta$ -position were investigated under optimized reaction conditions and results are shown in Table 2. The yields are based on the consumption of **1**, after column chromatography.

It was observed that compared to the reaction of MVK (**42**) (entry 1), acrolein (**44**) gave slightly low yield for corresponding product **52** (47%) (entry 2). However, it is significant to note that compared to simple  $\beta$ -unsubstituted alkenes **42**, **44** (entry 1, 2), reactions with corresponding  $\beta$ -phenyl electron deficient alkenes **45**, **46** proceeded smoothly to give the improved yields for the coupled product **53** (87%) and **54** (60%) respectively (entry 3, 4). The scope of this reaction was also evaluated with  $\beta$ -(2-furyl)alkene framework (**47**) (entry 5), however, the corresponding coupling product **55** was formed in low yield (41%).

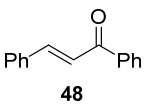
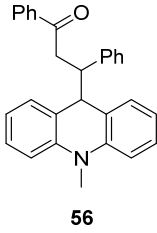
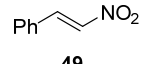
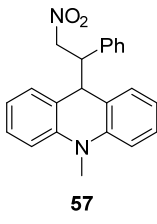
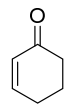
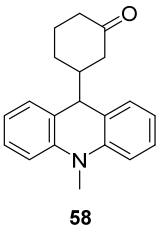
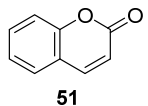
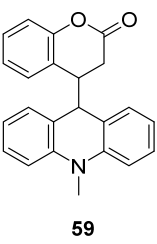
It may be significant to note that coupling of **1** with various kind of acyclic, cyclic and differently functionalized electron deficient alkenes, such as chalcone (**48**), nitrostyrene (**49**), cyclohexenone (**50**) and coumarin (**51**) proceeded with poor to moderate yield (30 - 58%, entries 6-9). In some cases (**42**, **44**, **46** and **50**), an excess of electron deficient alkene (3 equiv.) was used due to their competing self-polymerization reactions. Reaction with  $\beta$ -aromatic substituted alkenes (**45-49** and **51**) also produced small amounts of uncharacterized side products (5-10%).<sup>19</sup>



**Table 2.** Photocatalyzed  $\gamma$ -sp<sup>3</sup> C-H alkylation of **1** with electron deficient alkenes <sup>[a]</sup>

| Entry | Alkene | Equiv. | Product | Time(h) | Yield % <sup>[b]</sup> |
|-------|--------|--------|---------|---------|------------------------|
| 1     |        | 3      |         | 20      | 70                     |
| 2     |        | 3      |         | 18      | 47                     |
| 3     |        | 1      |         | 27      | 87                     |
| 4     |        | 3      |         | 22      | 60                     |
| 5     |        | 1      |         | 27      | 41                     |

continued....

| Entry | Alkene   | Equiv. | Product  | Time(h) | Yield % <sup>[b]</sup> |
|-------|--|--------|--|---------|------------------------|
| 6     | <br><b>48</b>   | 1      | <br><b>56</b>  | 20      | 56                     |
| 7     | <br><b>49</b>   | 1      | <br><b>57</b>  | 21      | 40                     |
| 8     | <br><b>50</b>   | 3      | <br><b>58</b>  | 21      | 58                     |
| 9     | <br><b>51</b> | 1      | <br><b>59</b> | 20      | 30                     |

<sup>[a]</sup> Reaction condition: **1** (0.51 mmol), **42**, **44-51** (0.51 or 1.53 mmol), Ru(bpy)<sub>3</sub>Cl<sub>2</sub> catalyst (5 mol %), Blue LED light irradiation, MeCN (2 mL) <sup>[b]</sup> Yield based on consumption of **1** after column chromatography. <sup>[c]</sup> Predominantly *cis* (95%).

It was interesting to note that reaction with **45-51** produced only *trans*-isomers, which was confirmed by NMR analyses and by single X-ray crystal structures of **56** and **57** (Figure 3).<sup>19</sup>

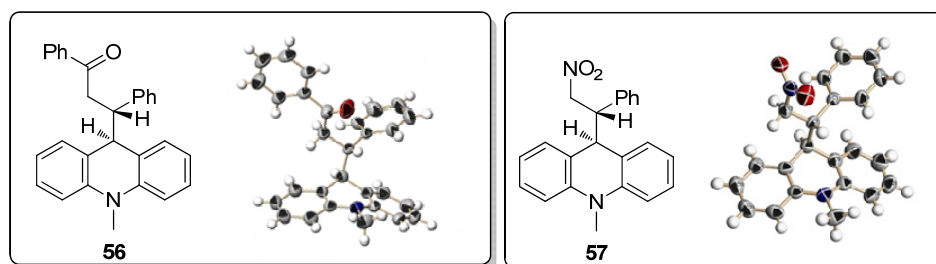


**Figure 3:** X-ray structure of **56** and **57**.

### 3.3.3 Proposed reaction mechanism:

In order to rationalize this photoreaction, a plausible reaction mechanism is proposed as shown in Figure 4. The excited  $\text{Ru}(\text{bpy})_3^{2+}$  is quenched by single electron transfer from **1** ( $\text{AcrH}_2$ )<sup>20</sup> producing **60** ( $\text{AcrH}_2$ )<sup>+</sup> and a  $\text{Ru}(\text{bpy})_3^+$ . The ( $\text{AcrH}_2$ )<sup>+</sup> undergoes deprotonation to generate  $\gamma$ -amino alkyl radical (**61**) ( $\text{AcrH}$ )<sup>·</sup> which upon addition to activated alkenes forms **62**. Reduction of **62** by  $\text{Ru}(\text{bpy})_3^+$  followed by protonation completes the reaction cycle with regeneration of the catalyst.<sup>19</sup>

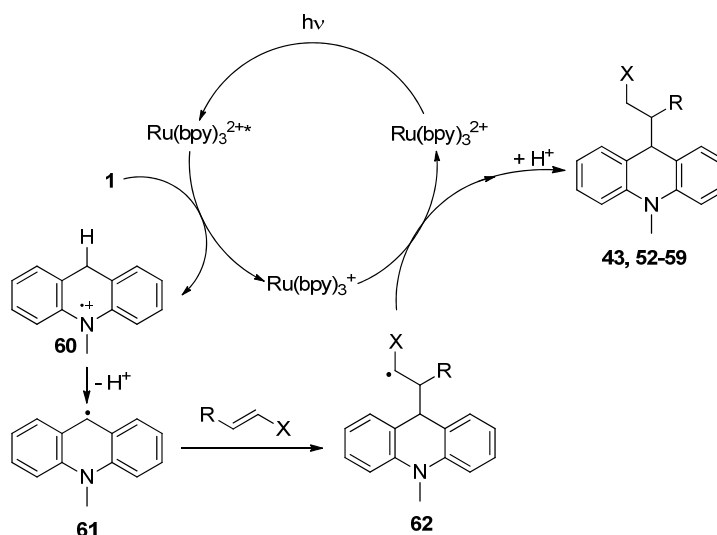


**Figure 4:** Proposed mechanism for photocatalytic  $\gamma$  C-H alkylation of **1**.

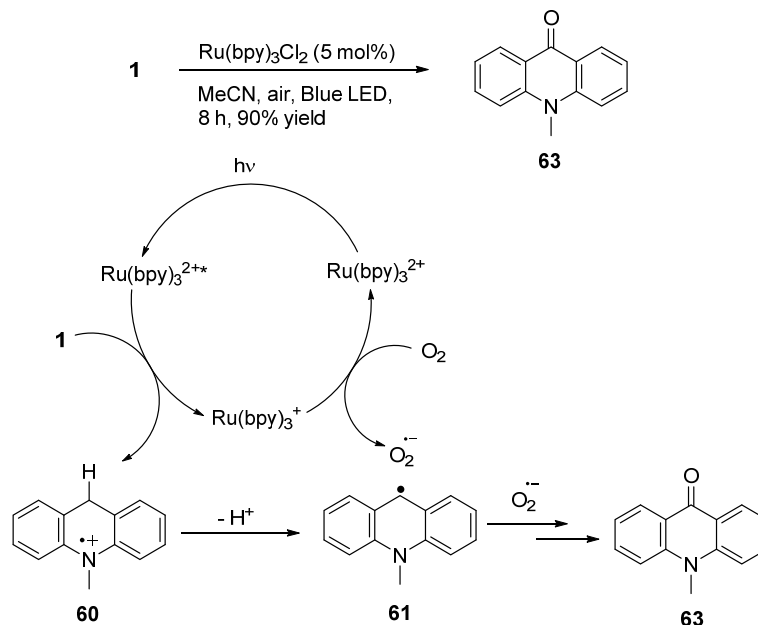
### 3.3.4 Synthesis of acridone:

Acridone and its derivatives show a wide range of biological and pharmacological activities<sup>21</sup> including anti-HIV,<sup>21a</sup> antiviral<sup>21f</sup> and therefore, their syntheses has attracted the attention of synthetic chemists. However, in most of the reported syntheses the requirement of stringent reaction conditions and tedious work-up, demands development of simpler strategy.<sup>22</sup>

The proposed intermediacy of  $\gamma$ -amino alkyl radical (**61**) ( $\text{AcrH}$ )<sup>·</sup> in the above reaction led us to envisage its application in the synthesis of acridone directly by the reaction of oxygen without using any consumable reagent. In this context, we found that identical photoirradiation of **1** in the presence of  $\text{Ru}(\text{bpy})_3\text{Cl}_2$  (5 mol%) in an open atmosphere produced **63** quantitatively (Scheme 9). The formation of **63** may be explained by the reaction of **61** [ $\text{AcrH}$ ]<sup>·</sup>, Scheme 9] either with ground state



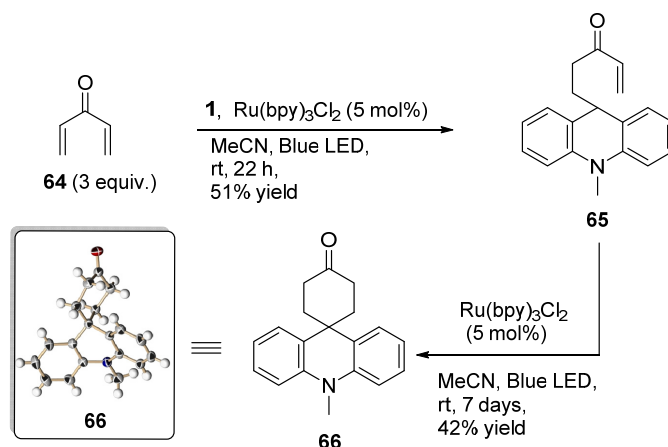
oxygen<sup>[23a]</sup> or by reaction with  $O_2^{\cdot-}$ , formed through regeneration of  $Ru(bpy)_3^{2+}$  via an electron transfer by  $Ru(bpy)_3^+$  to dissolved oxygen in the solvent.<sup>[23b]</sup>



**Scheme 9:** Photocatalyzed  $\gamma$   $sp^3$  C-H oxygenation of **1**.

### 3.3.5 Intramolecular coupling reaction:

After having successfully demonstrated that  $\gamma$ -aminoalkyl radical, generated by visible light photoredox reaction between a *t*-amine and  $Ru(bpy)_3Cl_2$ , undergoes alkylation reactions with activated olefins and oxygenation with air, further encouraged us to evaluate the scope of this work for the synthesis of important heterocyclic scaffold containing challenging all carbon quaternary centre by carrying



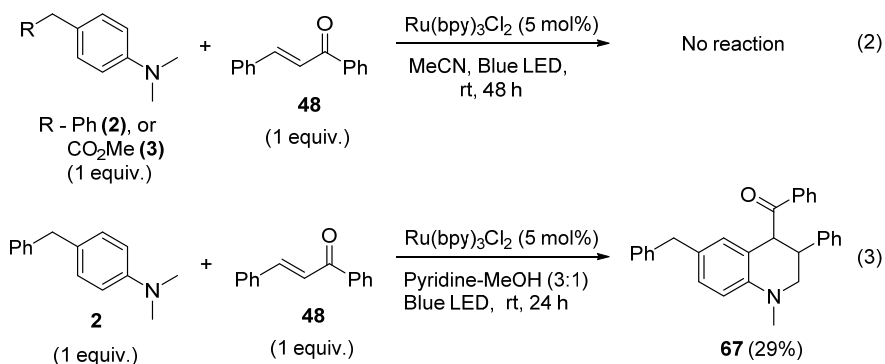
**Scheme 10:** Photocatalyzed sequential addition reaction of **1** with dienone (**64**).

out intramolecular reaction. In this regard, identical sequential photoredox catalysed alkylation reaction of **1** with **64** was carried out to produce spirocyclic product **66** (42% yield, based on consumption of **65**) whose structure was confirmed by X-ray analysis beside NMR and mass spectral analyses (Scheme 10).

### 3.4 Investigation of substrate scope of this reaction for various other *t*-amines:

#### 3.4.1 Initial results:

After successful demonstration of distal C-H functionalization of **1** by visible light photoredox catalysis, we proceeded to explore its further scope with other *t*-amines of type **2-3** having fairly acidic benzylic sp<sup>3</sup> C-H bond. Under identical reaction condition as described earlier for **1**, initially **2** (1 equiv.) was irradiated with **48** (1 equiv) in degassed CH<sub>3</sub>CN in the presence of Ru(bpy)<sub>3</sub>Cl<sub>2</sub> (5 mol%), however, there was no indication of any observable reaction (monitored by TLC) even after prolonged irradiation (48 h).<sup>19</sup> Identical reaction of **3** also did not result in the formation of any observable product (Scheme 11, eq 2).



**Scheme 11:** Photocatalytic reaction of *t*-anilines with **48**.

Ultimately, after some experimentation with different solvent systems, we found that irradiation (24 h) of **2** (1 equiv.) with **48** (1 equiv) in degassed dry pyridine-MeOH (3:1) by using Ru(bpy)<sub>3</sub>Cl<sub>2</sub> (5 mol%) produced unexpectedly tetrahydroisoquinoline framework (**67**) in 29% yield (calculated on the basis of the consumption of **2**, after column chromatographic purification) (Scheme 11, eq. 3). It is important to note that a careful LCMS analysis of the photolysate indicated complete consumption of **48** with appreciable amount of un-reacted **2** left and the formation of reduced chalcone. Furthermore, appropriate control experiments showed that both catalyst and visible light (blue LED) were needed for the formation of **67**. It

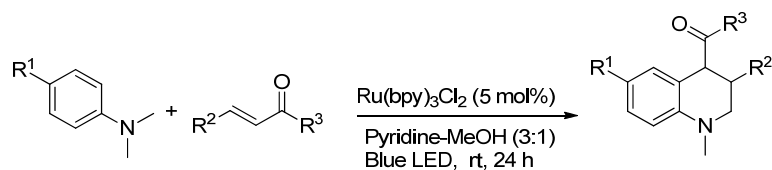
is also important to point that use of another photoredox catalyst [Ir(ppy)<sub>2</sub>(dtb-bpy)]PF<sub>6</sub> (5 mol%), did not help in improving the yield of **67**.

In addition, photo irradiation of **2** (1 equiv.) with **48** (1 equiv.) using Ru(bpy)<sub>3</sub>Cl<sub>2</sub> (5 mol%) in an open atmosphere in CH<sub>3</sub>CN did not show the formation of tetrahydroquinoline<sup>24</sup> (**67**) at all, however, it was formed in <5% yield in pyridine:MeOH (3:1) after prolonged irradiation (48 h). It is important to mention that in both of these last two reactions, a small amount N-demethylated product of **2** was observed (4-5% yield).<sup>25</sup>

### 3.4.2 Evaluation of the generality of the reaction:

In order to evaluate the generality of the above mentioned reaction (eq. 3), photo irradiation of various *t*-anilines with representative examples of electron deficient alkenes were investigated under identical experimental conditions and results are shown in Table 3. The yields are based on the consumption of *t*-anilines, after column chromatographic purification.

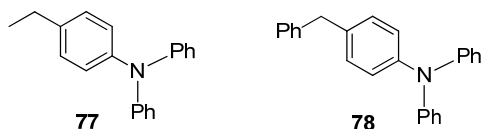
It was observed that irradiation of **2** with **45** gave corresponding tetrahydroquinoline **68** in slightly high yield (48%, entry 2). However, irradiation of **2** with **42** resulted in low yield of **69** (19%, entry 3), along with small amount of 5-((4-benzylphenyl)(methylamino)pentan-2-one (<5%) product. Analogous reaction pattern was observed for the reaction of **3** with **42**, **45** and **48** giving rise corresponding tetrahydroquinolines (13- 30%), (entries 4-6). To demonstrate further that this reaction is not limited to only *t*-amines of type **2-3**, identical reaction with **73-74** (entries 7-8) were also carried out with **48** which gave corresponding tetrahydroquinoline **75-76** (18-21%), respectively, albeit in low yields. Furthermore, the relative *trans* stereochemistry of tetrahydroquinolines were established by 2D NMR analyses and by MD simulation study of **71**.<sup>19</sup>

**Table 3:** Photocatalytic reaction of *t*-anilines with electron deficient alkenes.<sup>[a]</sup>

| Entry | <i>t</i> -Aniline | Alkene | Product | Yield <sup>[b]</sup>  |
|-------|-------------------|--------|---------|-----------------------|
| 1     |                   |        |         | 29(45) <sup>[c]</sup> |
| 2     |                   |        |         | 48                    |
| 3     |                   |        |         | 19                    |
| 4     |                   |        |         | 23                    |
| 5     |                   |        |         | 30                    |
| 6     |                   |        |         | 13                    |
| 7     |                   |        |         | 21 <sup>[c]</sup>     |
| 8     |                   |        |         | 18 <sup>[c]</sup>     |

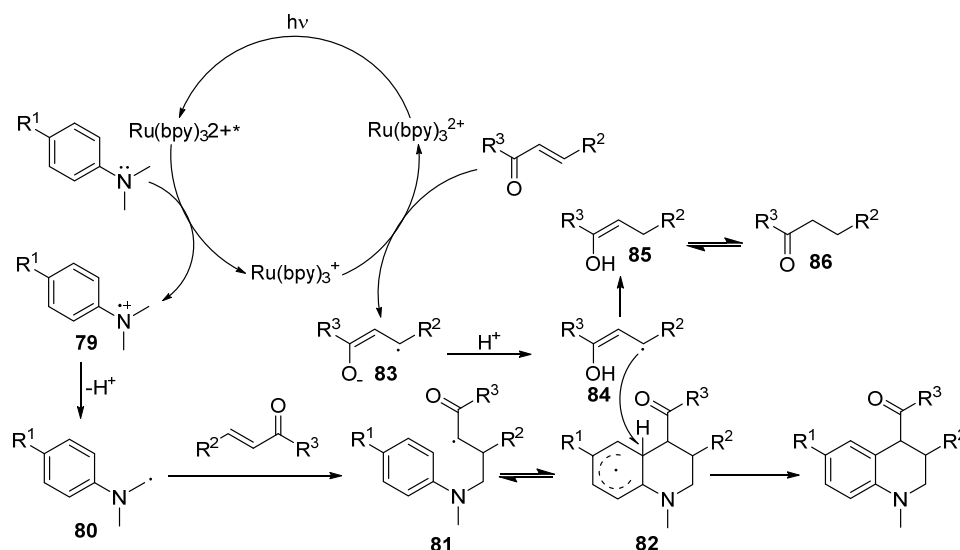
<sup>[a]</sup> Reaction condition: *t*-aniline (1 mmol), alkene (1 mmol), catalyst (5 mol%), blue LED light irradiation, pyridine : MeOH (3 : 1 mL), 24 h. <sup>[b]</sup> Yield based on consumption of *t*-aniline. <sup>[c]</sup> Yield based on consumption of **2** using **48** (2.5 mmol).

It should be noted that under the optimized reaction condition, identical activation of **77** or **78** (1 equiv.) with **48** (1 equiv.), either in degassed CH<sub>3</sub>CN or pyridine:MeOH (3:1) did not show any observable reaction.



### 3.4.3 Proposed reaction mechanism:

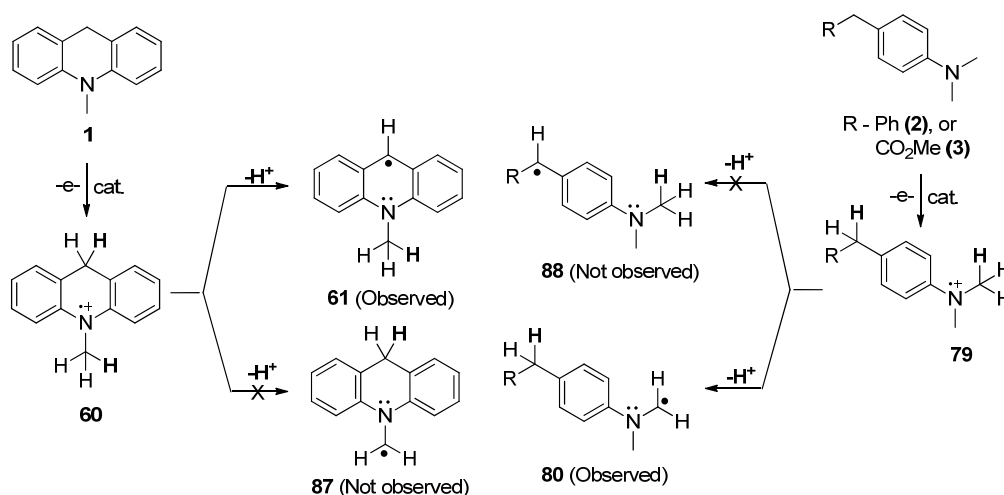
On the basis of observed results, a plausible reaction mechanism is proposed as shown in Figure-5. The support to this proposed mechanism discerns from the formation of **86** and improvement in yields of corresponding tetrahydroquinolines when photoreaction was carried out using 2.5 equivalents of enones (Table 3, entry 1).



**Figure 5:** Proposed mechanism for the photocatalytic reaction of *t*-anilines with electron deficient alkenes.

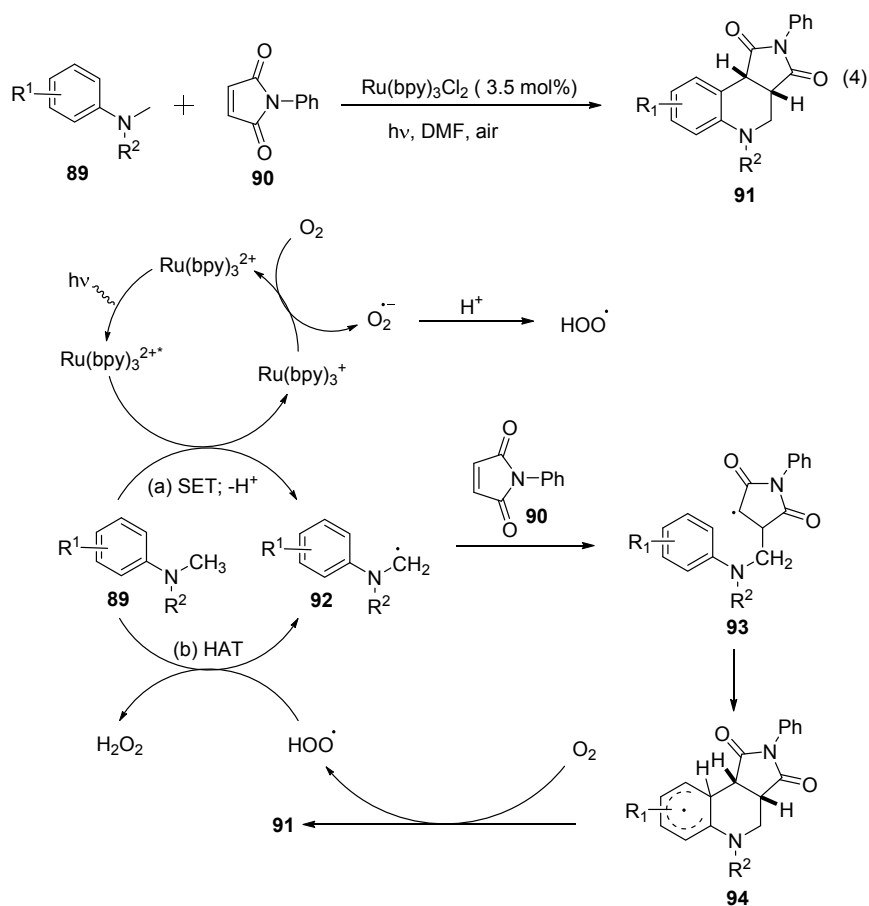
3.5 Proposed rationale for different deprotonation site of *t*-amines:

Although, at this stage we do not comprehend exactly the contrasting behavior in the observed deprotonation site between **60** and **79**, it appears that amine radical cation **60** ( $\text{AcrH}_2^{\cdot+}$ ) undergoes  $\gamma$  C-H deprotonation rather than  $\alpha$  C-H deprotonation owing to its higher acidity generating thermodynamically stable **61** ( $\text{AcrH}^{\cdot}$ ) rather than **87**<sup>20, 26</sup> (Figure 6). In contrast,  $\alpha$  C-H deprotonation from **79** could be mainly due to localization of charge on nitrogen contributing to low reaction barriers<sup>27</sup> for generating **80** compared to the formation of **88** by distal C-H deprotonation. Further mechanistic study in this regard is under progress.<sup>19</sup>

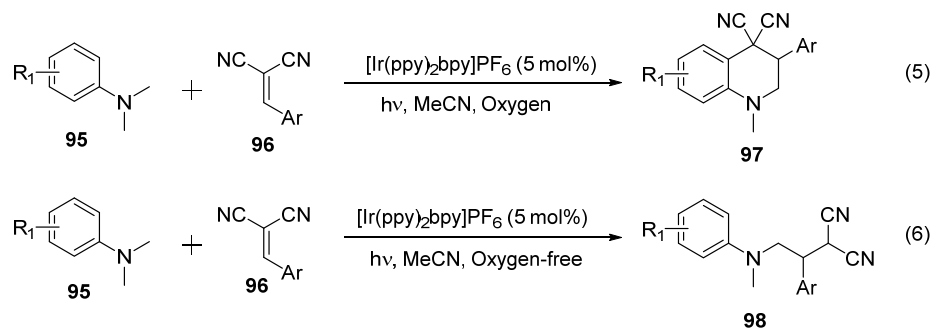


**Figure 6:** Possible deprotonation pathways of **60** and **79**.

It is important to mention that, while this work (Section 3.4) was in progress, two independent publications appeared simultaneously from the groups of Yu and Bian<sup>24a</sup> and Rueping<sup>24b</sup> reporting formation of tetrahydroquinoline frameworks from the reaction of *t*-anilines with various differently substituted olefins, by using visible light photoredox catalysis. Yu and Bian co-workers reported the formation of tetrahydroquinolines from *t*-anilines and N-aryl or N-benzyl maleimides using  $\text{Ru}(\text{bpy})_3\text{Cl}_2$  or  $[\text{Ir}(\text{ppy})_2(\text{dtb-bpy})]\text{PF}_6$  as catalyst and air as a terminal oxidant (Scheme 12, eq 4). The mechanism of this reaction is shown in Scheme 12.<sup>24a</sup>

Scheme 12: Photocatalytic reactions of *t*-anilines with 90.

Rueping and co-workers have reported the formation of cyclic and acyclic products from the photoreaction between *N,N*-dimethyl anilines and benzylidene malononitrile by using  $[\text{Ir}(\text{ppy})_2(\text{dtb-bpy})]\text{PF}_6$  as a catalyst in the presence and absence of oxygen respectively (Scheme 13, eq. 5-6).<sup>24b</sup>

Scheme 13: Photocatalytic reactions of *t*-anilines with 96.

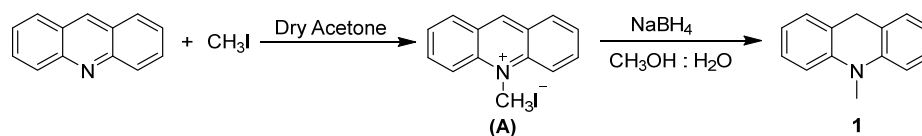
### 3.6 Summary:

In conclusion, we disclose an unprecedented, mechanistically interesting and synthetically useful one electron oxidative chemistry of *t*-amines having two possible sites for deprotonation through visible light photoredox catalysis. It has been found that deprotonation occurs either from  $\gamma$   $sp^3$  C-H or  $\alpha$   $sp^3$  C-H site, from their corresponding radical cations, depending on the structure of the amines. The activation of 10-methyl-9,10-dihydroacridine in the presence of electron deficient alkenes leads to  $\gamma$   $sp^3$  C-H alkylation whereas 4-alkyl-*N, N* dimethylanilines produces synthetically useful substituted tetrahydroquinolines through  $\alpha$   $sp^3$  C-H alkylation/cyclization sequence. Further, application of the methodology is demonstrated by the synthesis of 10-methylacridin-9(10H)-one without using any consumable reagent. This strategy may lead to an easy, economic and eco-friendly protocol for the syntheses of biologically active and pharmacologically important acridone derivatives.



## 3.7 Experimental section:

## 3.7.1 Preparation of substrates:

10-methyl-9,10-dihydroacridine **1** (AcrH<sub>2</sub>)<sup>28</sup>:

To a solution of acridine (1g, 5.58 mmol) in dry acetone (12 mL) was added methyl iodide (1.04 mL, 16.74 mmol) and the resulting reaction mixture refluxed under argon atmosphere for 24 h. The precipitated orange colored crystalline 10-methylacridin-10-ium iodide (**A**) was separated by filtration, dried and used as such for the next step without any purification.

A solution of 10-methylacridin-10-ium iodide (1.25 g, 3.89 mmol) in CH<sub>3</sub>OH:H<sub>2</sub>O (4:2, 60 mL) was charged in a 100 mL round bottom flask and stirred at 0 °C. NaBH<sub>4</sub> (0.294 g, 7.78 mmol) was slowly introduced in to the flask while stirring. After further stirring for another 1 h at 10 °C, solid separated from the solution was filtered, dried and crystallized [EtOH: H<sub>2</sub>O (95:5)] to obtain pure 10-methyl-9,10-dihydroacridine **1** (AcrH<sub>2</sub>) ( 0.505 g, 2.59 mmol) as a white solid.

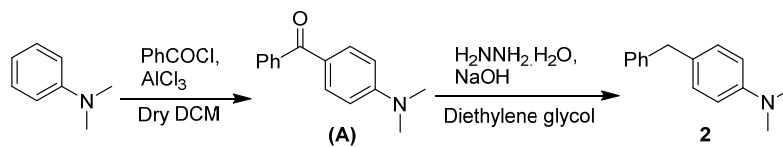
**R<sub>f</sub>** (49:1 Hexanes : EtOAc) = 0.65.

**IR** (neat): 2805, 1586, 1454, 1327, 1258, 1160, 1118, 1029, 917, 858, 740 cm<sup>-1</sup>.

**<sup>1</sup>H NMR** (400 MHz, CDCl<sub>3</sub>) δ 7.24 - 7.17 (m, 4 H), 6.95 (t, *J* = 7.4 Hz, 2 H), 6.90 (d, *J* = 8.0 Hz, 2 H), 3.91 (s, 2 H), 3.40 (s, 3 H)

**<sup>13</sup>C NMR** (100 MHz, CDCl<sub>3</sub>) δ 143.6, 127.5, 126.8, 124.2, 120.5, 111.8, 33.2, 33.1

**HRMS**: (ESI-MS) *m/z* calculated for C<sub>14</sub>H<sub>14</sub>N [M+H]<sup>+</sup>: 196.1121, found: 196.1118.

**4-Benzyl-*N,N*-dimethylaniline (2)**<sup>29</sup> :

To a mixture of  $\text{AlCl}_3$  (2.1 g, 15.74 mmol) and dry dichloromethane (50 mL) in 250 mL two neck round bottom flask was slowly added benzoyl chloride (2.21 g, 15.72 mmol) and *N,N*-dimethylaniline (2 g, 16.50 mmol) at  $0^\circ\text{C}$  under argon atmosphere. The reaction mixture was stirred for 4 h at  $0^\circ\text{C}$  and further 3 h at room temperature. Afterwards the reaction mixture was diluted with dichloromethane (50 mL), water (15 mL) and stirred for another 15 min. The separated organic layer was washed with water (2 x 20 mL), saturated aqueous  $\text{NaHCO}_3$  solution (2 x 20 mL), dried over  $\text{Na}_2\text{SO}_4$ , concentrated under reduced pressure and chromatographed to obtain pure 4-(dimethylamino)phenyl(phenyl)methanone (**A**) (2.3 g, 10.2 mmol) as a yellow solid.

A mixture of 4-(dimethylamino)phenyl(phenyl)-methanone (**A**) (2.3 g, 10.21 mmol), hydrazine-hydrate (2.56 g, 51.05 mmol),  $\text{NaOH}$  (2.04 g, 51.05 mmol) and diethylene glycol (65 mL) contained in a 250 mL round bottom flask, was heated at  $155^\circ\text{C}$  for 5 h. The reaction mixture was allowed to come to rt and diluted with ethyl acetate (100 mL) and water (100 mL). The organic layer was separated and the aqueous layer was extracted with ethyl acetate (2 x 100 mL). The combined organic layers were dried over  $\text{Na}_2\text{SO}_4$ , concentrated under reduced pressure and purified by column chromatography to obtain 4-benzyl-*N,N*-dimethylaniline (**2**) (1.8 g, 8.51 mmol) as a yellow liquid.

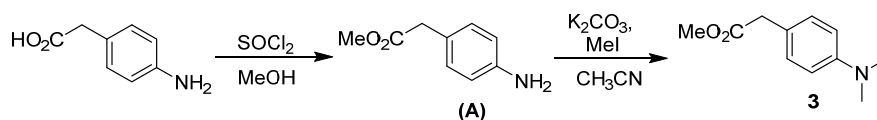
$R_f$  (19:1 Hexanes : EtOAc) = 0.8

**IR** (neat): 2900, 1615, 1520, 1493, 1346, 1218, 1162, 754  $\text{cm}^{-1}$

**$^1\text{H}$  NMR** (500 MHz,  $\text{CDCl}_3$ )  $\delta$  7.38 - 7.32 (m, 2 H), 7.30 - 7.23 (m, 3 H), 7.15 (d,  $J$  = 8.5 Hz, 2 H), 6.78 (d,  $J$  = 8.5 Hz, 2 H), 3.98 (s, 2 H), 2.99 (s, 6 H)

**$^{13}\text{C}$  NMR** (125 MHz,  $\text{CDCl}_3$ )  $\delta$  149.1, 142.0, 129.5, 129.3, 128.8, 128.3, 125.7, 113.0, 40.9, 40.8

**HRMS**: (ESI-MS)  $m/z$  calculated for  $\text{C}_{15}\text{H}_{18}\text{N}$   $[\text{M} + \text{H}]^+$ : 212.1434, found: 212.1434.

**Methyl 2-(4-(dimethylamino)phenyl)acetate (3)**<sup>30</sup>:

A 50 mL single neck round bottom flask containing mixture of 2-(4-aminophenyl)acetic acid (1 g, 6.62 mmol) and dry MeOH (20 mL) was charged with  $\text{SOCl}_2$  (0.53 mL, 7.28 mmol) drop-wise at 0 °C under argon atmosphere. After stirring at 0 °C for 30 min. and additionally 30 min. at rt, it was refluxed for 3 h. Excess of  $\text{SOCl}_2$  along with MeOH was distilled off under reduced pressure. The crude methyl 2-(4-aminophenyl)acetate (A) (1.04 g, 6.30 mmol) was used as such for the next step without any purification.

To a stirring mixture of crude methyl 2-(4-aminophenyl)acetate (A) (1.04 g, 6.30 mmol) and  $\text{K}_2\text{CO}_3$  (4.35 g, 31.48 mmol) in  $\text{CH}_3\text{CN}$  (20 mL), MeI (1.18 mL, 18.90 mmol) was introduced and refluxed for 8 h. Excess of MeI along with  $\text{CH}_3\text{CN}$  was evaporated off to obtain a solid mass which was treated with dichloromethane (50 mL) and water (50 mL). The organic layer was separated and the aqueous layer was extracted with dichloromethane (2 x 50 mL). The combined organic layer was washed with brine (20 mL), dried over  $\text{Na}_2\text{SO}_4$ , concentrated under reduced pressure and purified by column chromatography to obtain pure methyl 2-(4-(dimethylamino)phenyl)acetate (3) (0.8 g, 4.14 mmol) as a yellow liquid.

$R_f$  (9:1 Hexanes : EtOAc) = 0.4

IR (neat): 2951, 1733, 1615, 1523, 1436, 1347, 1259, 1154, 808  $\text{cm}^{-1}$

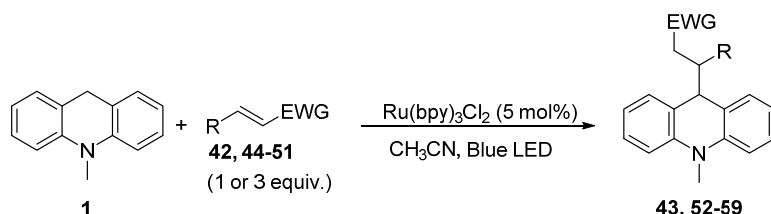
$^1\text{H NMR}$  (400 MHz,  $\text{CDCl}_3$ )  $\delta$  7.15 (d,  $J$  = 8.8 Hz, 2 H), 6.71 (d,  $J$  = 8.5 Hz, 2 H), 3.67 (s, 3 H), 3.53 (s, 2 H), 2.93 (s, 6 H)

$^{13}\text{C NMR}$  (100 MHz,  $\text{CDCl}_3$ )  $\delta$  172.7, 149.6, 129.8, 121.9, 112.8, 51.9, 40.7, 40.2

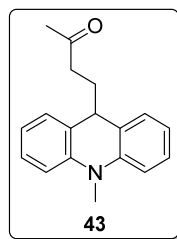
HRMS: (ESI-MS)  $m/z$  calculated for  $\text{C}_{11}\text{H}_{16}\text{NO}_2$   $[\text{M} + \text{H}]^+$ : 194.1176, found: 194.1171

### 3.7.2. General photoredox reaction for $\gamma$ sp<sup>3</sup> C-H alkylation of 10-methyl-9,10-dihydroacridine (**1**) with electron deficient alkenes:<sup>19</sup>

A dry 25 mL Schlenk or round bottom flask equipped with a magnetic stir bar was charged with a 10-methyl-9,10-dihydroacridine (**1**) (0.1 g, 0.51 mmol), electron deficient alkenes (0.51 mmol or 1.53 mmol), Ru(bpy)<sub>3</sub>Cl<sub>2</sub>•6H<sub>2</sub>O (0.019 g, 25.5  $\mu$ mol, 5 mol%) and HPLC grade acetonitrile (2 mL). The solution was degassed using three freeze-pump-thaw cycles and stirred at room temperature at a distance of approximately 3 cm from a blue light emitting diode. The photochemical reaction was monitored by TLC analysis. After completion, the solvent was removed under reduced pressure and residue purified by silica gel column chromatography using hexanes: ethyl acetate to obtain corresponding  $\gamma$  sp<sup>3</sup> C-H alkylation products. (The details of reaction conditions are summarized in Table 2).



#### 4-(10-methyl-9,10-dihydroacridin-9-yl)butan-2-one (**43**):



**Yield:** 70% (yellow oil).

**R<sub>f</sub>** (19:1 Hexanes : EtOAc) = 0.3.

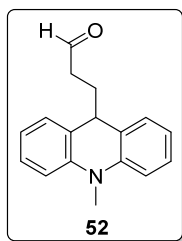
**IR** (neat): 2924, 2857, 1712, 1596, 1473, 1349, 1275, 1164, 1132, 1047, 754 cm<sup>-1</sup>.

**<sup>1</sup>H NMR** (500 MHz, CDCl<sub>3</sub>)  $\delta$  7.26 - 7.22 (m, 2 H), 7.14 (dd,  $J$  = 1.2, 7.3 Hz, 2 H), 6.98 - 6.93 (m, 4 H), 3.89 (t,  $J$  = 7.3 Hz, 1 H), 3.40 (s, 3 H), 2.34 (t,  $J$  = 7.6 Hz, 2 H), 2.06 (s, 3 H), 1.82 (q,  $J$  = 7.3 Hz, 2 H).

$^{13}\text{C}$  NMR (125 MHz,  $\text{CDCl}_3$ )  $\delta$  208.8, 142.4, 128.1, 127.0, 126.9, 120.5, 112.1, 43.0, 40.6, 32.9, 31.3, 29.9.

HRMS: (ESI-MS)  $m/z$  calculated for  $\text{C}_{18}\text{H}_{20}\text{NO}$   $[\text{M} + \text{H}]^+$ : 266.1539, found: 266.1538.

**3-(10-methyl-9,10-dihydroacridin-9-yl)propanal (52):**



**Yield:** 47% (yellow viscous oil)

$R_f$  (19:1 Hexanes : EtOAc) = 0.7

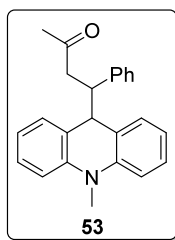
**IR** (neat): 2920, 2851, 1719, 1593, 1472, 1345, 1273, 1131, 1042, 748  $\text{cm}^{-1}$

$^1\text{H}$  NMR (500 MHz,  $\text{CDCl}_3$ )  $\delta$  9.61 (t,  $J = 1.5$  Hz, 1 H), 7.25 (dt,  $J = 1.5, 7.8$  Hz, 2 H), 7.15 (dd,  $J = 1.5, 7.3$  Hz, 2 H), 6.99 - 6.93 (m, 4 H), 3.93 (t,  $J = 7.2$  Hz, 1 H), 3.40 (s, 3 H), 2.35 (dt,  $J = 1.5, 7.5$  Hz, 2 H), 1.89 (q,  $J = 7.3$  Hz, 2 H)

$^{13}\text{C}$  NMR (125 MHz,  $\text{CDCl}_3$ )  $\delta$  202.4, 142.4, 128.2, 127.2, 126.5, 120.6, 112.2, 43.0, 40.9, 32.9, 29.9

**HRMS:** (ESI-MS)  $m/z$  calculated for  $\text{C}_{17}\text{H}_{18}\text{NO}$   $[\text{M} + \text{H}]^+$ : 252.1383, found: 252.1382.

**4-(10-methyl-9,10-dihydroacridin-9-yl)-4-phenylbutan-2-one (53):**



**Yield:** 87% (white solid)

$R_f$  (9:1 Hexanes : EtOAc) = 0.5.

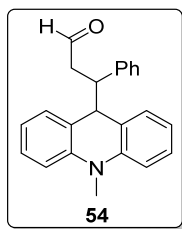
**IR** (neat): 3026, 2909, 1700, 1592, 1475, 1340, 1269, 1131, 756, 700  $\text{cm}^{-1}$ .

**$^1\text{H NMR}$**  (400 MHz,  $\text{CDCl}_3$ )  $\delta$  7.31 - 7.16 (m, 3 H), 7.15 - 7.05 (m, 3 H), 6.98 (t,  $J = 7.3$  Hz, 1 H), 6.86 - 6.77 (m, 3 H), 6.74 (d,  $J = 6.8$  Hz, 1 H), 6.64 (d,  $J = 5.3$  Hz, 2 H), 4.07 (d,  $J = 6.5$  Hz, 1 H), 3.37 (q,  $J = 7.1$  Hz, 1 H), 3.09 (s, 3 H), 2.87 - 2.74 (m, 2 H), 1.96 (s, 3 H)

**$^{13}\text{C NMR}$**  (100 MHz,  $\text{CDCl}_3$ )  $\delta$  207.5, 142.9, 142.8, 141.1, 128.9, 128.9, 128.2, 127.3, 127.2, 127.0, 126.3, 125.2, 124.0, 120.2, 119.7, 112.0, 111.9, 49.7, 47.4, 46.3, 32.8, 30.4

**HRMS:** (ESI-MS)  $m/z$  calculated for  $\text{C}_{24}\text{H}_{24}\text{NO}$   $[\text{M} + \text{H}]^+$ : 342.1852, found: 342.1851.

**3-(10-methyl-9,10-dihydroacridin-9-yl)-3-phenylpropanal (54):**



**Yield:** 60% (white crystalline solid).

$R_f$  (19:1 Hexanes : EtOAc) = 0.4

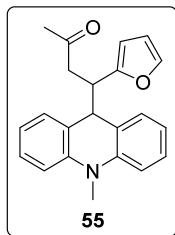
**IR** (neat): 2875, 1709, 1590, 1465, 1338, 1267, 1126, 747, 694  $\text{cm}^{-1}$ .

**$^1\text{H NMR}$**  (500 MHz,  $\text{CDCl}_3$ )  $\delta$  9.40 (t,  $J = 2.0$  Hz, 1 H), 7.30 - 7.24 (m, 1 H), 7.24 - 7.19 (m, 1 H), 7.17 - 7.11 (m, 3 H), 7.10 (dd,  $J = 1.4, 7.5$  Hz, 1 H), 6.98 (dt,  $J = 0.9, 7.3$  Hz, 1 H), 6.86 (dd,  $J = 2.0, 8.1$  Hz, 2 H), 6.83 - 6.79 (m, 1 H), 6.77 - 6.74 (m, 1 H), 6.73 - 6.67 (m, 2 H), 4.08 (d,  $J = 6.7$  Hz, 1 H), 3.46 - 3.37 (m, 1 H), 3.17 (s, 3 H), 2.79 - 2.74 (m, 2 H)

**$^{13}\text{C NMR}$**  (125 MHz,  $\text{CDCl}_3$ )  $\delta$  201.8, 142.9, 142.8, 140.6, 129.1, 129.0, 128.3, 127.6, 127.4, 127.2, 126.6, 124.5, 124.0, 120.3, 120.0, 112.1, 112.0, 50.2, 46.3, 46.0, 32.8.

**HRMS:** (ESI-MS)  $m/z$  calculated for  $C_{23}H_{22}NO$   $[M + H]^+$ : 328.1696, found: 328.1694.

**4-(furan-2-yl)-4-(10-methyl-9,10-dihydroacridin-9-yl)butan-2-one (55):**



**Yield:** (yellow oil):

$R_f$  (19:1 Hexanes : EtOAc) = 0.4

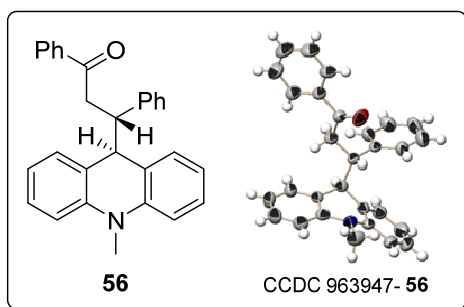
**IR** (neat): 2922, 1715, 1593, 1475, 1345, 1271, 1130, 751  $cm^{-1}$

**$^1H$  NMR** (500 MHz,  $CDCl_3$ )  $\delta$  7.27 (bs, 1 H), 7.26 - 7.15 (m, 2 H), 6.96 (d,  $J = 7.0$  Hz, 1 H), 6.93 - 6.86 (m, 3 H), 6.85 - 6.79 (m, 2 H), 6.14 (dd,  $J = 1.8, 2.7$  Hz, 1 H), 5.58 (d,  $J = 2.7$  Hz, 1 H), 4.18 (d,  $J = 7.6$  Hz, 1 H), 3.44 (ddd,  $J = 5.5, 7.6, 9.5$  Hz, 1 H), 3.33 (s, 3 H), 2.74 (dd,  $J = 9.5, 16.5$  Hz, 1 H), 2.58 (dd,  $J = 5.2, 16.5$  Hz, 1 H), 1.89 (s, 3 H)

**$^{13}C$  NMR** (125 MHz,  $CDCl_3$ )  $\delta$  207.2, 154.9, 143.0, 142.5, 140.8, 129.1, 128.5, 127.4, 127.1, 124.9, 124.1, 120.1, 112.1, 111.9, 110.0, 107.0, 48.0, 43.9, 40.8, 33.0, 30.1

**HRMS:** (ESI-MS)  $m/z$  calculated for  $C_{22}H_{22}NO_2$   $[M + H]^+$ : 332.1645, found: 332.1643.

**3-(10-methyl-9,10-dihydroacridin-9-yl)-1,3-diphenylpropan-1-one (56):**



**Yield:** 56% (white crystalline solid).

$R_f$  (19:1 Hexanes : EtOAc) = 0.4

**IR** (neat): 2885, 1677, 1589, 1466, 1338, 1272, 1126, 1036, 747, 690  $\text{cm}^{-1}$

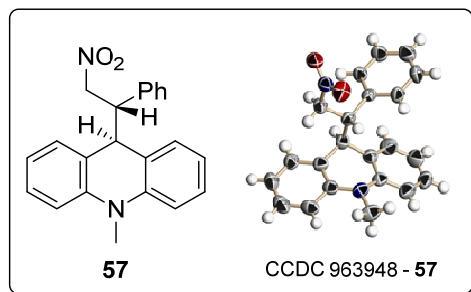
**$^1\text{H}$  NMR** (400 MHz,  $\text{CDCl}_3$ )  $\delta$  7.84 (d,  $J = 7.3$  Hz, 2 H), 7.56 (t,  $J = 7.3$  Hz, 1 H), 7.44 (t,  $J = 7.6$  Hz, 2 H), 7.29 - 7.19 (m, 3 H), 7.10 - 7.06 (m, 3 H), 6.98 (t,  $J = 7.4$  Hz, 1 H), 6.84 - 6.79 (m, 4 H), 6.67 - 6.65 (m, 2 H), 4.23 (d,  $J = 6.3$  Hz, 1 H), 3.60 (q,  $J = 6.9$  Hz, 1 H), 3.46 (dd,  $J = 6.5, 16.8$  Hz, 1 H), 3.29 (dd,  $J = 7.6, 16.9$  Hz, 1 H), 3.04 (s, 3 H)

**$^{13}\text{C}$  NMR** (100 MHz,  $\text{CDCl}_3$ )  $\delta$  198.8, 143.0, 142.8, 141.3, 137.2, 132.8, 129.1, 129.0, 128.4, 128.3, 127.9, 127.2, 127.0, 126.2, 125.4, 124.1, 120.3, 119.8, 111.9, 49.2, 47.7, 40.8, 32.8

**HRMS:** (ESI-MS)  $m/z$  calculated for  $\text{C}_{29}\text{H}_{26}\text{NO}$   $[\text{M} + \text{H}]^+$ : 404.2009, found: 404.2008.

CCDC-963947 contains the supplementary crystallographic data for **56**.

**10-methyl-9-(2-nitro-1-phenylethyl)-9,10-dihydroacridine (57):**



**Yield:** 40% (white crystalline solid)

$R_f$  (19:1 Hexanes : EtOAc) = 0.5

**IR** (neat): 2912, 1591, 1549, 1465, 1378, 1339, 1267, 1126, 1038, 740, 693, 639  $\text{cm}^{-1}$

**$^1\text{H}$  NMR** (400MHz,  $\text{CDCl}_3$ )  $\delta$  7.59 - 7.37 (m, 6 H), 7.30 - 7.27 (m, 1 H), 7.15 - 7.12 (m, 4 H), 6.94 (d,  $J = 6.8$  Hz, 2 H), 4.96 - 4.92 (m, 2 H), 4.48 (d,  $J = 6.5$  Hz, 1 H), 3.98 (td,  $J = 6.8, 8.9$  Hz, 1 H), 3.40 (s, 3 H)

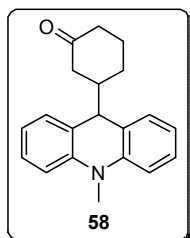
**$^{13}\text{C}$  NMR** (100 MHz,  $\text{CDCl}_3$ )  $\delta$  142.8, 142.7, 136.7, 128.9, 128.7, 128.1, 127.8, 127.7, 127.6, 127.4, 123.3, 122.7, 120.6, 120.3, 112.4, 112.2, 77.1, 50.1, 47.8, 32.8



**HRMS:** (ESI-MS)  $m/z$  calculated for  $C_{22}H_{21}N_2O_2$   $[M + H]^+$ : 345.1598, found: 345.1597.

CCDC-963948 contains the supplementary crystallographic data for **57**.

**3-(10-methyl-9,10-dihydroacridin-9-yl)cyclohexanone (58):**



**Yield:** 58% (white solid).

**R<sub>f</sub>** (19:1 Hexanes : EtOAc) = 0.5

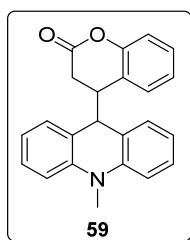
**IR** (neat): 2896, 1701, 1591, 1467, 1334, 1267, 1225, 1131, 1041, 883, 749  $cm^{-1}$

**<sup>1</sup>H NMR** (500 MHz,  $CDCl_3$ )  $\delta$  7.29 - 7.25 (m, 2 H), 7.14 (dt,  $J = 1.5, 7.2$  Hz, 2 H), 7.00 - 6.95 (m, 4 H), 3.80 (d,  $J = 6.4$  Hz, 1 H), 3.39 (s, 3 H), 2.29 - 2.21 (m, 2 H), 2.19 - 2.13 (m, 1 H), 2.05 - 1.91 (m, 3 H), 1.81 - 1.75 (m, 1 H), 1.46 (td,  $J = 4.0, 13.1$  Hz, 1 H), 1.37 - 1.29 (m, 1 H)

**<sup>13</sup>C NMR** (125 MHz,  $CDCl_3$ )  $\delta$  212.2, 142.8, 129.1, 129.0, 127.3, 127.2, 125.0, 124.5, 120.4, 120.3, 112.2, 49.4, 45.3, 45.2, 41.2, 32.9, 28.3, 25.1

**HRMS:** (ESI-MS)  $m/z$  calculated for  $C_{20}H_{22}NO$   $[M + H]^+$ : 292.1696, found: 292.1695.

**4-(10-methyl-9,10-dihydroacridin-9-yl)chroman-2-one (59):**



**Yield:** 30% (white solid).

**R<sub>f</sub>** (9:1 Hexanes : EtOAc) = 0.8

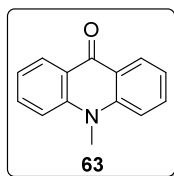
**IR** (neat): 2914, 1753, 1591, 1466, 1334, 1258, 1143, 1029, 908, 748 cm<sup>-1</sup>

**<sup>1</sup>H NMR** (400 MHz, CDCl<sub>3</sub>) δ 7.33 - 7.22 (m, 3 H), 7.01 - 6.95 (m, 5 H), 6.91 (t, *J* = 7.5 Hz, 1 H), 6.82 (t, *J* = 7.3 Hz, 1 H), 6.69 (d, *J* = 7.6 Hz, 1 H), 6.46 - 6.44 (m, 1 H), 3.95 (d, *J* = 8.1 Hz, 1 H), 3.40 (s, 3 H), 3.07 (t, *J* = 7.2 Hz, 1 H), 2.83 (dd, *J* = 1.5, 16.4 Hz, 1 H), 2.57 (dd, *J* = 6.6, 16.4 Hz, 1 H)

**<sup>13</sup>C NMR** (100MHz, CDCl<sub>3</sub>) δ 168.1, 151.7, 142.8, 142.7, 129.5, 129.2, 129.1, 128.4, 127.9, 127.6, 123.9, 123.6, 122.9, 120.7, 120.4, 116.6, 112.4, 111.9, 48.7, 41.1, 33.0, 31.7

**HRMS:** (ESI-MS) *m/z* calculated for C<sub>23</sub>H<sub>20</sub>NO<sub>2</sub> [M + H]<sup>+</sup>: 342.1489, found: 342.1488.

**10-methylacridin-9(10H)-one (63):**



**Yield:** 90% (white crystalline solid).

**R<sub>f</sub>** (6:4 Hexanes : EtOAc) = 0.4

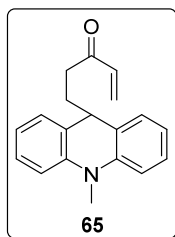
**IR** (neat): 2912, 1588, 1488, 1453, 1362, 1260, 1172, 1030, 799, 747, 667 cm<sup>-1</sup>

**<sup>1</sup>H NMR** (500 MHz, CDCl<sub>3</sub>) δ 8.56 (dd, *J* = 1.5, 7.9 Hz, 2 H), 7.71 (ddd, *J* = 1.7, 7.0, 8.7 Hz, 2 H), 7.49 (d, *J* = 8.9 Hz, 2 H), 7.32 - 7.25 (m, 2 H), 3.86 (s, 3 H)

**<sup>13</sup>C NMR** (125 MHz, CDCl<sub>3</sub>) δ 178.0, 142.4, 133.7, 127.6, 122.4, 121.2, 114.7, 33.5

**HRMS:** (ESI-MS) *m/z* calculated for C<sub>14</sub>H<sub>12</sub>NO [M + H]<sup>+</sup>: 210.0913, found: 210.0913.

**5-(10-methyl-9,10-dihydroacridin-9-yl)pent-1-en-3-one (65):**



**Yield:** 51% (yellow thick oil).

**R<sub>f</sub>** (19:1 Hexanes : EtOAc) = 0.5

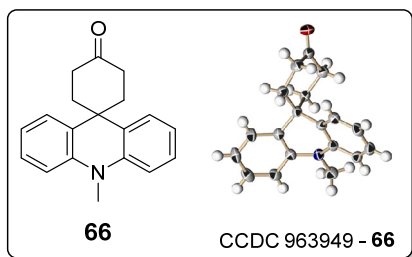
**IR** (neat): 2925, 1678, 1594, 1475, 1344, 1269, 1130, 1043, 755, 504 cm<sup>-1</sup>

**<sup>1</sup>H NMR** (200 MHz, CDCl<sub>3</sub>) δ 7.27 - 7.14 (m, 4 H), 7.00 - 6.92 (m, 4 H), 6.30 (dd, *J* = 10.2, 17.7 Hz, 1 H), 6.09 (dd, *J* = 1.5, 17.7 Hz, 1 H), 5.77 (dd, *J* = 1.5, 10.2 Hz, 1 H), 3.93 (t, *J* = 7.2 Hz, 1 H), 3.40 (s, 3 H), 2.51 (t, *J* = 7.5 Hz, 2 H), 1.87 (q, *J* = 7.4 Hz, 2 H)

**<sup>13</sup>C NMR** (50 MHz, CDCl<sub>3</sub>) δ 200.6, 142.3, 136.4, 128.1, 128.0, 127.9, 127.0, 126.9, 120.5, 112.1, 42.9, 36.4, 32.9, 31.2

**HRMS:** (ESI-MS) *m/z* calculated for C<sub>19</sub>H<sub>20</sub>NO [M + H]<sup>+</sup>: 278.1539, found: 278.1538.

**10-methyl-10H-spiro[acridine-9,1'-cyclohexan]-4'-one (66):**



**Yield:** 42% (white crystalline solid):

**R<sub>f</sub>** (9:1 Hexanes : EtOAc) = 0.7

**IR** (neat): 2923, 1716, 1590, 1465, 1346, 1270, 1130, 848, 750 cm<sup>-1</sup>

$^1\text{H NMR}$  (500 MHz,  $\text{CDCl}_3$ )  $\delta$  7.50 - 7.48 (m, 2 H), 7.32 - 7.29 (m, 2 H), 7.09 - 7.06 (m, 4 H), 3.52 (s, 3 H), 2.53 - 2.51 (m, 4 H), 2.48 - 2.45 (m, 4 H)

$^{13}\text{C NMR}$  (125 MHz,  $\text{CDCl}_3$ )  $\delta$  212.3, 142.8, 130.2, 126.9, 123.8, 120.9, 112.8, 39.1, 38.2, 33.4, 31.4

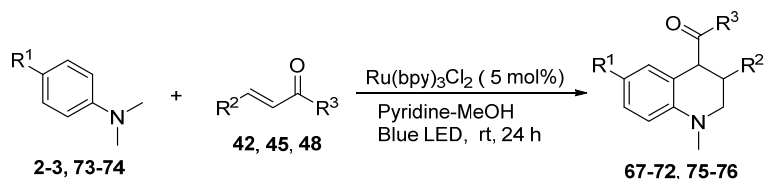
**HRMS:** (ESI-MS)  $m/z$  calculated for  $\text{C}_{19}\text{H}_{20}\text{NO}$   $[\text{M} + \text{H}]^+$ : 278.1539, found: 278.1538.

CCDC-963949 contains the supplementary crystallographic data for **66**.

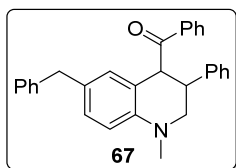
---

### 3.7.3 General procedure for photoredox reaction of *t*-anilines with electron deficient alkenes:

Identical irradiation, as described above (Section 3.7.2), set up was used to photolyze *t*-aniline (**2-3**, **73-74**) (1 mmol),  $\alpha$ ,  $\beta$ -unsaturated carbonyl compound (**42** or **45** or **48**) (1 or 2.5 mmol),  $\text{Ru}(\text{bpy})_3\text{Cl}_2 \cdot 6\text{H}_2\text{O}$  (5 mol%) in dry pyridine-MeOH (3:1 mL) for 24 h.<sup>19</sup> (The details of reaction conditions are summarized in Table 3).



#### (6-benzyl-1-methyl-3-phenyl-1,2,3,4-tetrahydroquinolin-4-yl)(phenyl)methanone (**67**):



**Yield:** 29% (using 1 equiv. of **48**) and 45% (using 2.5 equiv. of **48**), (yellow oil).

$R_f$  (19:1 Hexanes : EtOAc) = 0.4.

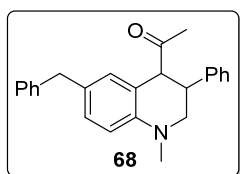
**IR** (neat): 3026, 1681, 1615, 1514, 1494, 1453, 1216, 757, 698  $\text{cm}^{-1}$

**<sup>1</sup>H NMR** (500 MHz, CDCl<sub>3</sub>) δ 7.81 - 7.80 (m, 2 H), 7.55 - 7.53 (m, 1 H), 7.42 - 7.39 (m, 2 H), 7.29 - 7.26 (m, 2 H), 7.23 - 7.20 (m, 3 H), 7.18 - 7.14 (m, 3 H), 7.07 (d, *J* = 7.0 Hz, 2 H), 7.01 (dd, *J* = 1.7, 8.4 Hz, 1 H), 6.74 - 6.72 (m, 2 H), 4.93 (d, *J* = 8.9 Hz, 1 H), 3.78 (s, 2 H), 3.70 (dt, *J* = 4.3, 8.9 Hz, 1 H), 3.45 (dd, *J* = 4.1, 11.4 Hz, 1 H), 3.38 (dd, *J* = 9.2, 11.3 Hz, 1 H), 2.98 (s, 3 H)

**<sup>13</sup>C NMR** (125 MHz, CDCl<sub>3</sub>) δ 202.1, 144.7, 141.8, 141.7, 137.2, 132.7, 129.4, 129.3, 128.8, 128.6, 128.6, 128.5, 128.2, 127.6, 127.0, 125.7, 121.2, 112.0, 55.8, 52.9, 42.6, 40.8, 39.4

**HRMS:** (ESI-MS) *m/z* calculated for C<sub>30</sub>H<sub>28</sub>NO [M + H]<sup>+</sup>: 418.2165, found: 418.2165.

**1-(6-benzyl-1-methyl-3-phenyl-1,2,3,4-tetrahydroquinolin-4-yl)ethanone (68):**



**Yield:** 48% (White solid).

**R<sub>f</sub>** (19:1 Hexanes : EtOAc) = 0.6

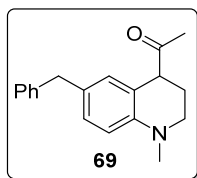
**IR** (neat): 3020, 2925, 1702, 1615, 1514, 1495, 1454, 1216, 757 cm<sup>-1</sup>

**<sup>1</sup>H NMR** (400 MHz, CDCl<sub>3</sub>) δ 7.37 - 7.28 (m, 5 H), 7.23 - 7.17 (m, 5 H), 7.05 (d, *J* = 8.3 Hz, 1 H), 6.77 (s, 1 H), 6.71 (d, *J* = 8.3 Hz, 1 H), 4.07 (d, *J* = 9.5 Hz, 1 H), 3.88 (s, 2 H), 3.52 (dt, *J* = 4.0, 9.5 Hz, 1 H), 3.38 (dd, *J* = 3.3, 11.3 Hz, 1 H), 3.31 - 3.26 (m, 1 H), 2.95 (s, 3 H), 2.04 (s, 3 H)

**<sup>13</sup>C NMR** (100MHz, CDCl<sub>3</sub>) δ 209.5, 144.5, 141.8, 141.1, 129.6, 129.1, 128.9, 128.8, 128.6, 128.3, 127.5, 127.2, 125.8, 119.6, 112.0, 58.6, 56.1, 42.0, 40.9, 39.3, 27.5

**HRMS:** (ESI-MS) *m/z* calculated for C<sub>25</sub>H<sub>26</sub>NO [M + H]<sup>+</sup>: 356.2009, found: 356.2008.

**1-(6-benzyl-1-methyl-1,2,3,4-tetrahydroquinolin-4-yl)ethanone (69):**



**Yield:** 19% (yellow oil).

**R<sub>f</sub>** (19:1 Hexanes : EtOAc) = 0.35

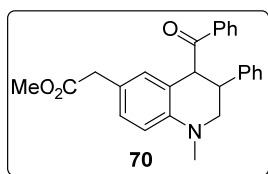
**IR** (neat): 2927, 1706, 1615, 1514, 1494, 1453, 1325, 1210, 702 cm<sup>-1</sup>

**<sup>1</sup>H NMR** (400 MHz, CDCl<sub>3</sub>) δ 7.32 - 7.28 (m, 2 H), 7.22 - 7.19 (m, 3 H), 7.02 (dd, *J* = 2.0, 8.3 Hz, 1 H), 6.83 (d, *J* = 1.5 Hz, 1 H), 6.63 (d, *J* = 8.3 Hz, 1 H), 3.90 (s, 2 H), 3.72 (t, *J* = 5.6 Hz, 1 H), 3.30 - 3.24 (m, 1 H), 3.16 - 3.10 (m, 1 H), 2.89 (s, 3 H), 2.35 - 2.27 (m, 1 H), 2.12 (s, 3 H), 2.07 - 1.99 (m, 1 H)

**<sup>13</sup>C NMR** (100 MHz, CDCl<sub>3</sub>) δ 210.3, 144.8, 141.9, 130.1, 129.0, 128.9, 128.7, 128.3, 125.8, 119.7, 111.7, 51.2, 48.3, 40.8, 39.0, 27.9, 24.5

**HRMS:** (ESI-MS) *m/z* calculated for C<sub>19</sub>H<sub>22</sub>NO [M + H]<sup>+</sup>: 280.1696, found: 280.1695.

**methyl 2-(4-benzoyl-1-methyl-3-phenyl-1,2,3,4-tetrahydroquinolin-6-yl)acetate (70):**



**Yield:** 23% (yellow oil).

**R<sub>f</sub>** (4:1 Hexanes : EtOAc) = 0.5

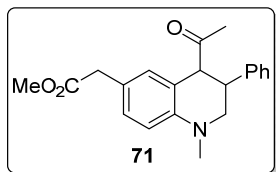
**IR** (neat): 3027, 2950, 1736, 1682, 1615, 1517, 1448, 1272, 1216, 1155, 1015, 756, 699 cm<sup>-1</sup>

**<sup>1</sup>H NMR** (400 MHz, CDCl<sub>3</sub>) δ 7.84 (d, *J* = 7.3 Hz, 2 H), 7.54 (t, *J* = 7.3 Hz, 1 H), 7.42 (t, *J* = 7.3 Hz, 2 H), 7.26 - 7.11 (m, 6 H), 6.76 - 6.74 (m, 2 H), 4.95 (d, *J* = 8.3 Hz, 1 H), 3.69 - 3.64 (m, 1 H), 3.61 (s, 3 H), 3.48 - 3.38 (m, 4 H), 2.98 (s, 3 H)

**<sup>13</sup>C NMR** (100 MHz, CDCl<sub>3</sub>) δ 202.0, 172.5, 145.5, 141.6, 137.1, 132.9, 129.6, 128.9, 128.7, 128.6, 128.5, 127.5, 127.0, 122.0, 121.2, 111.8, 55.4, 52.4, 51.8, 42.4, 40.1, 39.3

**HRMS:** (ESI-MS) *m/z* calculated for C<sub>26</sub>H<sub>26</sub>NO<sub>3</sub> [M + H]<sup>+</sup>: 400.1907, found: 400.1907.

**methyl 2-(4-acetyl-1-methyl-3-phenyl-1,2,3,4-tetrahydroquinolin-6-yl)acetate (71):**



**Yield:** 30% (yellow oil).

**R<sub>f</sub>** (4:1 Hexanes : EtOAc) = 0.5

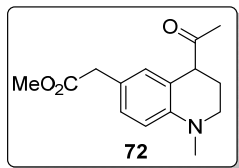
**IR** (neat): 3025, 2925, 1738, 1705, 1616, 1516, 1454, 1435, 1217, 1159, 1017, 757, 701 cm<sup>-1</sup>

**<sup>1</sup>H NMR** (500 MHz, CDCl<sub>3</sub>) δ 7.32 (t, *J* = 7.3 Hz, 2 H), 7.27 - 7.24 (m, 1 H), 7.22 - 7.19 (m, 2 H), 7.11 (dd, *J* = 1.8, 8.5 Hz, 1 H), 6.80 (s, 1 H), 6.69 (d, *J* = 8.2 Hz, 1 H), 4.06 (d, *J* = 9.5 Hz, 1 H), 3.67 (s, 3 H), 3.49 (s, 2 H), 3.48 - 3.46 (m, 1 H), 3.37 (dd, *J* = 4.1, 11.4 Hz, 1 H), 3.28 (dd, *J* = 9.5, 11.6 Hz, 1 H), 2.94 (s, 3 H), 2.06 (s, 3 H)

**<sup>13</sup>C NMR** (125 MHz, CDCl<sub>3</sub>) δ 209.5, 172.5, 145.2, 141.1, 129.5, 129.2, 128.9, 127.5, 127.3, 122.2, 119.6, 111.9, 58.4, 55.9, 51.9, 41.8, 40.1, 39.2, 27.7.

**HRMS:** (ESI-MS) *m/z* calculated for C<sub>21</sub>H<sub>24</sub>NO<sub>3</sub> [M + H]<sup>+</sup>: 338.1751, found: 338.1750.

**methyl 2-(4-acetyl-1-methyl-1,2,3,4-tetrahydroquinolin-6-yl)acetate (72):**



**Yield:** 13% (yellow oil):

**R<sub>f</sub>** (4:1 Hexanes : EtOAc) = 0.4.

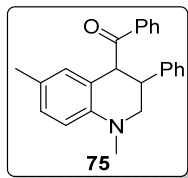
**IR** (neat): 2925, 1738, 1709, 1616, 1517, 1435, 1328, 1262, 1210, 1162, 1015 cm<sup>-1</sup>

**<sup>1</sup>H NMR** (500 MHz, CDCl<sub>3</sub>) δ 7.05 (dd, *J* = 2.1, 8.2 Hz, 1 H), 6.89 (d, *J* = 1.5 Hz, 1 H), 6.61 (d, *J* = 8.2 Hz, 1 H), 3.72 (t, *J* = 5.5 Hz, 1 H), 3.67 (s, 3 H), 3.49 (s, 2 H), 3.25 (ddd, *J* = 4.3, 9.7, 11.4 Hz, 1 H), 3.15 - 3.10 (m, 1 H), 2.87 (s, 3 H), 2.31 - 2.25 (m, 1 H), 2.14 (s, 3 H), 2.04 - 1.97 (m, 1 H)

**<sup>13</sup>C NMR** (125 MHz, CDCl<sub>3</sub>) δ 210.0, 172.6, 145.3, 130.4, 129.2, 121.6, 119.7, 111.7, 51.9, 51.0, 48.1, 40.1, 38.9, 28.1, 24.2

**HRMS:** (ESI-MS) *m/z* calculated for C<sub>15</sub>H<sub>20</sub>NO<sub>3</sub> [M + H]<sup>+</sup>: 262.1438, found: 262.1438.

**(1,6-dimethyl-3-phenyl-1,2,3,4-tetrahydroquinolin-4-yl)(phenyl)methanone (75):**



**Yield:** 21% (yellow oil).

**R<sub>f</sub>** (19:1 Hexanes : EtOAc) = 0.4.

**IR** (neat): 3028, 2920, 1679, 1514, 1449, 1277, 1243, 1002, 804, 759, 698 cm<sup>-1</sup>

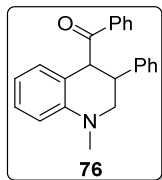
**<sup>1</sup>H NMR** (400 MHz, CDCl<sub>3</sub>) δ 7.84 (d, *J* = 8.1 Hz, 2 H), 7.54 (t, *J* = 7.3 Hz, 1 H), 7.41 (t, *J* = 7.6 Hz, 2 H), 7.29 - 7.13 (m, 5 H), 7.02 (d, *J* = 8.3 Hz, 1 H), 6.72 (d, *J* = 8.3 Hz, 1 H), 6.68 (s, 1 H), 4.93 (d, *J* = 8.6 Hz, 1 H), 3.66 (dt, *J* = 4.0, 8.7 Hz, 1 H), 3.46 - 3.28 (m, 2 H), 2.96 (s, 3 H), 2.15 (s, 3 H)



$^{13}\text{C}$  NMR (100 MHz,  $\text{CDCl}_3$ )  $\delta$  202.2, 144.3, 141.8, 137.1, 132.8, 129.2, 128.7, 128.7, 128.6, 128.5, 127.5, 126.9, 126.1, 121.3, 111.9, 55.7, 52.7, 42.7, 39.4, 20.2

HRMS: (ESI-MS)  $m/z$  calculated for  $\text{C}_{24}\text{H}_{24}\text{NO}$   $[\text{M} + \text{H}]^+$ : 342.1852, found: 342.1850

**(1-methyl-3-phenyl-1,2,3,4-tetrahydroquinolin-4-yl)(phenyl)methanone (76):**



**Yield:** 18% (yellow oil).

**R<sub>f</sub>** (19:1 Hexanes : EtOAc) = 0.35.

**IR** (neat): 3028, 2925, 1680, 1600, 1504, 1449, 1325, 1277, 1216, 1001, 745, 697  $\text{cm}^{-1}$

$^1\text{H}$  NMR (400 MHz,  $\text{CDCl}_3$ )  $\delta$  7.87 (d,  $J = 7.3$  Hz, 2 H), 7.55 (t,  $J = 7.3$  Hz, 1 H), 7.42 (t,  $J = 7.6$  Hz, 2 H), 7.26 (d,  $J = 7.3$  Hz, 2 H), 7.24 - 7.15 (m, 4 H), 6.86 (d,  $J = 7.5$  Hz, 1 H), 6.79 (d,  $J = 8.1$  Hz, 1 H), 6.63 (t,  $J = 7.3$  Hz, 1 H), 5.00 (d,  $J = 8.6$  Hz, 1 H), 3.70 (dt,  $J = 4.1, 8.5$  Hz, 1 H), 3.49 (dd,  $J = 4.2$  Hz,  $J = 11.5$  Hz, 1 H), 3.43 - 3.39 (m, 1 H), 3.00 (s, 3 H)

$^{13}\text{C}$  NMR (100 MHz,  $\text{CDCl}_3$ )  $\delta$  202.0, 146.3, 141.7, 137.2, 132.9, 128.7, 128.7, 128.6, 128.5, 128.1, 127.5, 127.0, 121.1, 116.8, 111.6, 55.6, 52.3, 42.3, 39.3

HRMS: (ESI-MS)  $m/z$  calculated for  $\text{C}_{23}\text{H}_{22}\text{NO}$   $[\text{M} + \text{H}]^+$ : 328.1696, found: 328.1696

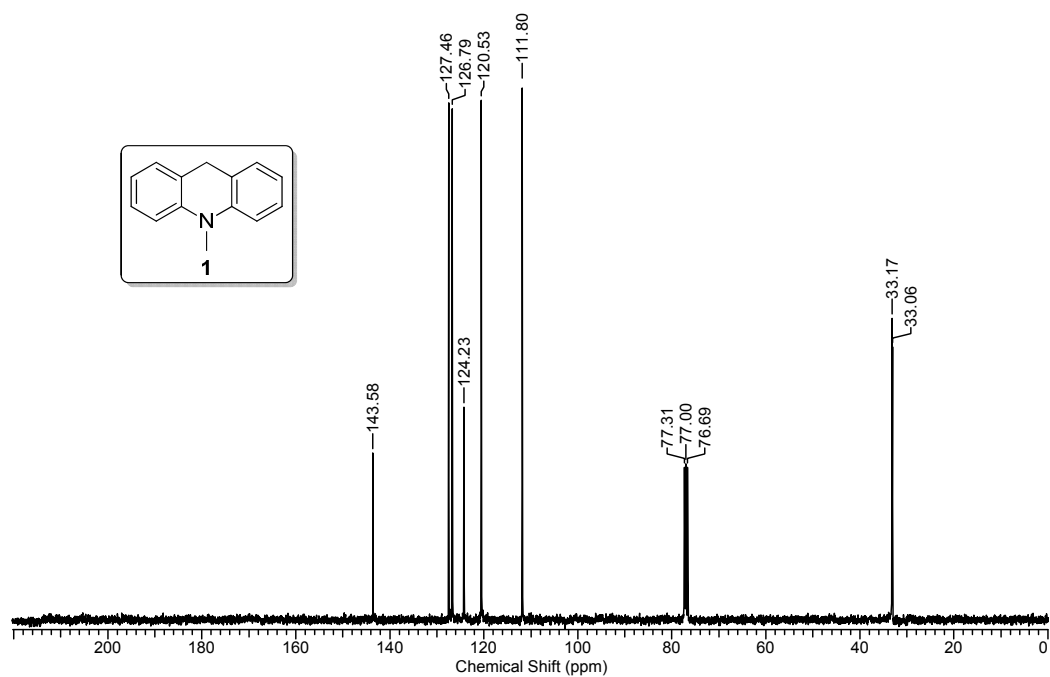
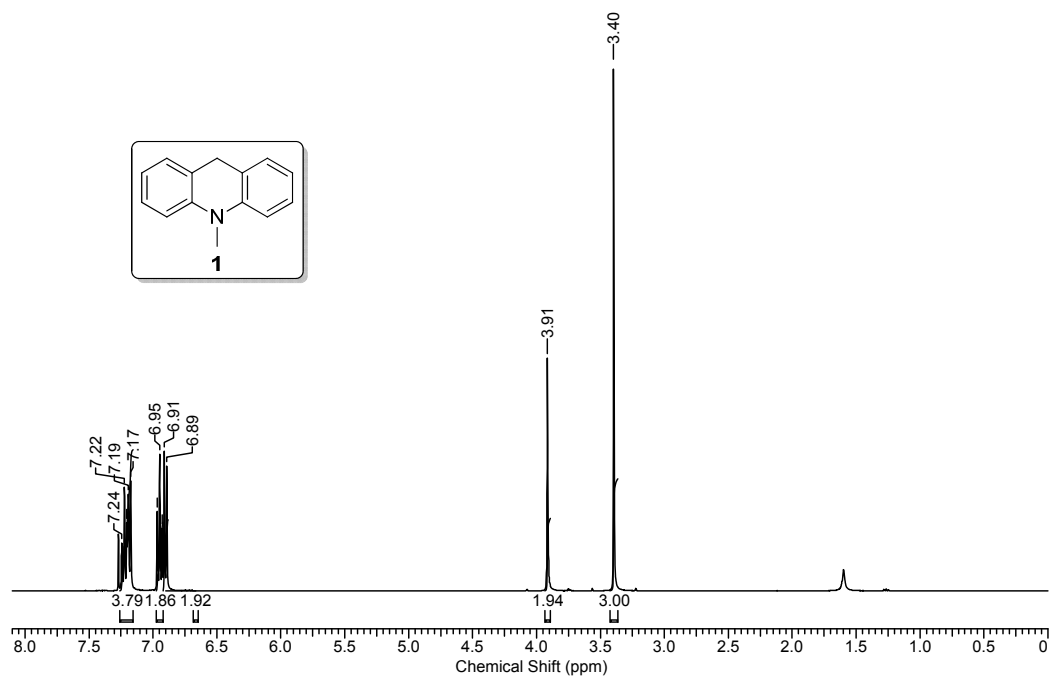
**3.8 References:**

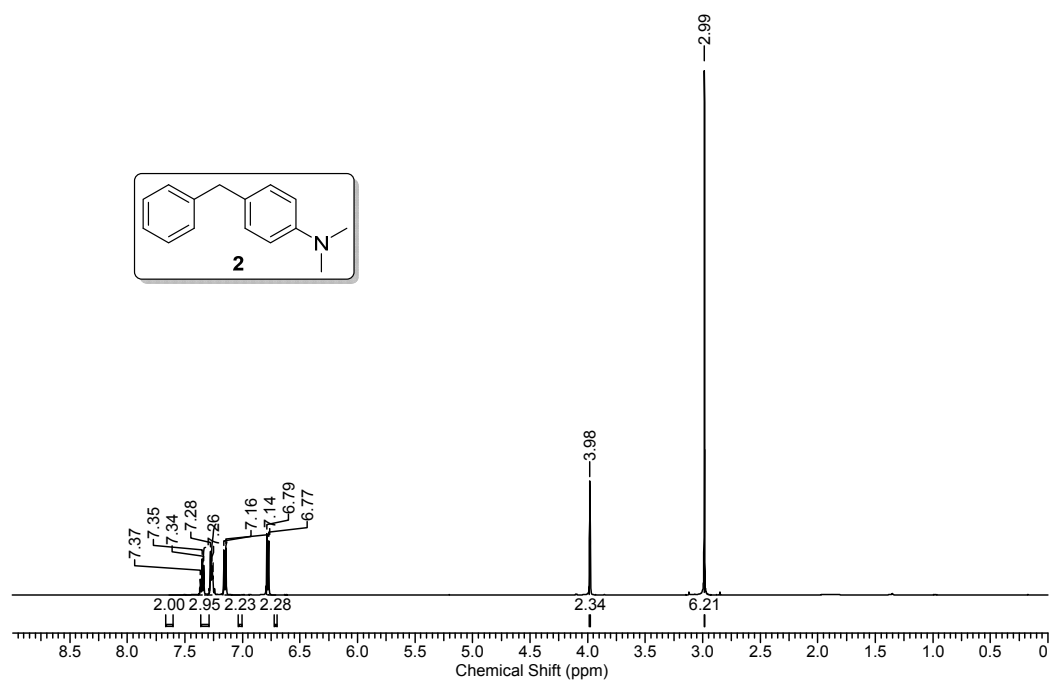
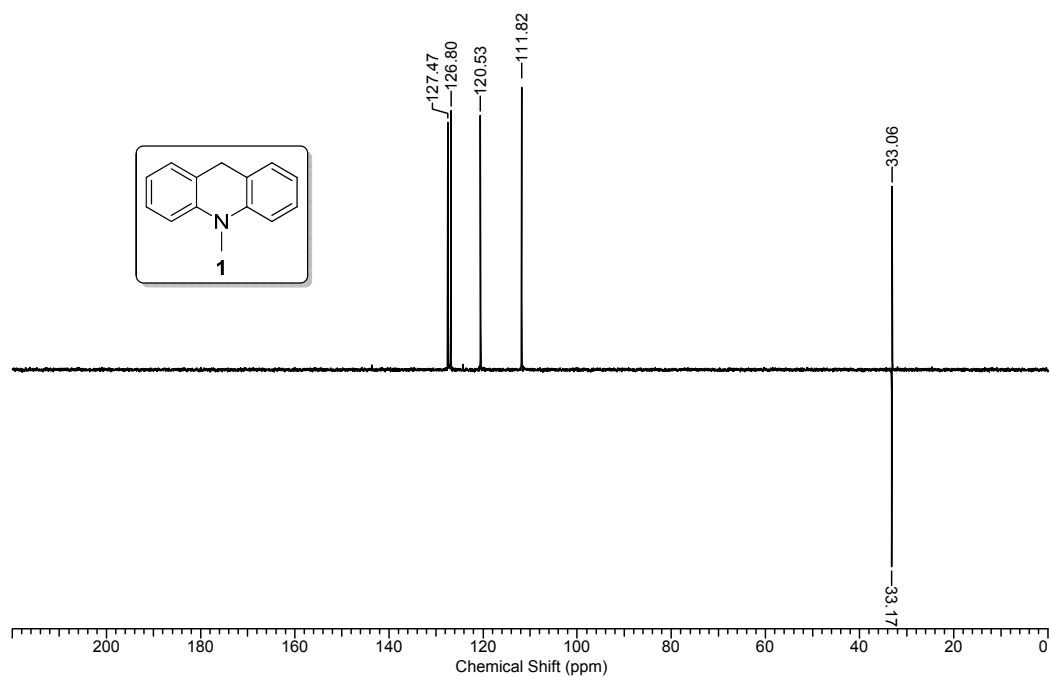
- (a) Filip, T. *Collect. Czech. Chem. Commun.* **2011**, *76*, 859–917. (b) Narayanam, J. M. R.; Stephenson, C. R. J. *Chem. Soc. Rev.* **2011**, *40*, 102-113. (c) Xuan, J.; Xiao, W.-J. *Angew. Chem. Int. Ed.* **2012**, *51*, 6828-6838. (d) Hari, D. P.; König, B. *Angew. Chem. Int. Ed.* **2013**, *52*, 4734-4743. (e) Prier, C. K.; Rankic, D. A.; MacMillan, D. W. C. *Chem. Rev.* **2013**, *113*, 5322-5363. (f) Xi, Y.; Yi, H.; Lei, A. *Org. Biomol. Chem.* **2013**, *11*, 2387-2403.
- (a) Maity, S.; Zheng, N. *Synlett* **2012**, *23*, 1851-1856. (b) Shi, L.; Xia, W. *Chem. Soc. Rev.* **2012**, *41*, 7687-7697. (c) Hu, J.; Wang, J.; Nguyen, T. H.; Zheng, N. *Beilstein J. Org. Chem.* **2013**, *9*, 1977-2001.
- (a) McNally, A.; Prier, C. K.; MacMillan, D. W. C. *Science* **2011**, *334*, 1114-1117. (b) Miyake, Y.; Nakajima, K.; Nishibayashi, Y. *J. Am. Chem. Soc.* **2012**, *134*, 3338-3341.
- (a) Condie, A. G.; González-Gómez, J. C.; Stephenson, C. R. J. *J. Am. Chem. Soc.* **2010**, *132*, 1464-1465. (b) Hari, D. P.; König, B. *Org. Lett.* **2011**, *13*, 3852-3855. (c) Rueping, M.; Vila, C.; Koenigs, R. M.; Poscharny, K.; Fabry, D. C. *Chem. Commun.* **2011**, *47*, 2360-2362. (d) Freeman, D. B.; Furst, L.; Condie, A. G.; Stephenson, C. R. J. *Org. Lett.* **2012**, *14*, 94-97. (e) Rueping, M.; Koenigs, R. M.; Poscharny, K.; Fabry, D. C.; Leonori, D.; Vila, C. *Chem. Eur. J.* **2012**, *18*, 5170-5174. (f) Zhao, G.; Yang, C.; Guo, L.; Sun, H.; Chen, C.; Xia, W. *Chem. Commun.* **2012**, *48*, 2337-2339.
- (a) Pandey, G. *Synlett* **1992**, 546-552. (b) Dileep Kumar, J. S.; Das, S. *Res. Chem. Intermed.* **1997**, *23*, 755-800. (c) Das, S.; Suresh, V., Electron-transfer Reactions of Amines. In *Electron Transfer in Chemistry*, Balzani, V., Ed. Wiley-VCH Verlag GmbH: Weinheim, Germany, 2008; pp 379-456.
- (a) Pac, C.; Ihama, M.; Yasuda, M.; Miyauchi, Y.; Sakurai, H. *J. Am. Chem. Soc.* **1981**, *103*, 6495-6497. (b) Pac, C.; Miyauchi, Y.; Ishitani, O.; Ihama, M.; Yasuda, M.; Sakurai, H. *J. Org. Chem.* **1984**, *49*, 26-34.
- Richardson, R. D.; Carpenter, B. K. *J. Am. Chem. Soc.* **2008**, *130*, 3169-3180.
- (a) Pandey, G. *Top. Curr. Chem.* **1993**, *168*, 175-221. (b) Pandey, G.; Pal, S.; Laha, R. *Angew. Chem. Int. Ed.* **2013**, *52*, 5146-5149.
- (a) Pandey, G.; Kumaraswamy, G. *Tetrahedron Lett.* **1988**, *29*, 4153-4156. (b) Pandey, G.; Kumaraswamy, G.; Reddy, P. Y. *Tetrahedron* **1992**, *48*, 8295-

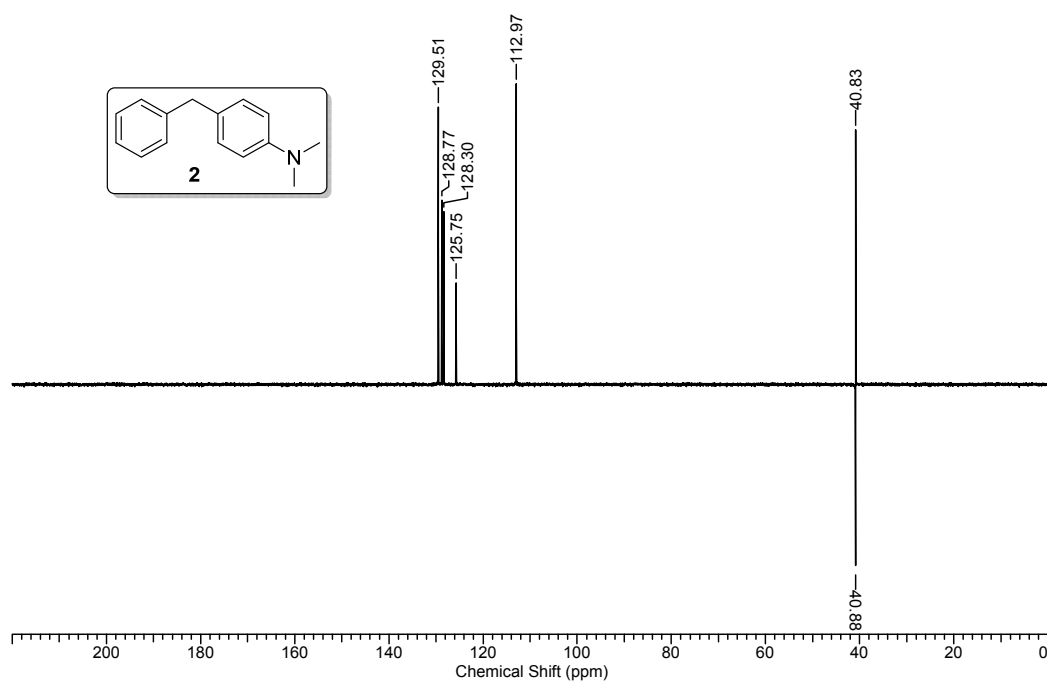
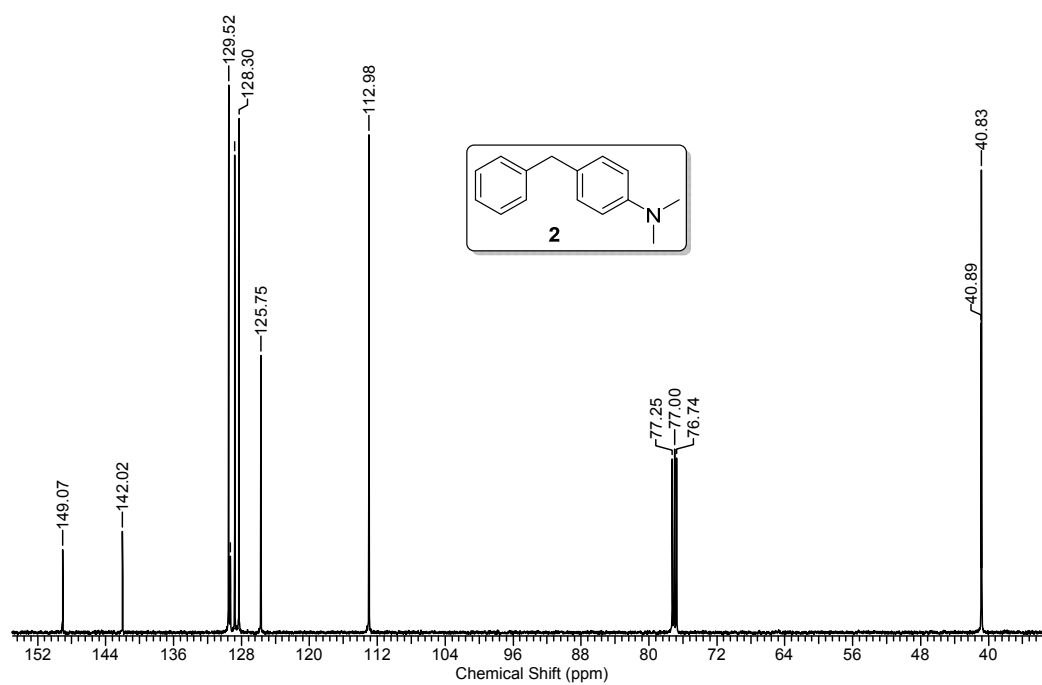
8308. (c) Pandey, G.; Rani, K. S.; Lakshmaiah, G. *Tetrahedron Lett.* **1992**, *33*, 5107-5110. (d) Pandey, G.; Gadre, S. R. *Arkivoc* **2003**, 45-54.
10. Kohls, P.; Jadhav, D.; Pandey, G.; Reiser, O. *Org. Lett.* **2012**, *14*, 672-675.
11. Xia, X.-F.; Shu, X.-Z.; Ji, K.-G.; Yang, Y.-F.; Shaukat, A.; Liu, X.-Y.; Liang, Y.-M. *J. Org. Chem.* **2010**, *75*, 2893-2902.
12. Takasu, N.; Oisaki, K.; Kanai, M. *Org. Lett.* **2013**, *15*, 1918-1921.
13. Sundararaju, B.; Achard, M.; Sharma, G. V. M.; Bruneau, C. *J. Am. Chem. Soc.* **2011**, *133*, 10340-10343.
14. Pintér, Á.; Sud, A.; Sureshkumar, D.; Klusmann, M. *Angew. Chem. Int. Ed.* **2010**, *49*, 5004-5007.
15. Zhang, B.; Cui, Y.; Jiao, N. *Chem. Commun.* **2012**, *48*, 4498-4500.
16. Fukuzumi, S.; Tanaka, T., in *Photoinduced Electron Transfer, Part C* (Eds.: M. A. Fox, M. Chanon), Elsevier, Amsterdam, Chapters 4.10, pp. 578-636, **1988**.
17. (a) Fukuzumi, S.; Ishikawa, M.; Tanaka, T. *J. Chem. Soc., Chem. Commun.* **1985**, 1069-1071. (b) Fukuzumi, S.; Ishikawa, M.; Tanaka, T. *Tetrahedron* **1986**, *42*, 1021-1034. (c) Fukuzumi, S.; Mochizuki, S.; Tanaka, T. *J. Phys. Chem.* **1990**, *94*, 722-726.
18. Jiang, H.; Liu, Y.-C.; Li, J.; Wang, G.-W.; Wu, Y.-D.; Wang, Q.-M.; Mak, T. C. W. *Chem. Commun.* **2002**, 882-883.
19. Pandey, G.; Jadhav, D.; Tiwari, S. K.; Singh, B. *Adv. Synth. Catal.* **2014**, In press (Manuscript ID adsc.201400107).
20. (a) Fukuzumi, S.; Koumitsu, S.; Hironaka, K.; Tanaka, T. *J. Am. Chem. Soc.* **1987**, *109*, 305-316. (b) Yuasa, J.; Fukuzumi, S. *J. Am. Chem. Soc.* **2006**, *128*, 14281-14292.
21. (a) Fujiwara, M.; Okamoto, M.; Okamoto, M.; Watanabe, M.; Machida, H.; Shigeta, S.; Konno, K.; Yokota, T.; Baba, M. *Antiviral Research* **1999**, *43*, 189-199. (b) Harrison, R. J.; Reszka, A. P.; Haider, S. M.; Romagnoli, B.; Morrell, J.; Read, M. A.; Gowan, S. M.; Incles, C. M.; Kelland, L. R.; Neidle, S. *Bioorg. Med. Chem. Lett.* **2004**, *14*, 5845-5849. (c) Tabarrini, O.; Manfroni, G.; Fravolini, A.; Cecchetti, V.; Sabatini, S.; De Clercq, E.; Rozenski, J.; Canard, B.; Dutartre, H.; Paeshuyse, J.; Neyts, J. *J. Med. Chem.* **2006**, *49*, 2621-2627. (d) Ngoumfo, R. M.; Jouda, J.-B.; Mouafo, F. T.; Komguem, J.; Mbazono, C. D.; Shiao, T. C.; Choudhary, M. I.; Laatsch, H.; Legault, J.; Pichette, A.; Roy, R. *Bioorg. Med. Chem.* **2010**, *18*, 3601-3605. (e) Marques,

- E. F.; Bueno, M. A.; Duarte, P. D.; Silva, L. R. S. P.; Martinelli, A. M.; dos Santos, C. Y.; Severino, R. P.; Brömme, D.; Vieira, P. C.; Corrêa, A. G. *Eur. J. Med. Chem.* **2012**, *54*, 10-21. (f) Sepulveda, C. S.; Fascio, M. L.; Garcia, C. C.; D'Accorso, N. B.; Damonte, E. B. *Curr. Med. Chem.* **2013**, *20*, 2402-2414.
22. (a) Huang, P.-C.; Parthasarathy, K.; Cheng, C.-H. *Chem. Eur. J.* **2013**, *19*, 460-464. (b) Li, X.-A.; Wang, H.-L.; Yang, S.-D. *Org. Lett.* **2013**, *15*, 1794-1797. And refer- ences cited therein.
23. (a) Fukuzumi, S.; Ishikawa, M.; Tanaka, T. *J. Chem. Soc., Perkin Trans. 2* **1989**, 1037-1045. (b) Anderson, C. P.; Salmon, D. J.; Meyer, T. J.; Young, R. *J. Am. Chem. Soc.* **1977**, *99*, 1980-1982.
24. (a) Ju, X.; Li, D.; Li, W.; Yu, W.; Bian, F. *Adv. Synth. Catal.* **2012**, *354*, 3561-3567. (b) Zhu, S.; Das, A.; Bui, L.; Zhou, H.; Curran, D. P.; Rueping, M. *J. Am. Chem. Soc.* **2013**, *135*, 1823-1829.
25. Rueping, M.; Vila, C.; Szadkowska, A.; Koenigs, R. M.; Fronert, J. *ACS Catal.* **2012**, *2*, 2810-2815.
26. (a) Zhu, X.-Q.; Li, H.-R.; Li, Q.; Ai, T.; Lu, J.-Y.; Yang, Y.; Cheng, J.-P. *Chem. Eur. J.* **2003**, *9*, 871-880. (b) Gębicki, J.; Marcinek, A.; Zielonka, J. *Acc. Chem. Res.* **2004**, *37*, 379-386. (c) Zhu, X.-Q.; Tan, Y.; Cao, C.-T. *J. Phys. Chem. B* **2010**, *114*, 2058-2075.
27. Parker, V. D.; Tilset, M. *J. Am. Chem. Soc.* **1991**, *113*, 8778-8781.
28. Roberts R. M. G.; Ostovic D.; Kreevoy M. M. *Faraday Discuss. Chem. Soc.* **1982**, *74*, 257- 265
29. Amatore M.; Gosmini C. *Chem. Commun.* **2008**, 5019-5021.
30. Owston N. A.; Parker, A. J.; Williams J. M. J. *Chem. Commun.* **2008**, 624-625

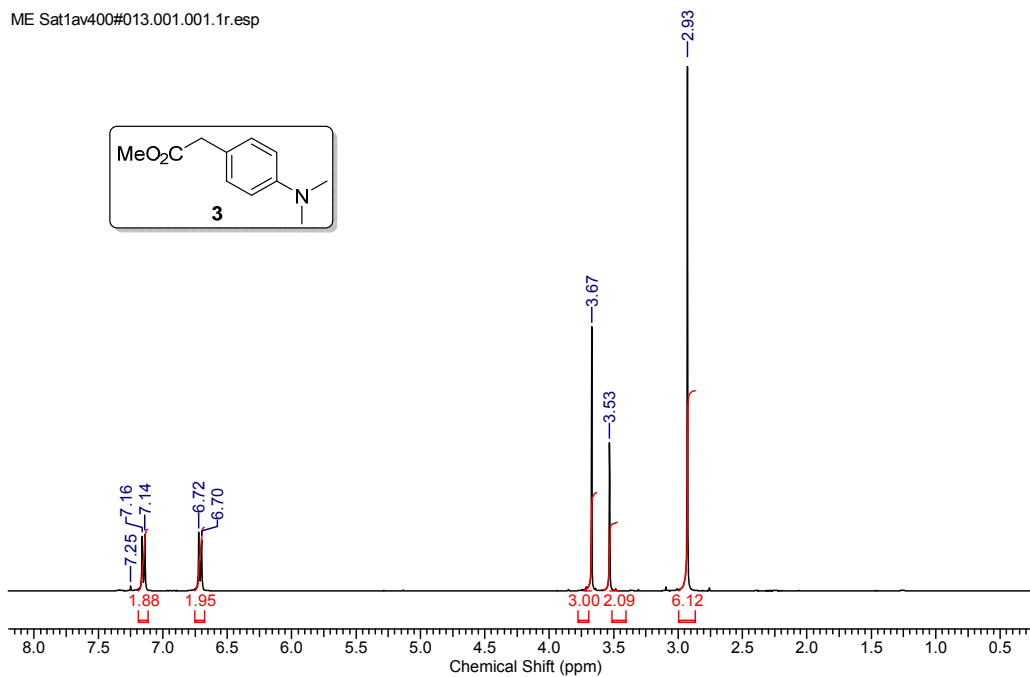
3.9 Spectra:



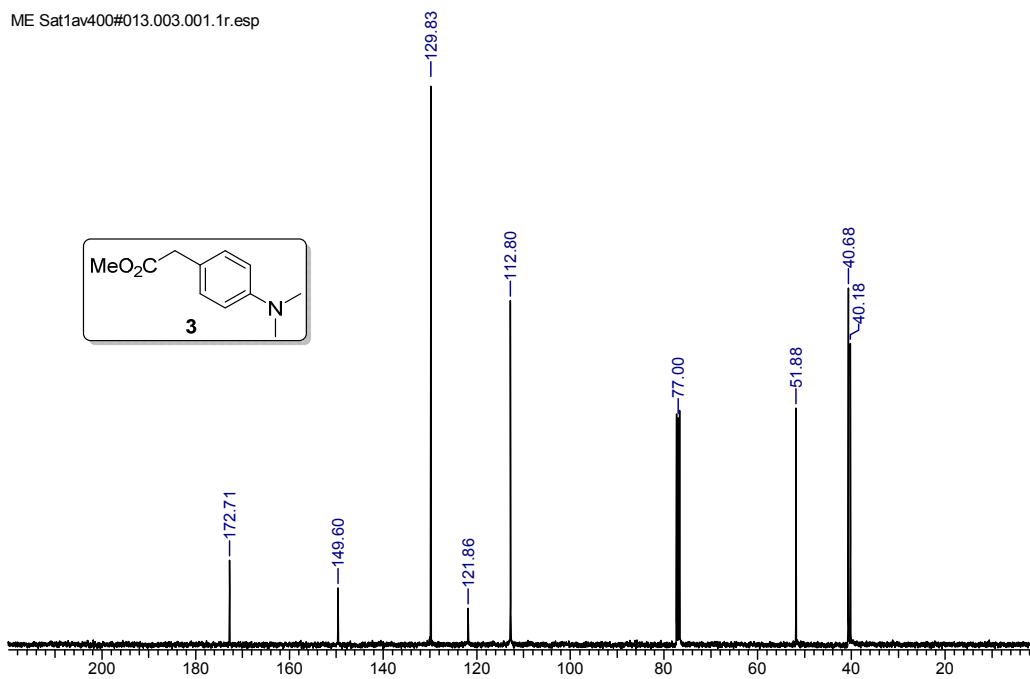




ME Sat1av400#013.001.001.1r.esp

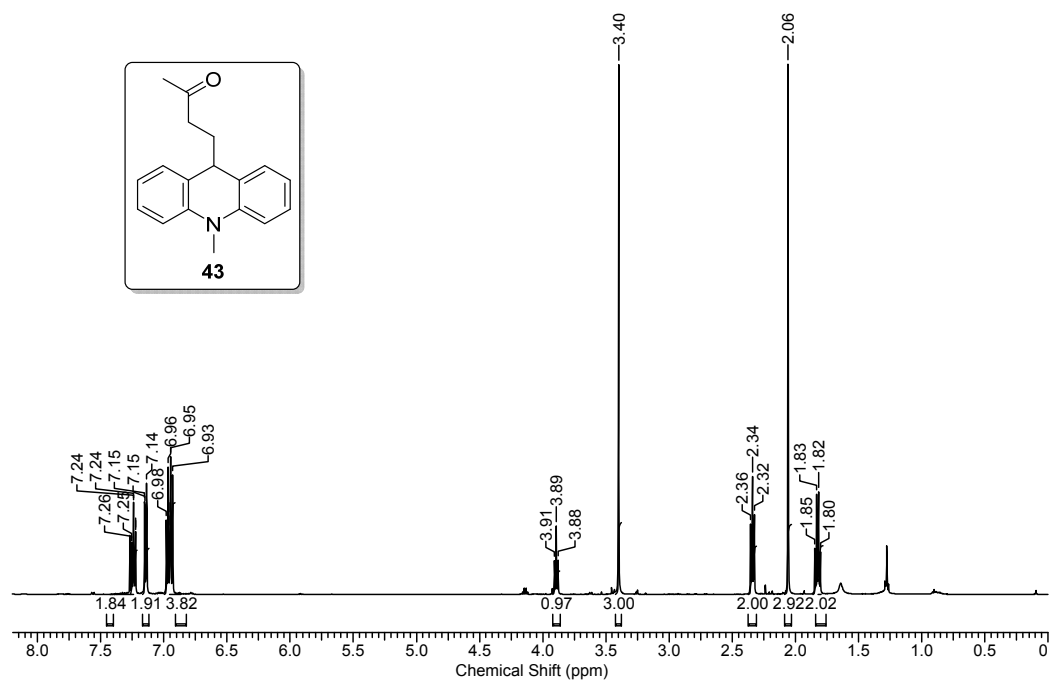
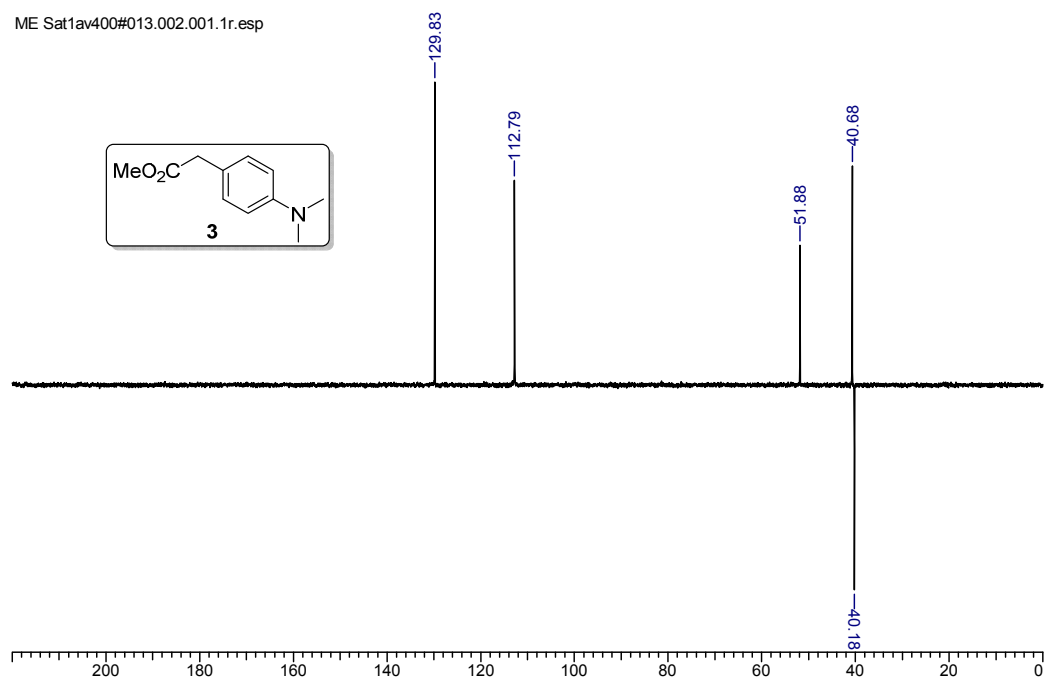


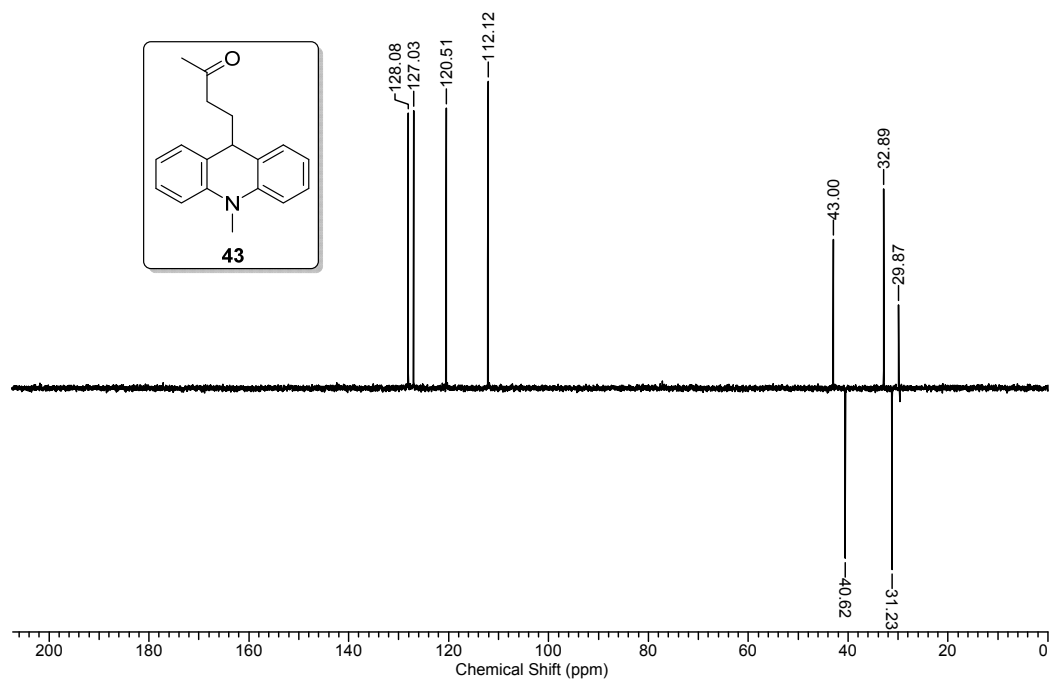
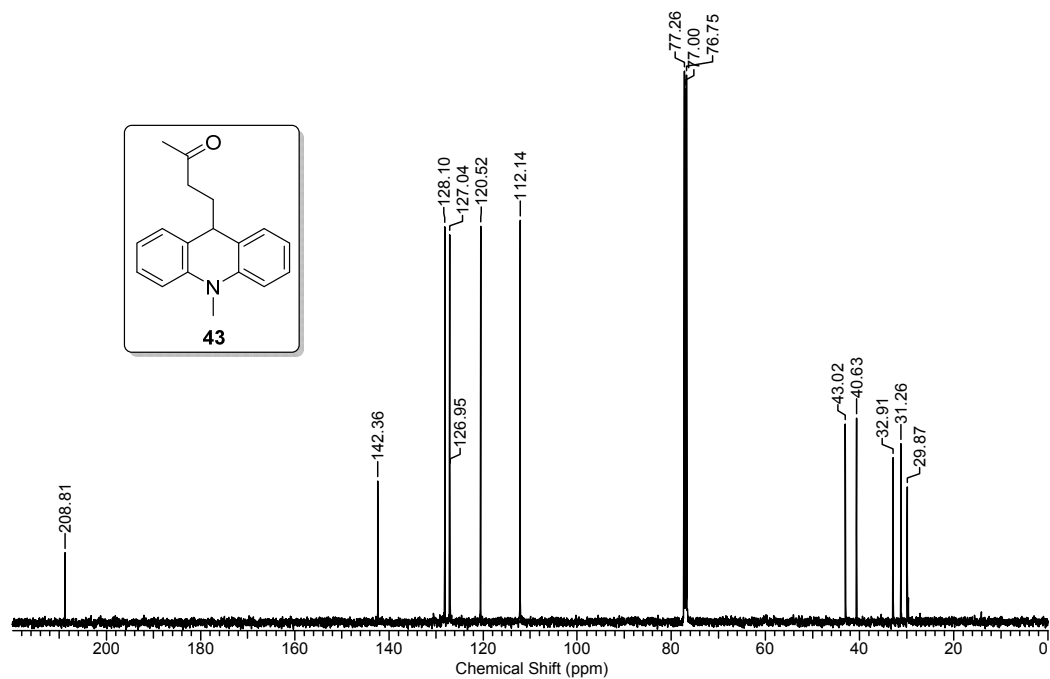
ME Sat1av400#013.003.001.1r.esp

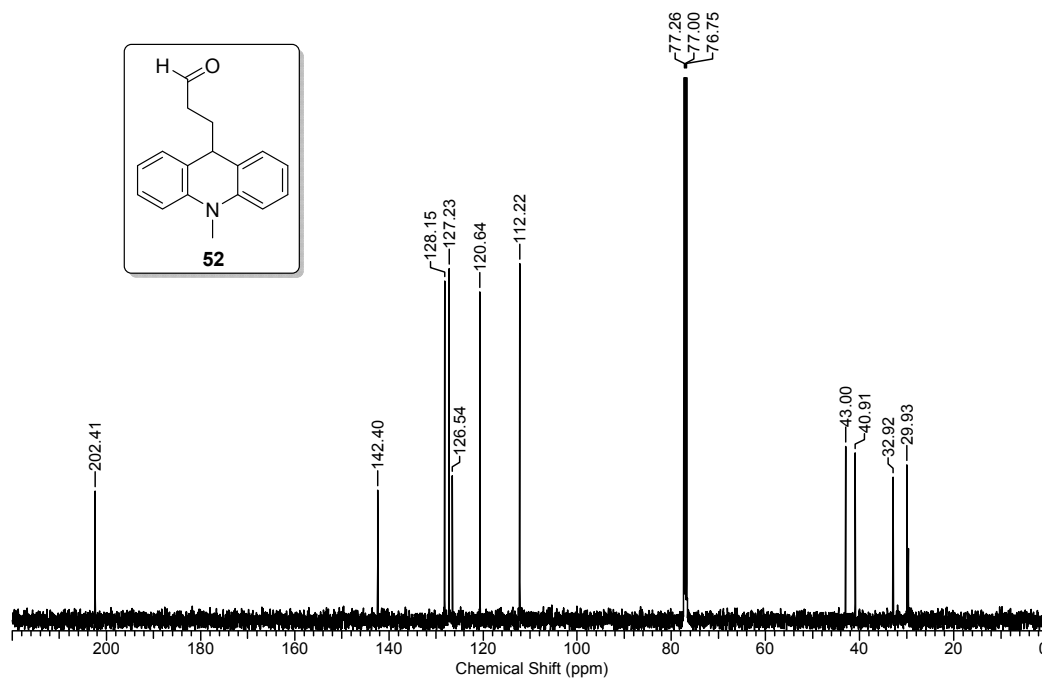
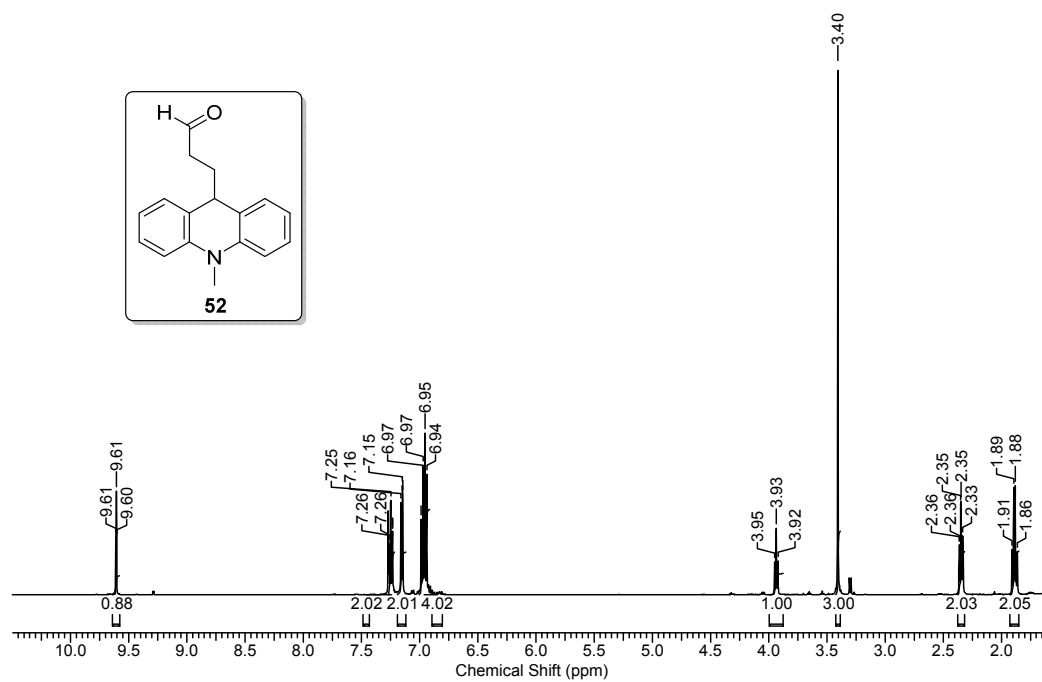


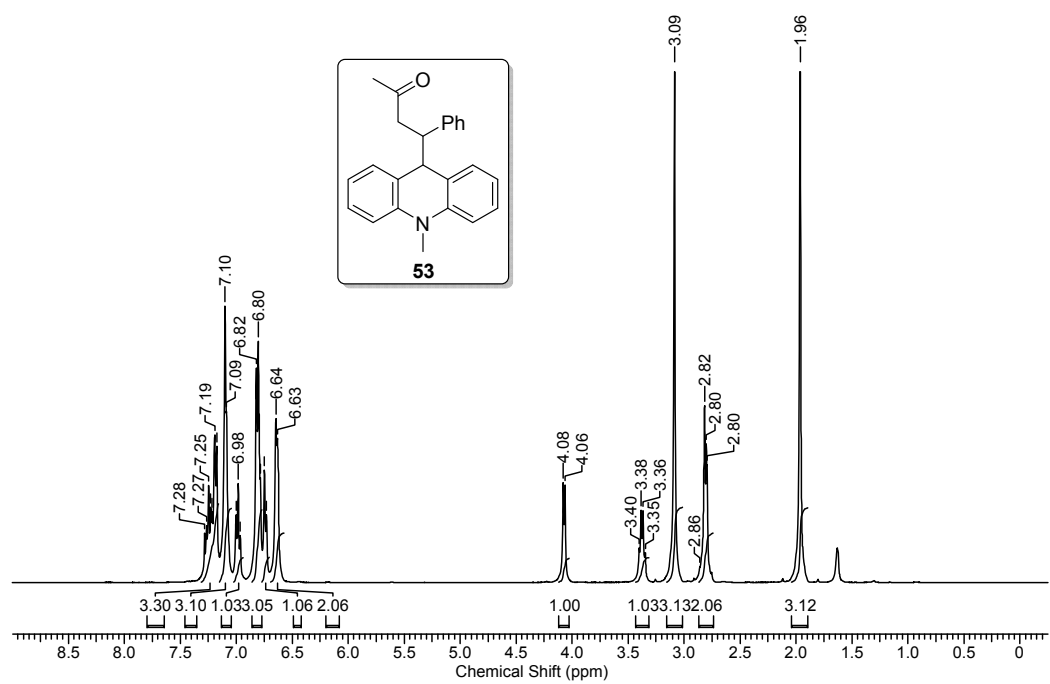
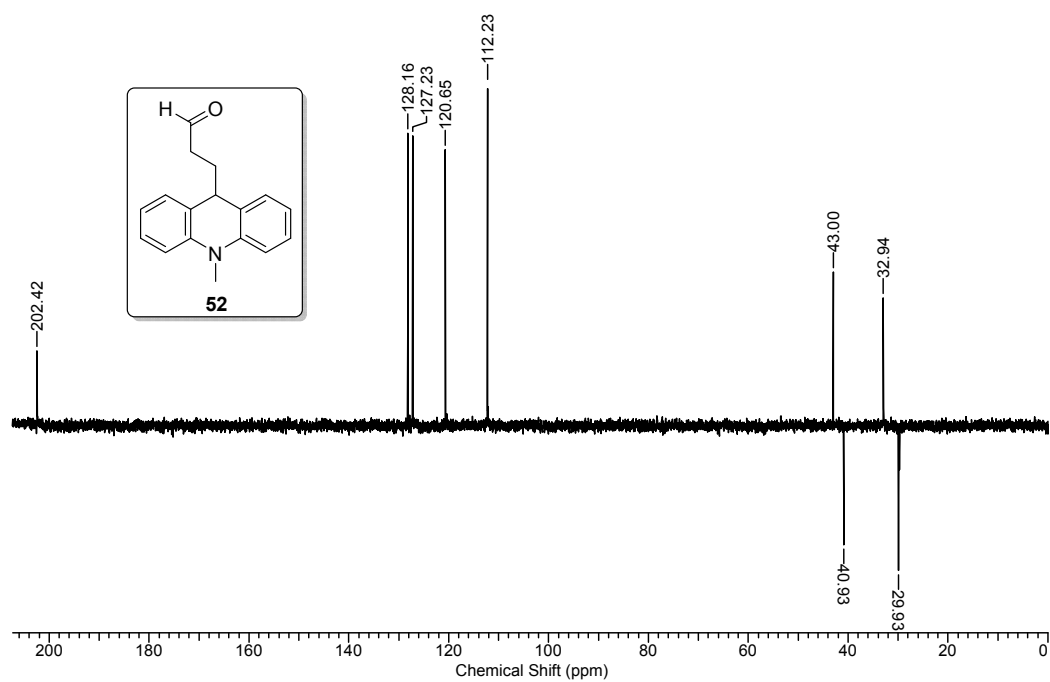


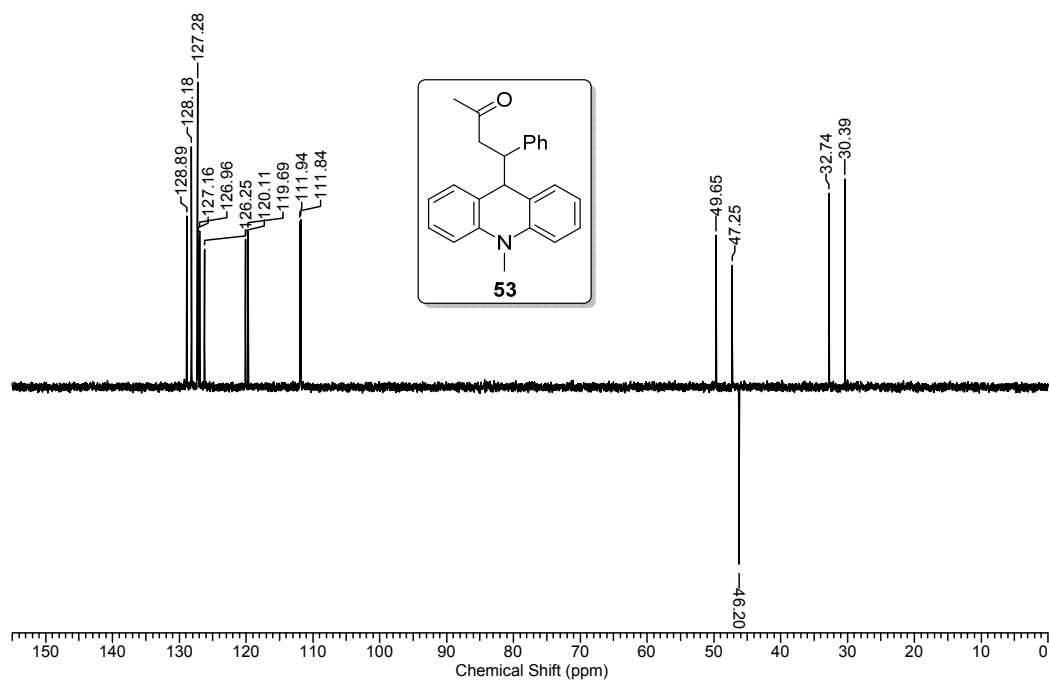
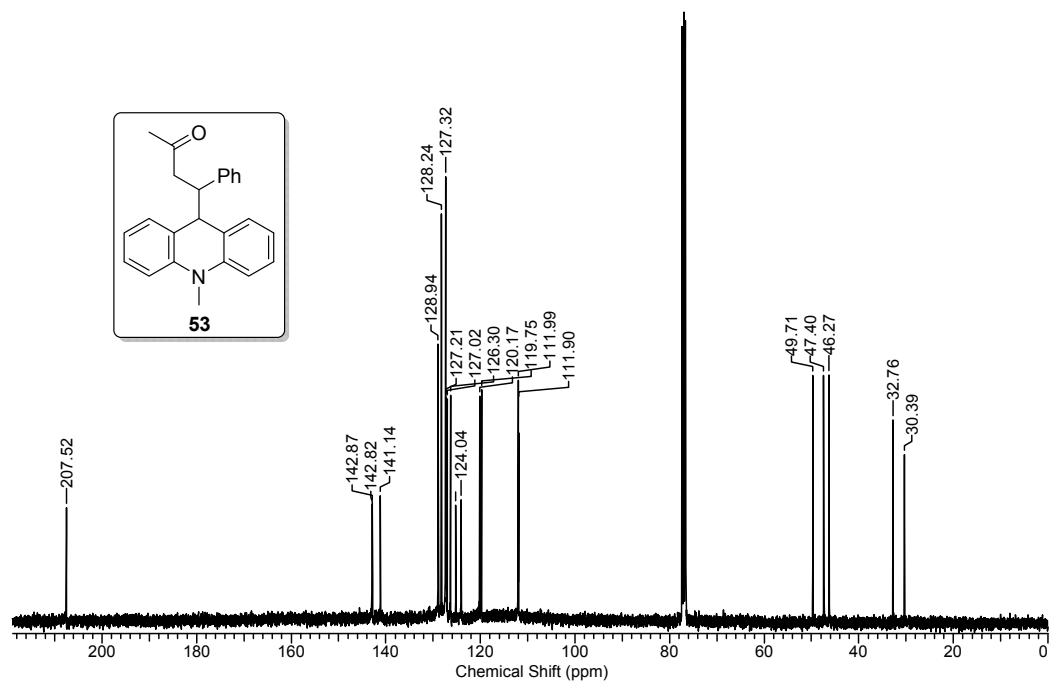
ME Sat1av400#013.002.001.1r.esp

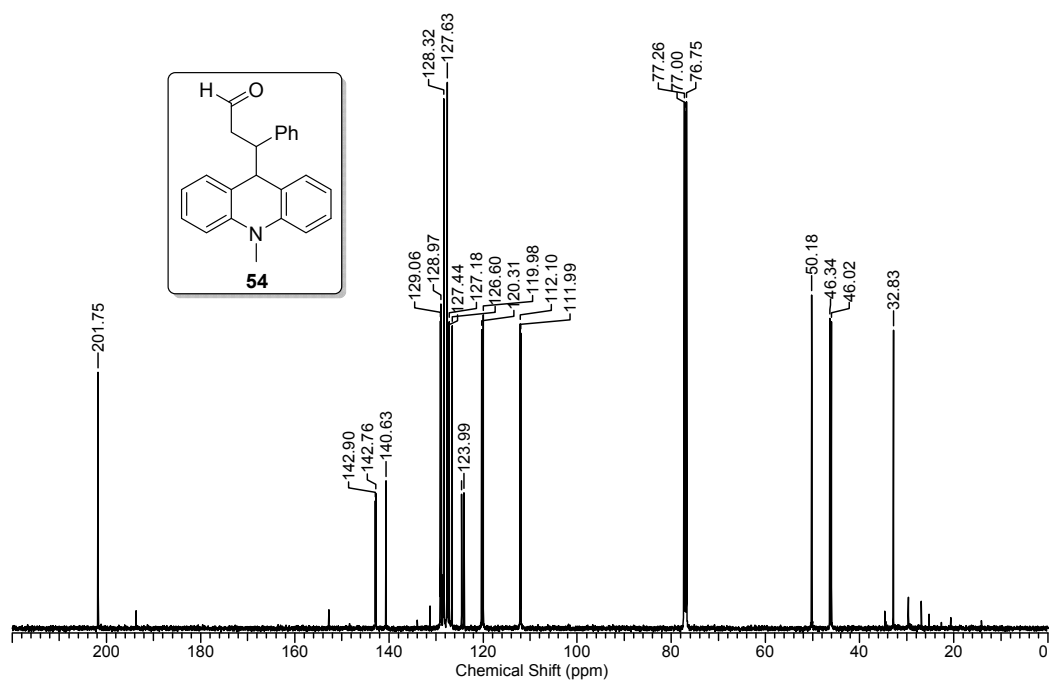
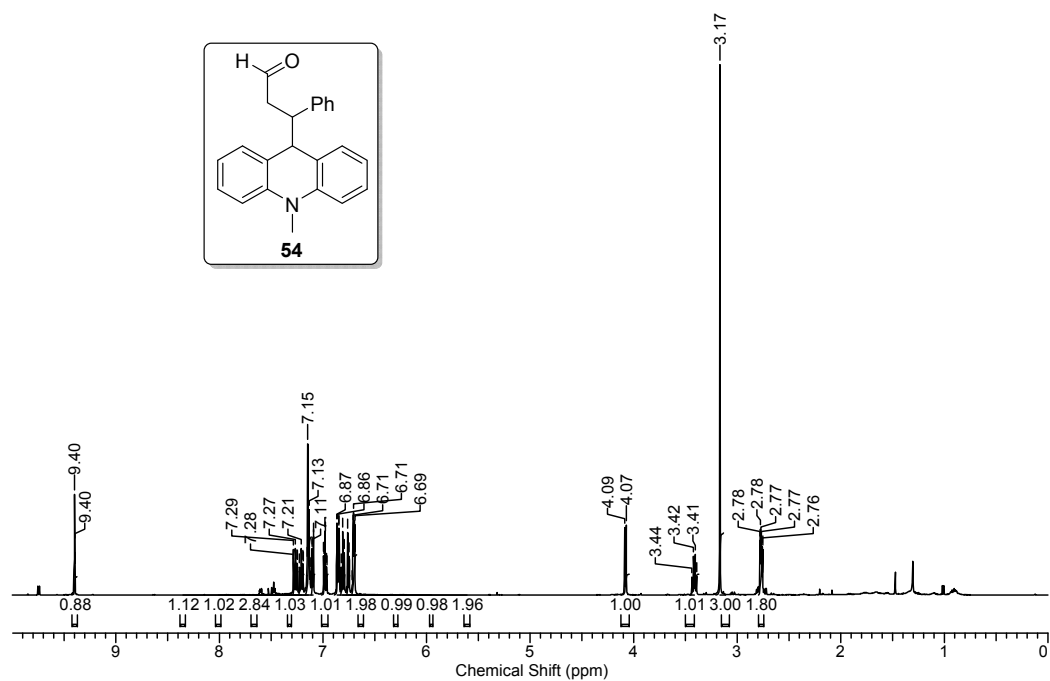


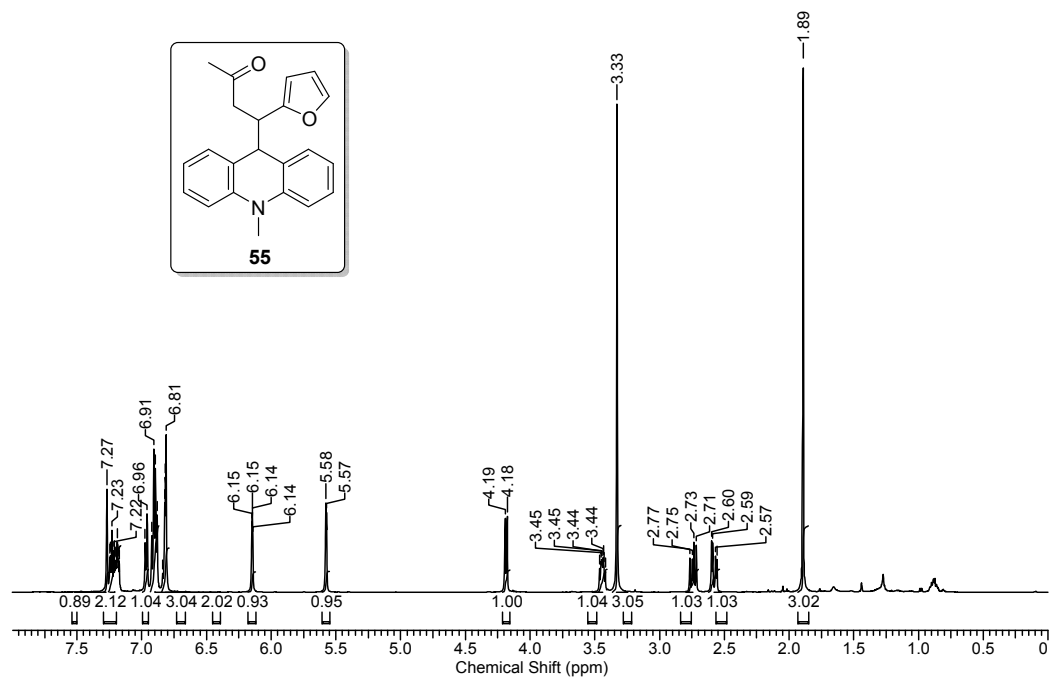
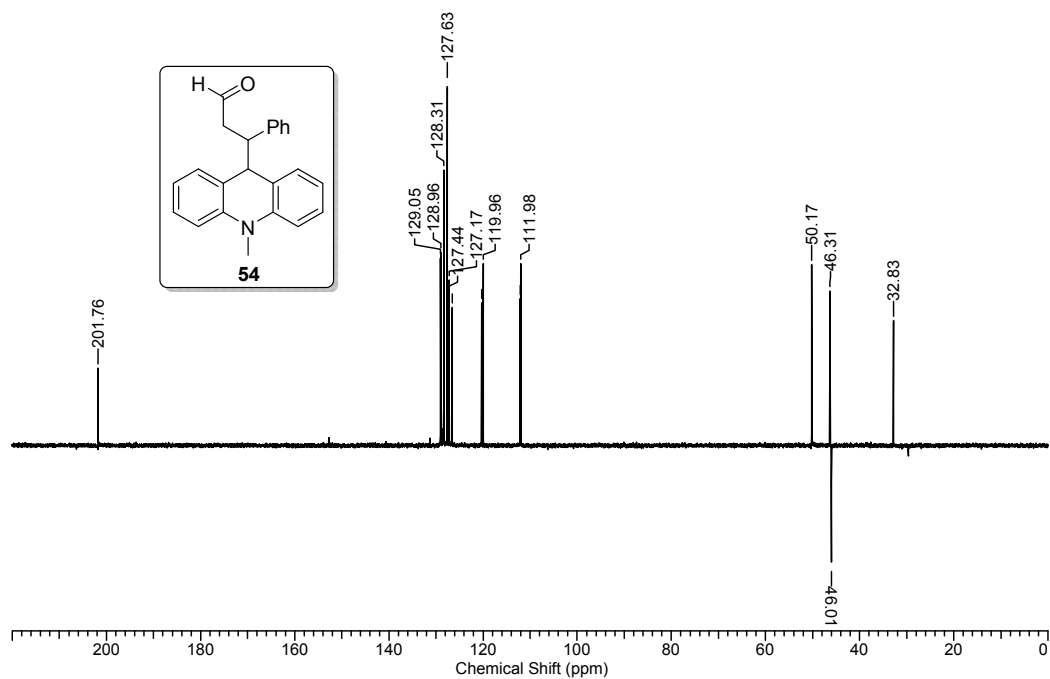


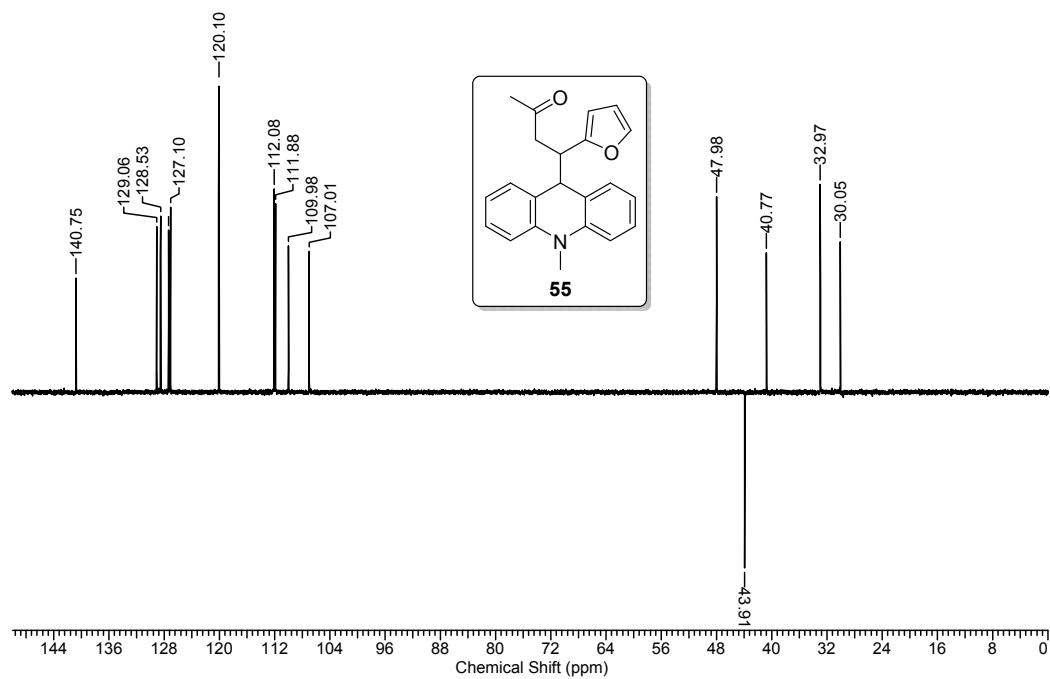
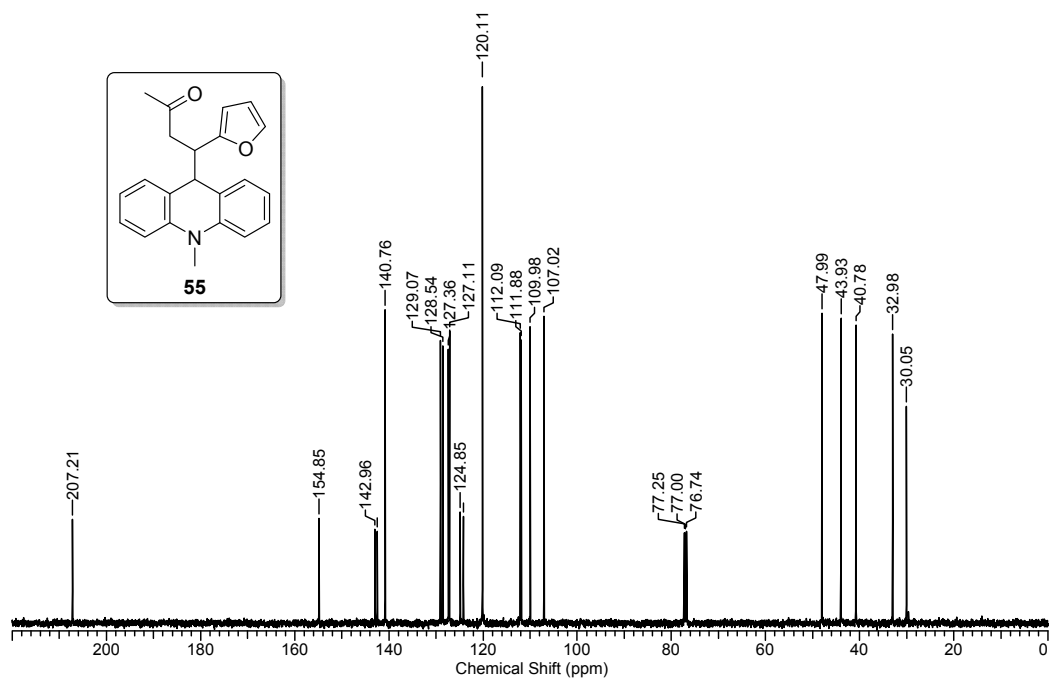




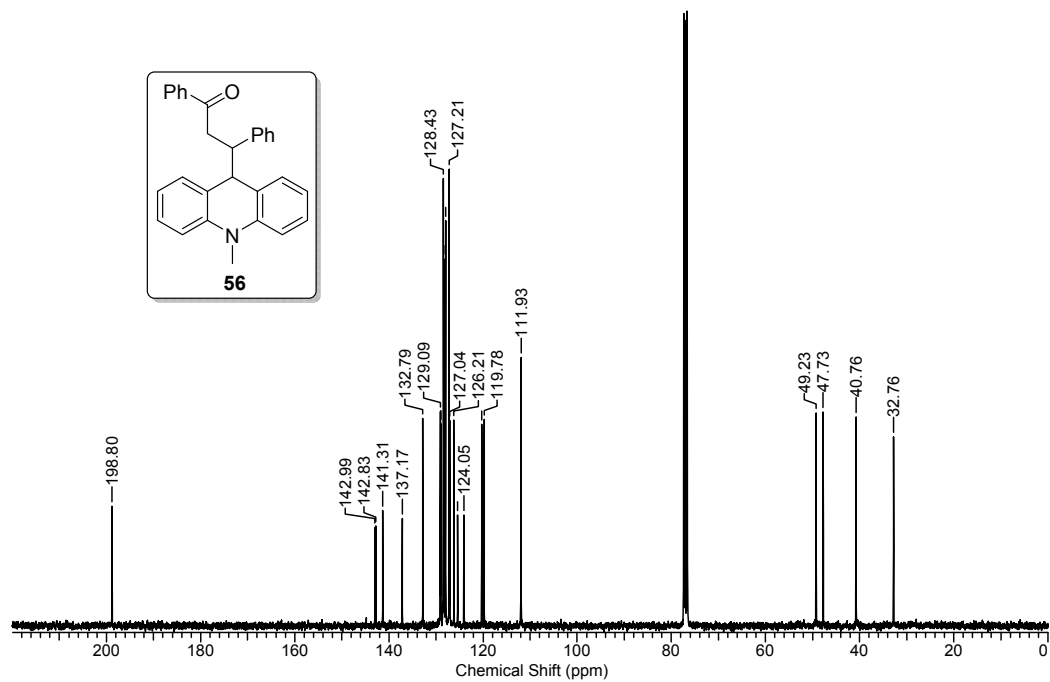
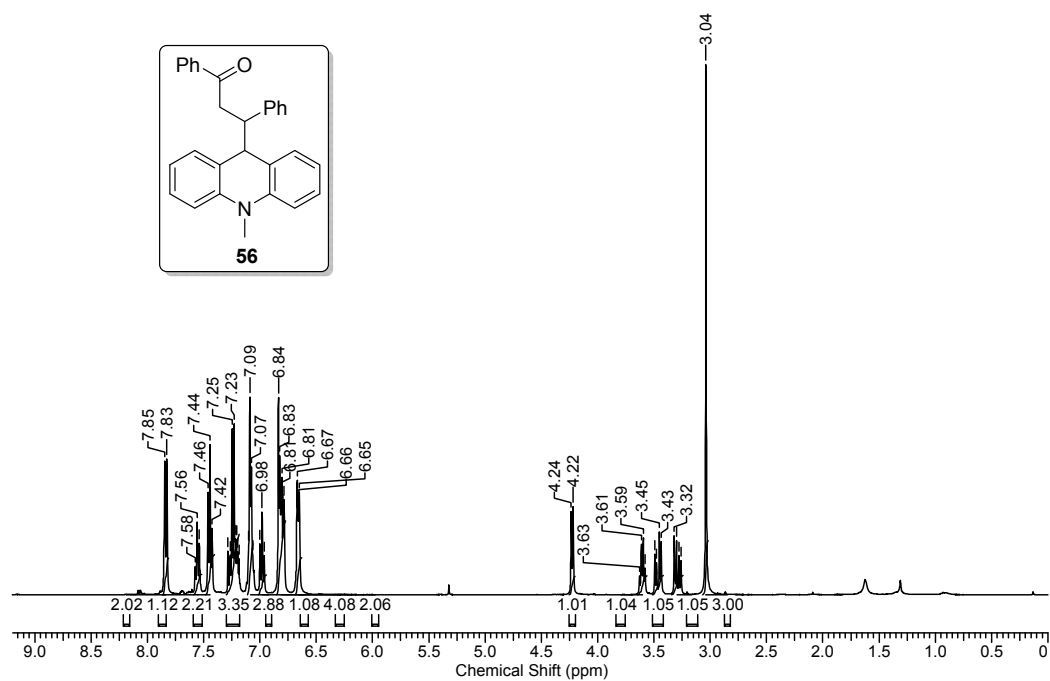


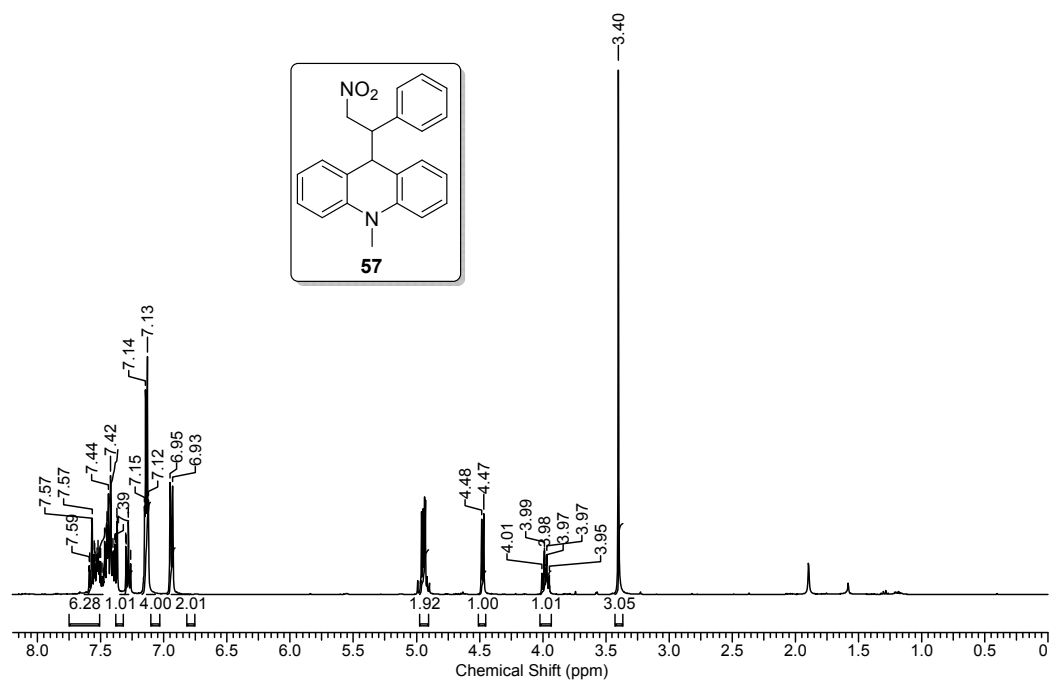
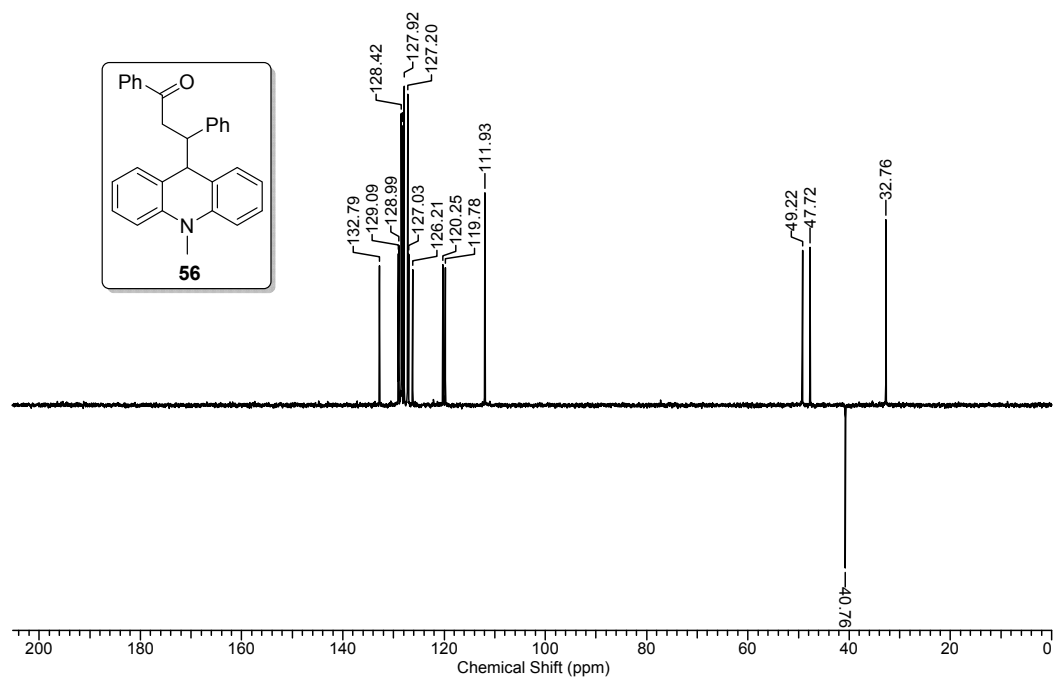


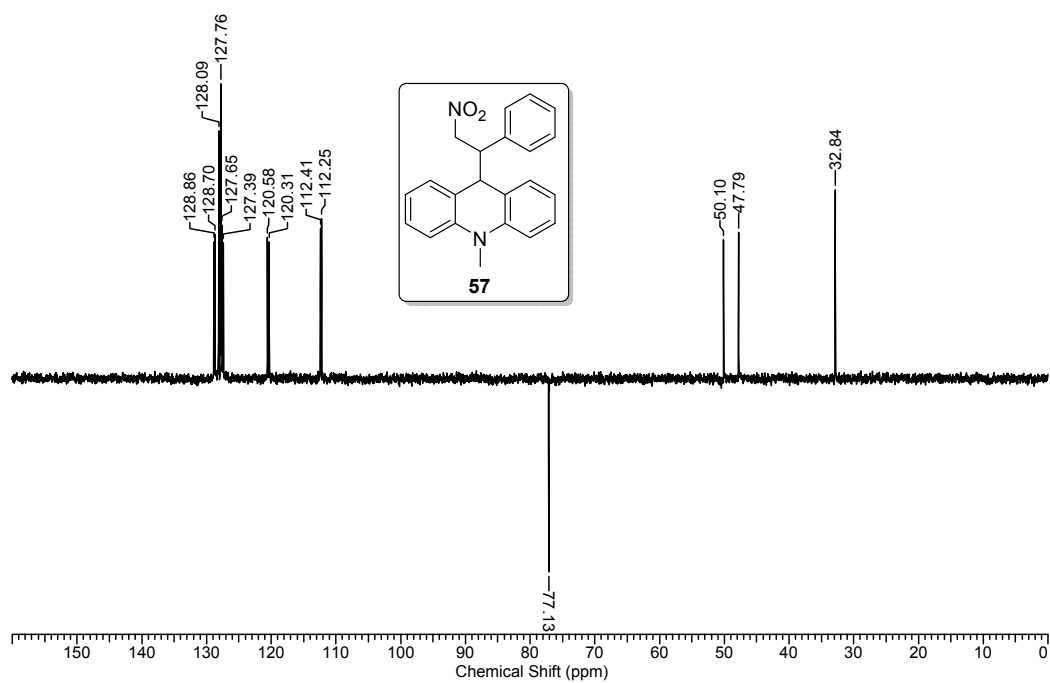
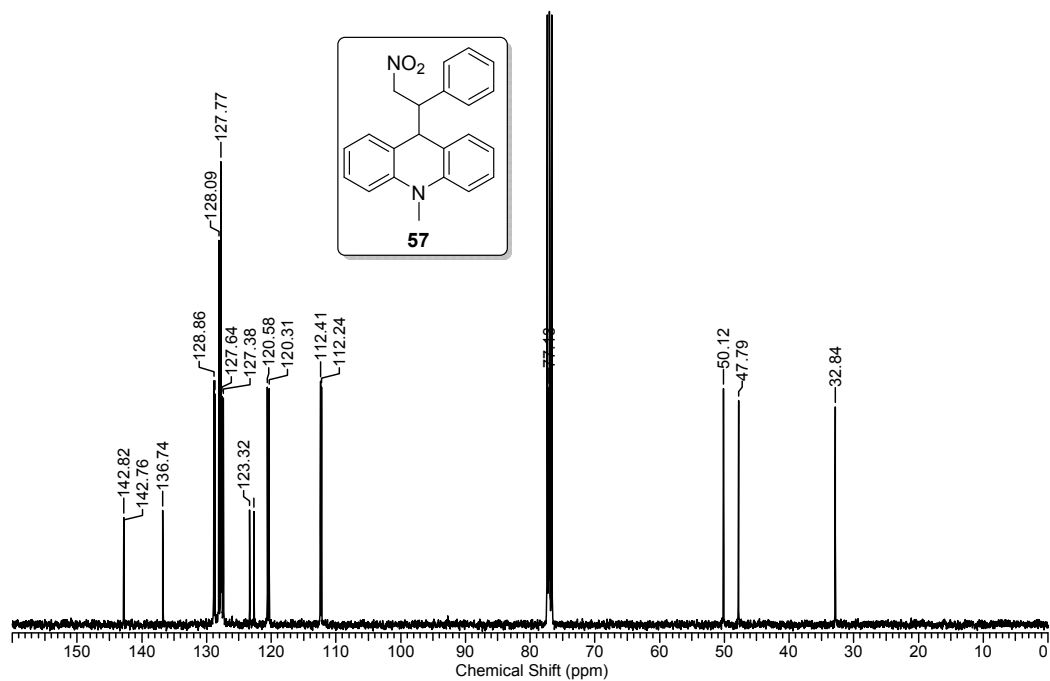


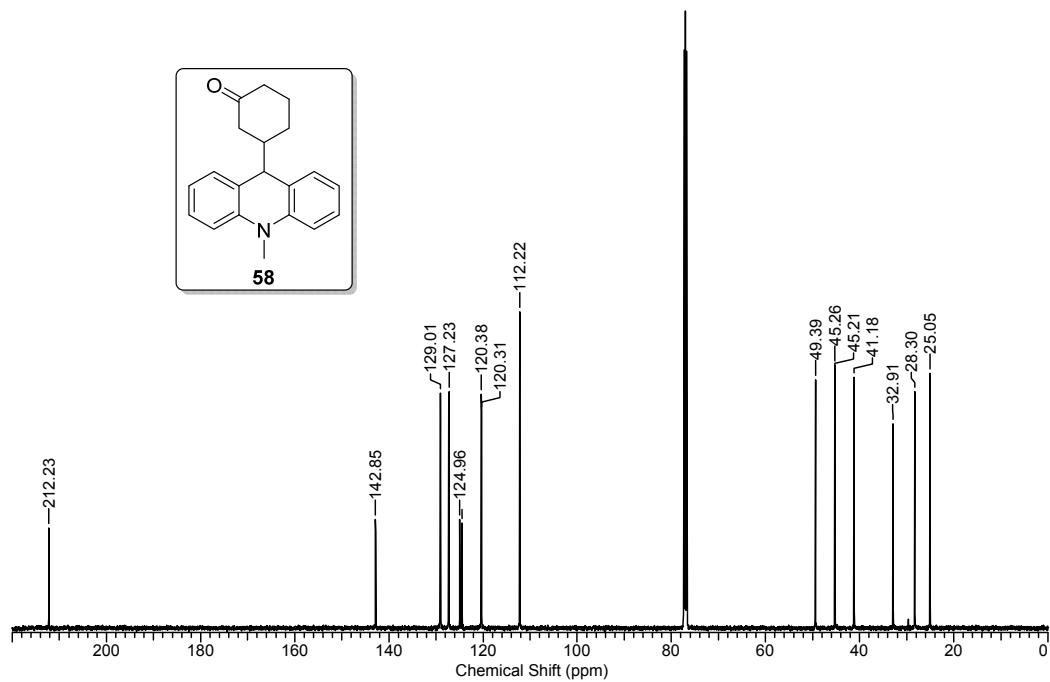
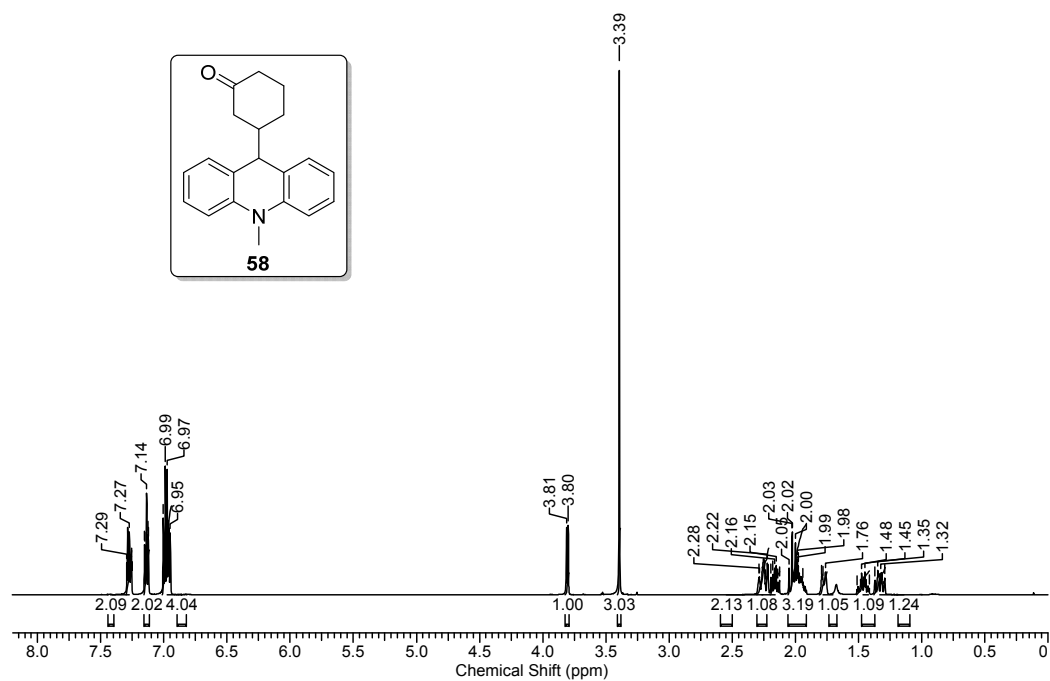


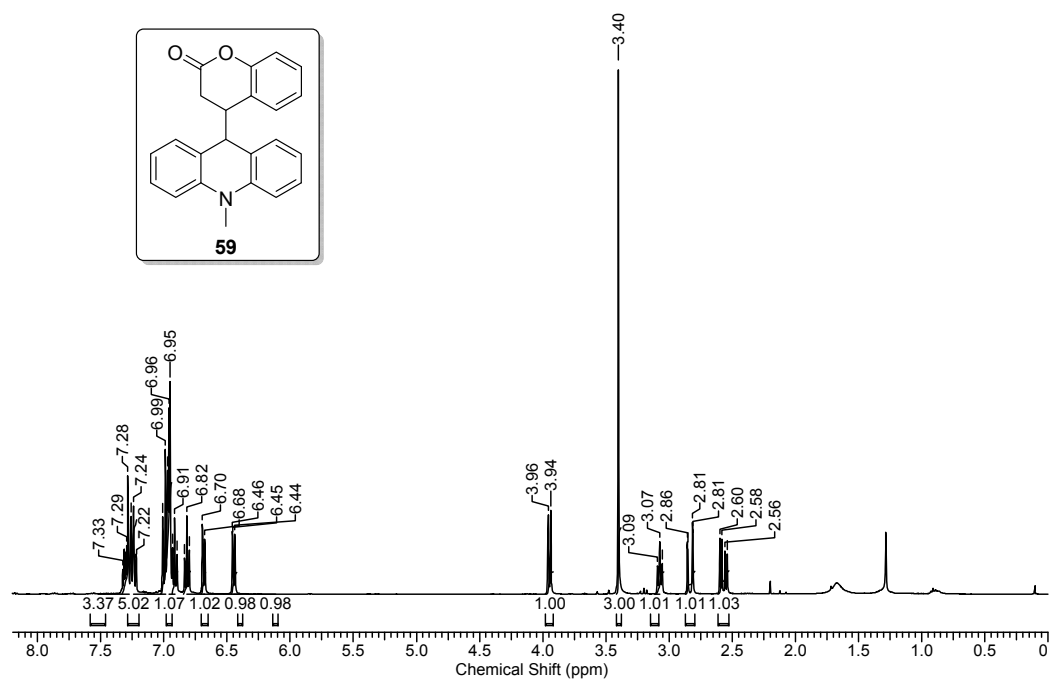
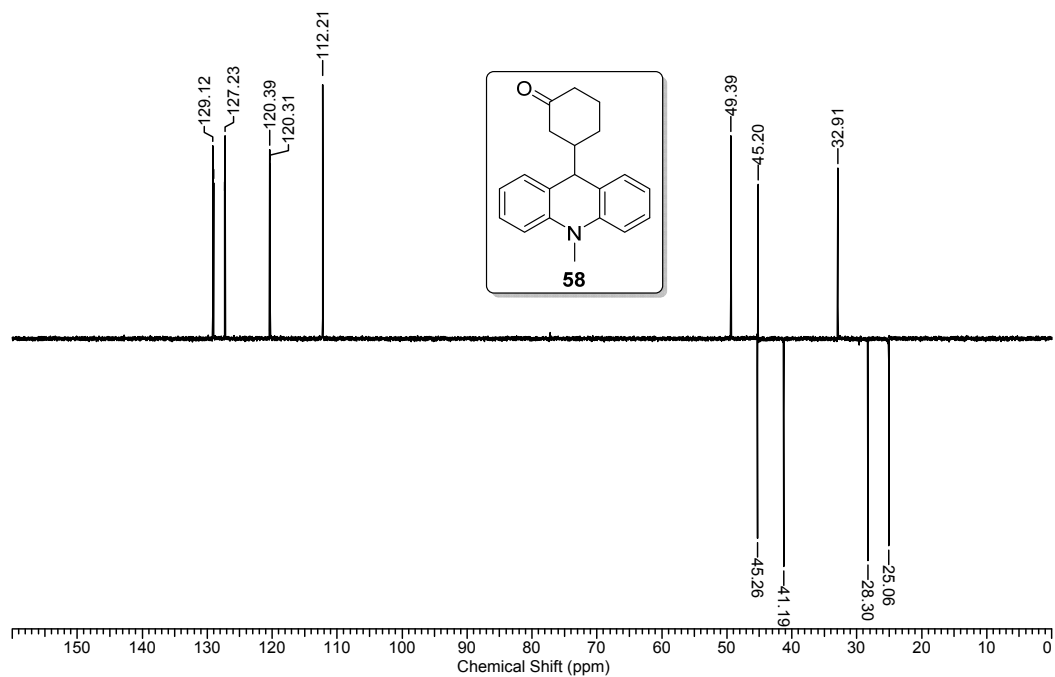


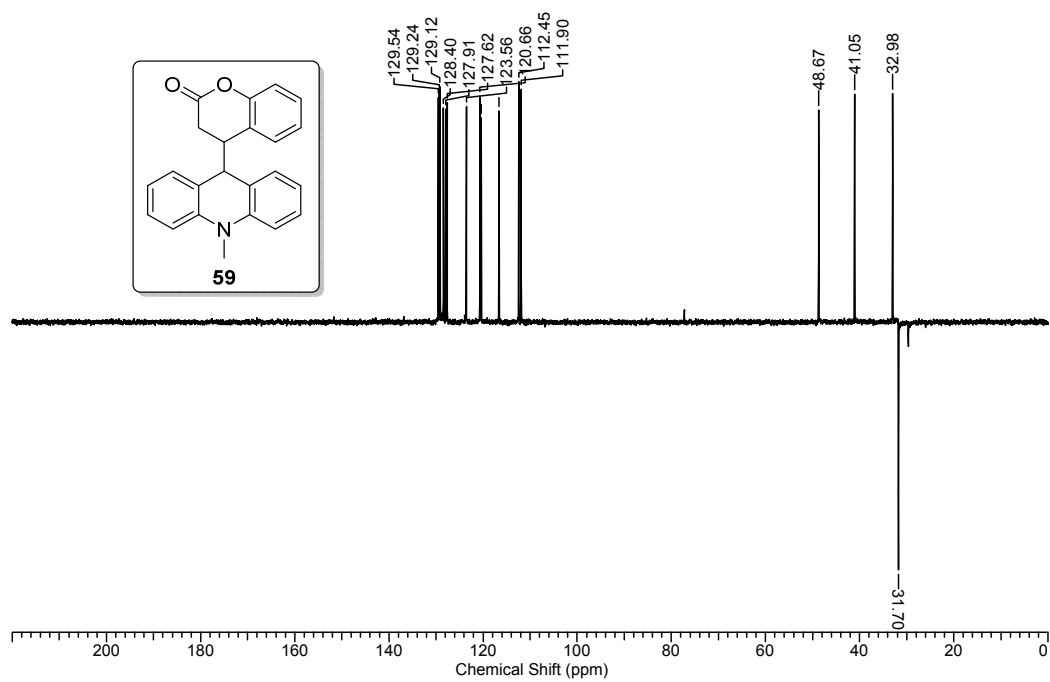
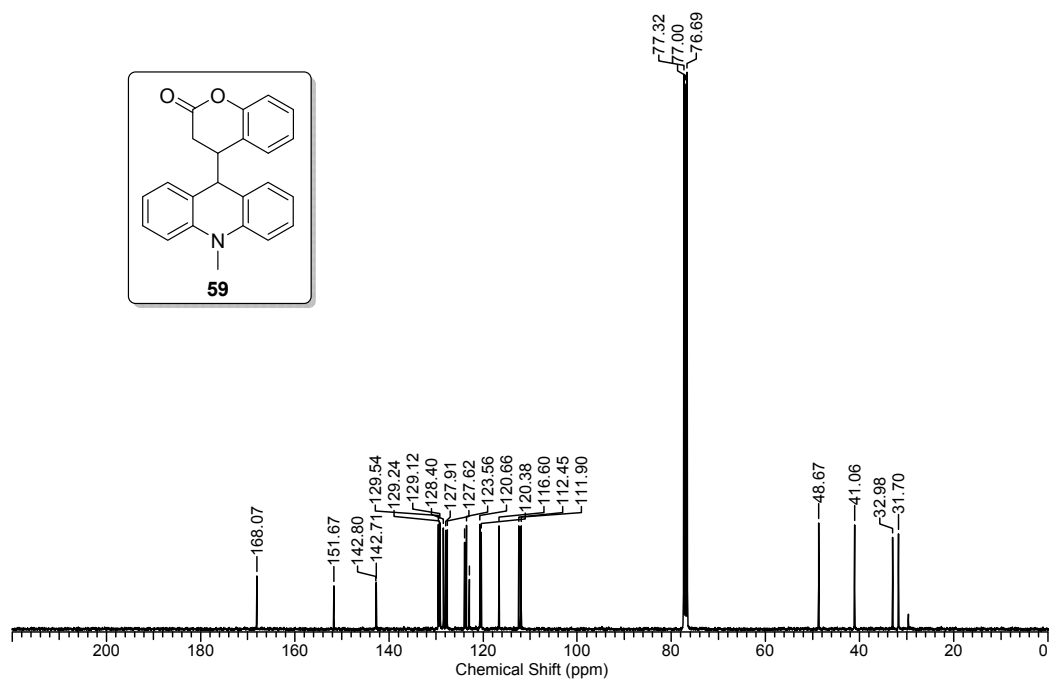


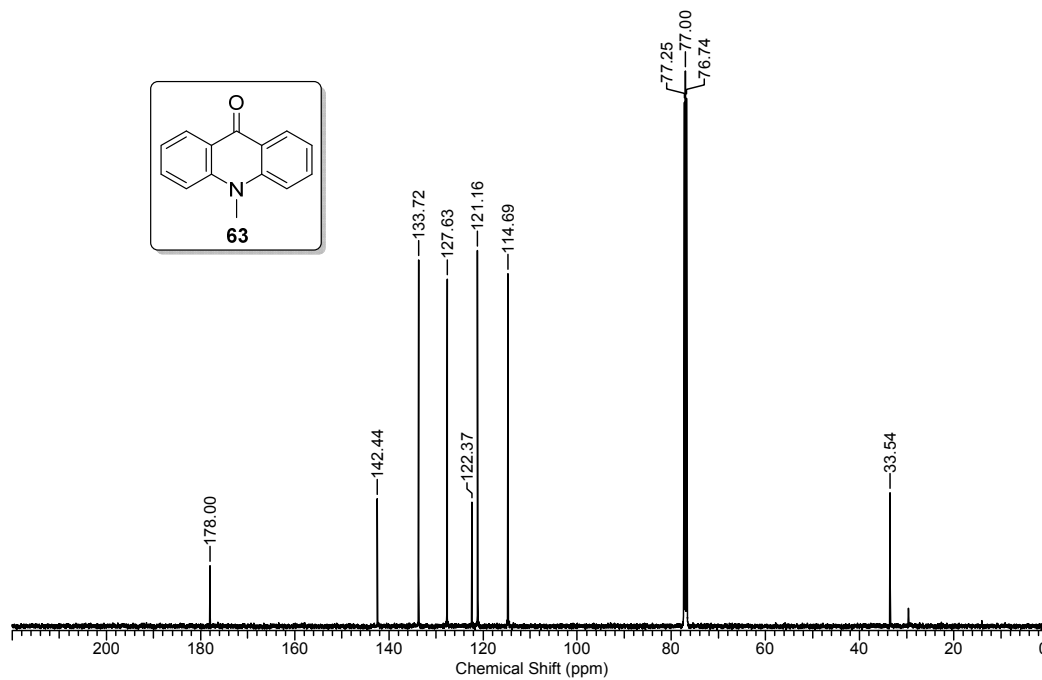
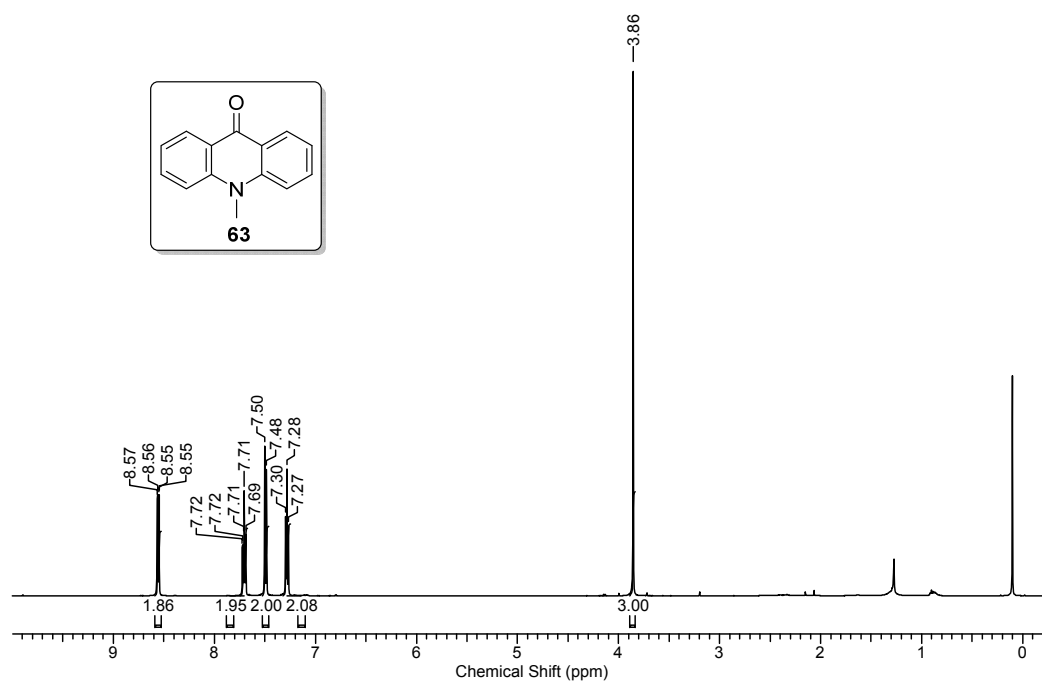


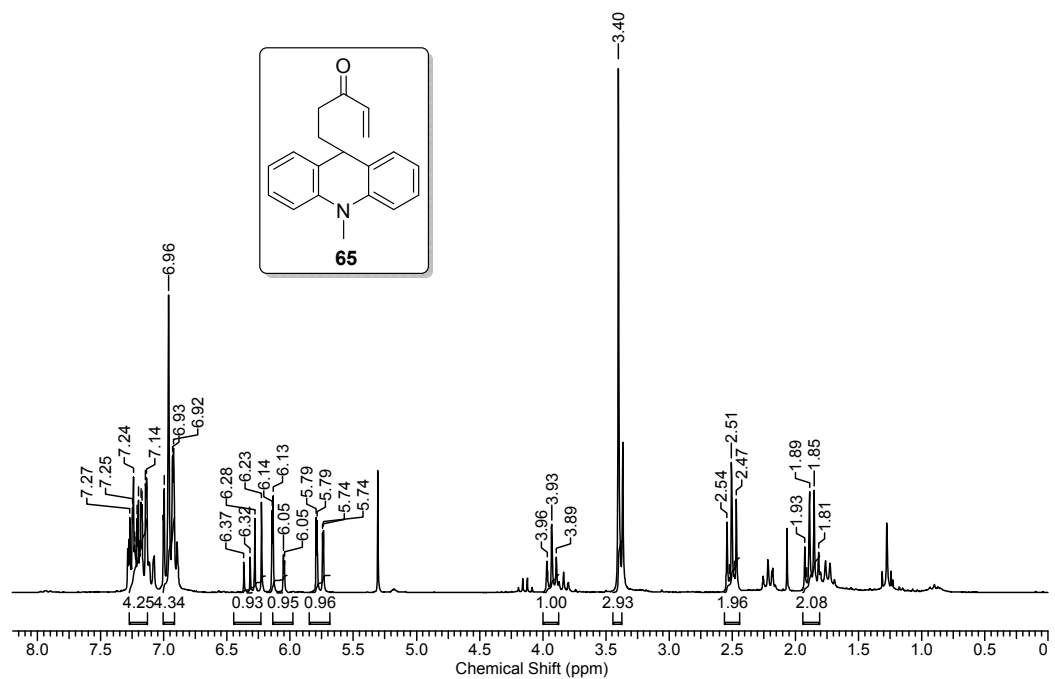
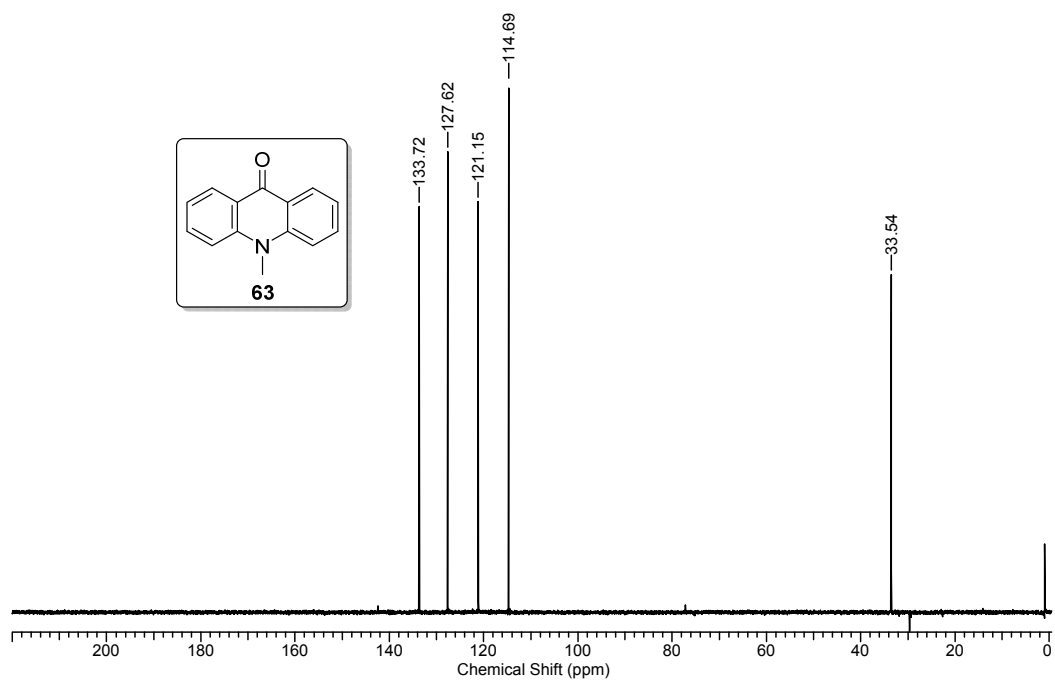




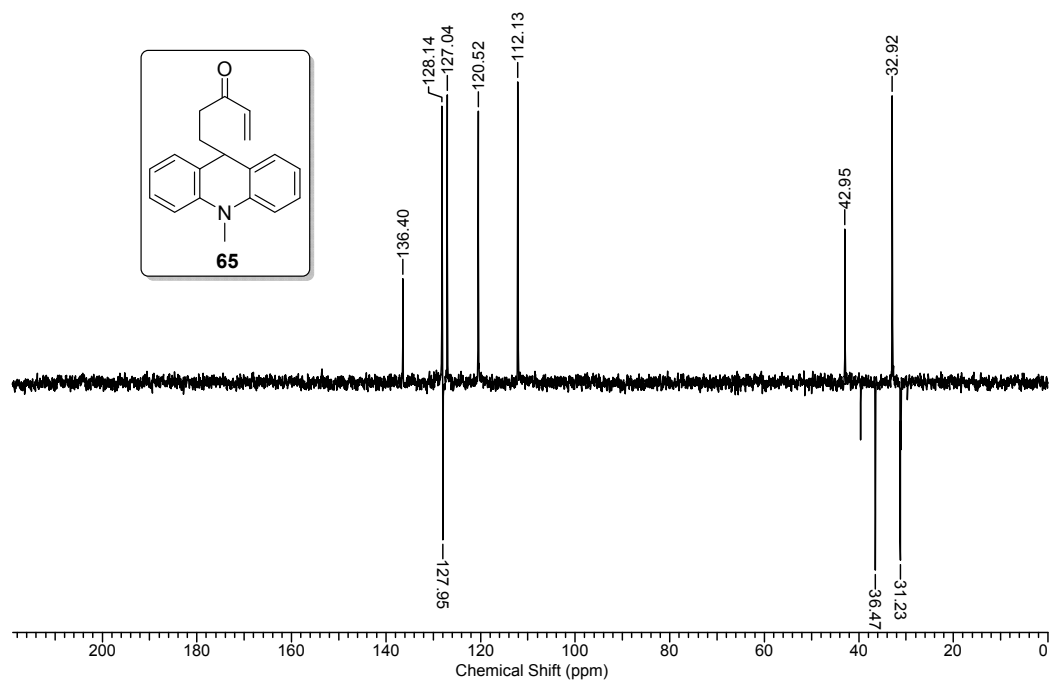
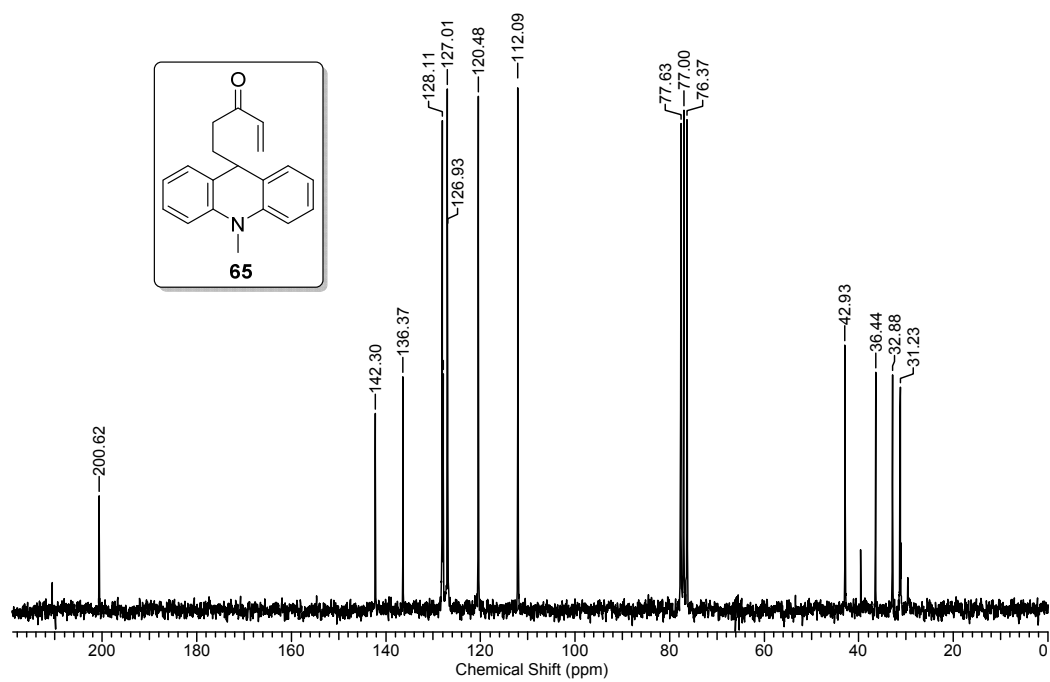


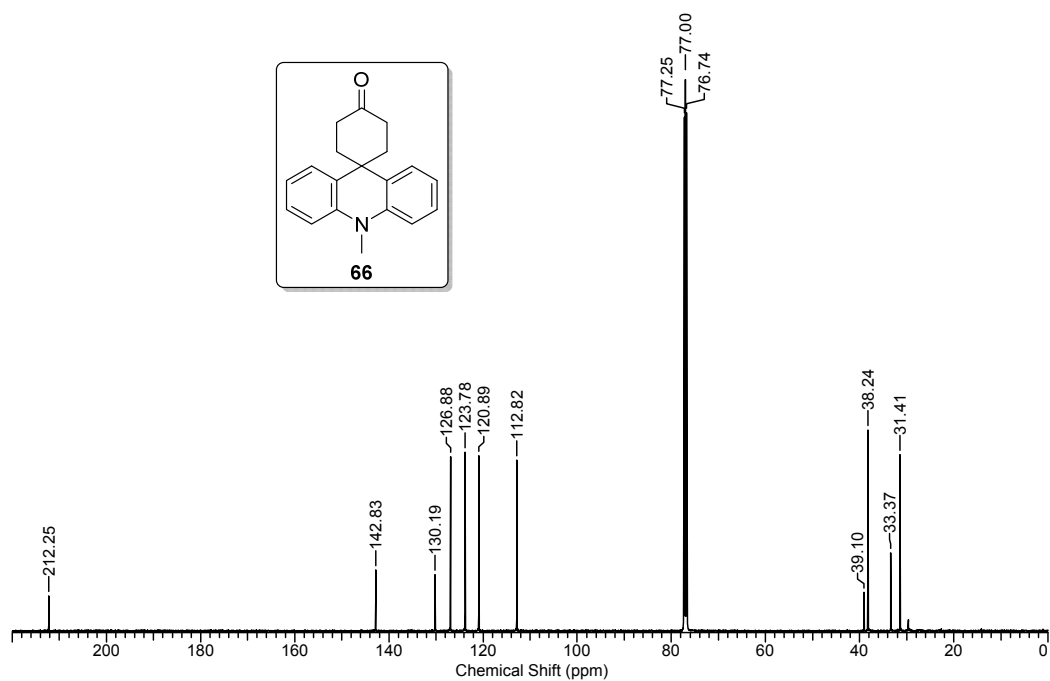
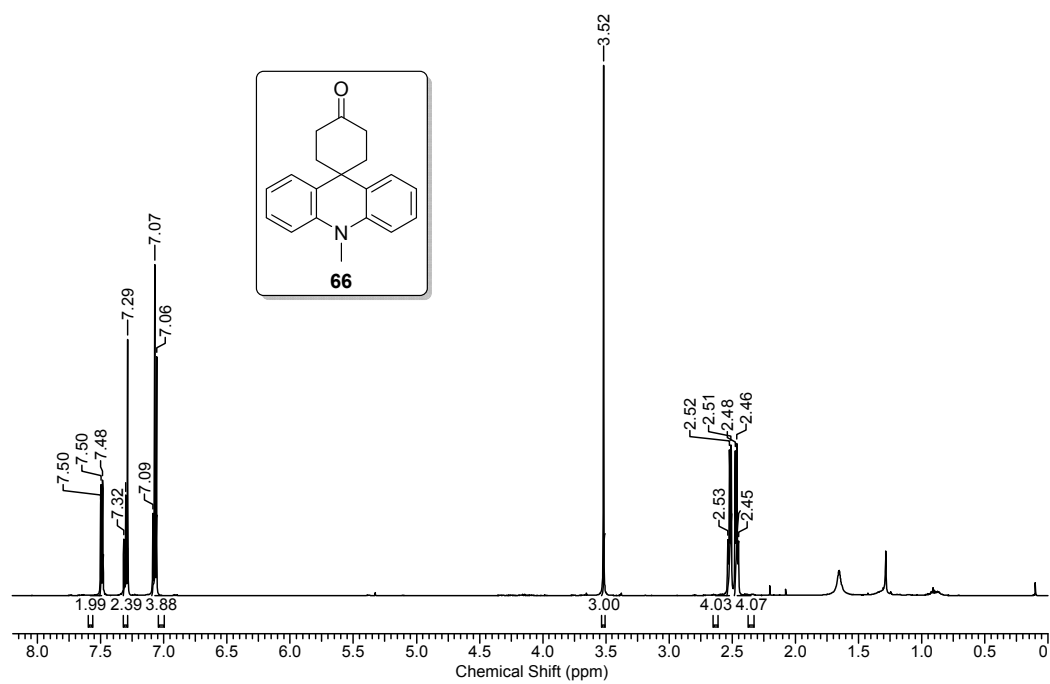


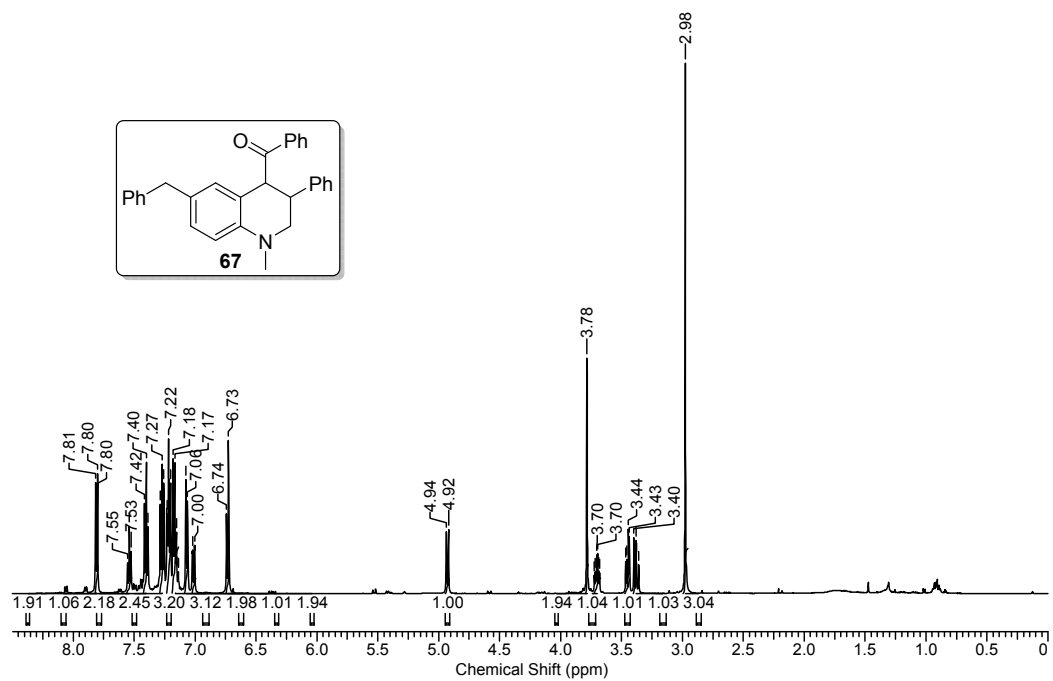
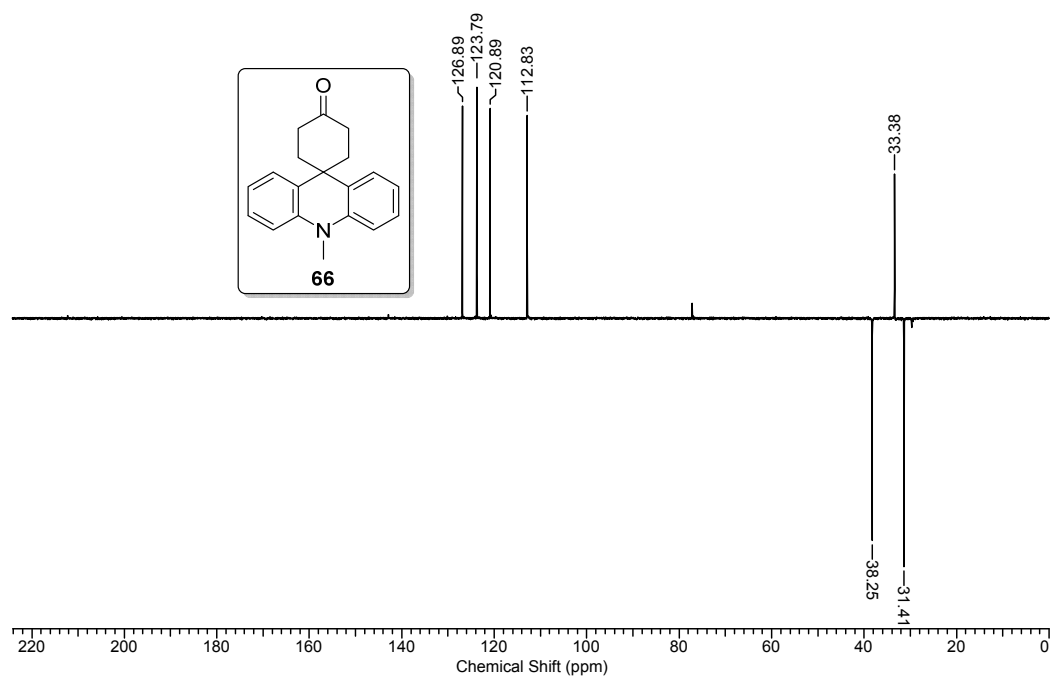


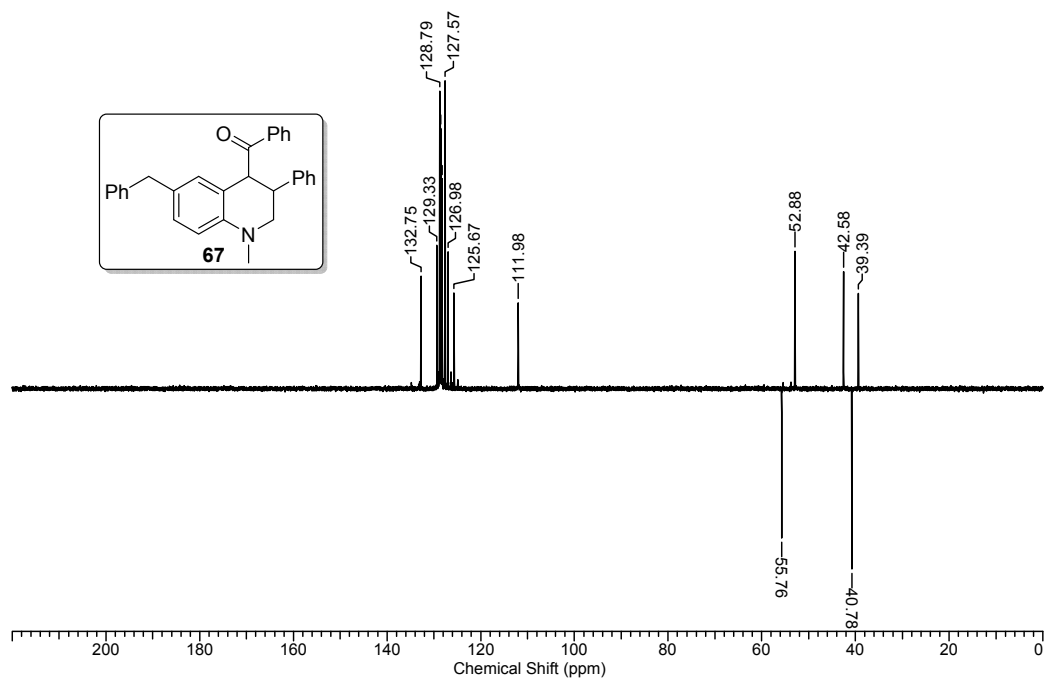
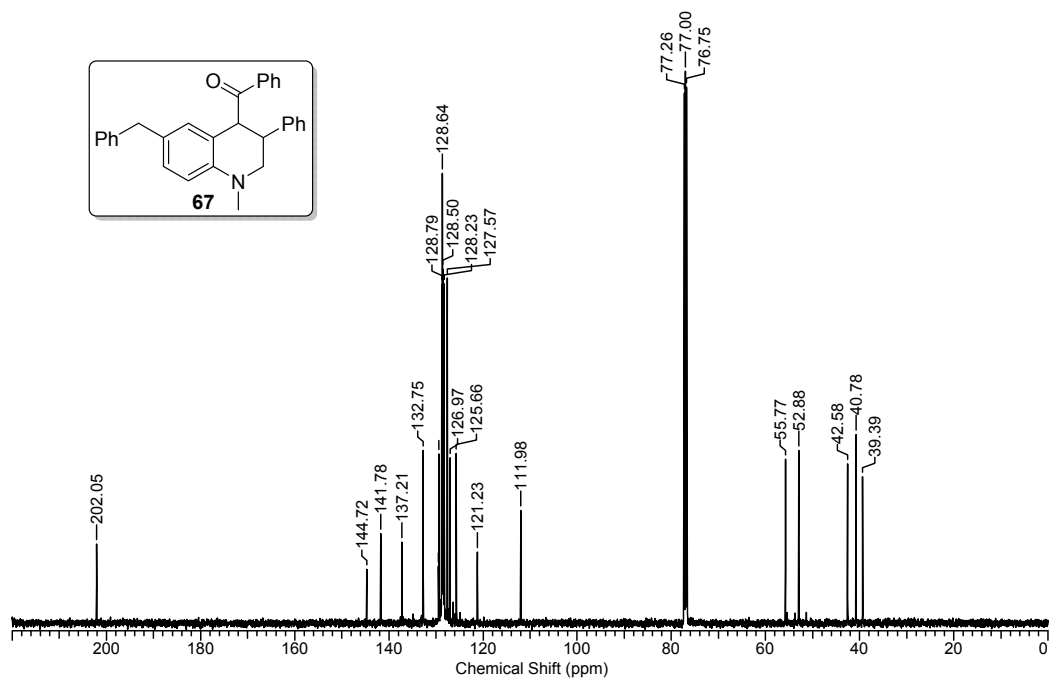




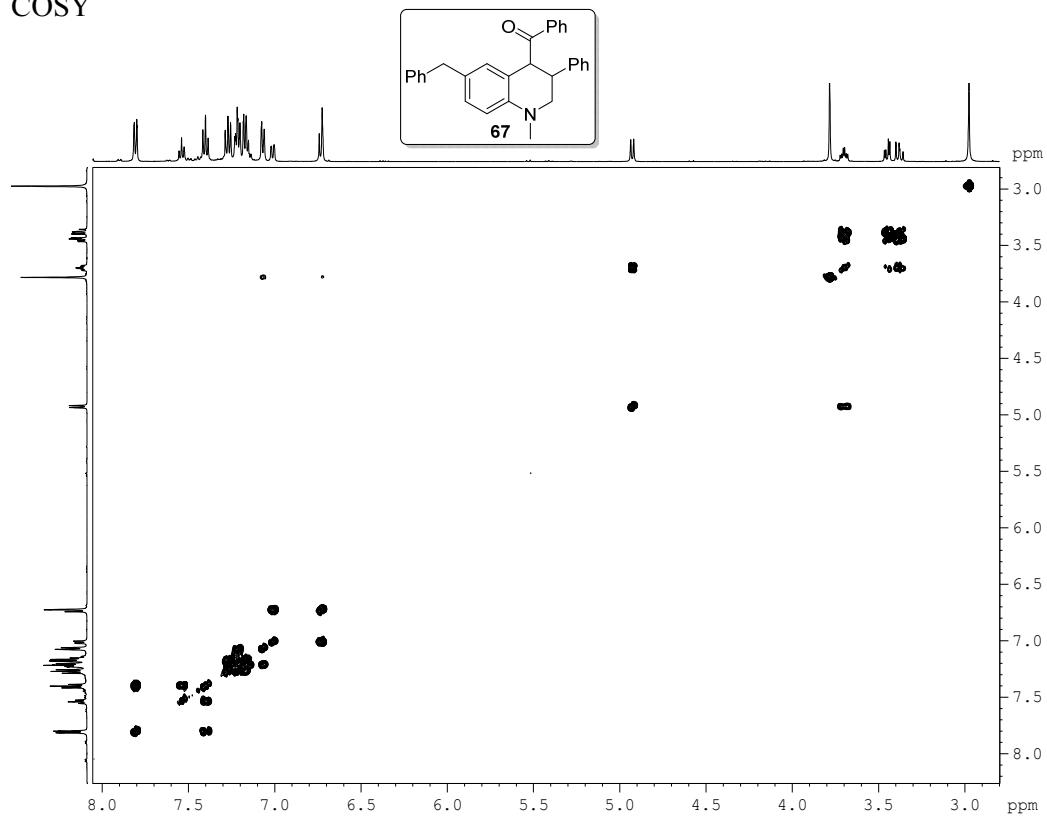




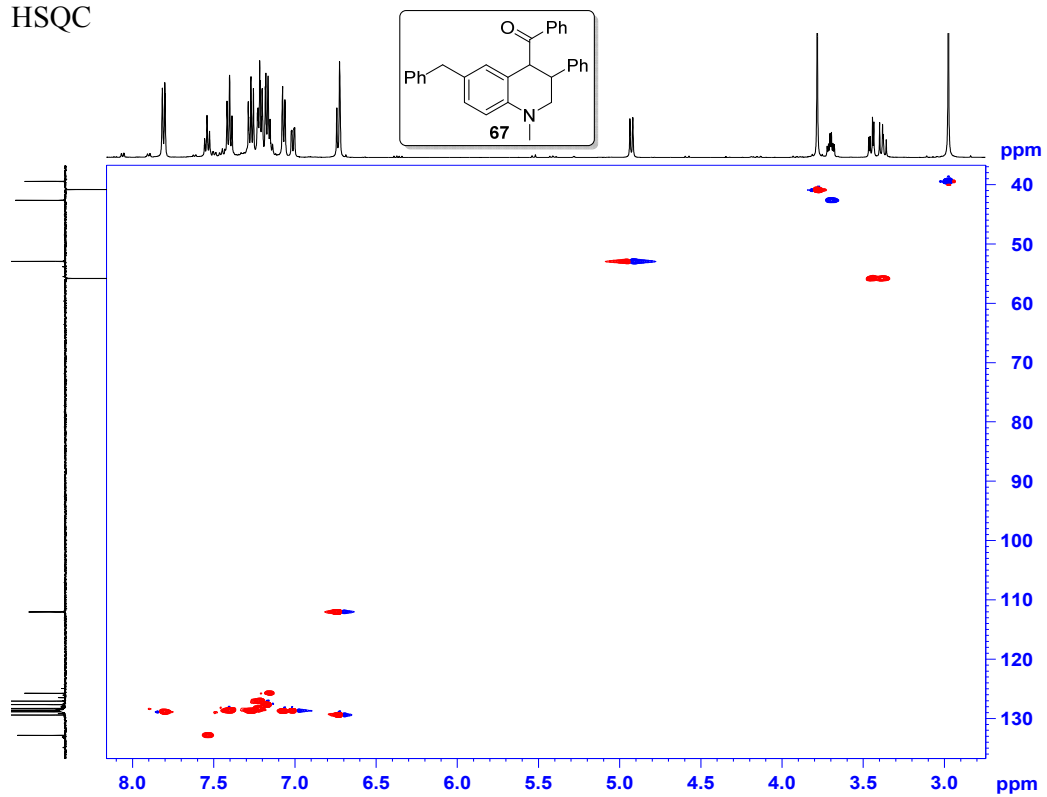




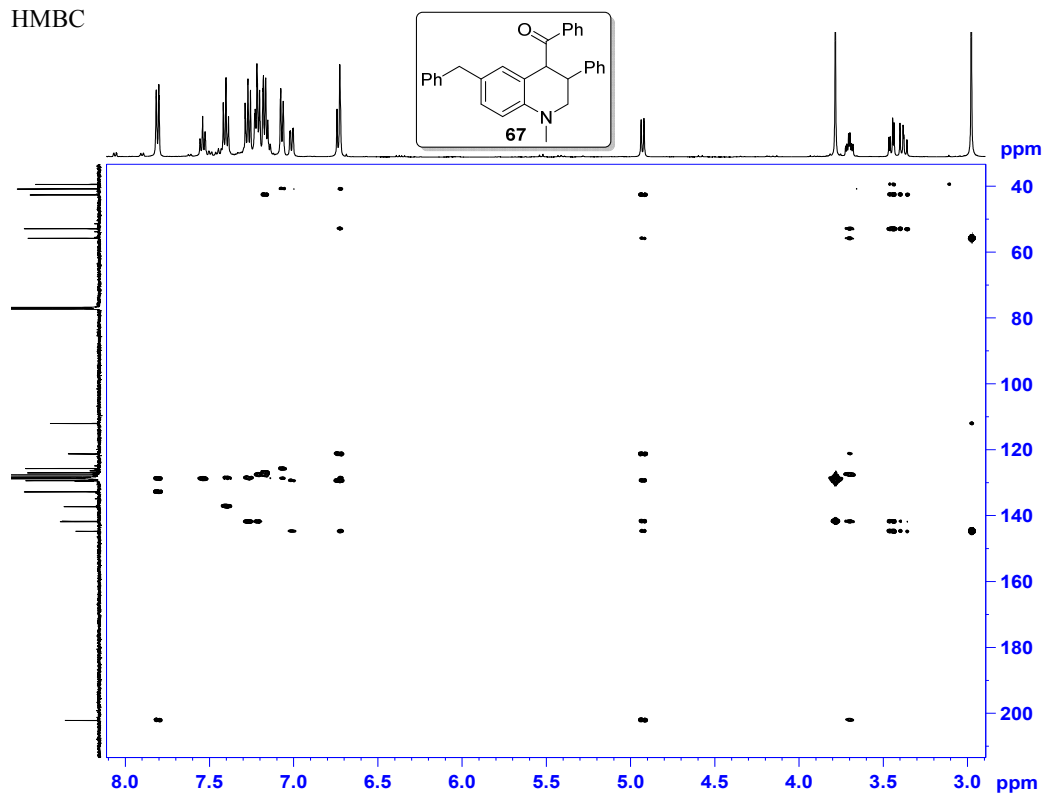
COSY



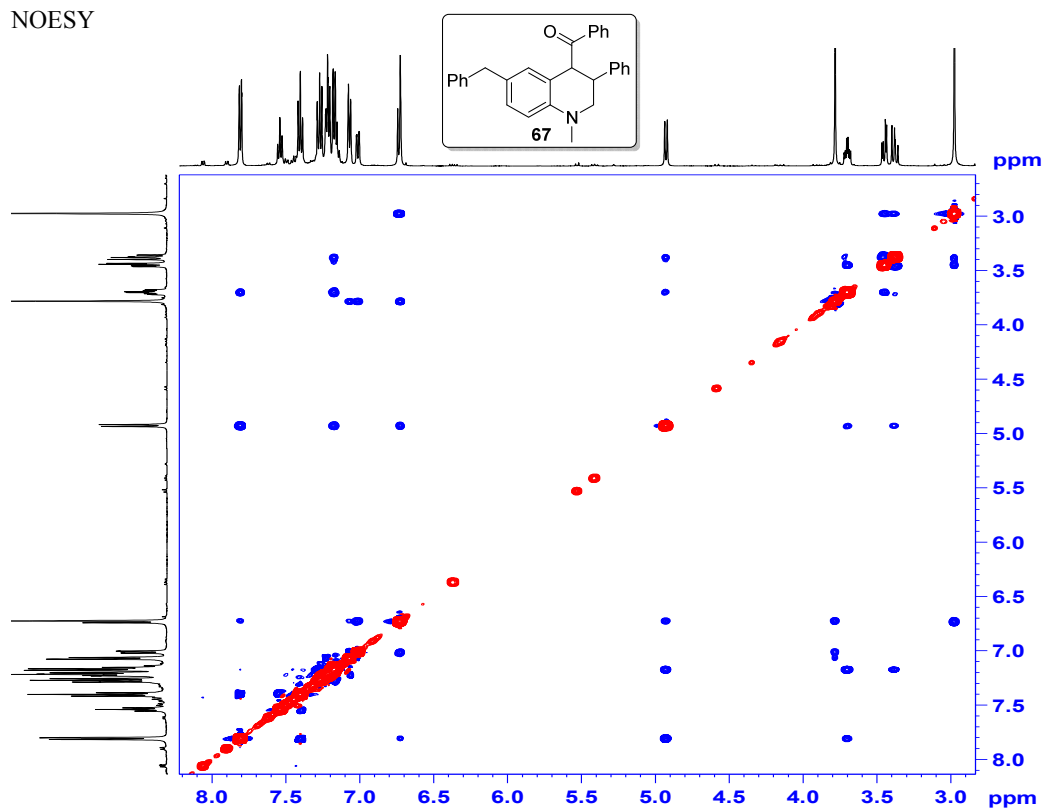
HSQC

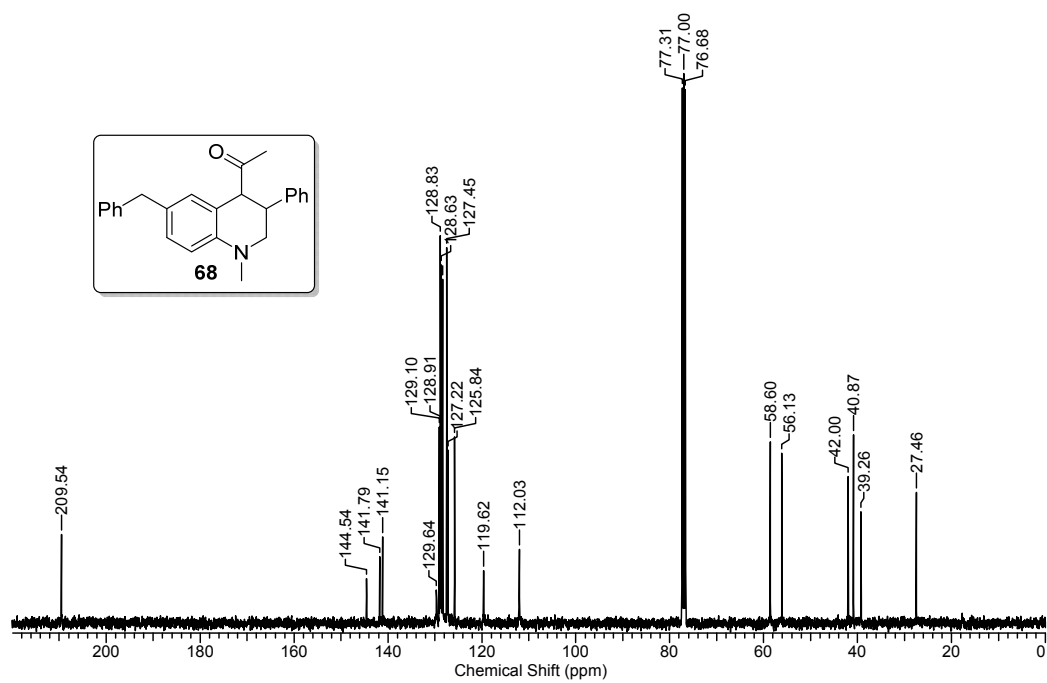
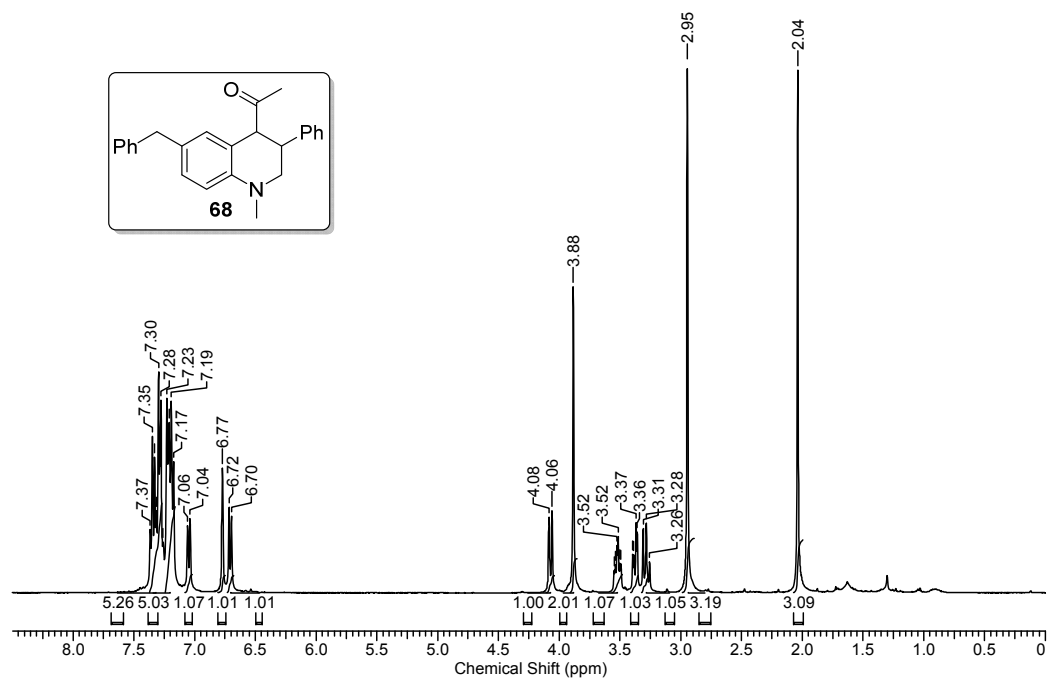


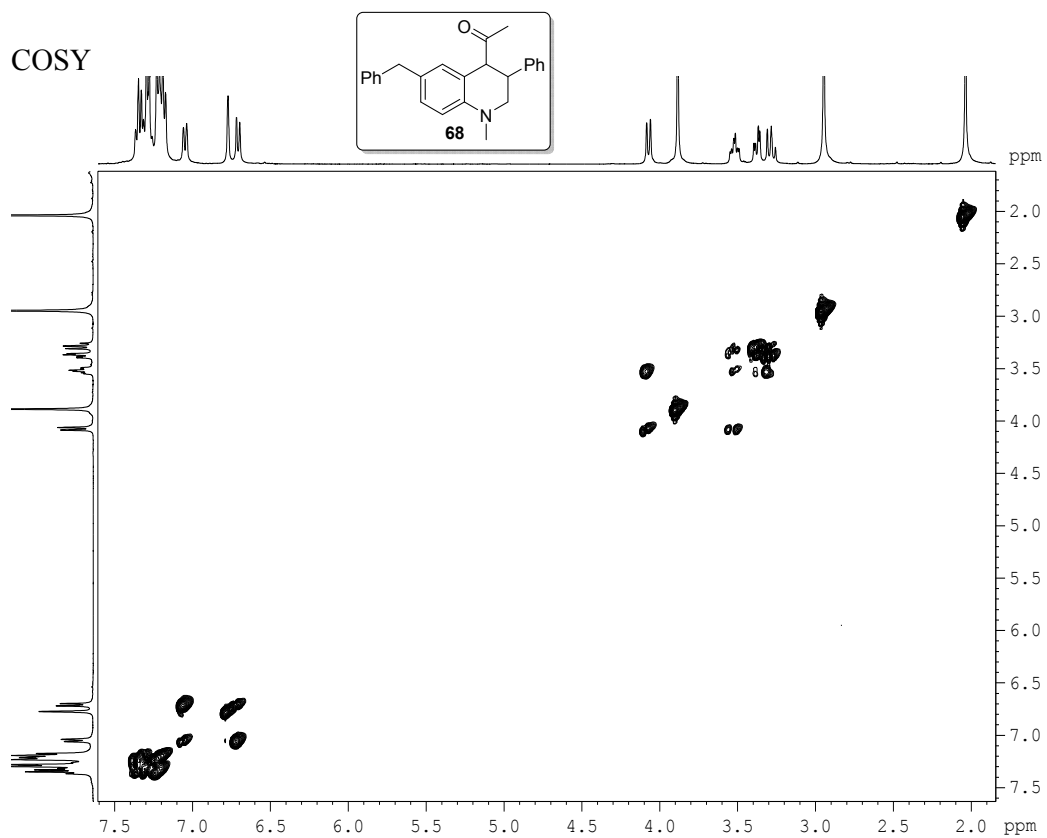
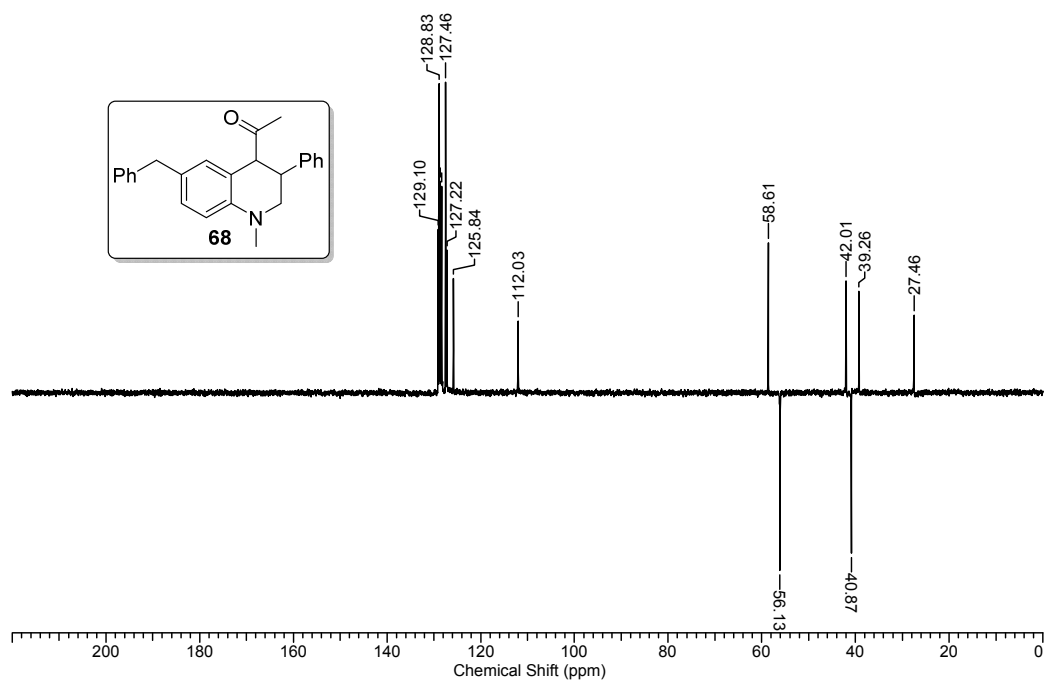
HMBC



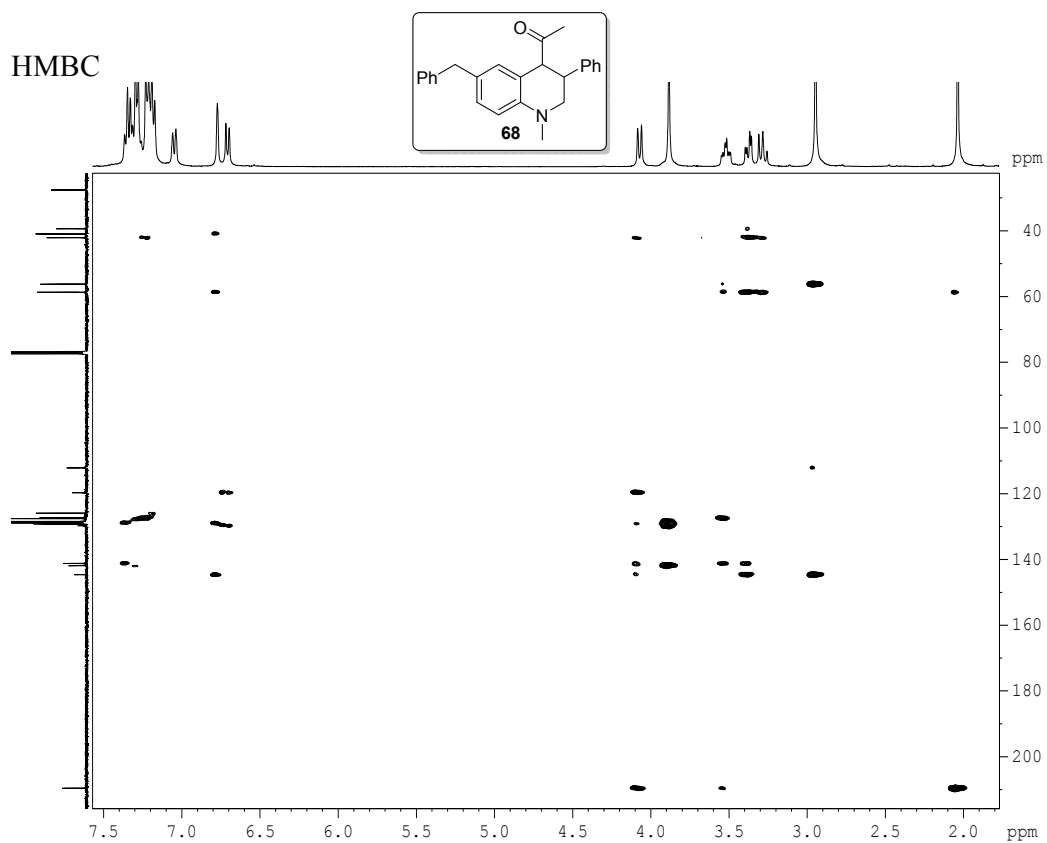
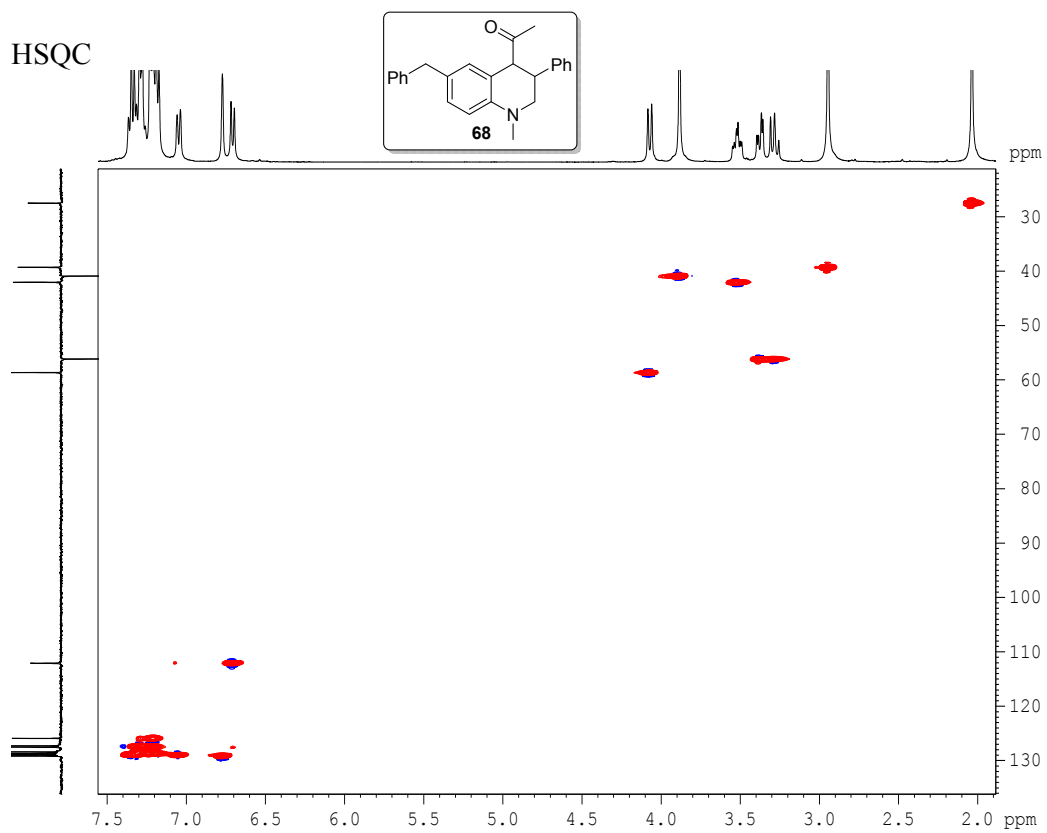
NOESY



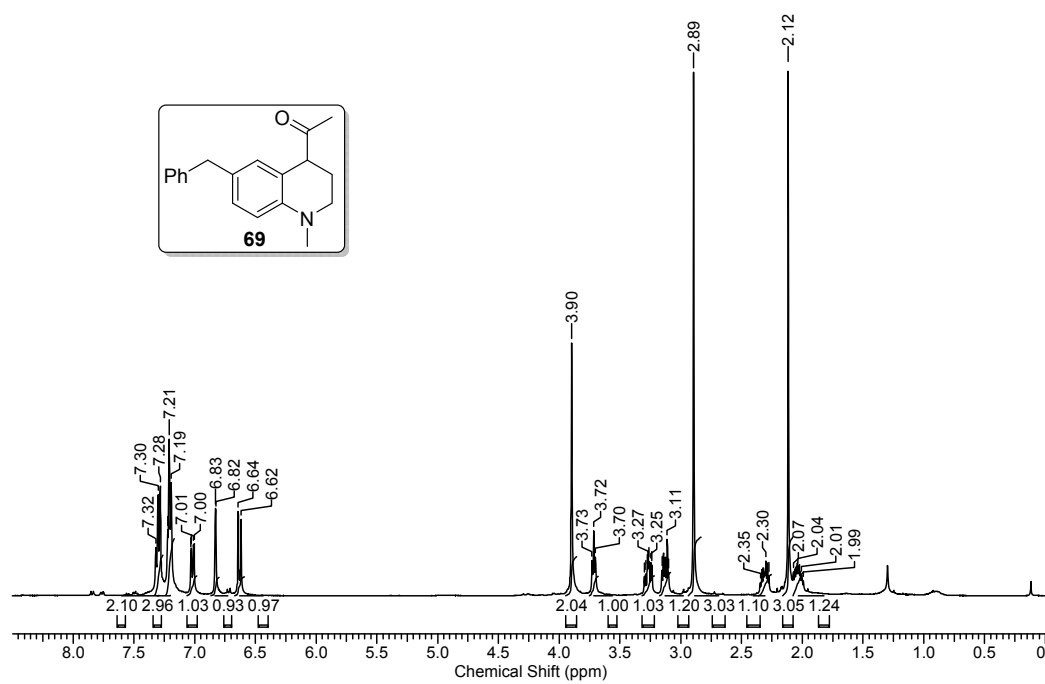
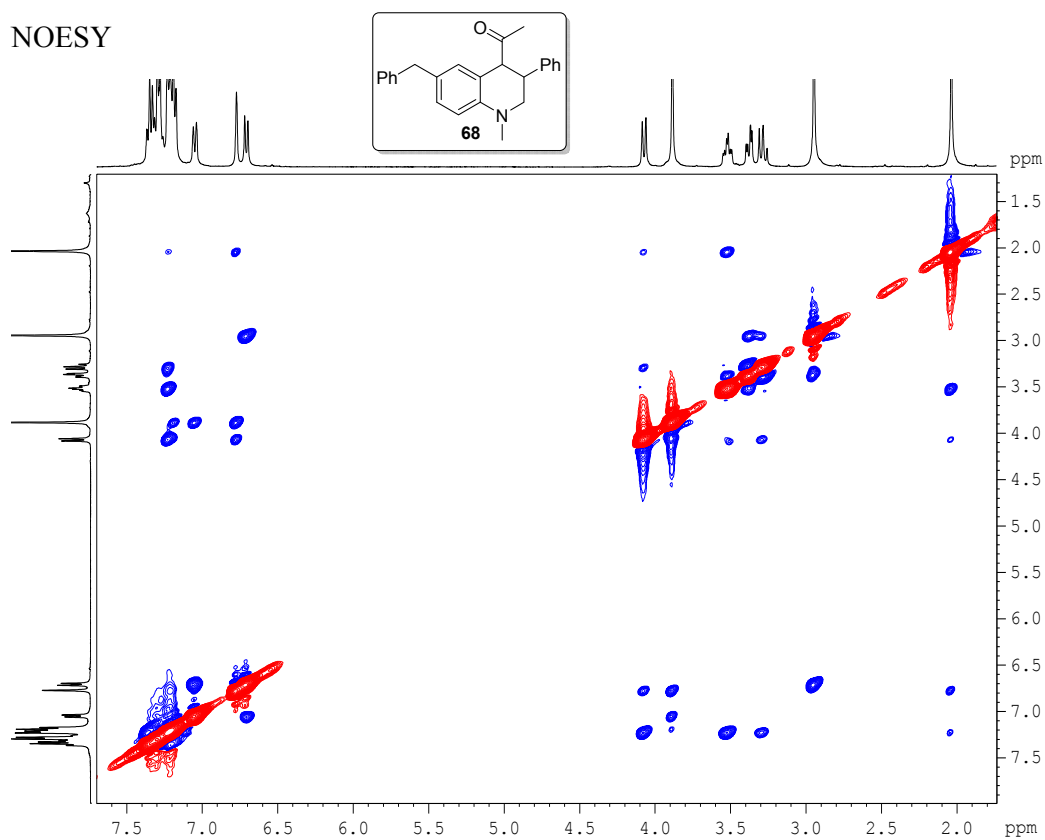


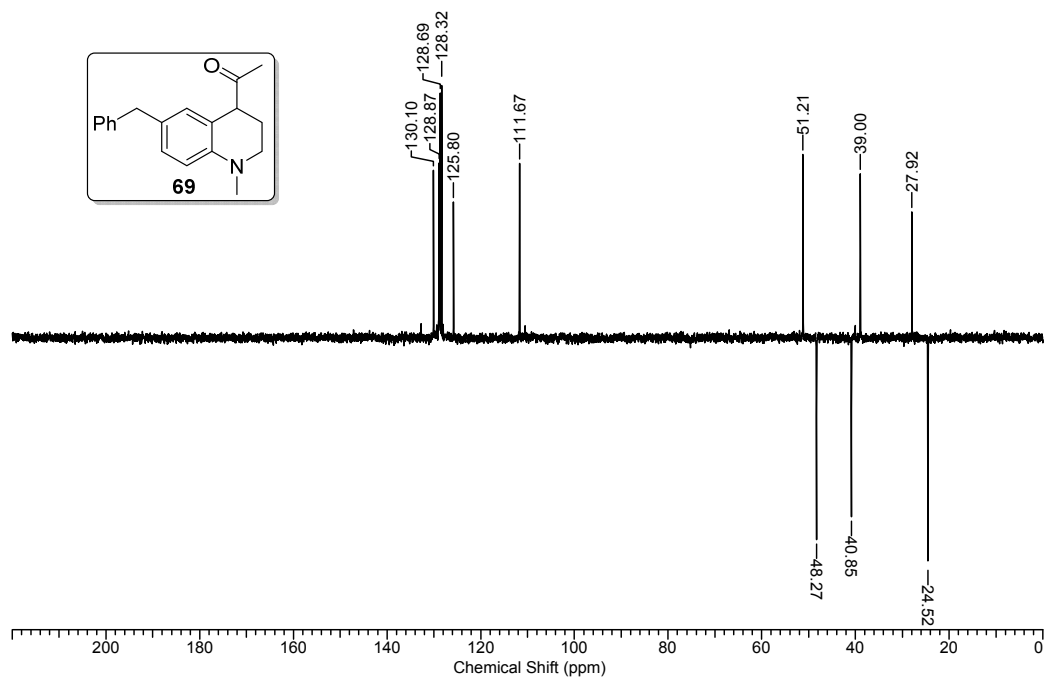
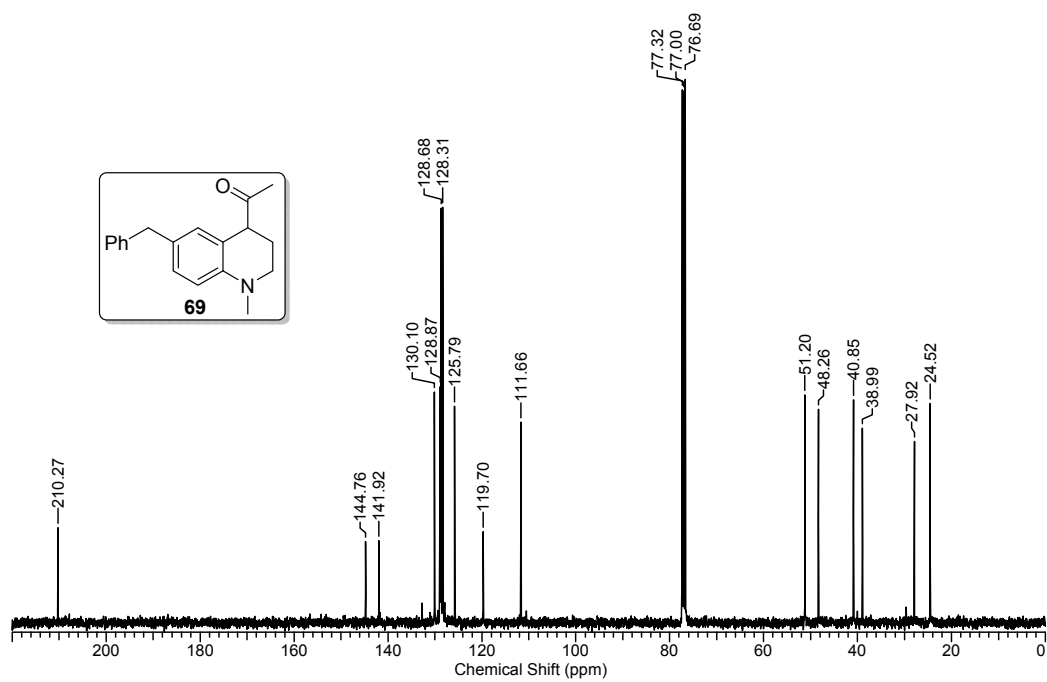


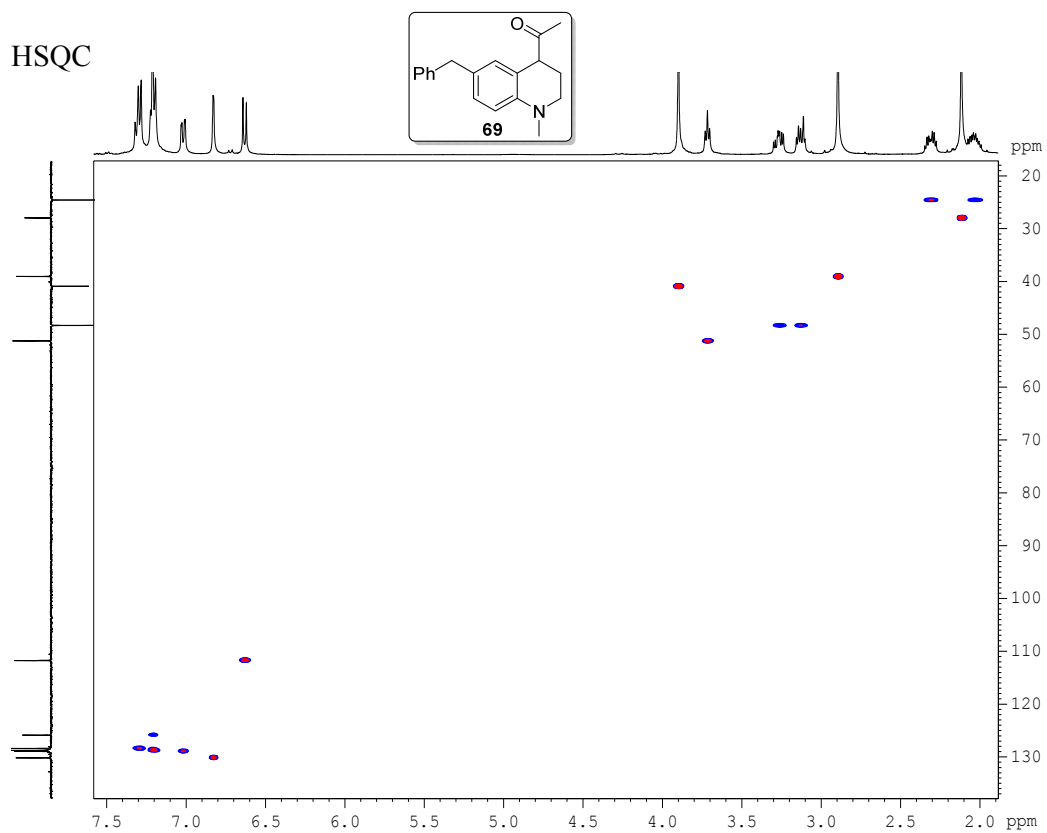
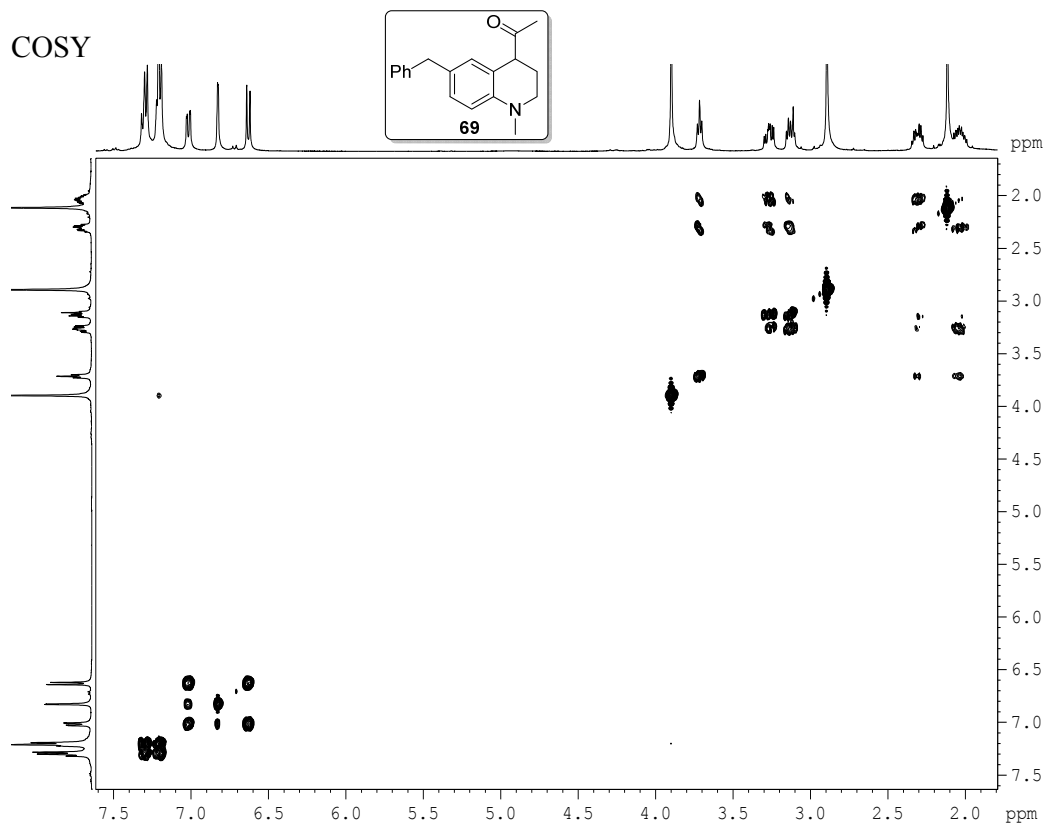


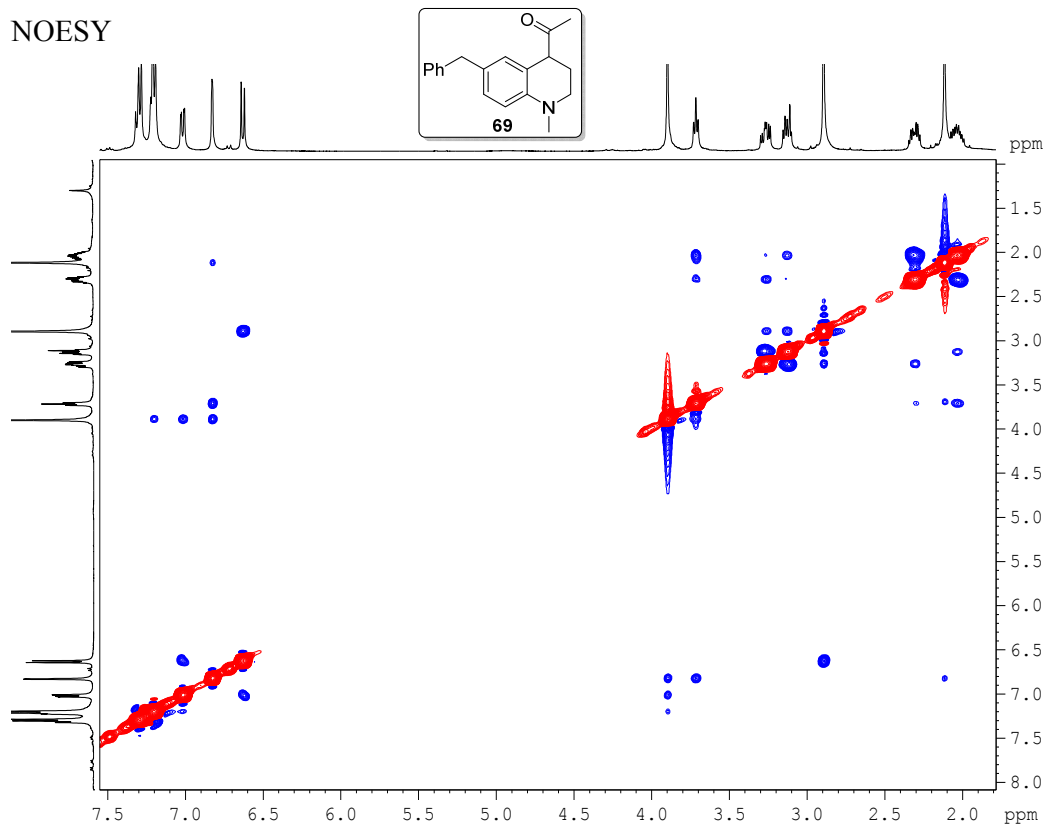
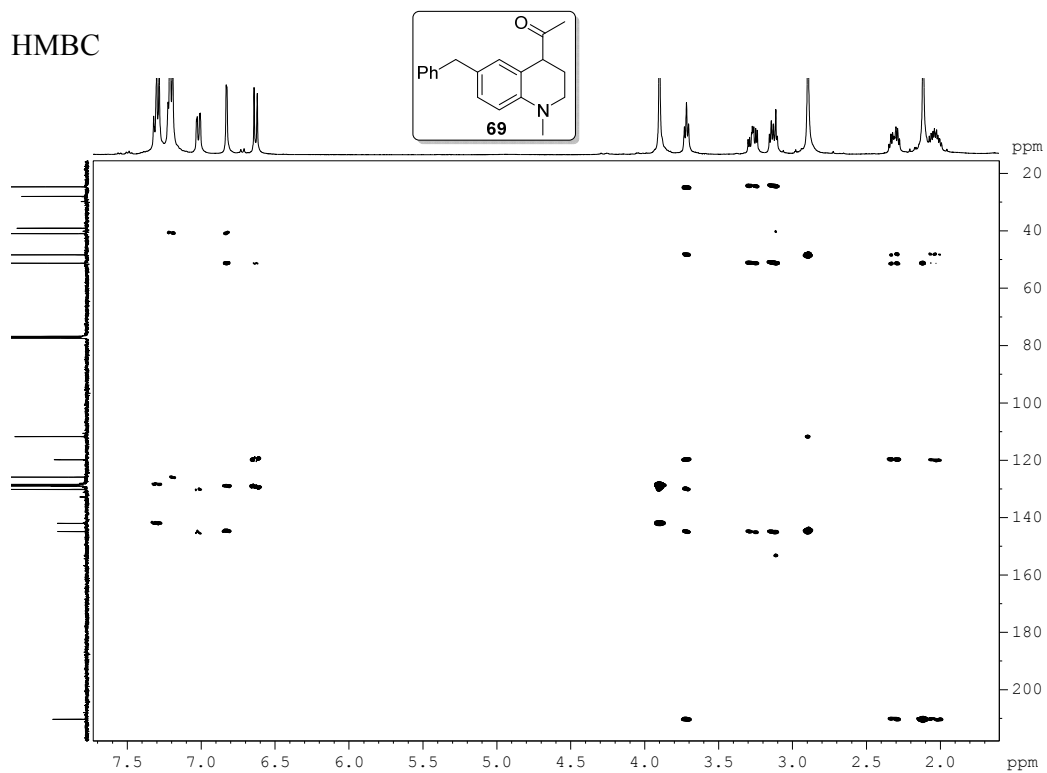


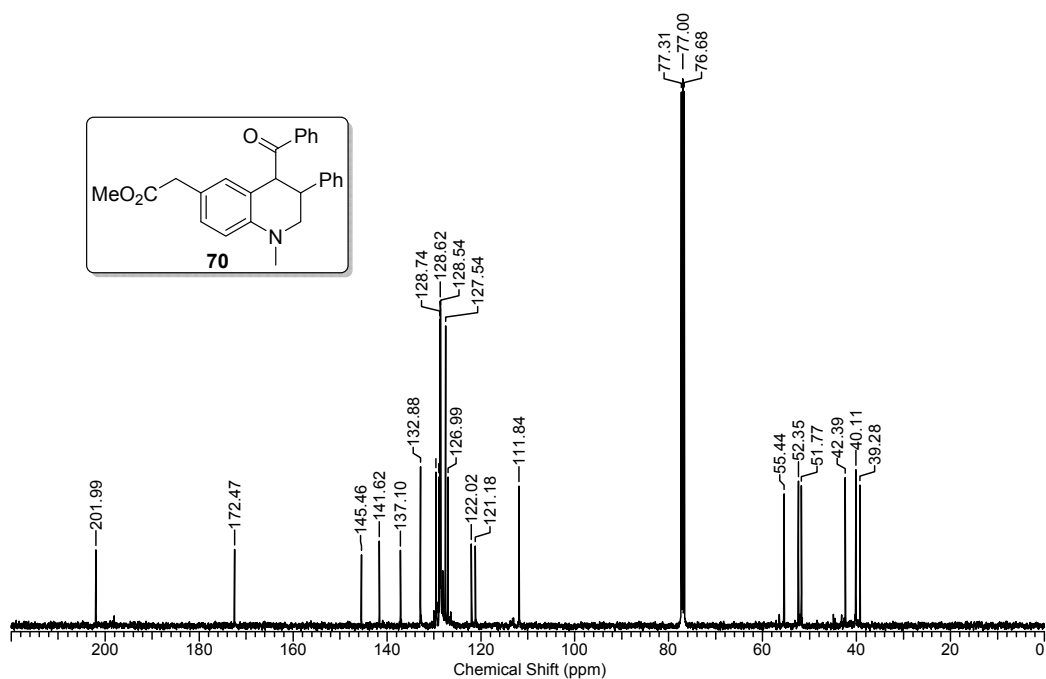
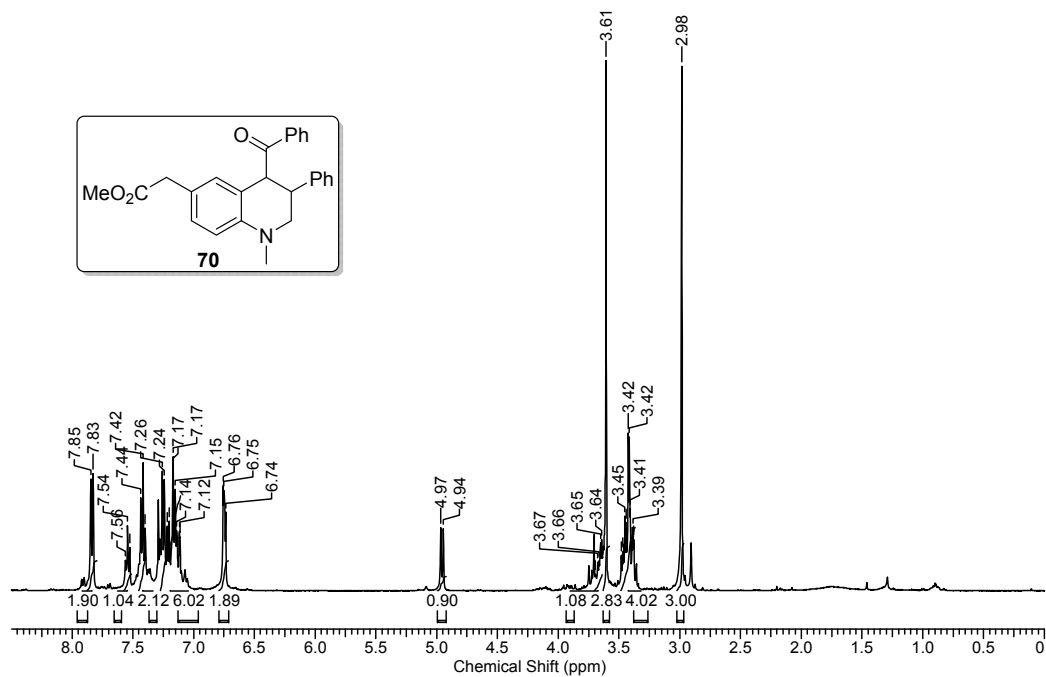
NOESY

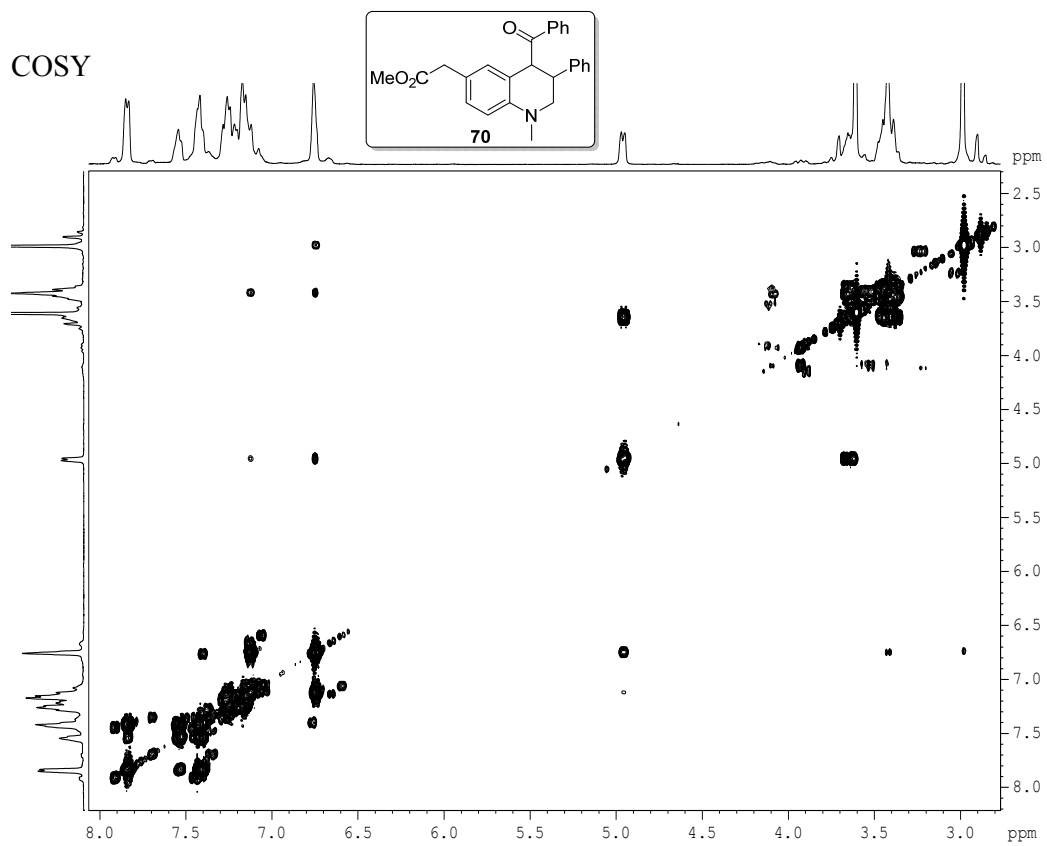
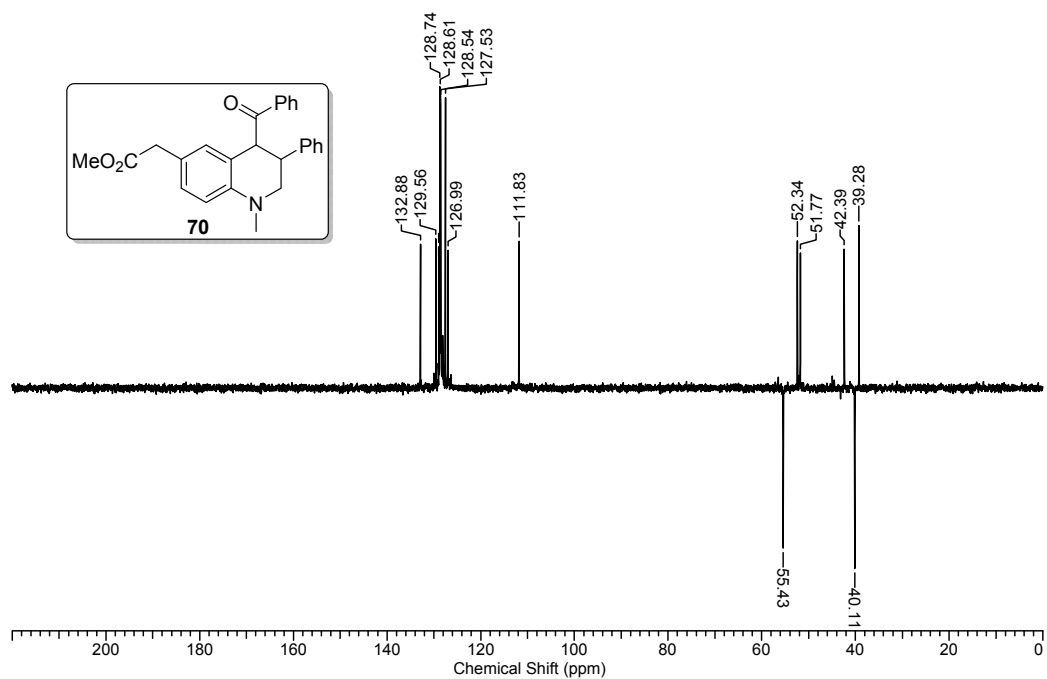


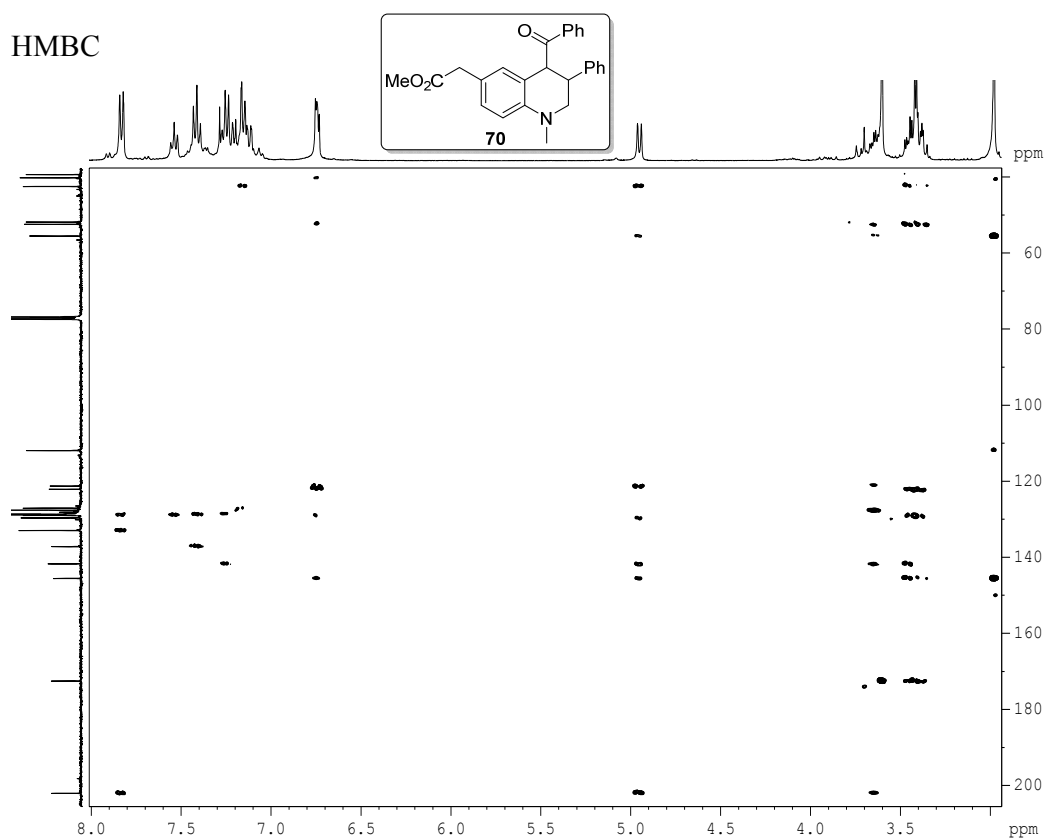
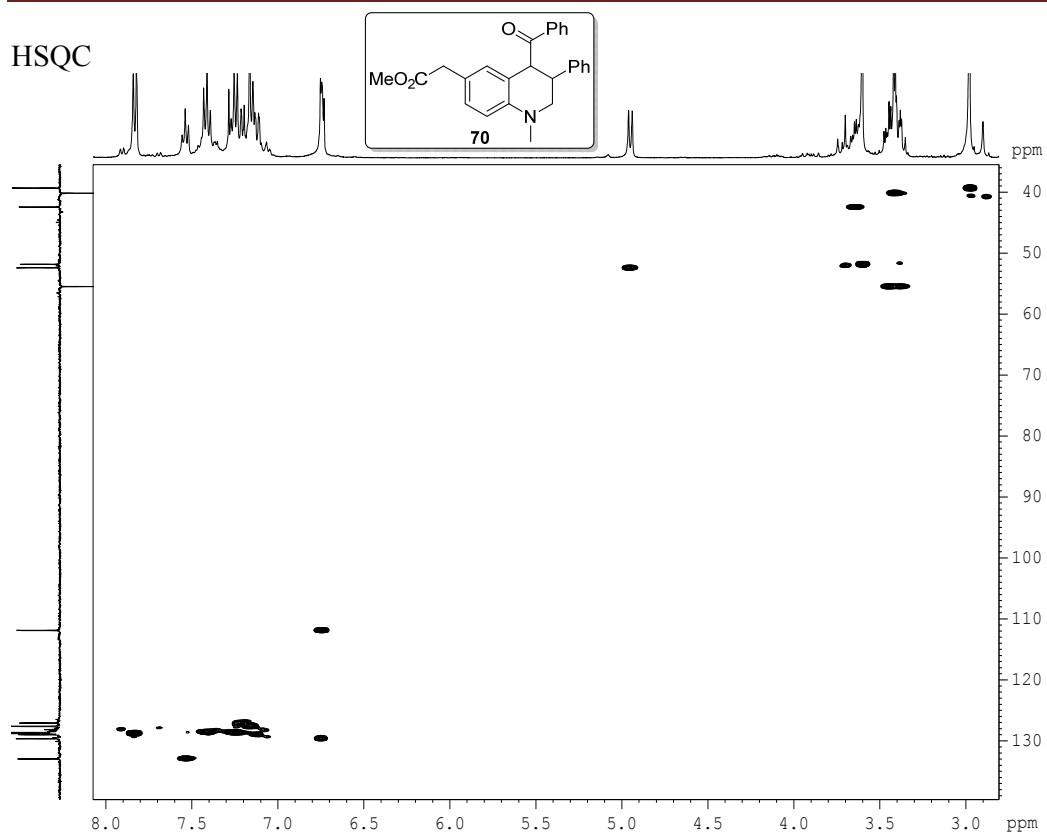






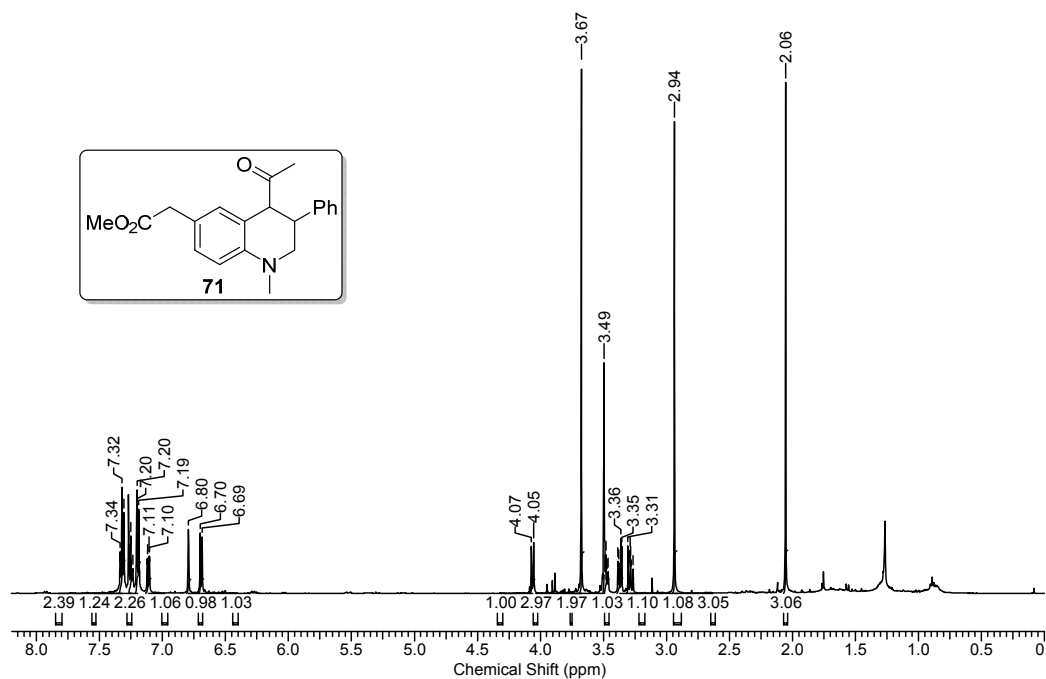
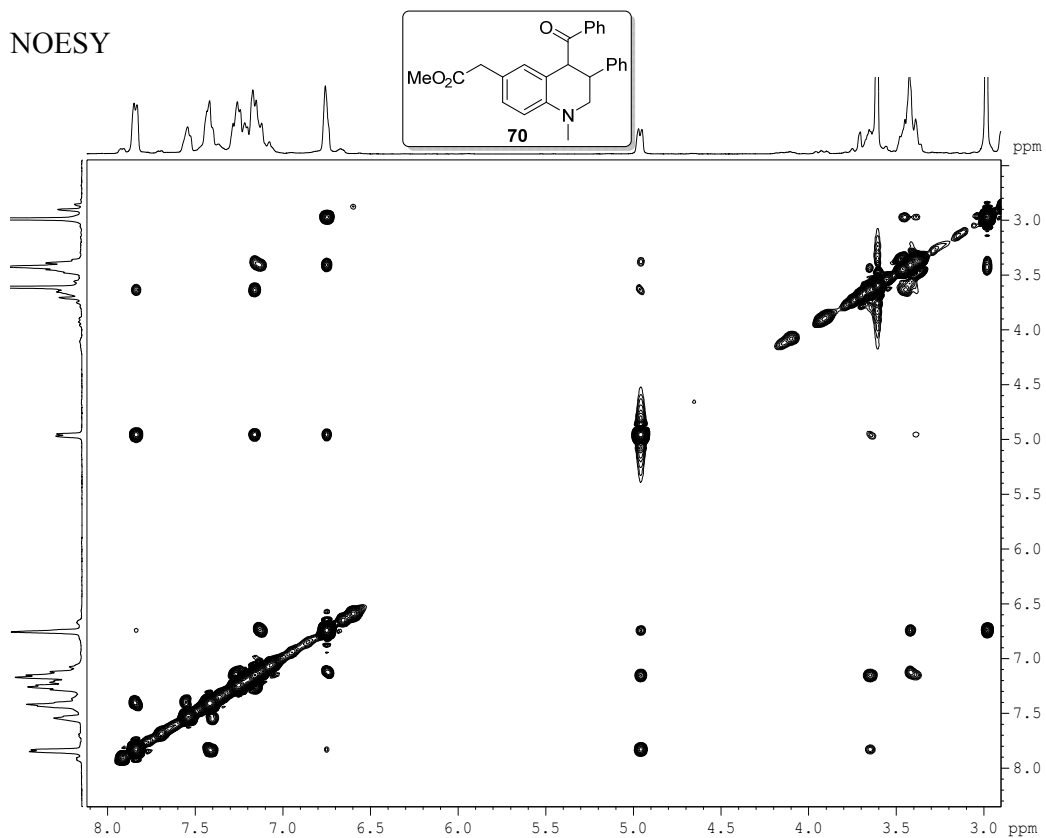


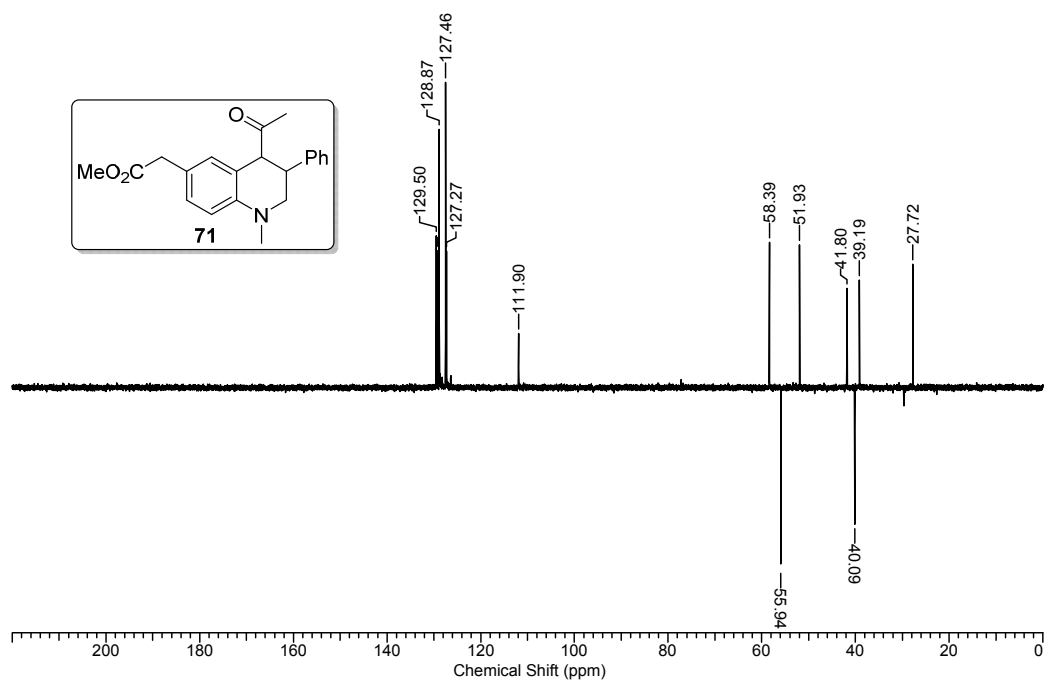
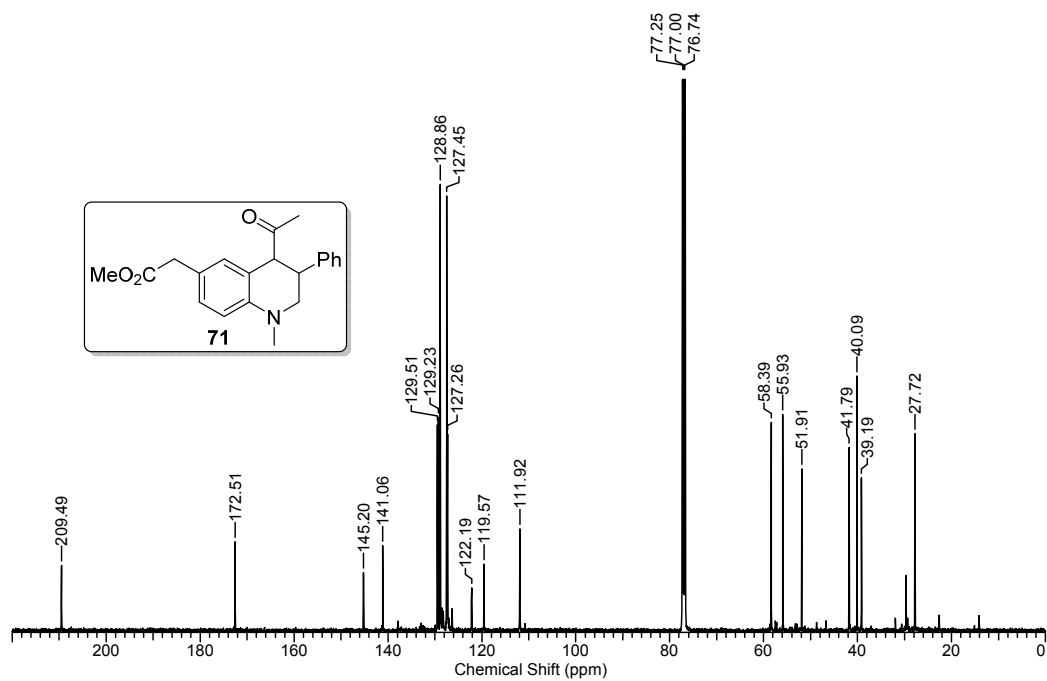




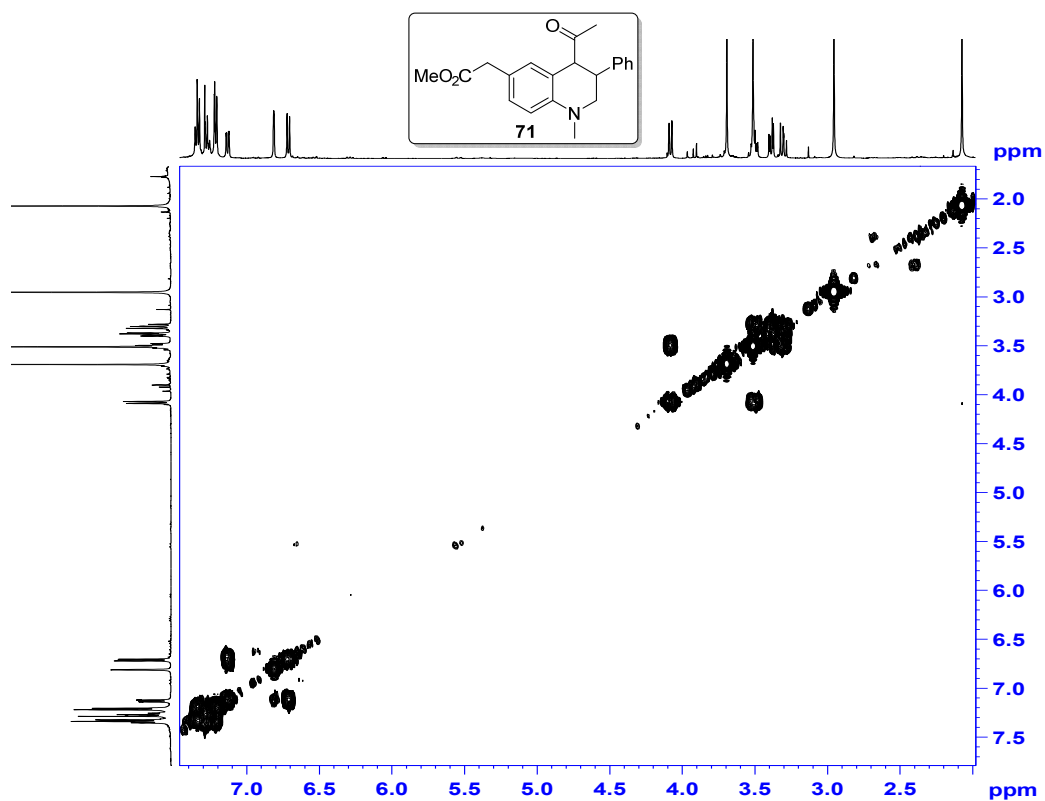


NOESY

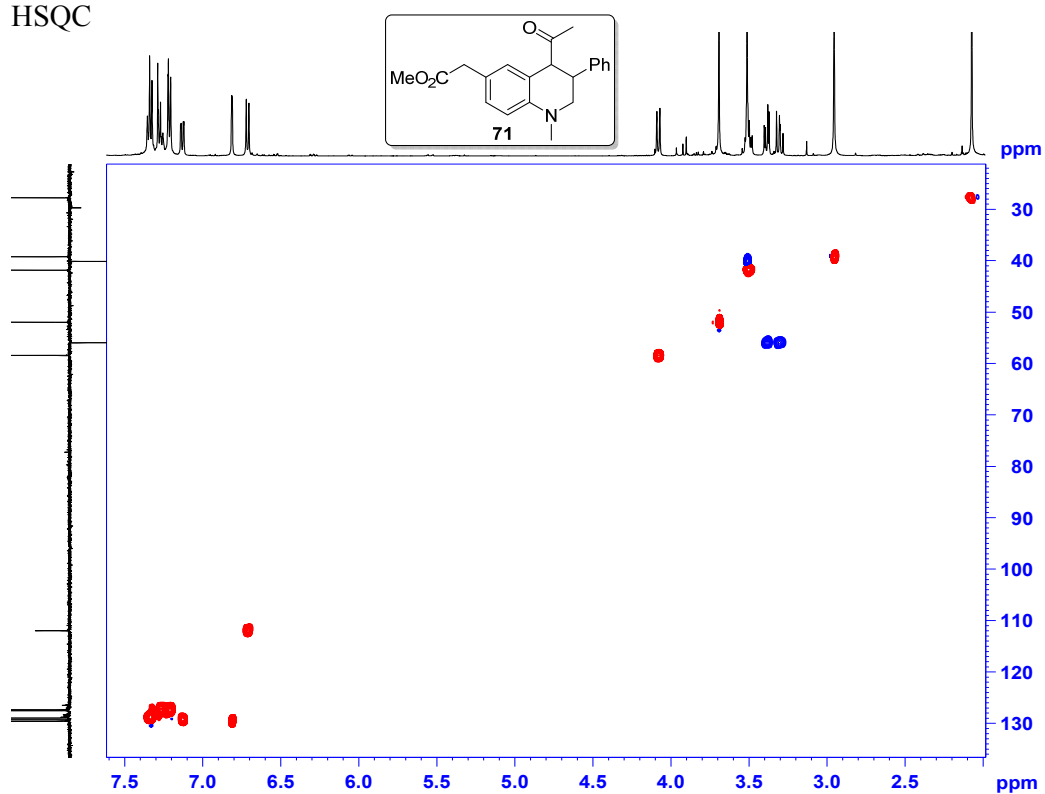




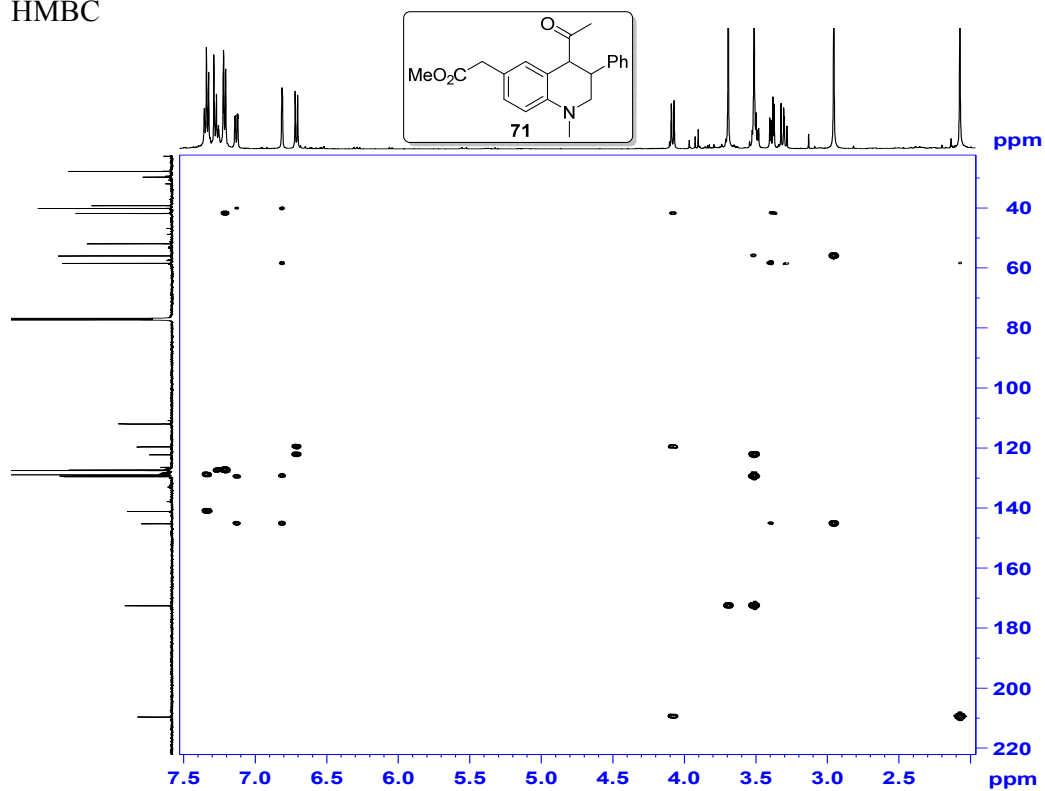
COSY



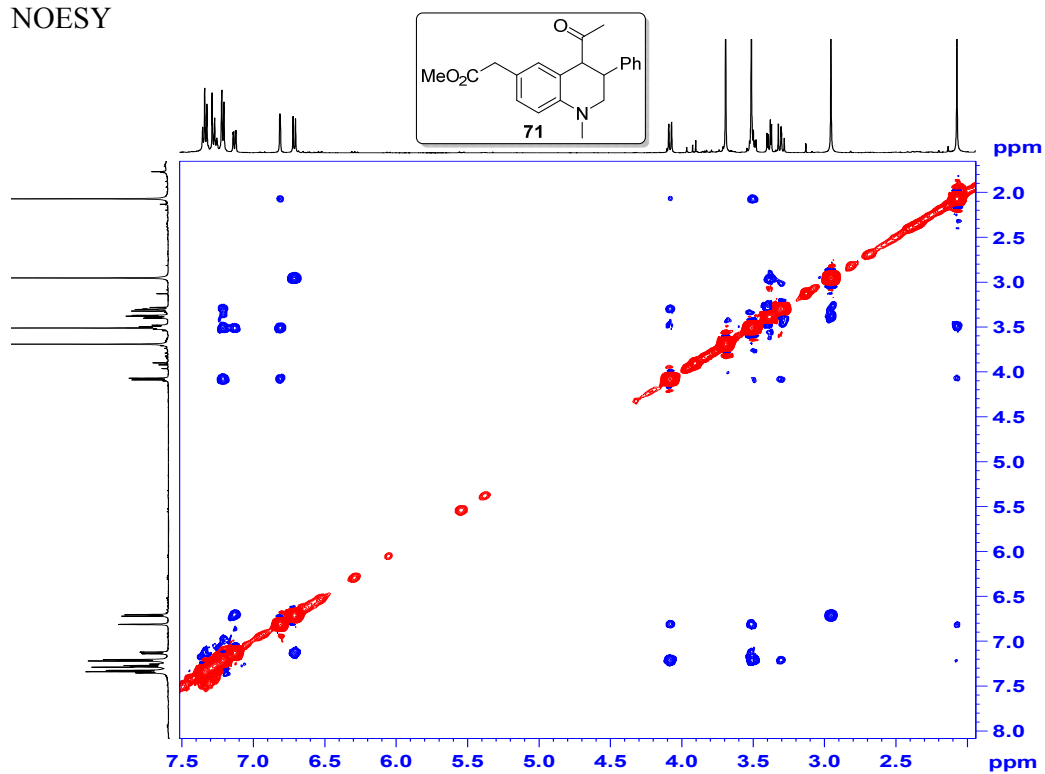
HSQC

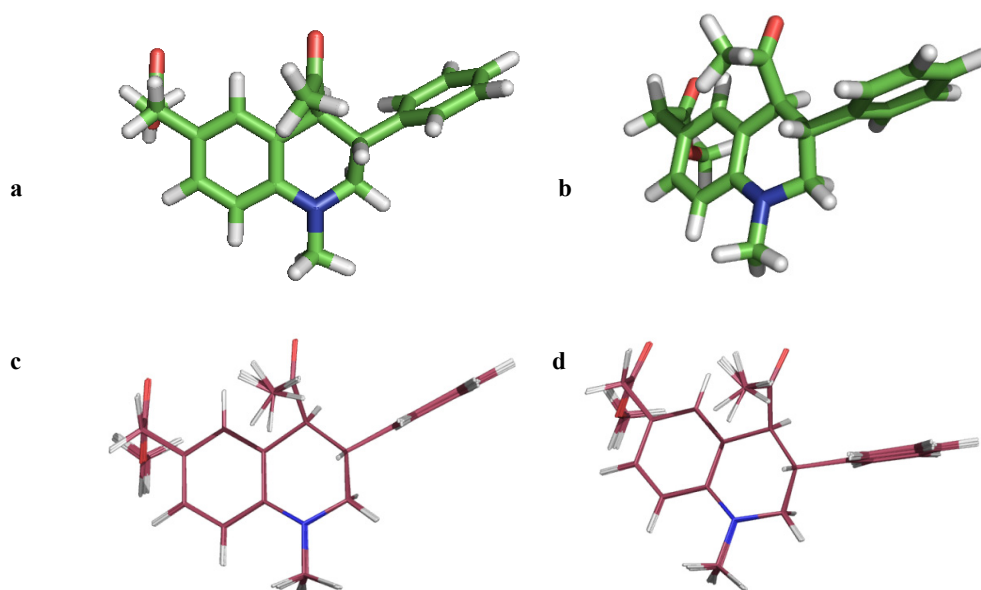


HMBC



NOESY



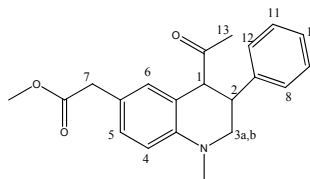
**MD Simulation :**

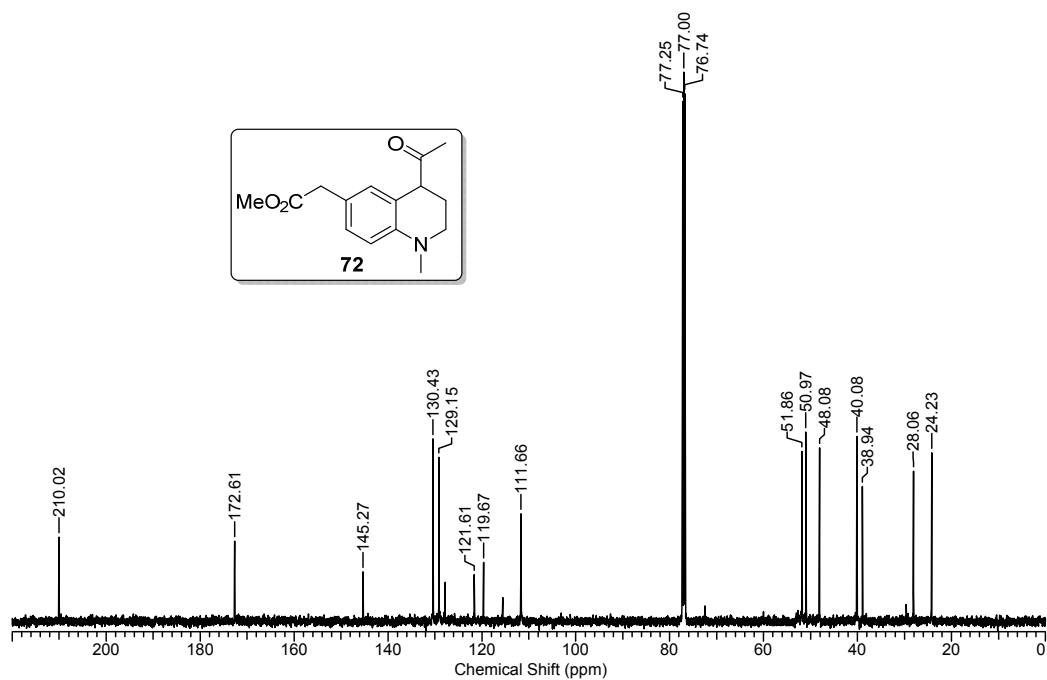
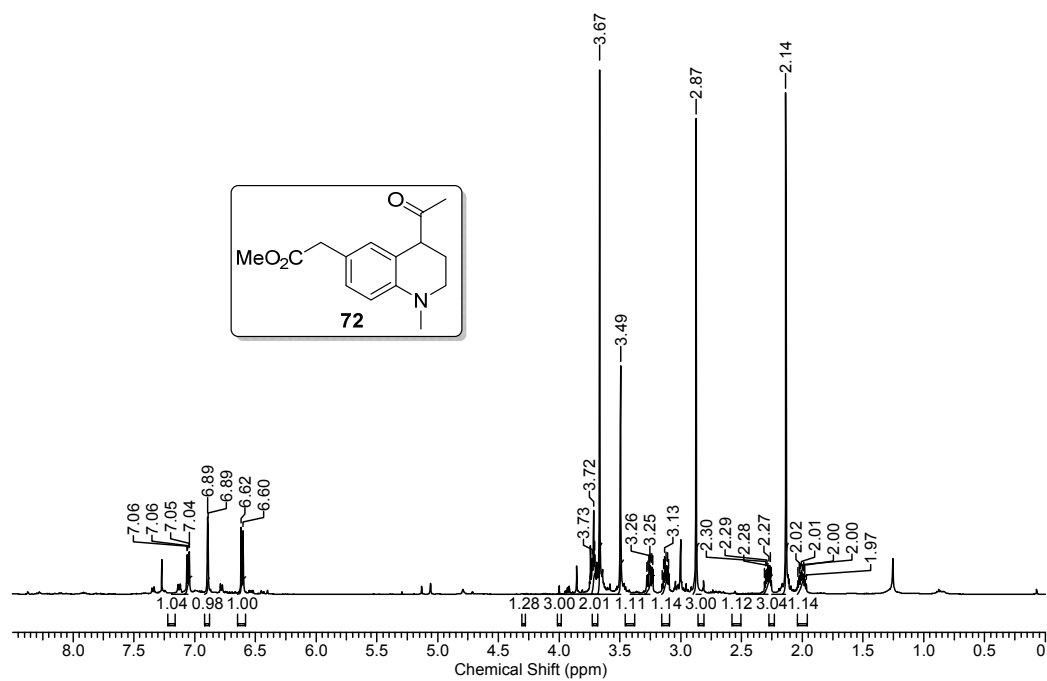
**Figure 1.** Stereo view of minimized structures (**a, b**) and superimposed 20 minimum energy structures (**c, d**) for compound **71**.

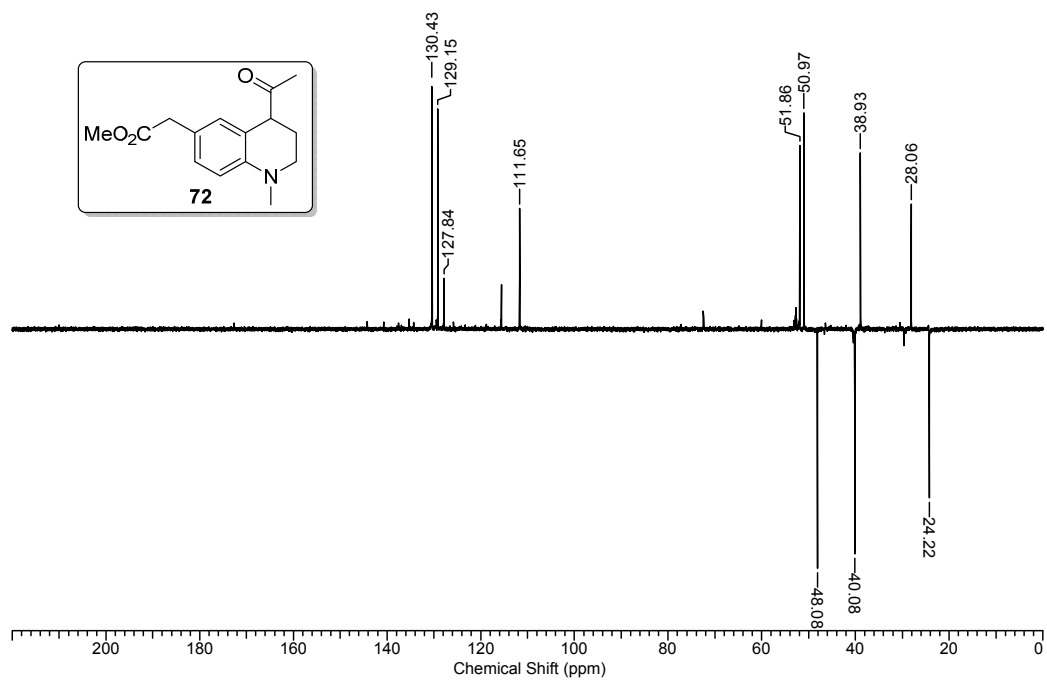
Distance constraints used in MD calculations for compound **71** derived from 2D NOESY experiment are given in table **4**. MD simulation was done on Schrodinger software by using macro module tool. This calculation has produced 100 minimized structures out of that 20 best superimposed structures are shown in fig **c & d**. The superimposed structure shows less than 0.1 Å RMSD values.

**Table 4 :**

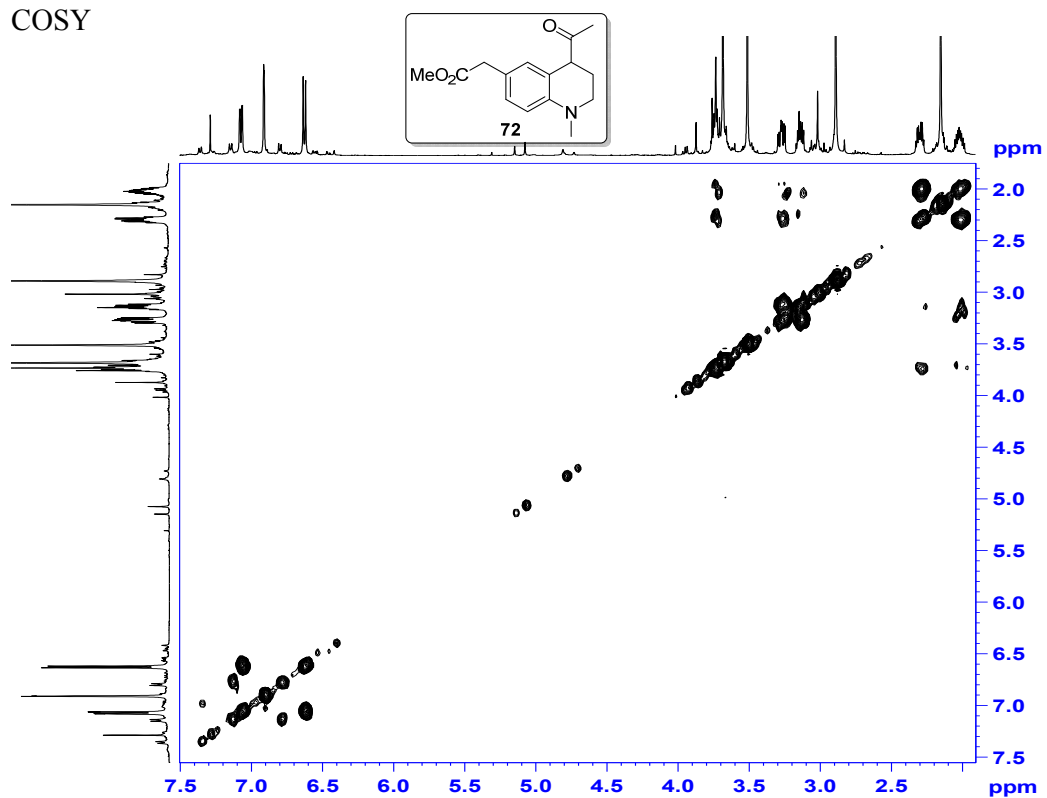
| (F2)<br>[ppm] | (F1) [ppm] | Upper<br>Bound | Lower<br>Bound | Between |
|---------------|------------|----------------|----------------|---------|
| 6.7061        | 7.1172     | 2.684          | 2.196          | 5H/4H   |
| 4.0798        | 6.8071     | 3.13121        | 2.561899       | 1H/6H   |
| 4.0823        | 7.21       | 2.574525       | 2.106429       | 1H/12H  |
| 3.5111        | 6.8046     | 2.864897       | 2.344006       | 7H/6H   |
| 3.4965        | 7.1978     | 2.530739       | 2.070605       | 2H/8H   |
| 3.3037        | 7.1978     | 3.081239       | 2.521014       | 3B/12H  |
| 3.494         | 4.0843     | 3.696374       | 3.024306       | 1H/2H   |
| 3.3061        | 4.0794     | 3.306417       | 2.70525        | 1H/3B   |
| 3.3915        | 3.486      | 3.169193       | 2.592976       | 2H/3A   |
| 2.9546        | 3.3858     | 2.682984       | 2.195168       | Nme/3A  |
| 2.9522        | 3.2589     | 2.997168       | 2.452228       | Nme/3B  |
| 2.0711        | 3.4884     | 2.808011       | 2.297464       | 13/2H   |
| 2.9546        | 6.707      | 2.412529       | 1.973887       | Nme/4H  |
| 2.0711        | 6.8095     | 3.591313       | 2.938347       | 13H/6H  |
| 2.0735        | 7.2076     | 3.986811       | 3.261936       | 13H/8H  |



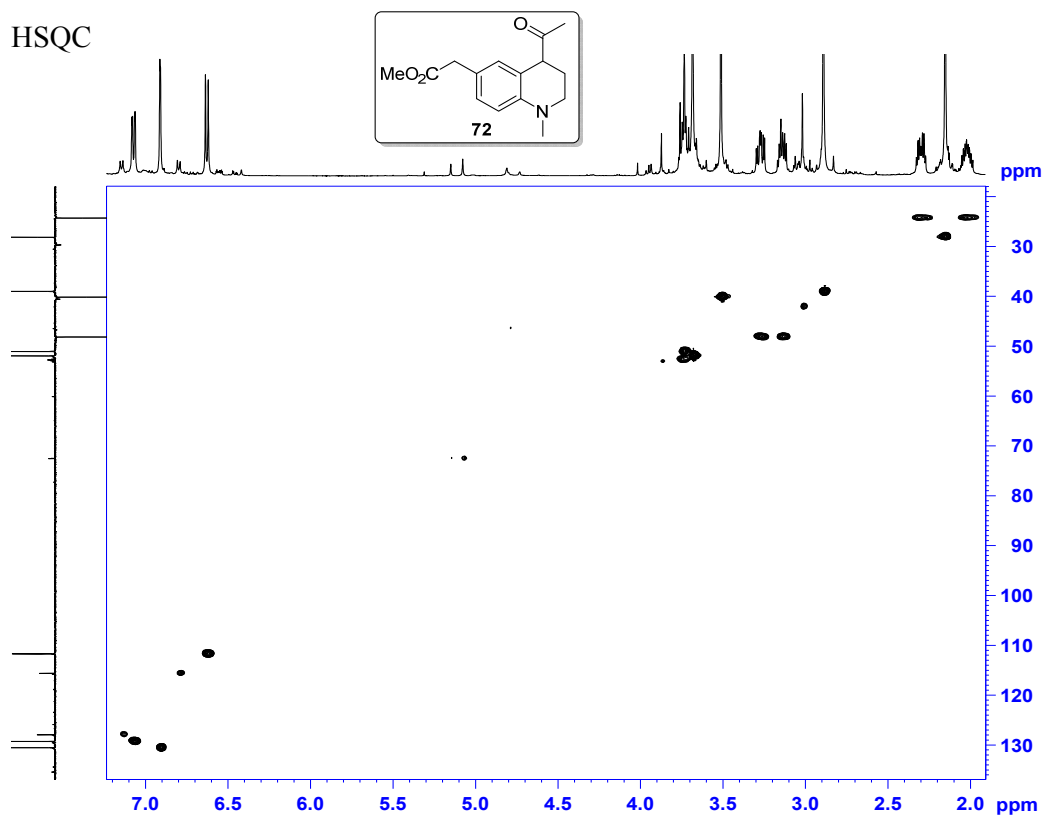




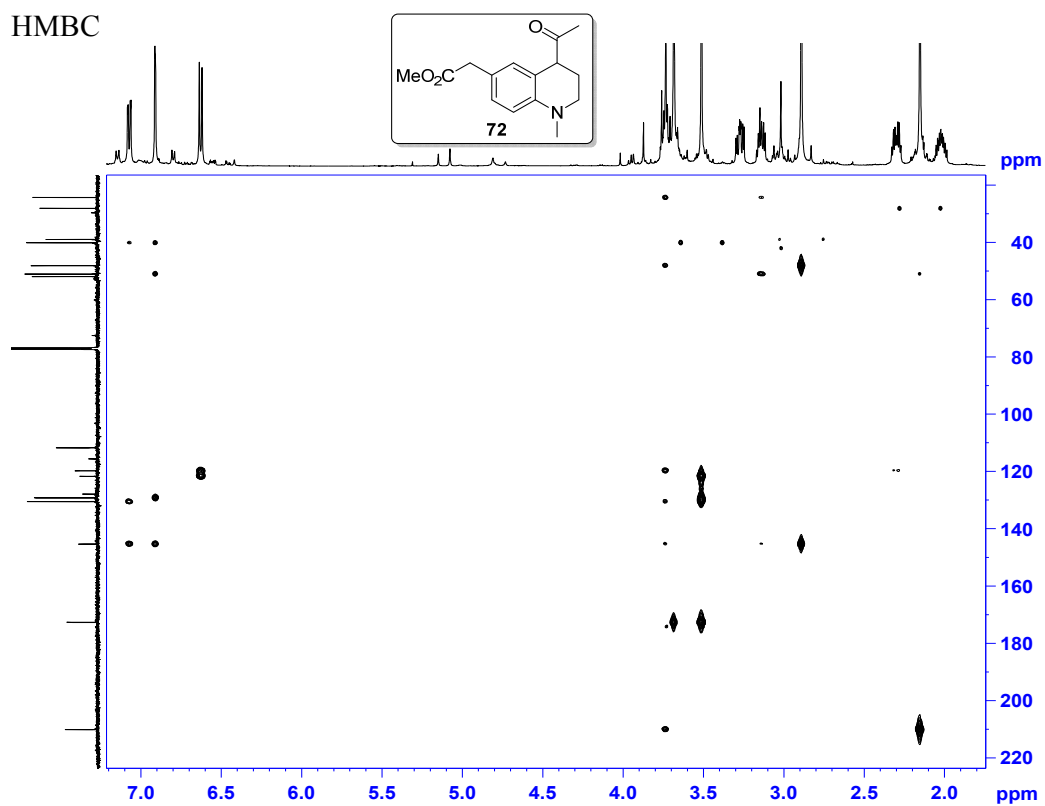
COSY



HSQC

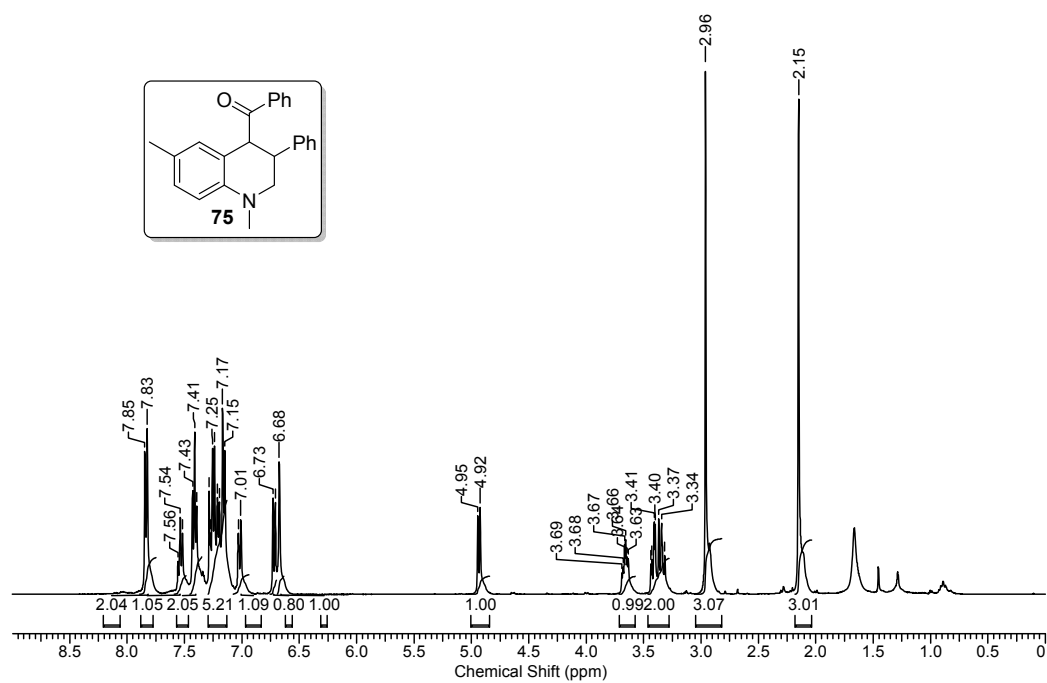
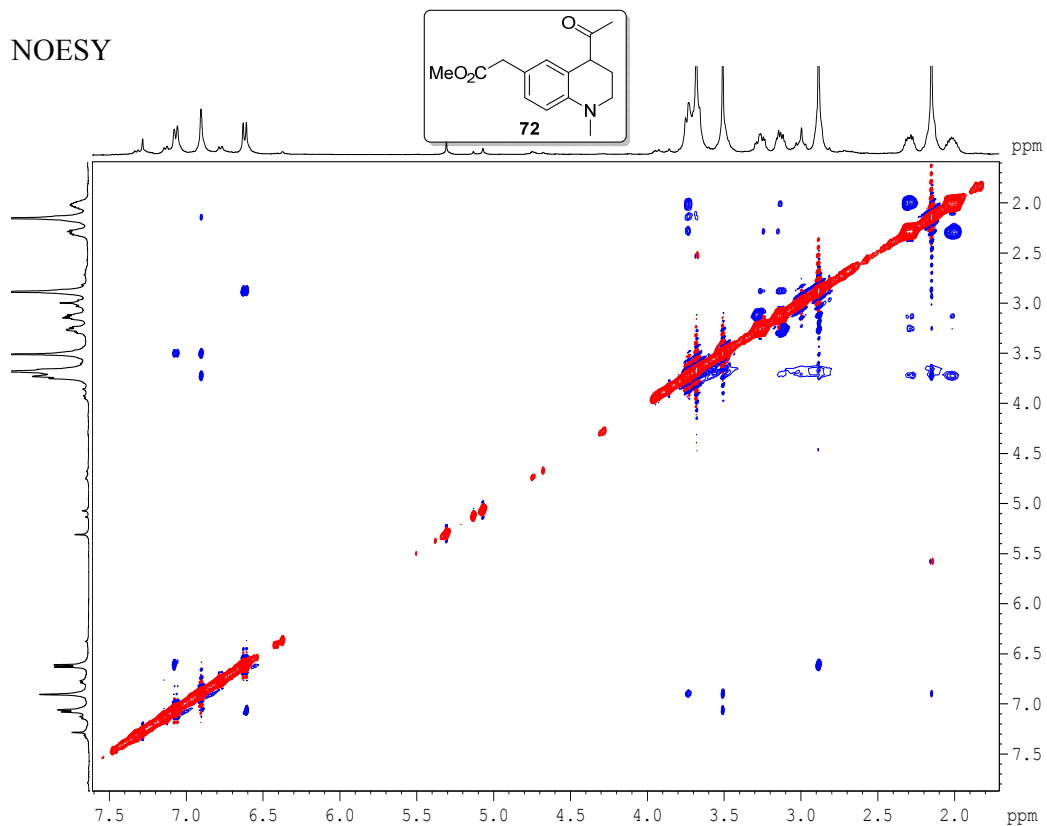


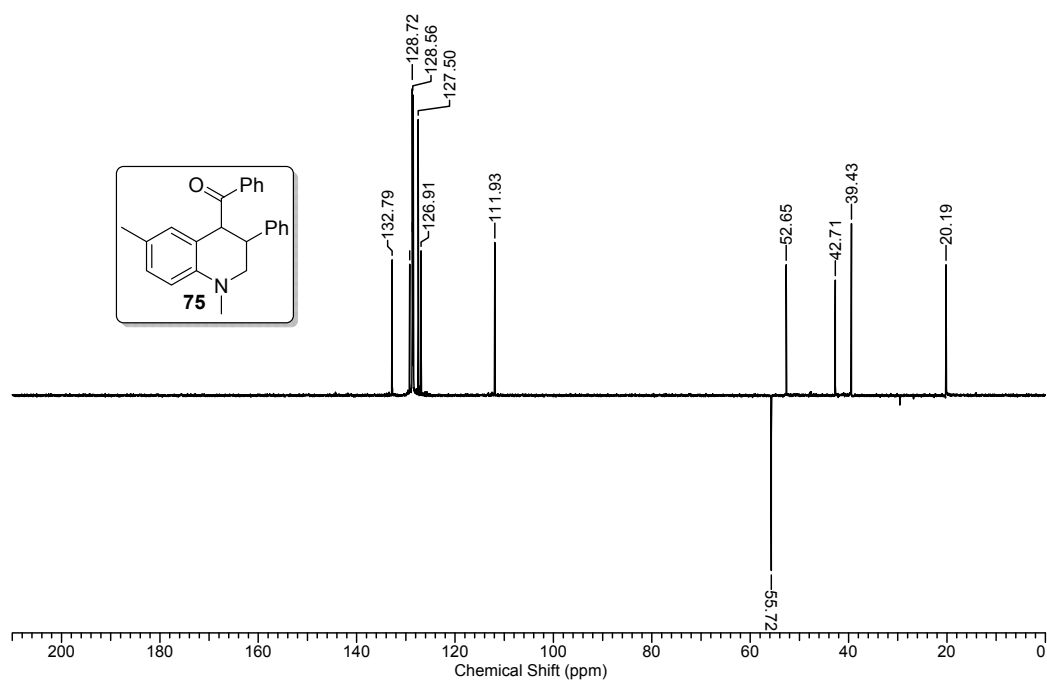
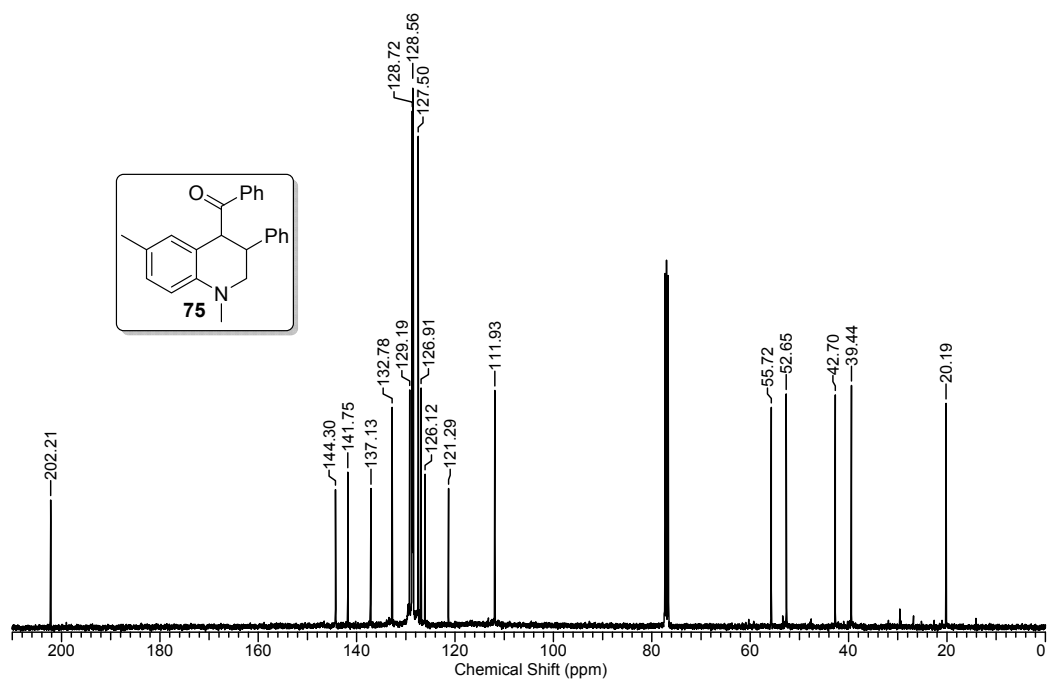
HMBC

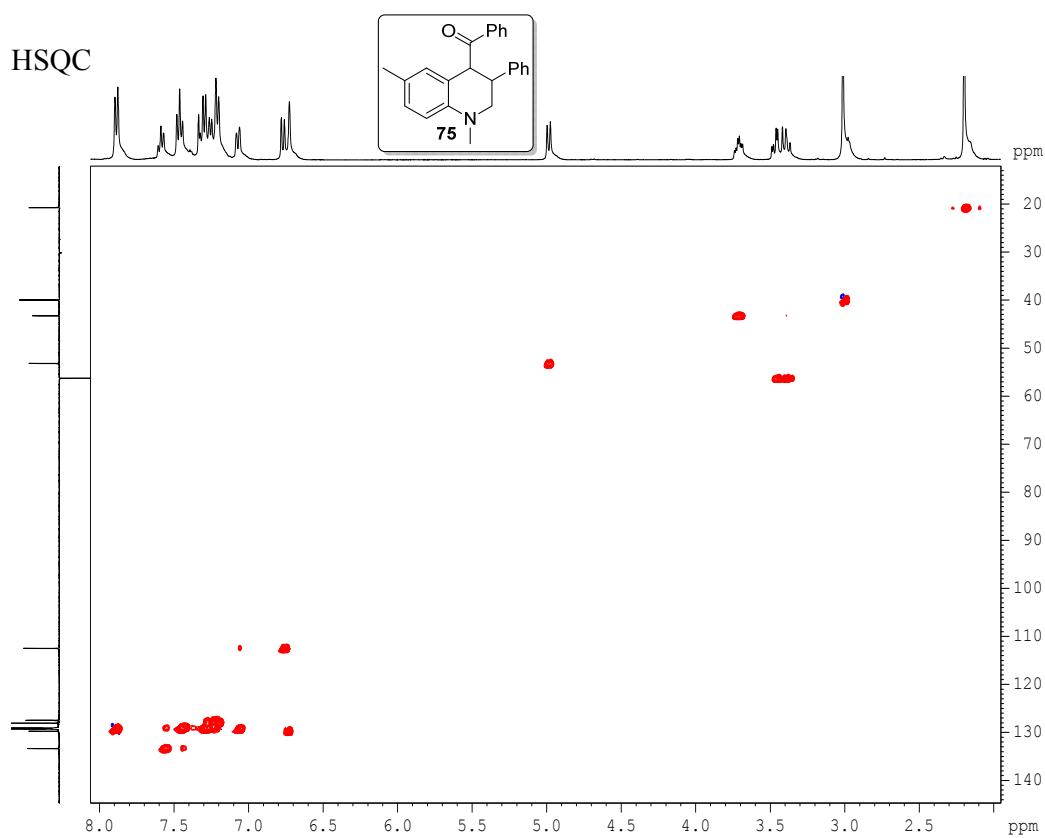
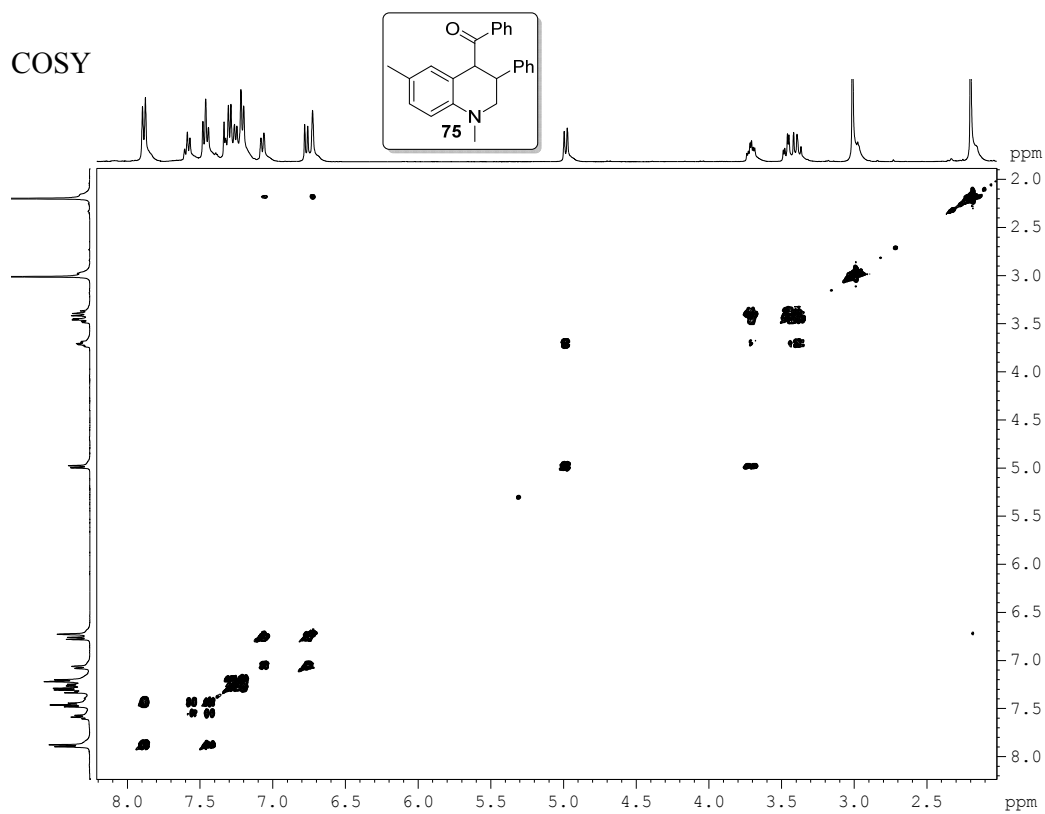


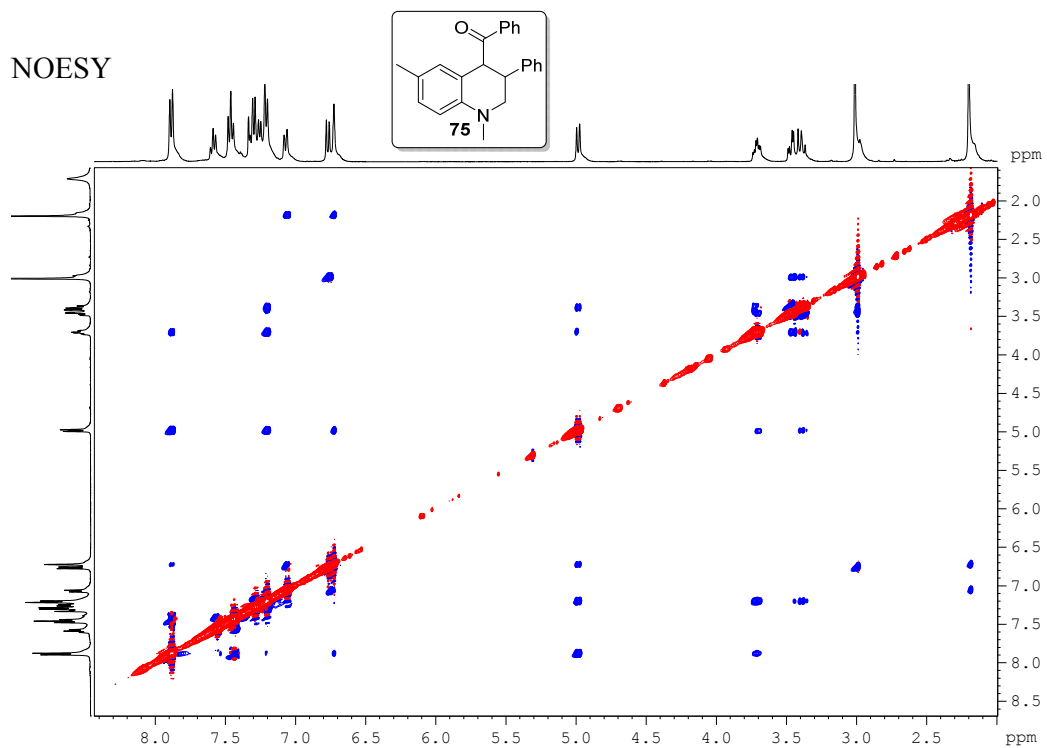
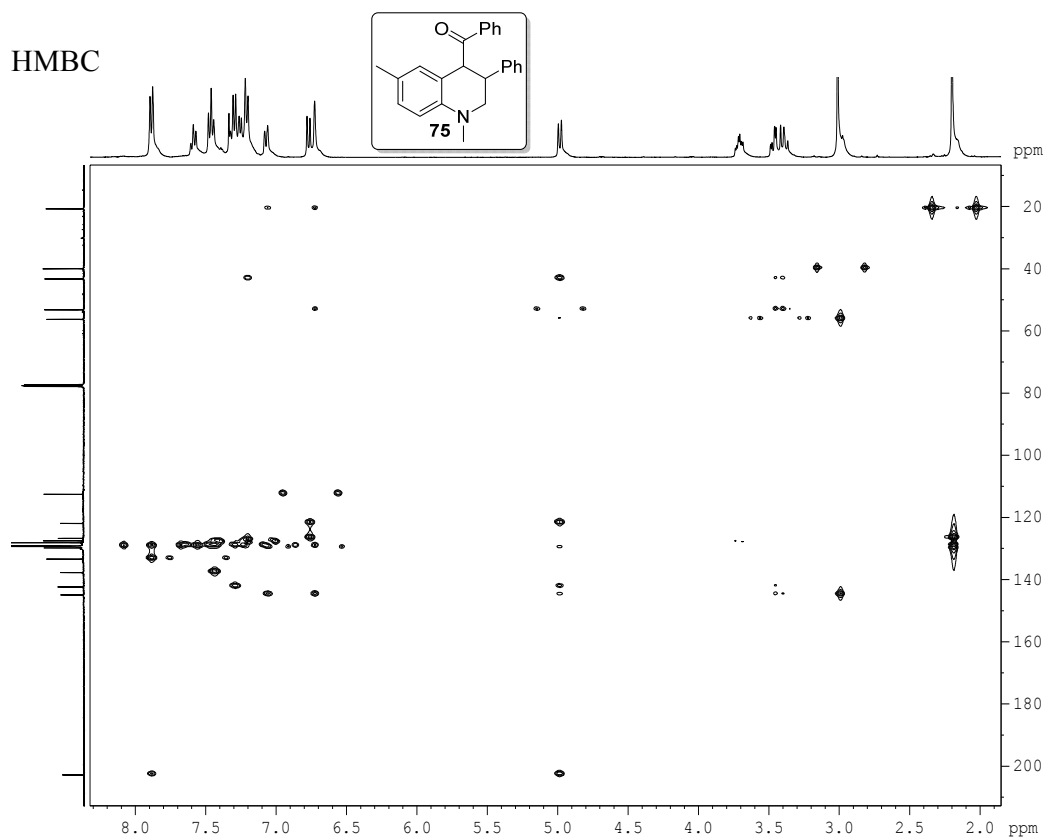


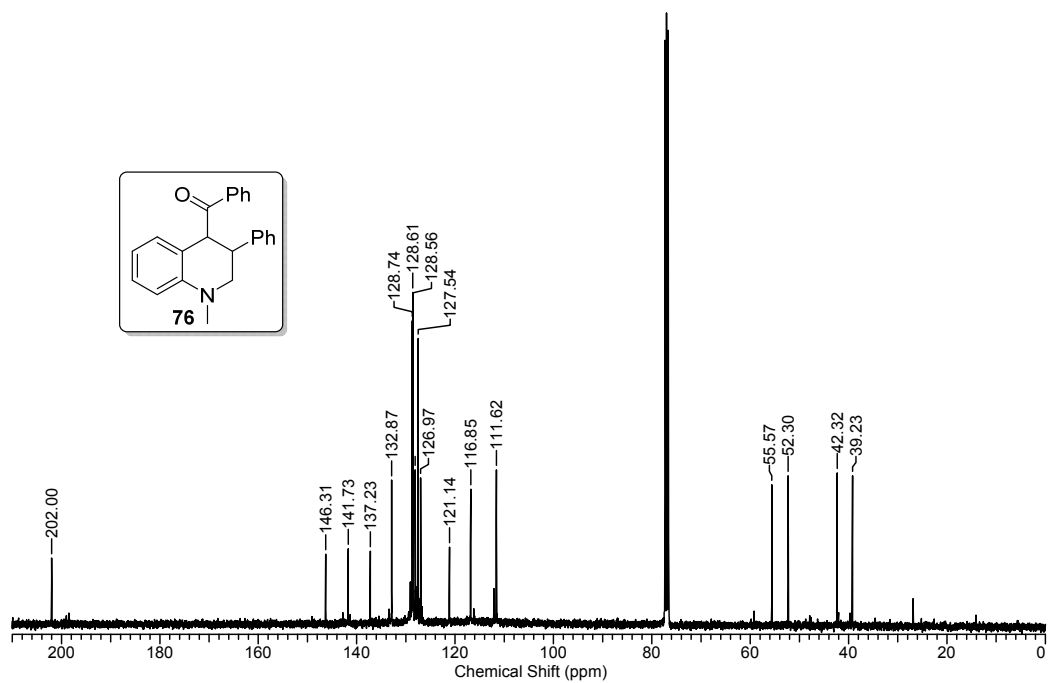
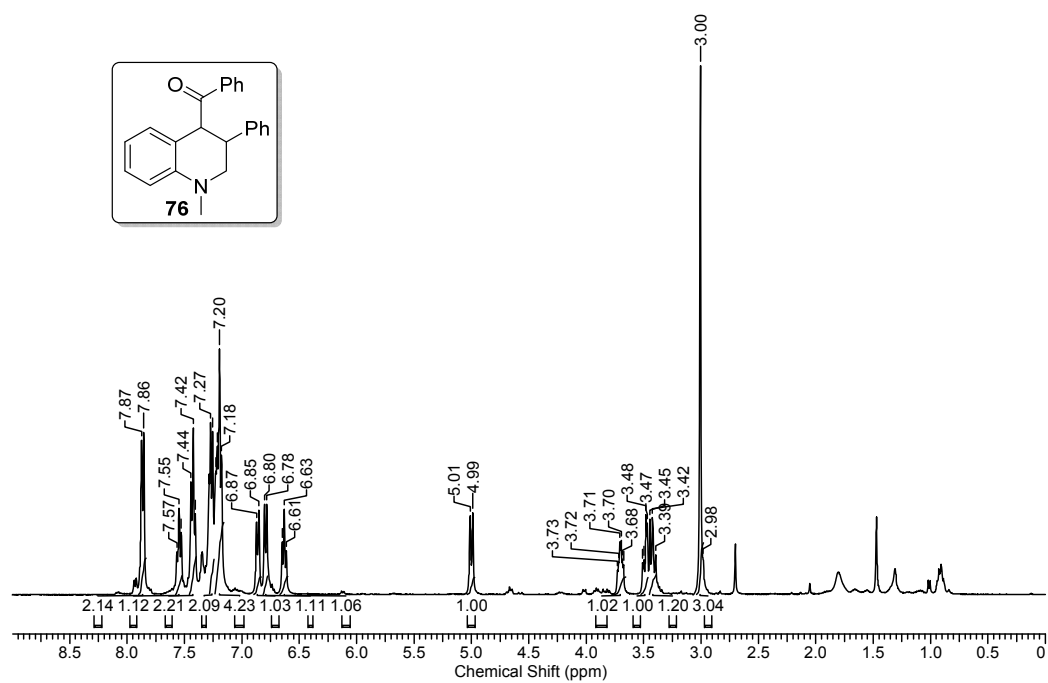
NOESY

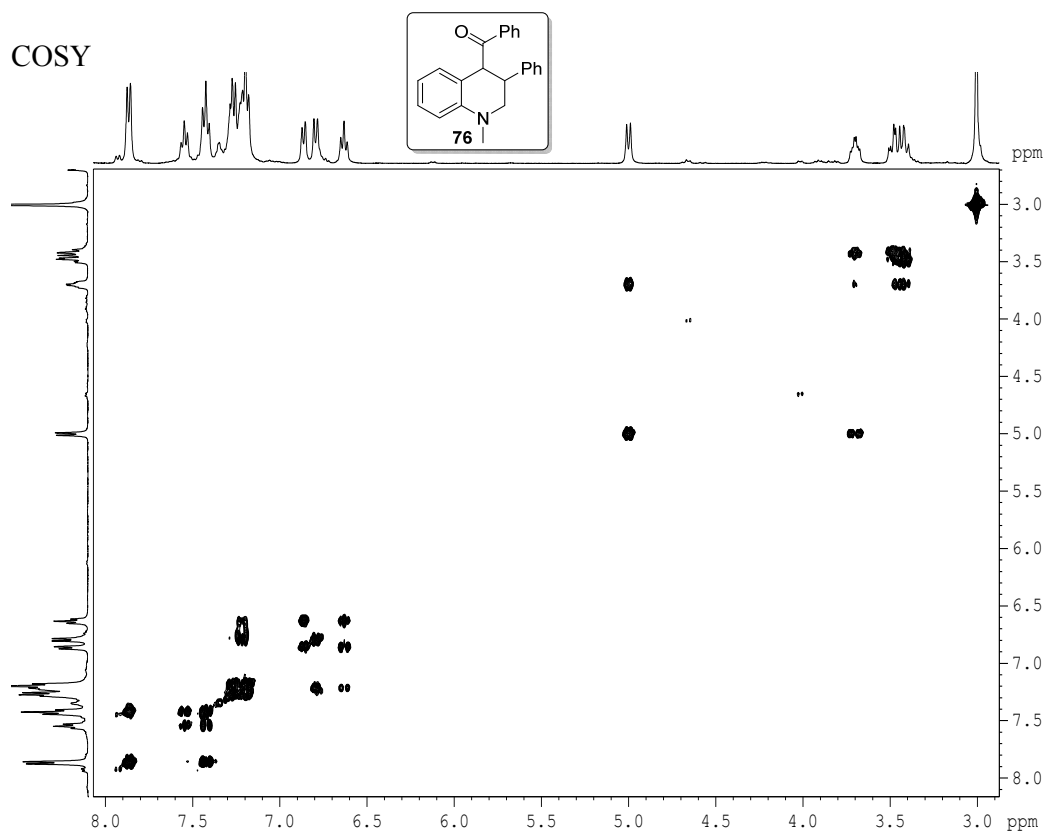
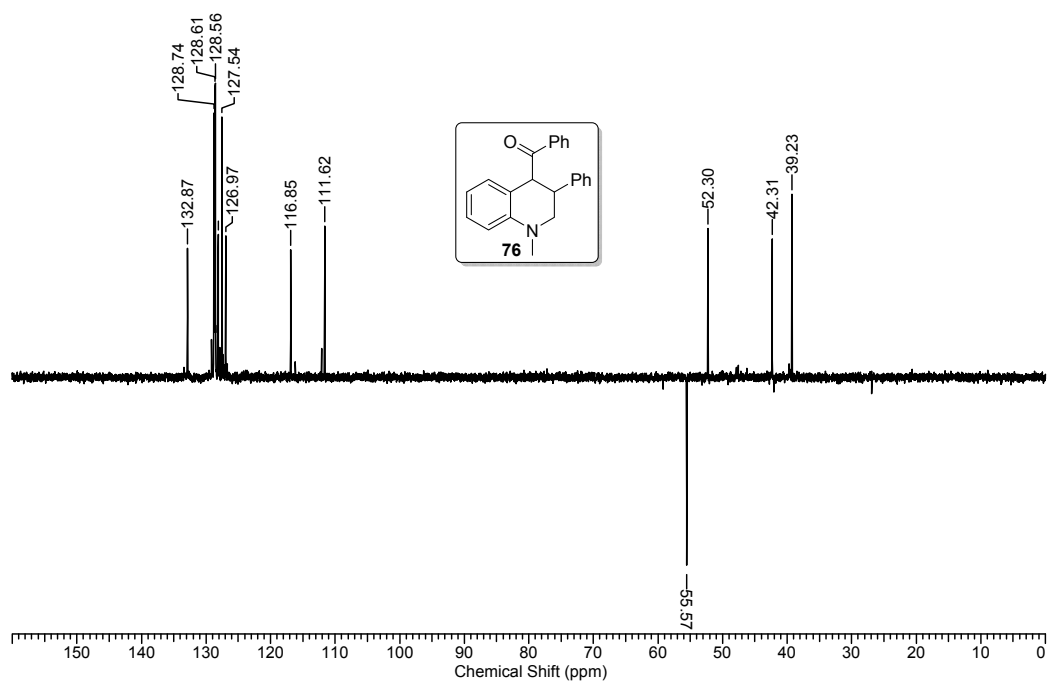


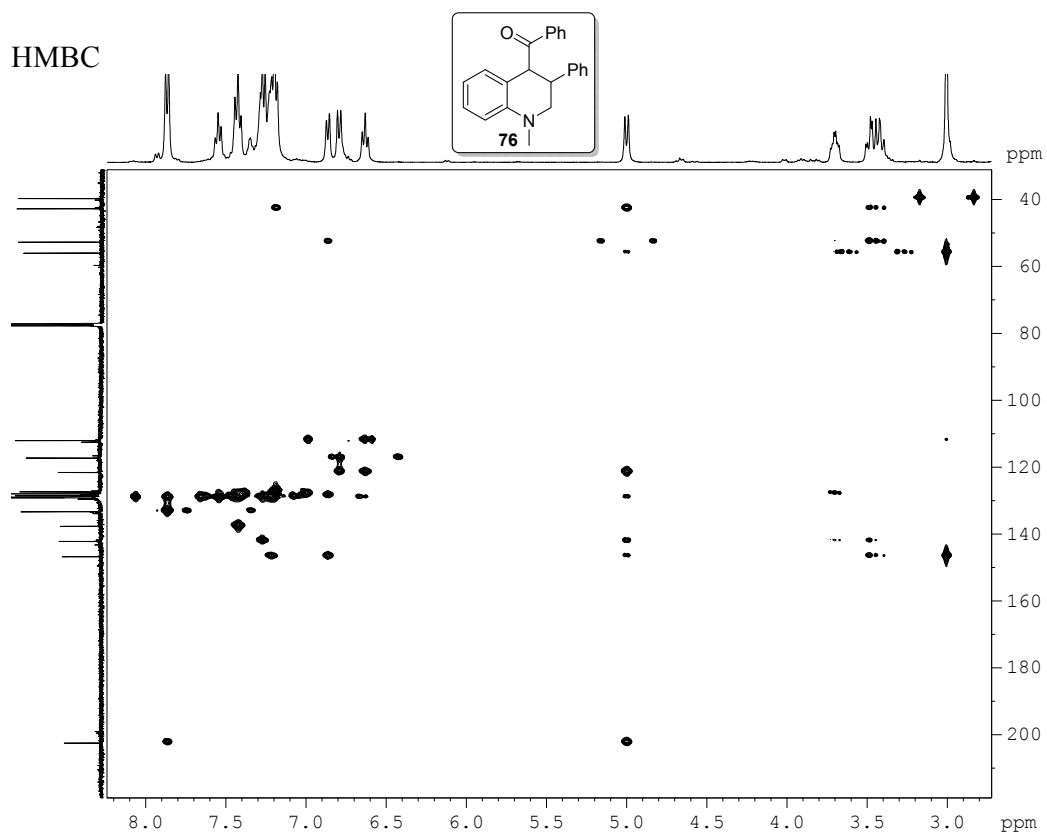
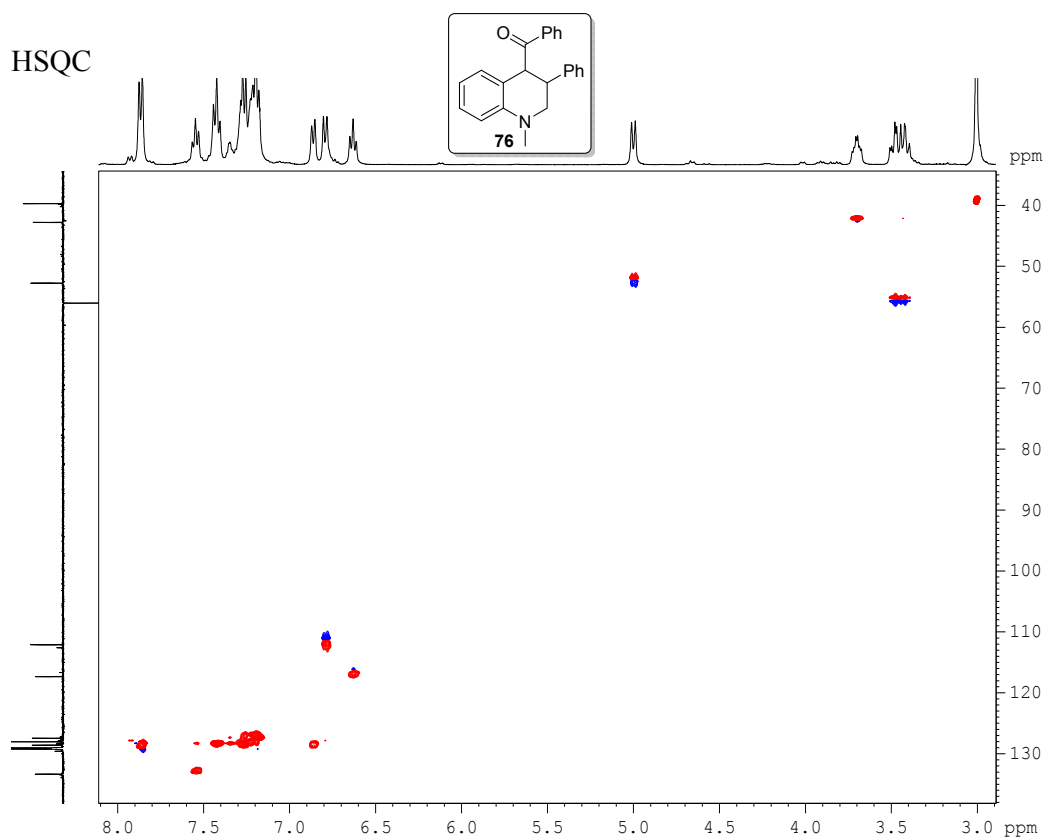


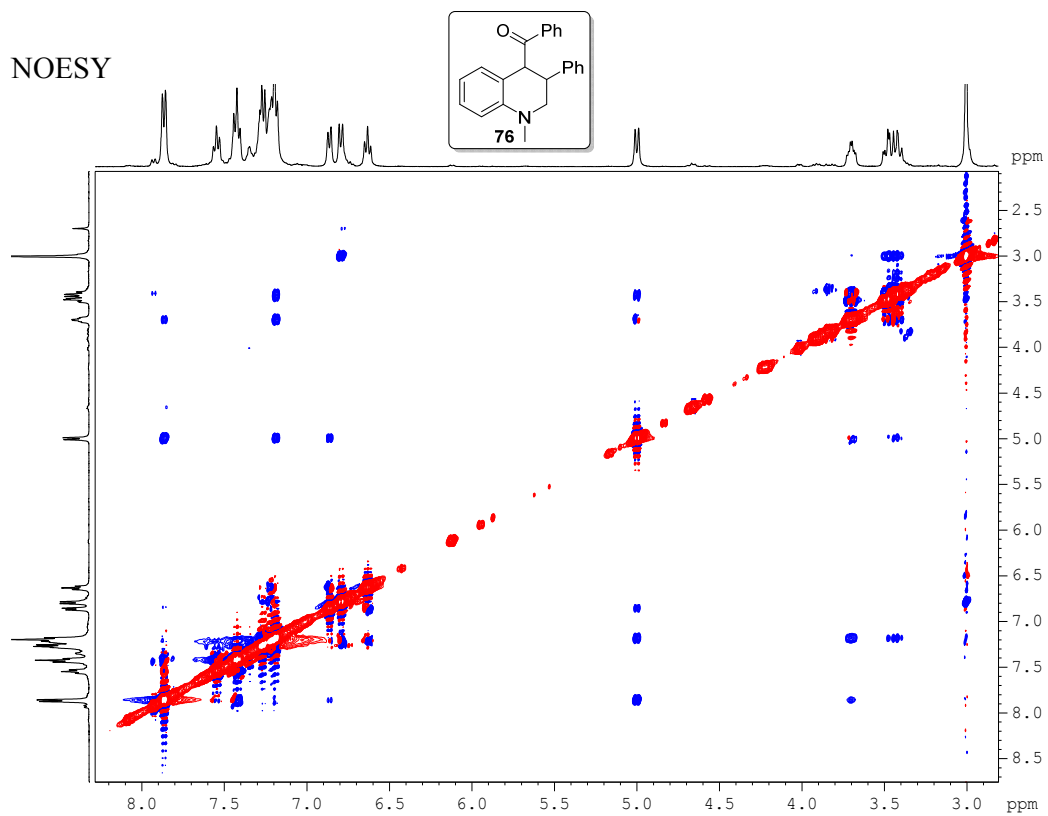












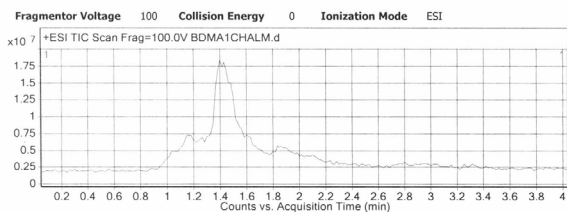


## LCMS analysis of photoirradiation reaction between 2 and 48 (eq 3):

## Qualitative Compound Report

Data File: BDMA1CHALM.d      Sample Name: BDMA1CHALM  
Sample Type: Sample      Position: 11  
Instrument Name: Instrument 1      User Name: CBMR-PC\admin  
Acq Method: Direct Mass.m      Acquired Time: 9/14/2013 8:06:40 PM  
IRM Calibration Status: Success      DA Method: Default.m  
Comment: +Ve MODE

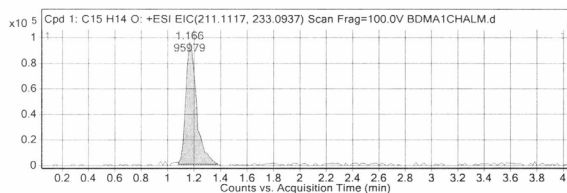
Acquisition SW: 6200 series TOF/6500 series  
Version: Q-TOF B.05.00 (B5042.0)



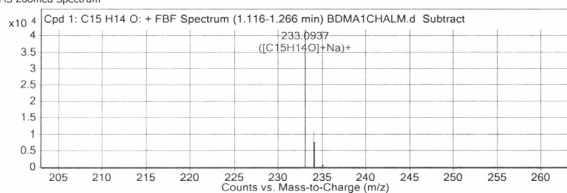
Compound Table

| Compound Label     | RT    | Mass     | Abund   | Formula     | Tgt Mass | Diff (ppm) | MFG Formula | DB Formula  |
|--------------------|-------|----------|---------|-------------|----------|------------|-------------|-------------|
| Cpd 1: C15 H14 O   | 1.166 | 210.104  | 41793   | C15 H14 O   | 210.1045 | -2.11      | C15 H14 O   | C15 H14 O   |
| Cpd 2: C15 H17 N   | 1.433 | 211.1365 | 1510973 | C15 H17 N   | 211.1361 | 1.69       | C15 H17 N   | C15 H17 N   |
| Cpd 3: C30 H27 N O | 1.55  | 417.2097 | 324505  | C30 H27 N O | 417.2093 | 1.06       | C30 H27 N O | C30 H27 N O |

| Compound Label   | m/z      | RT    | Algorithm       | Mass    |
|------------------|----------|-------|-----------------|---------|
| Cpd 1: C15 H14 O | 233.0937 | 1.166 | Find By Formula | 210.104 |



MS Zoomed Spectrum

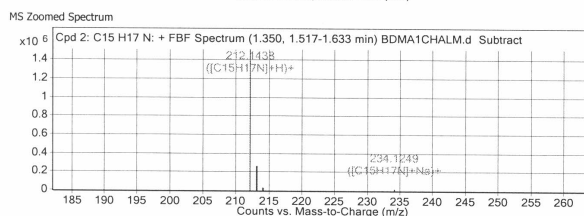
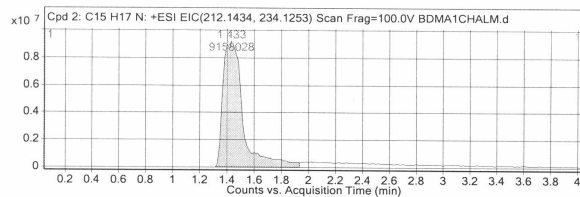


MS Spectrum Peak List

| m/z      | z | Abund    | Formula | Ion     |
|----------|---|----------|---------|---------|
| 233.0937 | 1 | 41793.27 | C15H14O | (M+Na)+ |
| 234.0952 | 1 | 10933.06 | C15H14O | (M+Na)+ |
| 235.0969 | 1 | 564.33   | C15H14O | (M+Na)+ |

| Compound Label   | m/z      | RT    | Algorithm       | Mass     |
|------------------|----------|-------|-----------------|----------|
| Cpd 2: C15 H17 N | 212.1438 | 1.433 | Find By Formula | 211.1365 |

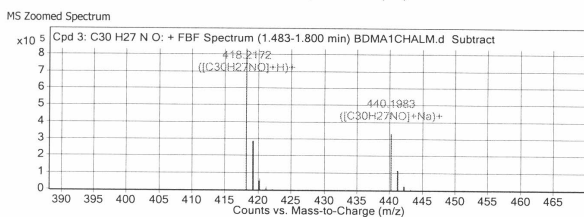
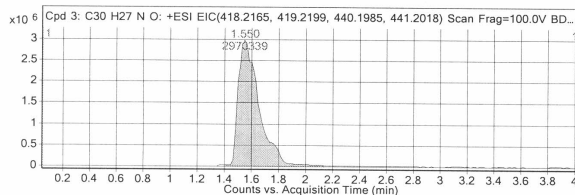
## Qualitative Compound Report



MS Spectrum Peak List

| m/z      | z | Abund      | Formula | Ion     |
|----------|---|------------|---------|---------|
| 212.1438 | 1 | 1510972.63 | C15H17N | (M+H)+  |
| 213.1465 | 1 | 245330.28  | C15H17N | (M+H)+  |
| 214.1495 | 1 | 18597.85   | C15H17N | (M+H)+  |
| 215.1426 | 1 | 1051.04    | C15H17N | (M+H)+  |
| 234.1249 | 1 | 12224.32   | C15H17N | (M+Na)+ |
| 235.1277 | 1 | 2402.13    | C15H17N | (M+Na)+ |

| Compound Label     | m/z      | RT   | Algorithm       | Mass     |
|--------------------|----------|------|-----------------|----------|
| Cpd 3: C30 H27 N O | 440.1983 | 1.55 | Find By Formula | 417.2097 |



MS Spectrum Peak List

| m/z      | z | Abund     | Formula  | Ion     |
|----------|---|-----------|----------|---------|
| 418.2172 | 1 | 831862.13 | C30H27NO | (M+H)+  |
| 419.2201 | 1 | 271396.97 | C30H27NO | (M+H)+  |
| 420.2261 | 1 | 66023.95  | C30H27NO | (M+H)+  |
| 421.2311 | 1 | 16041.01  | C30H27NO | (M+H)+  |
| 422.2335 | 1 | 3522.03   | C30H27NO | (M+H)+  |
| 440.1983 | 1 | 324504.66 | C30H27NO | (M+Na)+ |
| 441.2006 | 1 | 110515.73 | C30H27NO | (M+Na)+ |
| 442.2047 | 1 | 23190.71  | C30H27NO | (M+Na)+ |

## Qualitative Compound Report

|          |   |         |          |         |
|----------|---|---------|----------|---------|
| 443.2098 | 1 | 4285.61 | C30H27NO | (M+Na)+ |
|----------|---|---------|----------|---------|

--- End Of Report ---

## 3.10 Single crystal structure analysis:

Crystal structure of 3-(10-methyl-9,10-dihydroacridin-9-yl)-1,3-diphenylpropan-1-one (**56**):

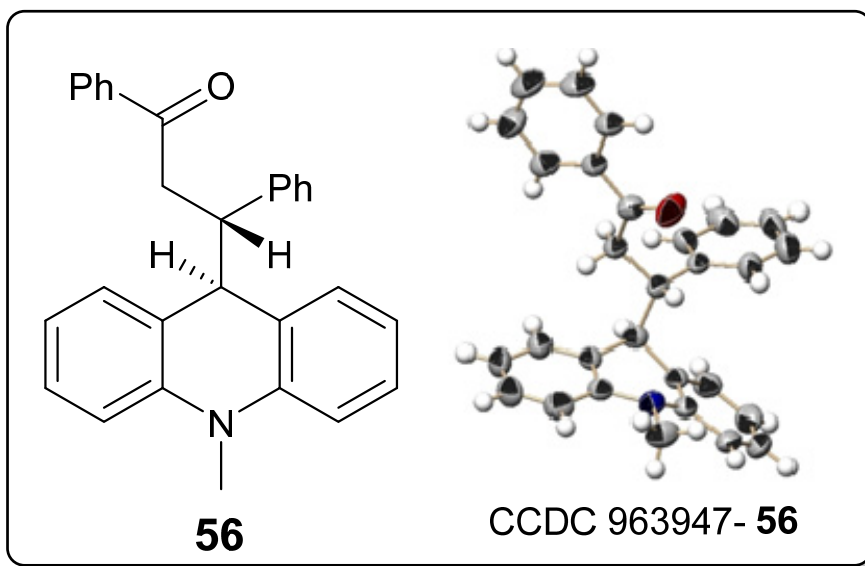


**Table 5:** Crystal data and structural refinement for **56**.

| Crystal Data                             |                                    |
|--|------------------------------------|
| Empirical formula                        | C <sub>29</sub> H <sub>25</sub> NO |
| Formula weight                           | 403.50                             |
| Temperature/K                            | 293(2)                             |
| Crystal system                           | monoclinic                         |
| Space group                              | C2/c                               |
| a/Å                                      | 44.695(6)                          |
| b/Å                                      | 5.6461(7)                          |
| c/Å                                      | 18.771(3)                          |
| $\alpha$ /°                              | 90.00                              |
| $\beta$ /°                               | 114.034(16)                        |
| $\gamma$ /°                              | 90.00                              |
| Volume/Å <sup>3</sup>                    | 4326.3(10)                         |
| Z  | 8                                  |
| $\rho_{\text{calc}}$ /mg/mm <sup>3</sup> | 1.239                              |
| m/mm <sup>-1</sup>                       | 0.074                              |
| F(000)                                   | 1712.0                             |

| Data Collection                             |   |
|---|---|
| Crystal size/mm <sup>3</sup>                | 0.14 × 0.12 × 0.10                                |
| 2 $\theta$ range for data collection        | 5.86 to 58.3°                                     |
| Index ranges                                | -60 ≤ h ≤ 58, -7 ≤ k ≤ 5, -25 ≤ l ≤ 25            |
| Reflections collected                       | 10408   |
| Independent reflections                     | 4984[R(int) = 0.0397]                             |
| Data/restraints/parameters                  | 4984/0/282  |
| Goodness-of-fit on F <sup>2</sup>           | 1.049   |
| Final R indexes [I ≥ 2 $\sigma$ (I)]        | R <sub>1</sub> = 0.0702, wR <sub>2</sub> = 0.1381 |
| Final R indexes [all data]                  | R <sub>1</sub> = 0.1430, wR <sub>2</sub> = 0.1763 |
| Largest diff. peak/hole / e Å <sup>-3</sup> | 0.19/-0.26  |

**Crystal Structure of 10-methyl-9-(2-nitro-1-phenylethyl)-9,10-dihydroacridine (57):**

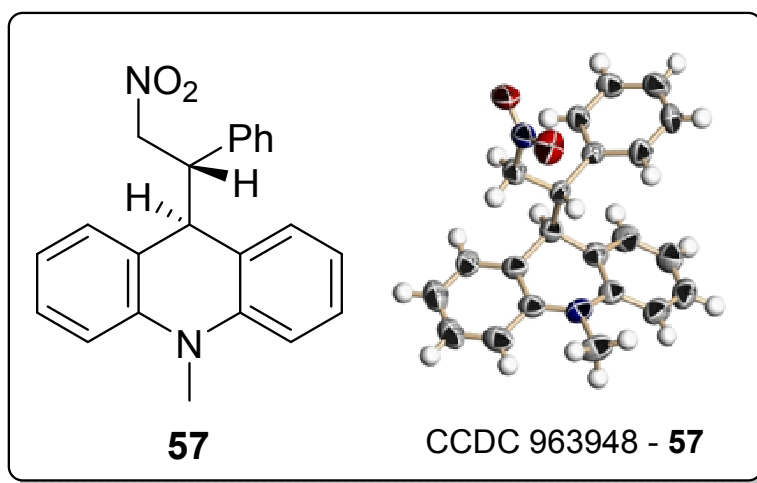


**Table 6:** Crystal data and structural refinement for **57**.

| Crystal Data      |   |
|-------------------|---|
| Empirical formula | C <sub>22</sub> H <sub>20</sub> N <sub>2</sub> O <sub>2</sub> |
| Formula weight    | 344.40  |
| Temperature/K     | 293.01(10)  |
| Crystal system    | monoclinic  |
| Space group       | P2 <sub>1</sub> /c  |
| a/Å               | 18.092(2)   |

|   |   |
|---|---|
| b/Å   | 5.5893(7)   |
| c/Å   | 19.173(3)   |
| $\alpha$ /°                                 | 90.00   |
| $\beta$ /°                                  | 115.022(17)                                       |
| $\gamma$ /°                                 | 90.00   |
| Volume/Å <sup>3</sup>                       | 1756.9(4)   |
| Z   | 4   |
| $\rho_{\text{calc}}$ /mm <sup>3</sup>       | 1.302   |
| m/mm <sup>-1</sup>                          | 0.084   |
| F(000)                                      | 728.0   |
| <b>Data Collection</b>                      |   |
| Crystal size/mm <sup>3</sup>                | 0.35 × 0.14 × 0.11                                |
| 2 $\Theta$ range for data collection        | 6.92 to 58.1°                                     |
| Index ranges                                | -24 ≤ h ≤ 20, -7 ≤ k ≤ 7, -24 ≤ l ≤ 25            |
| Reflections collected                       | 7251  |
| Independent reflections                     | 3975[R(int) = 0.0661]                             |
| Data/restraints/parameters                  | 3975/0/236  |
| Goodness-of-fit on F <sup>2</sup>           | 0.935   |
| Final R indexes [I ≥ 2 $\sigma$ (I)]        | R <sub>1</sub> = 0.0765, wR <sub>2</sub> = 0.1691 |
| Final R indexes [all data]                  | R <sub>1</sub> = 0.1728, wR <sub>2</sub> = 0.2185 |
| Largest diff. peak/hole / e Å <sup>-3</sup> | 0.28/-0.22  |

**Crystal Structure of 10-methyl-10H-spiro[acridine-9,1'-cyclohexan]-4'-one (66):**

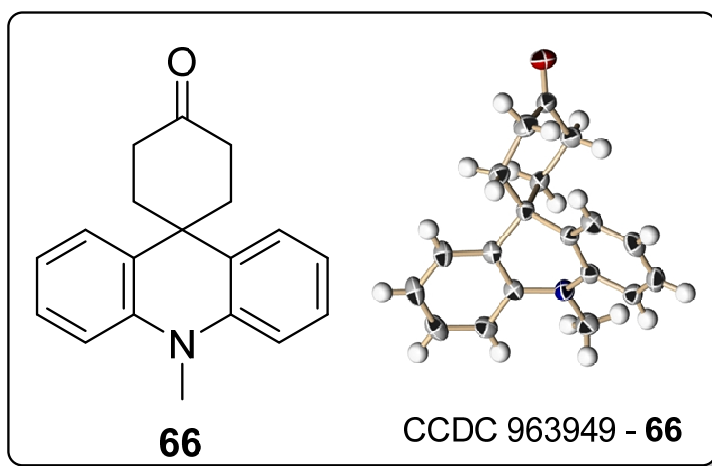


**Table 7:** Crystal data and structural refinement for **66**.

| <b>Crystal Data</b>                         |   |
|---|---|
| Empirical formula                           | C <sub>19</sub> H <sub>19</sub> NO                |
| Formula weight                              | 277.35  |
| Temperature/K                               | 219.99(10)  |
| Crystal system                              | triclinic   |
| Space group                                 | P-1   |
| a/Å   | 8.6574(8)   |
| b/Å   | 9.3517(8)   |
| c/Å   | 10.6769(9)  |
| α/°   | 103.888(7)  |
| β/°   | 108.883(8)  |
| γ/°   | 108.807(8)  |
| Volume/Å <sup>3</sup>                       | 714.71(11)  |
| Z   | 2   |
| ρ <sub>calc</sub> /mg/mm <sup>3</sup>       | 1.289   |
| m/mm <sup>-1</sup>                          | 0.079   |
| F(000)                                      | 296.0   |
| <b>Data Collection</b>                      |   |
| Crystal size/mm <sup>3</sup>                | 0.28 × 0.21 × 0.15                                |
| 2θ range for data collection                | 6.8 to 58.38°                                     |
| Index ranges                                | -11 ≤ h ≤ 9, -12 ≤ k ≤ 12, -11 ≤ l ≤ 13           |
| Reflections collected                       | 5158  |
| Independent reflections                     | 3264[R(int) = 0.0250]                             |
| Data/restraints/parameters                  | 3264/0/191  |
| Goodness-of-fit on F <sup>2</sup>           | 1.033   |
| Final R indexes [I ≥ 2σ(I)]                 | R <sub>1</sub> = 0.0510, wR <sub>2</sub> = 0.1209 |
| Final R indexes [all data]                  | R <sub>1</sub> = 0.0656, wR <sub>2</sub> = 0.1357 |
| Largest diff. peak/hole / e Å <sup>-3</sup> | 0.23/-0.22  |

### **List of research publications:**

1. "Visible Light Photoredox Catalysis: Generation and Addition of N-Aryltetrahydroisoquinoline-Derived  $\alpha$ -Amino Radicals to Michael Acceptor." Paul Kohls, **Deepak Jadhav**, Ganesh Pandey\*, Oliver Reiser\* *Org.Lett.* **2012**, 14, 672-675.
2. "Visible Light Photoredox Catalysis: Investigation of Distal  $sp^3$  C-H Functionalization of *t*-Amines for Alkylation Reaction" Ganesh Pandey\*, **Deepak Jadhav**, Sandip Kumar Tiwari, Bhawana Singh, *Adv. Synth. Catal.* **2014**, In press (accepted manuscript ID: 201400107).

### **Symposia /conferences and awards:**

- Participation in "Joint International Conference on Building Bridges, Forging Bonds for 21<sup>st</sup> Century Organic Chemistry and Chemical Biology (ACS-CSIR-OCCB 2006)," held at CSIR-National Chemical Laboratory, Pune, Maharashtra, India, on January 6-9, 2006.
- Participation in "4<sup>th</sup> J-NOST Conference", held at Madurai Kamaraj University, Madurai, Tamil Nadu, India, on December 6-9, 2008.
- Participation in "Indo-Korean Symposium in Organic Chemistry", held at CSIR-National Chemical Laboratory, Pune, Maharashtra, India, on January 12-13, 2009.
- Best Discussion Leader Award in "1<sup>st</sup> Indian-German Graduate School of Advanced Organic Synthesis for a Sustainable Future (INDIGO) Ph.D. Research Conference and Intensive Course" held at Aalankrita Resort, Hyderabad, Andhra Pradesh, India, on March 1- 4, 2009,
- Received "Indian-German Graduate School of Advanced Organic Synthesis for a Sustainable Future (INDIGO)" Fellowship to do Research as an Exchange Student for Ph. D. Studies in Germany from January-August 2010.
- Participation in "Next Two Decades of Chemical Sciences and Technology" Workshop Organized by Maharashtra Academy of Sciences jointly with NCL & UoP, at National Chemical Laboratory, Pune, Maharashtra, India, on September 23, 2011.
- Participation in "American Chemical Society on Campus" Event held at CSIR-National Chemical Laboratory, Pune, Maharashtra, India, on October 10, 2012.

## **Erratum**